Investigating the effects of repeat ketamine exposure linking brain structural imaging changes to cellular alterations

Chesters, Robert Anthony

Awarding institution:
King's College London

Investigating the effects of repeat ketamine exposure: linking brain structural imaging changes to cellular alterations

Thesis submitted for the degree of Doctor of Philosophy

Robert Chesters

Department of Basic & Clinical Neuroscience

Institute of Psychiatry, Psychology and Neuroscience

King's College London

2018

Abstract

Ketamine has been used over the last 10-12 years as a surprisingly effective therapy for treatment resistant depression. This has led to the establishment of specialised ketamine treatment clinics in the United Kingdom and United States. However, treatment at these clinics is expensive and there is a concern that people suffering with depression will self-medicate with “street” ketamine and run the risk of using too high and too frequent doses. This might lead to detrimental changes in psychological wellbeing, brain functional activity, metabolism and brain structure; as has been observed in recreational ketamine users.

There is a lack of evidence regarding the long-term effects and safety profile of ketamine exposure, and moreover the psychological and neurological changes observed in recreational ketamine users are likely confounded by additional psychotropic drug use.

To investigate the long-term effects of ketamine, with and without these confounds, I conducted structural magnetic resonance imaging in both recreational ketamine users and mice (that received repeated doses of ketamine). In humans, repeat ketamine exposure induced decreases in brain volume in the frontal cortex, striatum and cerebellum. In mice, repeat ketamine exposure induced an increase in volume in the frontal cortex, which was associated with an increase in the amount of neurofilament and synaptophysin within the prefrontal cortex. I observed further decreases and increases in volume within the parietal, temporal and occipital cortices, striatum and cerebellum. Diffusion tensor imaging in mice revealed alterations in brain structure in the neuropil and corpus callosum, which partially replicates previously published changes observed in human ketamine users. These changes in the corpus callosum were associated with an increase in the amount of neurofilament and myelin basic protein.

These data suggest remodelling of neural circuits under repeat ketamine exposure, the functional and behavioural consequences of which require further investigation.

Statement of originality

All work in this thesis, other than where explicitly stated, was carried out by me.

Recruitment of participants, in chapter 2, was performed by Professor Celia Morgan, University College London, and assessments of psychological wellbeing were performed by Dr James Stone, King's College London.

Publications and presentations

Results from chapters 2-4 of this thesis have been presented in different formats at the following scientific research conferences:

- **Brain volumetric change following chronic ketamine exposure in both humans and mice: Similarities and differences.** Poster @ The British Association for Psychopharmacology Summer Meeting (Brighton) 2016
- **Comparing the effects of intermittent and daily chronic ketamine administration on brain microstructure in mice as seen by MRI.** Poster @ The British Chapter of the International Society for Magnetic Resonance in Medicine Meeting (London) 2016
- **Translational neuroimaging reveals differential effects of chronic ketamine on brain macrostructure in humans and mice.** Talk and poster @ European College of Neuropsychopharmacology Workshop for Early Career Scientists in Europe (Nice) 2016
- **Translational neuroimaging reveals differential effects of chronic ketamine on brain macrostructure in humans and mice.** Talk @ European College of Neuropsychopharmacology Congress (Vienna) 2016
- **Repeat ketamine exposure induces microstructural changes in mouse brain tissue.** Poster @ The British Association for Psychopharmacology Summer Meeting (Harrogate) 2017
- **Neuroadaptations to chronic ketamine exposure: a parallel human and mouse MR imaging study.** Poster @ Society of Biological Psychiatry Annual Meeting (San Diego) 2017

Acknowledgements

For helping me through the writing of this thesis and for all your support throughout my PhD, thank you

1. Dr Pop
2. The Iron
3. Jiu Jitsu and everyone at TRICCS
4. Omi
5. The pocket rocket and Brown Bear
6. Mr McGhee and Dutchy

"The Iron never lies to you. You can walk outside and listen to all kinds of talk, get told that you're a god or a total bastard. The Iron will always kick you the real deal. The Iron is the great reference point, the all-knowing perspective giver. Always there like a beacon in the pitch black. I have found the Iron to be my greatest friend. It never freaks out on me, never runs. Friends may come and go…

But two hundred pounds is always two hundred pounds."

-Henry Rollins

Table of contents

List of Figures

List of tables

Abbreviations

1H-MRS	proton magnetic resonance spectroscopy
ACC	anterior cingulate cortex
AD	axial diffusivity
AMPA	α-amino-3-hydroxy-5-methyl-4-isoxazolepropionic acid
AP	axon potential
CAARMS	comprehensive assessment of at-risk mental state
CAT	computational anatomy toolbox
CD68	cluster of differentiation 68
CNS	central nervous system
DAB	3’3-diaminobenzidine
DSM	diagnostic and statistical manual for mental disorder
DTI	diffusion tensor imaging
EAAT	excitatory amino acid transporter
EEG	electroencephalography
FA	fractional anisotropy
FDR	false discovery rate
fMRi	functional MRI
GABA	γ-aminobutyric acid
GAD67	glutamic acid decarboxylase 67
GAT	GABA transporter
GFAP	glial fibrillary acidic protein
GLM	general linear model
IL-18	interleukin 18
IL-6	interleukin 6
IP	intraperitoneal
logJ	logarithmic Jacobian
MAOI	monoamine oxidase inhibitor
MBP	myelin basic protein
MD	mean diffusivity

MDMA	3,4-Methylenedioxymethamphetamine
mIPSC	miniature inhibitory post-synaptic potential
MK-801	dizocilpine
MNI	Montreal neurological institute
MR	magnetic resonance
MRI	magnetic resonance imaging
NAA	N-acetyl-aspartate
NMDA	N-methyl-D-aspartate
NO	nitric oxide
OPC	oligodendrocyte precursor protein
PANSS	positive and negative syndrome scale
PBS	phosphate buffered saline
PBS-T	phosphate buffered saline with triton
PCP	phencyclidine
RD	radial diffusivity
ROI	region of interest
sMRI	structural MRI
SNRI	serotonin and noradrenaline reuptake inhibitor
SOD	superoxide dismutase
SPM	statistical parametric mapping
SPQ	schizotypal personality questionnaire
SSRI	selective serotonin reuptake inhibitor
TBM	tensor based morphometry
TIV	total intracranial volume
TNFα	tumour necrosis factor alpha
UK	United Kingdom
USA	United States of America
VBM	voxel based morphometry

Chapter 1 General Introduction

1.1 What is ketamine?

Ketamine is a drug, more specifically an N-methyl-D-aspartate (NMDA) receptor antagonist. It was originally developed as an anaesthetic in the 1960's. In developed countries such as the United Kingdom it is mostly used in paediatric medicine and in veterinary medicine (Bokor and Anderson, 2014). The reason being that when it is used in adults it elicits psychotropic changes in thinking and behaviour. Such changes include altered thinking patterns, delusional thinking, altered sensory perception, memory deficits, hallucinations and disrupted sleep (Malhotra *et al.*, 1996; Morgan, Mofeez, *et al.*, 2004; Morgan, Riccelli, *et al.*, 2004; Krystal *et al.*, 2005; Morgan, Muetzelfeldt and Curran, 2010; Driesen *et al.*, 2013; Morgan *et al.*, 2014). However, ketamine continues to be used as an anaesthetic in situations and parts of the world where other anaesthetics are not available. The reason being that ketamine preserves breathing reflexes, normal blood pressure and cardiac function, unlike other anaesthetics which require additional supporting machinery to maintain these functions within the patient (Wolff and Winstock, 2006; Domino, 2010).

As mentioned, ketamine can elicit psychotropic changes in adults. In a clinical setting this is undesirable and has limited the use of ketamine in the western world. However, the psychotropic effects of ketamine have led to its wide spread use as a recreational drug, used by people of all ages and demographics. Recreational ketamine use is particularly popular amongst people in their late teens and early twenties. This is true in the United Kingdom, United States of America, China and South East Asia (Global Drug Survey, 2011; Fang, Wang, Shi, Liu, & Lu, 2006; Joe-Laidler & Hunt, 2008; Leung et al., 2008; Lua, Lin, Tseng, Hu, & Yeh, 2003) (Daly, 2016). Recreational ketamine use is also widespread throughout mainland Europe (Hatton, 2015; Daly, 2016; Codrea-Racio, 2016; Malta, 2010; Labu 2017) (Reynaud-Maurupt *et al.*, 2007; Papaseit *et al.*, 2014; Anderson *et al.*, 2017).

The euphoric effects of ketamine, altered sensory perceptions, altered thought, abstract thinking and a feeling of freedom and floating are the reasons why people use ketamine recreationally. Furthermore, ketamine is relatively cheap; £20-£30 pounds per gram (Oliver, 2017), and is readily available which is probably why it is a popular drug, especially amongst younger adults looking to party for cheap.

Unfortunately, ketamine use can lead to both temporary and persistent sub-threshold psychotic symptoms like those experienced by psychotic and schizophrenic patients. These include, but are not limited to; difficulty concentrating, depressed mood, disrupted sleep, anxiety, suspiciousness, withdrawal from friends and family, delusions, hallucinations, disorganised speech and suicidal thoughts and actions. When these symptoms are present in a person but not together or at a great enough severity and/or frequency for a clinical diagnosis of a psychiatric illness then they are said to be at a sub-threshold level (Krystal *et al.*, 1994, 2005; Malhotra *et al.*, 1996; Morgan, Mofeez, *et al.*, 2004; Morgan, Riccelli, *et al.*, 2004; Pomarol-Clotet *et al.*, 2006; Morgan, Muetzelfeldt and Curran, 2010; Driesen *et al.*, 2013; Morgan *et al.*, 2014).

Alongside psychotropic changes repeat ketamine use has been reported to cause changes in brain structure, function and metabolism. These changes include a reduction in brain volume in the grey matter of the frontal cortex, altered white matter brain structure underlying the frontal cortex, disrupted neuronal activity in the hippocampus and altered brain metabolism in the thalamus (Liao *et al.*, 2010, 2011; Edward Roberts *et al.*, 2014; Morgan *et al.*, 2014; Stone *et al.*, 2014).

It may seem surprising then that ketamine over the last 10-12 years has been used as an "off-label" therapy against treatment resistant depression (Zarate and Singh, 2006; DiazGranados *et al.*, 2010; Lapidus *et al.*, 2014).

1.2 Ketamine as a therapy against treatment resistant depression

Depression is a psychiatric disorder and there are many subtypes including but not limited to:

- Major depression; this is the type of depression most people immediately think of when they hear the term depression. This type is characterised by low mood, loss of pleasure and/or interest in activities, feelings of guilt and/or worthlessness, lack of energy and feeling tired, disrupted and lack of sleep, agitation, lethargy and thoughts of suicide.

- Bipolar depression (AKA: manic depression); this is characterised by phases of high energy and elation, feelings of joy, excitement and happiness and phases of major depression.
- Seasonal affective disorder; this is a form of major depression which typically occurs during winter and when there are low natural light levels. This form of major depression typically recedes in the spring and summer months.
- Psychotic depression; people with this subtype of depression experience both major depression and psychotic symptoms.

Depression is typically treated through cognitive behavioural therapy or anti-depressant medication or a combination of both (Mind, 2016; NHS, 2016). Types of anti-depressant medication include:

- Selective serotonin reuptake inhibitors (SSRIs)
- Serotonin and noradrenaline reuptake inhibitors (SNRIs)
- Tricyclics and tricyclic-related drugs
- Monoamine oxidase inhibitors (MAOIs)

Tricyclic antidepressants and MAOIs were developed in the 1950s. Tricyclics work by blocking the reuptake of biogenic amines (dopamine, noradrenaline and adrenaline) and serotonin from the synaptic cleft / extracellular space, whereas MAOIs act by blocking the breakdown of noradrenaline and serotonin by the enzyme monoamine oxidase (Feighner, 1999; Artigas, Nutt and Shelton, 2002; Taylor *et al.*, 2005). The effectiveness of these drugs in treating depression led to the monoamine hypothesis of depression (Delgado, 2000; Hirschfeld, 2000). In a nutshell this hypothesis states that depression arises due to a deficiency in noradrenergic and / or serotonergic signalling within the brain. In turn this led to the development of more specific drugs which target the noradrenergic and serotonergic neurotransmitter systems. In the 1980s SSRIs were developed. SSRIs function by blocking the reuptake of serotonin from the synaptic cleft/extracellular space (Feighner, 1999; Artigas, Nutt and Shelton, 2002). SNRIs were then developed in the 1990s. SNRIs act similarly to SSRIs but also block the reuptake of noradrenaline (Lambert and Bourin, 2002).

Although tricyclics, MAOIs, SSRIs and SNRIs are effective in alleviating the symptoms of depression in a lot of people, they take 3-4 weeks to work and have limited efficiency in

others. Furthermore, 10-30% of people with major and bipolar depression are resistant to these types of drugs (Zarate and Singh, 2006; Al-Harbi, 2012; McIntyre *et al.*, 2014; Ionescu, Rosenbaum and Alpert, 2015; Singh *et al.*, 2017b).

However, quite surprisingly, over the last 10-12 years ketamine has become a successful alternative to conventional antidepressant medication and has been shown to be effective in relieving depressive symptoms in patients who were previously resistant to pharmacological interventions. A single intravenous infusion of 0.5mg/kg of ketamine has been shown to have rapid, strong symptom relief in as little as 2 hours with effects lasting up to 1-2 weeks (Zarate and Singh, 2006; Coyle and Laws, 2015; Kirby, 2015; Kraus *et al.*, 2017; Singh *et al.*, 2017b). Furthermore, these effects have been shown to occur in at least 70% of treatment resistant patients, of which roughly 1/3 achieved symptom remission within 24 hours (Murrough *et al.*, 2013; Serafini *et al.*, 2014; Han *et al.*, 2016). The rapid and strong symptom relief incudes decreased depression ratings, elevated mood and a reduction in suicidal thoughts (Price *et al.*, 2014; Feifel, 2016; Vande Voort *et al.*, 2016).

1.3 Proposed mechanism of action of ketamine's antidepressant affect

The primary mechanism of action of ketamine's antidepressant effect is thought to involve the restoration of synaptic connectivity and glutamatergic signalling (which is thought to be disrupted in depression) (Abdallah *et al.*, 2014). Within depression, and particularly within the prefrontal cortex, synaptic connectivity is significantly reduced. This is expressed as a reduction in glutamate neurotransmission due to decreased excitatory amino acid transporter (EAAT) levels, reduced BDNF expression and release, and reduced mTORC1 signalling resulting in a decrease in post-synaptic AMPA receptors. Upon treatment with ketamine, rapid restoration of prefrontal synaptic connectivity is believed to result within the prefrontal cortex of the depressed brain. This is thought to occur as follows: Ketamine preferentially inhibits NMDA receptors on inhibitory GABAergic interneurons, this causes a widespread prefrontal glutamate surge which activates post-synaptic AMPA receptors. Combined with ketamine's blockade of extra synaptic NMDA receptors on post-synaptic neurons, BDNF release in the post-synaptic

neuron is increased and activates mTORC1 signalling. The increase in mTORC1 signalling in turn increases post-synaptic protein synthesis and AMPA cycling. This results in the restoration of AMPA receptors to the post-synaptic membrane and the restoration of glutamatergic neurotransmission to normal levels.

For a detailed discussion of the proposed mechanisms of action of ketamine in depression please see the following reviews; (Duman *et al.*, 2012; Abdallah *et al.*, 2014; Abdallah, Averill and Krystal, 2015).

1.4 Ketamine treatment clinics and concerns moving forward

The effectiveness of ketamine in helping to alleviate symptoms in treatment-resistant depression has led to the establishment of specialised ketamine treatment clinics in both the United Kingdom (UK) and United States of America (USA). These clinics offer ketamine infusions to patients with depression. These infusions are administered by medical professionals following a psychiatric assessment of the patient and a review of their medical history, as well as a clinical diagnosis for depression (Oxford Health, 2017; Portland Ketamine Clinic, n.d.; Ketamine Health Centres, n.d.; NY Ketamine Infusions LLC, 2018; Ketamine Wellness Centres, 2018). Examples of such clinics include:

- Oxford Health NHS Foundation Trust (UK)
- Portland Ketamine Clinic (USA)
- Ketamine Health Centres Florida and Arizona (USA)
- NY Ketamine Infusions (USA)
- Ketamine Wellness Centres (USA)

Ketamine infusions provided by such clinics have had widespread success and have been publicised widely in the media:

- *"Ketamine can have a "truly remarkable" effect on people with depression".* Independent Newspaper Online (Forster, 2017).
- *"Ketamine helps patients with severe depression 'when nothing else works', doctors say*". Independent Newspaper Online (Forster, 2017).

- *"In the past 20 years, I've not seen anything like this……. Studies have shown that 60% to 70% of people with treatment-resistant depression respond to ketamine".* Time Magazine Online (Oaklander, 2017)
- *"Ketamine could help thousands with severe depression, doctors say*". The Guardian Online (Marsh, 2017)
- *"Ketamine depression treatment should be rolled out"* (BBC News, 2017).

However, this service comes at a price. As the ketamine treatments are given "off-label" (prescribed for a condition other than that for which the drug has been officially approved) they are not provided free of charge by the National Health Service (NHS) in the UK (Oxford Health, 2017), nor are they covered by medical insurance companies in the USA (Ketamine Advocacy Network, 2015; Ketamine Wellness Centres, 2018). It costs roughly £200 per ketamine infusion in the UK; following an initial £150 consultancy fee for a clinical psychiatric assessment (Oxford Health, 2017). Whereas in the USA, ketamine infusions cost between $400-$800 depending on the clinic (Portland Ketamine Clinic, n.d.; Ketamine Health Centres, n.d.; NY Ketamine Infusions LLC, 2018; Ketamine Advocacy Network, 2015; Ketamine Wellness Centres, 2018).

With an initial proposed treatment regime of 6 infusions over 2-3 weeks this type of therapy can get expensive quickly; costing over £1,200 in the UK and $2400-$4800 in the USA (NY Ketamine Infusions LLC, 2018; Portland Ketamine Clinic, n.d.; Ketamine Health Centres, n.d.). There is also no guarantee that 6 infusions are enough to keep symptoms of depression at bay and follow up booster infusions are recommended every 3-5 weeks (Oxford Health, 2017; Portland Ketamine Clinic, n.d.).

It is my opinion that such high costs for specialised treatment may lead patients to seek cheaper and more readily available alternatives, such as "street" ketamine. At £20-£30 per gram "street" ketamine is a far cheaper alternative compared to infusions at a clinic. Furthermore, "street" ketamine is readily available from your local drug dealer and this form of ketamine powder is arguably easier to obtain off the street than ketamine infusions are following appointments for psychiatric assessment, clinical diagnosis and treatment at a clinic (Discussions with regular ketamine users in London (UK), 2015-2018).

An obvious concern for public health in my opinion is that if patients with depression choose to self-medicate with "street" ketamine they run the risk of misusing the drug; taking too high a dose too frequently and potentially becoming addicted to the psychotropic effects of the drug (Zhu *et al.*, 2016; Sanacora *et al.*, 2017; Wilkinson *et al.*, 2017; Canuso *et al.*, 2018). Indeed, an example of this can be seen in the literature: a case study of a man prescribed intranasal ketamine to treat his depression found that he was overusing. The man was prescribed 70-150mg every 4 hours as needed but self-reported taking higher doses up to 12 times a day. The man reported doing this as ketamine was the only drug that had ever helped with his depression (Schak *et al.*, 2016).

Furthermore, there is a paucity of studies and/or clinical trials which have investigated the long term effects and/or safety profile of ketamine treatment for depression (Melvyn W. Zhang, Harris and Ho, 2016; Zhu *et al.*, 2016; Singh *et al.*, 2017b). This is an issue which has recently been reviewed in depth by Short et al (2017). In their paper Short and colleagues analysed 60 clinical trial studies, including 899 study participants, for their assessment of the safety profile and side effects of ketamine infusions for treatment resistant depression. The authors highlight the following:

- 55 (of 60) studies reported on the short-term immediate side effects of ketamine following infusion but fail to follow this up at later time points. The main side effects reported include headaches, dizziness, dissociation, increased blood pressure, blurred vision, nausea, drowsiness, anxiety elevated heart rate and difficulty concentrating (Short *et al.*, 2017). These side effects also desist shortly after the infusion.
- Only 12 (of 60) studies reported on the long-term side effects but reporting was ad-hoc and there was no enough data to conclude on the risks of cognitive impairment, drug dependency and systemic damage (e.g. urinary tract damage / structural, functional and metabolic brain alterations). Furthermore, no long-term psychotropic side effects were reported on (Short *et al.*, 2017).

Short et al (2017) conclude that more investigations into the long-term effects of ketamine infusions are required to confidently state whether this drug should be continued as a treatment for depression. This is a conclusion shared by many in the field (Feifel, 2016; Melvyn W Zhang, Harris and Ho, 2016; Sanacora *et al.*, 2017; Singh *et al.*, 2017b, 2017a).

As well as a need to better understand the long-term effects of ketamine at clinical doses, I would argue that we also need to better understand the effects of ketamine at doses evident of misuse / overuse. The reason being that, as previously mentioned, people may choose to self-medicate with "street" ketamine as a cheaper and more easily attainable substitute to ketamine infusions offered by specialist clinics. Of interest to me is understanding the potential impact of repeat ketamine use (at higher than clinical doses, >0.05mg/kg) on brain structure, function and metabolism.

In the next section I will provide an overview of the current literature on how repeat ketamine use effects brain structure, function and metabolism in humans.

1.5 Structural, functional and metabolic effects of ketamine on the brain

Attempts to understand the structural, functional and metabolic effects of ketamine on the brain have been performed using structural magnetic resonance imaging (sMRI), functional magnetic resonance imaging (fMRI) and proton magnetic resonance spectroscopy (^{1}H-MRS).

a) Functional brain alterations under ketamine

fMRI is a technique used to study the brain's intrinsic functional organization, i.e. how the brain works (Fornito, Zalesky, & Breakspear, 2015). Studies of resting state functional brain activity in the absence of any specific task (rs-fMRI) have shown changes in activity within the prefrontal cortex following a single (acute) infusion of ketamine in healthy individuals (Honey *et al.*, 2004, 2008; Deakin *et al.*, 2008; De Simoni *et al.*, 2013; Doyle *et al.*, 2013a; Driesen, McCarthy and Bhagwagar, 2013). Such changes in acute studies have also been shown to correlate with psychotic symptoms and cognitive deficits often seen in schizophrenic patients (Deakin et al., 2008; N. Driesen, McCarthy, & Bhagwagar, 2013; G. D. Honey et al., 2008; R. a E. Honey et al., 2004). Furthermore, these changes have been shown to correlate with psychotic symptoms (at a sub-threshold level for clinical diagnosis) and cognitive deficits in healthy volunteers and patients with schizophrenia (Lahti, Holcomb, *et al.*, 1995; Lahti, Koffel, *et al.*, 1995; Lahti

et al., 1999, 2001). Another fMRI study by Stone and colleagues (2015) found that increased paracentral lobule activity, in healthy participants given a single ketamine infusion, correlated with self-reported perceptual distortions and delusions of thought.

Whilst the effects of single ketamine infusions on brain function have been studied in detail (Morgan and Curran, 2006; Bokor and Anderson, 2014; Sassano-Higgins *et al.*, 2016; Short *et al.*, 2018), in contrast, the effects of repeat (chronic) ketamine use on brain function remain mostly unexplored in humans. However, it is plausible to hypothesise that repeat ketamine use may continue to alter functional activity in a given brain region leading to prolonged psychotropic side effects.

One report from a Chinese cohort provides preliminary evidence for the effects of repeat ketamine use on functional activity: Liao and colleagues (2012) examined functional connectivity in ketamine-dependent individuals (n=41) compared to age-matched healthy controls (n=44). They found that functional connectivity was decreased in the right anterior cingulate cortex of ketamine users but increased in the left precentral gyrus. Increased connectivity in the left precentral gyrus also correlated negatively with both estimated lifetime ketamine consumption and indices of ketamine craving. This suggests a potential relationship between left precentral gyrus function and ketamine addiction (Liao *et al.*, 2012).

The localisation of functional changes in the anterior cingulate cortex (ACC) resonates with previous rs-fMRI studies in users of other psychotropic drugs such as opioids, nicotine and alcohol, but the direction of change is opposite in ketamine users, who show a decrease, rather than increase as reported for these other drugs (Ma, Tai and Leung, 2012). This is potentially important, in light of meta-analytical evidence suggesting the presence of decreased functional connectivity in the ACC in both individuals at ultra-high risk for psychosis and in the first episode of psychosis (Fusar-Poli *et al.*, 2012; Cooper *et al.*, 2014). Speculatively, ketamine may therefore lead to brain dysfunction that closely recapitulates psychotic disorders when used repeatedly (Liao et al., 2012). Moreover, the ACC represents part of a brain network involving the frontal cortex that is critical for emotional aspects of behaviour, decision-making, response selection, and general cognition (Allman *et al.*, 2001; Kennerley *et al.*, 2006; Walton *et al.*, 2007; Kennerley and Wallis, 2009; Shackman *et al.*, 2011). Decreases in ACC functional activity may therefore be consistent with the negative impact of

ketamine on cognition and executive function (Moghaddam *et al.*, 1997; Liao *et al.*, 2011).

More recently, a second study by Morgan and colleagues examined repeat ketamine use and the impairment of spatial memory processing (Morgan *et al.*, 2014). By comparing frequent ketamine users (n=11) to poly-drug control subjects (users of multiple other psychotropic drugs, n=15) in a virtual reality task of spatial memory they found ketamine users to have spatial memory deficits. fMRI data collected during the task revealed that spatial memory deficits in ketamine users were associated with decreased activation (i.e. less neural activity) in the right hippocampus and left parahippocampal gyrus during a navigation task. The authors also found a similar association in decreased activity in the left caudate nucleus during updating of spatial memory. Clinical observations further found that frequent ketamine users exhibited schizotypal symptoms (symptoms like those present in schizophrenia) and dissociation, which were correlated to lower levels of hippocampal activation.

Taken together the above two repeat ketamine studies provide evidence to suggest that repeat ketamine use causes alterations in neural network activity and brain activation, particularly in the frontal lobe and in the medial temporal lobe. The location of functional alterations in the frontal cortex of repeat ketamine users appear to partially overlap with those seen in healthy individuals given a single ketamine infusion. It is tempting then to speculate that acute neural plasticity changes induced by ketamine manifest into enduring disruptions in functional brain activity upon repeated usage. In turn, these changes may relate to impaired cognition and schizophrenia-like symptoms in repeat users.

b) Metabolic brain alterations under ketamine

Alongside fMRI, proton magnetic resonance spectroscopy (^{1}H-MRS) has been used to examine the neurochemical changes which arise through ketamine use. ^{1}H-MRS is a non-invasive technique used to examine the neurochemistry of the living brain. Altered neurochemistry of the brain can indirectly indicate altered structure and function (Gujar *et al.*, 2005)

Three reports describe glutamate metabolite estimation with ^{1}H-MRS following single ketamine administration in humans. One reported increased anterior cingulate glutamine (Rowland *et al.*, 2005), one reported increased anterior cingulate glutamate (Stone *et al.*, 2012), and one reported no change in anterior cingulate glutamate + glutamine levels (Taylor *et al.*, 2012). None of these studies reported any change in N-acetyl-aspartate (NAA), a commonly used marker of neural activity and/or integrity, following acute ketamine treatment.

Until recently, there were no ^{1}H-MRS studies in repeat ketamine users. However, Stone and colleagues (2014) recently reported 1H-MRS data from ketamine users (n=15) as compared to poly-drug controls (n=13). The ketamine users, although not well matched for amphetamine use, displayed significantly greater severity of sub-threshold psychotic symptoms, assessed using the Comprehensive Assessment of At-Risk Mental State (CAARMS) (Yung *et al.*, 2005. Ketamine users had significantly lower levels of thalamic NAA (scaled to creatine), but there were no significant group-level differences in either NAA, glutamate or glutamine (all scaled to creatine) in either the medial temporal lobe or anterior cingulate cortex (Stone *et al.*, 2014). Anterior cingulate glutamate levels were positively correlated to the severity of abnormal perceptions measured using CAARMS, although this did not survive correction for multiple comparisons (Stone *et al.*, 2014).

These data are broadly in line with 1H-MRS findings in patients with schizophrenia. Recent meta-analyses suggest schizophrenia is associated with both psychotic state and age-dependent decreases in NAA (Brugger *et al.*, 2011), and glutamate (Marsman *et al.*, 2013). Specifically, reductions in NAA have been reported in the thalamus of individuals at high clinical or genetic risk of psychosis, leading to more widespread reductions in patients with chronic schizophrenia, including the frontal cortex (Steen, Hamer and Lieberman, 2005; Brugger *et al.*, 2011). Reports of changes in glutamate are more variable, but there is evidence to support age-related decreases in the frontal cortex, that may be more pronounced in chronic schizophrenia patients. In contrast, 1H-MRS studies in individuals at high clinical or genetic risk for schizophrenia, or patients in their first episode of psychosis have suggested higher levels of glutamate, particularly in the medial prefrontal cortex (Bartha *et al.*, 1997; Théberge *et al.*, 2004; Stone *et al.*, 2009; Marsman *et al.*, 2013); although some studies found no difference (Wood *et al.*, 2007; Yoo *et al.*, 2009).

How these neurochemical data relate to the effects of ketamine remains unclear, but it is interesting to note that ^{1}H-MRS studies have generally reported decreases in either NAA or glutamate in those individuals dependent on alcohol (Jagannathan, Desai and Raghunathan, 1996; Parks *et al.*, 2002), opiates (Haselhorst *et al.*, 2002; Yücel *et al.*, 2007) and methamphetamine (Ernst *et al.*, 2000; Biswal *et al.*, 2010; Howells *et al.*, 2014).

c) Structural brain alterations under ketamine

Like functional and metabolic changes described in fMRI and ^{1}H-MRS studies, little is known about any structural changes to the brain which might arise through repeat ketamine use. To my knowledge only four such studies exist in the literature:

In the same Chinese cohort in whom the fMRI analyses were conducted, Liao and colleagues (2011) reported voxel-based morphometry (VBM) (John Ashburner and Friston, 2000; Giuliani *et al.*, 2005) analysis of the brain of ketamine-dependent users (n=41) versus age-matched healthy controls (n=44). VBM is a method for analysing differences in brain volume between two distinct groups, as measured using MRI (John Ashburner and Friston, 2000). As with the fMRI dataset, subjects were excluded if they met criteria for dependence on other substances, but not nicotine dependence (Liao *et al.*, 2011). Subjects were required to abstain from ketamine for at least 48 hours and nicotine for at least 12 hours before scanning and from other psychoactive substances for at least 2 weeks. Ketamine-dependent subjects displayed significant ($p<0.05$ Family Wise Error rate corrected) clusters (minimum voxel size = 100) of reduced grey matter volume in the left superior frontal cortex and right middle frontal cortex, as compared to controls. These apparent reductions in grey matter volume in both frontal cortex regions were negatively correlated with the duration of ketamine use, and the reduction in left superior frontal gyrus volume was negatively correlated with estimated total lifetime ketamine consumption (Liao *et al.*, 2011). These structural changes appear to be consistent, at least in the direction of change, with observations reported from studies of brain morphometry in heroin and cocaine dependent-users (Lim *et al.*, 2008; Liu *et al.*, 2009), but strikingly, also in those with nicotine (Li *et al.*, 2015) and/or alcohol dependence (Grodin *et al.,* 2013). Notably, ketamine-dependent users were significantly

impaired in tests of executive function, but no explicit correlations were made between these data and the results of the VBM analysis (Liao *et al.*, 2011). Nevertheless, these data suggest that the functional abnormalities that occur in the frontal cortex of repeat ketamine users are accompanied by structural alterations, which may be related to cognitive impairments in these individuals.

In a second, independent Chinese cohort of ketamine addicts (n=21) compared to a very small number of healthy controls (n=3), Wang and colleagues (2013) reported on signs of cortical atrophy and hyperintense lesions in numerous brain regions, including the cortex, superficial white matter, striatum and brainstem (Wang *et al.*, 2013). The density and size of these lesions increased in proportion to the amount of (self-reported) ketamine consumption and duration of ketamine use, although no statistical correlations were performed and the assessment of lesions was entirely qualitative (Wang *et al.*, 2013).

In addition to the Wang et al (2013) study, white matter changes in repeat ketamine users have been observed in diffusion tensor imaging (DTI) studies.

DTI is a non-invasive MRI technique used to quantify structural changes in white (and grey) matter structure. This is based on changes to water diffusion in neural tissue (Le Bihan *et al.*, 2001). DTI is based on the assumption that water molecules preferentially diffuse along axonal fibre bundles as opposed to across them (i.e. the path of least residence) (Mori and Zhang, 2006; Walhovd, Johansen-Berg and Karadottir, 2014). The diffusion of tissue water in a given neural tissue voxel is comprised primarily of axial diffusion (AD), which runs parallel to the axonal fibres. Secondary and tertiary diffusion run orthogonally to axonal fibres and are averaged together to calculate radial diffusivity (RD). These diffusivity measurements (axial diffusivity and radial diffusivity) can be combined and averaged to give a value of mean diffusivity (MD) or fractional anisotropy (FA). Values of FA range from 0 (isotropic); water molecules have the same likelihood to diffuse in all directions, to 1 (anisotropic); water molecules tend to diffuse in a single direction.

In MRI voxels of the brain containing densely myelinated axon fibres, such as the corpus callosum and anterior commissure FA values are very close to 1 and axial diffusivity is high, suggesting that water preferentially diffuses along these fibres as opposed to

across the fibres. It is thought that disruption to myelination or damage to axons will allow water molecules to move freely in more directions (closer to anisotropic diffusion), resulting in lower axial diffusion and decreased FA (Concha, 2014). There is also some evidence to suggest that radial diffusivity may be related to the degree of myelination, whereas axial diffusivity may be more closely related to the level of axonal density (Song *et al.*, 2003, 2005). Therefore, by examining radial and axial components separately, this may provide more detailed information about the structural basis for any differences observed.

In repeat ketamine users white matter structural alterations have been observed by Liao and colleagues (2010), this is in the same cohort of repeat ketamine users (n=41) from which fMRI and VBM abnormalities were previously reported (Liao *et al.*, 2011, 2012). In the DTI study, voxel-wise analysis of the white matter revealed bilateral reductions in FA in the frontal and left temporoparietal cortices, as compared to control subjects, suggesting altered brain structure in these regions (Liao *et al.*, 2010). Furthermore, frontal cortex white matter FA values were negatively correlated with the severity of ketamine use (measured by estimated total ketamine consumption). However, there were no significant correlations between FA values and the age of onset of ketamine use, perhaps suggesting that the white matter changes reflect cumulative use (Liao *et al.*, 2010).

As with the fMRI and VBM findings, these white matter alterations following repeat ketamine use parallel similar observations in other forms of repeat drug use (Goldstein and Volkow, 2002): Bilateral frontal cortex white matter FA alterations have been reported in alcoholics (Pfefferbaum *et al.*, 2009) as well as amphetamine (Thompson, 2004), methamphetamine (Alicata *et al.*, 2009), cannabis (Arnone *et al.*, 2008), heroin (Liu *et al.*, 2008) and nicotine dependent individuals (Wang *et al.*, 2009). These white matter changes overlap remarkably with reports of white matter changes in the frontal lobe of individuals at high-risk of psychosis and who subsequently transitioned to psychosis (Muñoz Maniega *et al.*, 2008; Bloemen *et al.*, 2010), in first episode psychosis patients prior to antipsychotic medication (Cheung *et al.*, 2008; Reis Marques *et al.*, 2014) and in chronic patients receiving antipsychotic medication (Pomarol-Clotet *et al.*, 2010). However, there were no significant correlations between lower FA values and

ketamine-associated symptoms (hallucinations, dissociation, sleep disturbances or schizophrenia-like symptoms) in the repeat ketamine users (Liao *et al.*, 2010).

Therefore, whilst these findings suggest that ketamine use is clearly associated with alterations in white matter structure, they do not support a relationship with psychotic or schizophrenia-like symptoms.

A second DTI study by Roberts and colleagues (2014) compared repeat ketamine users (n=16) and poly-drug controls (n=16). They found significant clusters of altered white matter structure (reduced axial diffusivity) in the frontal, parietal and somatosensory cortices. No differences in radial diffusivity were reported and the decreases in axial diffusivity were not significantly correlated to any measure of ketamine use or consumption (Edward Roberts *et al.*, 2014). However, there was a significant positive correlation between dissociative symptoms in ketamine users and caudate–prefrontal cortex connectivity in the right hemisphere. These data partially concur with the findings of Liao and colleagues (2010) and show that the white matter underlying the frontal cortex is an area of structural alteration following repeat ketamine use.

1.6 Limitations of human neuroimaging studies in repeat ketamine users

Taken together, although the number of studies is sparse, the results of fMRI, sMRI and ^{1}H-MRS studies converge to suggest that repeat ketamine use leads to distinct alterations in brain structure and function. Specifically in the frontal lobe, repeat ketamine use leads to perturbations in brain function (Liao *et al.*, 2012) which are accompanied by decreases in grey matter volume (Liao *et al.*, 2011; Wang *et al.*, 2013) and alterations in white matter structure (Liao *et al.*, 2010; Edward Roberts *et al.*, 2014). However, one should perhaps be cautious in making too many conclusions since there have been very few neuroimaging studies of repeat ketamine users; three of which come from one cohort (Liao *et al.*, 2010, 2011, 2012). As such, they all suffer from several limitations.

Ketamine users, across the available studies tend to take a variety of other psychotropic drugs. In the studies of Liao and colleagues (Liao *et al.*, 2010, 2011, 2012) ketamine-dependent individuals were not compared to poly-drug user controls, moreover, nicotine-dependent subjects were not excluded and there were differences in the levels of education between the ketamine users and the controls. The study by Wang and colleagues (2013) did not robustly control for these variables and had a very small control group for comparison (n=3). Subsequent studies have improved on this design by comparing ketamine users to poly-drug user controls, which are well matched for levels of education (Edward Roberts *et al.*, 2014; Morgan *et al.*, 2014; Stone *et al.*, 2014). However, it is extremely difficult to find individuals that have exclusively used more ketamine, as compared to other drugs. For example, in the sample analysed using ^{1}H-MRS by Stone and colleagues (2014), ketamine users were not well matched for amphetamine use. This difficulty in finding suitable subjects is reflected in the smaller sample sizes reported in these studies, which may potentially reduce statistical power to detect subtle effects.

Importantly, as discussed earlier, many of the other drugs used by ketamine users have been shown to impact on brain structure and function in similar ways to ketamine. Furthermore, drugs such as nicotine and alcohol have been shown to impact on the effects that other drugs have on the brain. For example, a recent study of cannabis users provides clear evidence that when cannabis users are compared to controls, there is a

distinct influence of co-morbid alcohol use on the directionality and effect size of the structural MRI results (Weiland *et al.*, 2015). In addition, across the available repeat ketamine studies there is considerable variance in the frequency of use and the amount of ketamine consumed. Whilst some studies find evidence for correlations between brain structural and functional alterations and lifetime ketamine consumption (Liao *et al.*, 2010, 2011, 2012), others do not (Edward Roberts et al., 2014; James M Stone et al., 2014). Lastly, these studies cannot definitively rule out that the neuroimaging abnormalities observed in ketamine users do not represent pre-existing differences related to genetic or other environmental factors, as has recently been suggested for cannabis use (French *et al.*, 2015; Pagliaccio *et al.*, 2015). Together, these caveats render it extremely difficult to precisely infer the effects of ketamine alone in these individuals.

One potential approach to address these limitations is to apply the same neuroimaging methods to rodents, where the timing, dose and duration of ketamine administration, as well as the background genetics and housing environment may be strictly controlled. This translational approach has several advantages (Finlay, Duty and Vernon, 2014). First, the effects of ketamine may be precisely modelled and studied using comparable methods in the absence of additional variables that are associated with human studies (e.g. other drug use). Second and perhaps more importantly, because rodent models permit invasive post-mortem investigations at the cellular and molecular level, the biological correlates of MRI signals altered by ketamine exposure may be investigated to reveal the underlying mechanisms. The power of this approach is exemplified by studies linking the effects of antipsychotic drugs on brain imaging to neuropathological changes at the cellular level, as well as the effects of therapeutic interventions in disease models (Vernon *et al.*, 2011, 2012; Finlay, Duty and Vernon, 2014; Harrison *et al.*, 2015).

1.7 Alterations in neuronal structure and function following repeat ketamine exposure in rodents

The idea to examine the pathophysiology of repeat ketamine exposure in rodent models is not a new one and there already exists a wealth of literature upon this topic. However, there are two important limitations which apply to these data. First, very few studies have employed a translational approach to link neuroimaging signals to neuropathological changes, although there are notable exceptions (Kim *et al.*, 2012; Schobel, Chaudhury and Khan, 2013). Second, the majority of rodent studies on ketamine, including those using MRI, have focussed principally on neuronal elements at the expense of other central nervous system (CNS) components, including astrocytes, oligodendrocytes, myelin, microglia and the vasculature, all of which may contribute to MRI-detectable alterations in either brain structure or function (Zatorre, Fields and Johansen-Berg, 2012; Finlay, Duty and Vernon, 2014). Nevertheless, these pre-existing studies have revealed important observations that are worth brief discussion.

A consistent finding from rodent studies following both single and repeat ketamine administration is a marked reduction in parvalbumin (a calcium binding protein) expression within γ-aminobutyric acid (GABA) interneurons of the prefrontal cortex and hippocampus (Keilhoff *et al.*, 2004; Behrens *et al.*, 2007; Zhang, Behrens and Lisman, 2008; Kittelberger *et al.*, 2012; Schobel, Chaudhury and Khan, 2013). Moreover, ketamine acting as an NMDA receptor antagonist, has been shown to preferentially inhibit parvalbumin positive interneurons in the prefrontal cortex (Quirk *et al.*, 2009) as well as reduce GAD67 levels (an isoform of glutamic acid decarboxylase, the rate limiting enzyme in GABA synthesis) within these cells. Unsurprisingly, these structural alterations to GABAergic interneurons are accompanied by parallel functional changes in hippocampal and cortical networks, probed using electroencephalography (EEG) and other electrophysiological methods (Zhang, Behrens and Lisman, 2008; Featherstone *et al.*, 2012, 2014; Kittelberger *et al.*, 2012; Hinman *et al.*, 2013). An example of this is decreased theta power in the hippocampus, which coincides with impairments in episodic memory encoding (Hinman *et al.*, 2013) and behavioural extinction learning (Featherstone *et al.*, 2012).

In addition to EEG and electrophysiological changes in the hippocampus, Schobel et al (2013) utilised fMRI to show that repeat intermittent ketamine administration in mice leads to increased functional activity in the hippocampus. In this study these fMRI changes predated atrophy of the hippocampus, as seen by sMRI and were brought about by ketamine induced increases in extracellular glutamate (Schobel, Chaudhury and Khan, 2013). Schobel et al (2013) also measured functional activity and atrophy of the hippocampus in a longitudinal study of individuals at high risk for psychosis; some of whom subsequently transitioned to psychosis during the follow up phase of the study. Interestingly, those individuals who went on to develop psychosis presented with the highest hippocampal activation. Again, these functional changes predated structural changes in hippocampal atrophy, as seen by structural MRI. It would appear then that structural and functional alterations, brought about by repeat ketamine administration in mice, may model some of the changes which occur in human subjects who go on to develop psychosis and suggest glutamate as a pathological driver of psychosis.

As discussed in preceding sections, ^{1}H-MRS studies in patients in their first episode of psychosis have also suggested higher levels of glutamate in the medial prefrontal cortex (Bartha *et al.*, 1997; Théberge *et al.*, 2004; Tibbo *et al.*, 2004; Stone *et al.*, 2009; Marsman *et al.*, 2013). Single ketamine infusions in healthy volunteers have shown increases in glutamate and glutamine levels in the prefrontal cortex (Rowland *et al.*, 2005; Stone *et al.*, 2012), although no studies have reported similar findings in human repeat ketamine users. There is evidence, however, for increased glutamate levels in the prefrontal cortex of rats (Kim *et al.*, 2011a). In the study by Kim et al (2011), in-vivo ^{1}H-MRS and ex-vivo ^{1}H high-resolution magic angle spinning (HR-MAS) spectroscopy were used to assess glutamate levels in the medial prefrontal cortex of rats repeatedly administered ketamine. Both ^{1}H-MRS and HR-MAS spectroscopy demonstrated an increase in glutamate levels in the prefrontal cortex of ketamine administered rats. Furthermore, ex-vivo high resolution mass spectroscopy revealed a decrease in the ratio of glutamate: glutamine, which may suggest altered glutamate-glutamine cycling between neurons and astrocytes (Kim *et al.*, 2011a), something which has not been pursued further.

Taken together then, the functional changes in the brain that occur under repeat ketamine administration, appear to be initiated by local increases in extracellular

glutamate levels which may stem from changes to GABAergic interneurons and a suppressed inhibitory neurotransmitter system. Indeed, evidence from acute ketamine studies demonstrates that reductions in parvalbumin and GAD67 expression, in the prefrontal cortex and hippocampus, are related to reductions in miniature post-synaptic current (mIPSC) amplitude and frequency in layer 5 projection neurons, as well as increased extracellular glutamate levels (Zhang, Behrens and Lisman, 2008; Wang *et al.*, 2014). Furthermore, these changes reflect a model of glutamate disinhibition brought about by dysfunctional GABAergic interneurons. This model suggests that the preferential inhibition of GABAergic interneurons in the cortex and hippocampus leads to disinhibition of glutamatergic projection neurons and subsequently impaired regulation of the activity of these projection neurons (Anticevic *et al.*, 2013; Frohlich and Van Horn, 2014; Heckers and Konradi, 2014).

Whilst these are important findings, there remains a relative paucity of published data on cellular changes that may occur to glial cells and/or myelin because of repeat ketamine administration. This is somewhat surprising given the significantly higher proportions of glia to neurons in the CNS and the critical role these cells play in plasticity, regulating neural transmission and monitoring the neuropil (Eroglu and Barres, 2010; Eyo and Dailey, 2013; Pajevic, Basser and Fields, 2014; Wang and Young, 2014; Chung, Allen and Eroglu, 2015; Gundersen, Storm-Mathisen and Bergersen, 2015; Khakh and Sofroniew, 2015; Wu *et al.*, 2015). Moreover, this represents a significant gap in our knowledge of the cellular effects of ketamine that contribute to alterations in brain structure and function following repeat use. In the following sections I shall discuss the importance of glia and myelin in the CNS and speculate on how they may be impacted by repeat ketamine exposure.

1.8 The importance of myelin and oligodendrocyte integrity

Myelin is a membranous sheath consisting of various lipids and proteins (Schmitt, Cantuti Castelvetri and Simons, 2014), which wraps around axons in a spiral-like fashion, and alongside oligodendrocytes, fibrous astrocytes and microglia, forms the white matter. Axons are myelinated by several oligodendrocytes which each myelinate a small stretch of the axon. Each myelinated portion of the axon is known as an internode and the gap between myelinated regions a node of Ranvier. Not all neurons in the brain have myelinated axons, for example only 28% of axons in the mouse corpus callosum are myelinated (Sturrock) compared to 98.8% in the optic nerve (Honjin, Sakato and Yamashita, 1977). Similarly, the degree of myelination along axons differs between neurons in a particular region (Tomassy *et al.*, 2014). The dense lipid nature of myelin causes it to act as a barrier against the diffusion of ions, which may only diffuse across the axonal membrane at nodes of Ranvier. This means that during action potential (AP) propagation along the axon, ions carry the AP further down the axon before diffusing across the membrane. This phenomenon is known as saltatory conduction and facilitates rapid, energy efficient, conduction along the axon (Harris and Attwell, 2012).

Myelination, the elaboration of myelin surrounding neuronal axons, is essential for normal brain function. The development of the myelin sheath enables rapid synchronized communication between the neural systems responsible for higher order cognitive functioning. The importance of this is highlighted in thalamocortical neurons, which relay sensory signals from the thalamus to different cortical areas. Different cortical areas are different distances away from the thalamus, thus signals arising from thalamocortical neurons tend to travel over different distances on their way to the cortex. As these signals enter the cortex, they tend to travel similar distances to their target. However, signals arriving in different cortical areas do so within a narrow time window of each other, roughly 2ms. This is possibly due to greater myelination of axons in the thalamus and in white matter tracts leading to cortex than within the cortex itself. Such regional myelination facilitates rapid conduction of action potentials along longer axons, which travel greater distances to their cortical terminus. This selective myelination of longer axons allows for synchronous information processing across the thalamocortical network (Salami *et al.*, 2003).

Any disruption to myelin integrity would therefore be predicted to radically alter the synchronicity of neural networks. This prediction is confirmed by the findings of Kim et al (Kim, Renden and von Gersdorff, 2013) at the calyx of held synapse, in the ascending auditory pathway. Here the exact timing of incoming signals is crucial for computing sound source localisation. In a genetically altered rat model that lacks compacted myelin, there are inconsistencies in the reliability of action potentials arriving at the synapse at specific times. Thus, disruption to myelination would lead to alterations in signalling within neural networks. A similar example can be seen in the olivary nuclei (of the medulla) and Purkinje cells (of the cerebellum). In these pathways synchronous activity is important for coordinating the timing of voluntary movement. Lang and Rosenbluth (2003) found that disrupted myelination in this neural network decreased the conduction velocity of signals from the olivary nuclei and led to desynchronous activity across the network (Lang and Rosenbluth, 2003). Hence, correct myelination is important for the synchronous activity of neurons within neural networks (Vicente *et al.*, 2008; Pajevic, Basser and Fields, 2014).

Damage to white matter and myelin integrity and subsequent disruptions to neural network activity is highly likely then to have adverse functional consequences on behaviour. Indeed, impaired white matter and myelin integrity has shown to be present in schizophrenia, bipolar depression, major depression and neurodegenerative disorders such as multiple sclerosis and Alzheimer disease (Fields, 2008; Nave, 2010; Yu *et al.*, 2012; Mighdoll *et al.*, 2014). More specifically, DTI studies in both schizophrenic and psychosis patients have shown that decreased FA values and increased diffusivity within white matter tracts of the frontal and parietal lobes are correlated with psychosis (Garver, Holcomb and Christensen, 2008) and negative symptom severity (Peters *et al.*, 2013). Furthermore, reduced FA values in psychotic patients not only correlate with the severity of negative symptoms, but also with a decrease in plasma levels of polyunsaturated fatty acids (Peters *et al.*, 2013). As polyunsaturated fatty acids are necessary for myelin formation this would suggest a correlation between myelin impairment and negative symptom severity. Furthermore, reductions in FA values across the brain have been linked to cognitive impairments in traumatic brain injury, multiple sclerosis, ischemia and stroke (Kraus *et al.*, 2007; Sigal *et al.*, 2012; Sierra, 2014). Alongside neuroimaging data, myelin and oligodendrocyte deficits have been reported

from post-mortem brain samples from schizophrenia and depressed patients (Hof *et al.*, 2003; Uranova *et al.*, 2004; Byne *et al.*, 2006; Regenold *et al.*, 2007; Parlapani *et al.*, 2009; Takahashi *et al.*, 2011). Similarly, altered myelin and oligodendrocyte integrity has been linked to impairments in spatial working memory, recognition, social interaction and anxiety in rodents (Makinodan *et al.*, 2009, 2012; Tanaka *et al.*, 2009; Xu *et al.*, 2009; Liu *et al.*, 2012; Blasi *et al.*, 2014). Clearly then, correct myelination is vital for functional brain activity and alterations to myelin structure can lead to cognitive and/or emotional changes.

As discussed in previous sections, repeat ketamine use has been shown to alter white matter structure in the frontal lobe (Liao *et al.*, 2010; Edward Roberts *et al.*, 2014). One might speculate then, that this is the result of altered myelin structure and this alteration might contribute to cognitive and behavioural changes. However, altered myelin structure is just one of many possible cellular correlates of changing values in DTI parameters such as FA and AD. Other potential cellular correlates include changes in axonal size, density, and membrane structure; lipid, protein, and macromolecule content; and water compartmentalization or a combination of these events (Deoni *et al.*, 2008; Almeida and Lyons, 2017; Stolp *et al.*, 2018). Consequently, in the absence of post-mortem findings, the observed DTI signal changes in repeat ketamine users are ambiguous, hindering meaningful inferences between imaging findings, cellular correlates and changes to cognition and behaviour.

To the best of my knowledge, there are no published animal studies which have investigated specifically the effects of ketamine administration on oligodendrocytes and myelin. There are, however, five studies which have investigated the effects of repeat administration of more potent NMDA receptor antagonists on oligodendrocytes and myelin, which provide useful generalisations. Two of these studies investigated the neurodevelopmental effects of early phencyclidine (PCP) administration on white matter integrity (Lindahl *et al.*, 2008; R. Zhang *et al.*, 2012). Whereas the other three studies investigated the effect of chronic dizocilpine (MK-801) administration on white matter integrity (Xiu *et al.*, 2014, 2015; Wu *et al.*, 2016).

PCP and MK-801, like ketamine, are NMDA-receptor antagonists which act in the same manner to antagonize these receptors (Morris, Cochran and Pratt, 2005; Lim, Taylor and Malone, 2012; Blot, Bai and Otani, 2013; Steeds, Carhart-Harris and Stone, 2014). All three antagonists bind within the ion channel pore of the NMDA receptor and ultimately prevent the flow of ions across the receptor (Foster and Fagg, 1987). MK-801 has greater affinity for the NMDA receptor than PCP, which in turn is more potent than ketamine (Daniell, 1990).

The first PCP study conducted by Lindahl et al (2008) investigated the effects of daily intraperitoneal (IP) administration of 10mg/kg PCP in pregnant rats, starting from conception to embryonic day 20, relative to measurements in control mice whose mothers received daily injections of saline during pregnancy. Using a combination of western blotting and thresholding analysis of immunostained tissue sections, the authors found a reduction in NG2 positive oligodendrocyte precursor cells (OPCs) at post-natal day 2 (P2). At later stages; P16, P22 and P60, CNPase expression was also reduced. At all these stages the expression of myelin basic protein (MBP) was also reduced. As both markers of OPCs (NG2) and mature myelinating oligodendrocytes were reduced, but CNPase expression was increased, these results would suggest that exposure to PCP during embryonic development may delay oligodendrocyte maturation and subsequently lead to reduced levels of myelination at a given postnatal stage.

A second neonatal PCP study by Zhang et al (2012), also found reductions in the level of MBP as confirmed by western blot analysis and optical density measurements of MBP-stained tissue sections. These reductions were seen at P16, P22 and P32 in rats exposed to daily injections of PCP (10mg/kg; i.p.) during P2 to P14. Again, such results would suggest that early exposure to PCP leads to a maturational delay in oligodendrocyte development and myelination. The findings from these two studies are broadly consistent with the DTI findings from chronic ketamine users reported by Roberts et al (2014) and Liao et al (2010); in that administration of a non-competitive NMDA receptor leads to frontal white matter alteration.

In a study by Wu and colleagues (2016), MK-801 (0.2mg/kg) was systemically administered to adult mice for 14 consecutive days. Using DTI the authors found a significant impairments in the white matter of the corpus callosum (Wu *et al.*, 2016).

In an earlier study, Xiu et al (2014) administered MK-801 (1mg/kg) systemically to adult mice for 14 consecutive days and observed a reduction in the volume of the total white matter across the entire cerebrum, as measured by post-mortem stereology. Focussing on the corpus callosum, a significant decrease in white matter volume, MBP and CNPase expression and disrupted myelin architecture were all reported in these MK-801 treated mice. In a follow up study Xiu et al (2015) found that the myelinated fibres of the corpus callosum, of mice treated with MK-801, were impaired with splitting lamellae of myelin sheaths and segmental demyelination. Furthermore, the total length of the myelinated fibres in the corpus callosum significantly decreased when compared to those of the mice treated with saline (Xiu *et al.*, 2015).

Given that NMDA receptor antagonism induces changes in both myelination and expression of various cell markers across the oligodendrocyte lineage it is feasible to hypothesize that similar cellular changes may occur under repeat ketamine administration. If so, understanding such cellular changes will allow better interpretation of white matter perturbations seen in repeat ketamine users (Liao *et al.*, 2010; Edward Roberts *et al.*, 2014). In this context, pre-clinical studies directly linking neuroimaging findings to post-mortem histology have great potential.

1.9 Ketamine induced excitotoxicity and potential myelin damage?

If repeat ketamine administration does induce similar cellular changes in the white matter, as have been seen for PCP and MK-801, then the next logical question is what might be the mechanism responsible for such changes and how are myelination and/or oligodendrocyte lineage cells affected by ketamine. One potential mechanism might be glutamate excitotoxicity.

Like most cells containing surface NMDA receptors, oligodendrocytes and their progenitors are susceptible to excitotoxic damage (Matute, 2006). In vitro work has shown that excitotoxic levels of kainite, α-amino-3-hydroxy-5-methyl-4-isoxazolepropionic acid (AMPA) and glutamate cause reductions in the number of mature oligodendrocytes (Mcdonald, Althomsons and Hyrc, 1998; McDonald, Levine and Qu, 1998). Glutamatergic excitotoxicity in the optic nerve can trigger the

degradation of oligodendrocyte myelinating processes (Káradóttir *et al.*, 2005). Furthermore, glutamatergic excitotoxicity has been shown to cause the loss of myelin at paranodes, the initial region of myelination next to the node. This results in an increase in nodal length and exposes repolarizing kv1.2 channels to the neuropil. Together these changes contribute to a 'leakier' membrane along axons resulting in an action potential of lower amplitude and faster refractory period (Fu *et al.*, 2009). Taken together, it is clear how this pathological cascade, driven by excess glutamate would lead to myelin damage, impaired neuronal synchrony within networks and aberrant behaviour.

In support of a role for glutamate in NMDA antagonist mediated demyelination, ketamine administration is known to lead to an increase in prefrontal cortex glutamate levels in both humans (Stone, Dietrich and Edden, 2012; Wang *et al.*, 2014) and rodents (Kim *et al.*, 2011b; Wang *et al.*, 2014). It is therefore conceivable that glutamate spill over may occur at synapses (Danbolt, 2001). Excess glutamate may then bind to NMDA receptors expressed on oligodendrocytes and cause excitotoxic damage. Over time and with repeat ketamine use, this may lead to oligodendrocyte cell death and damage to myelin. Such changes in turn may alter neural network activity and subsequently lead to deficits in cognition and/or to the emergence of psychosis, delusions and memory impairments as seen in repeat ketamine users.

Evidence of possible NMDA receptor antagonist induced excitotoxicity can be seen in the study of Olney et al (1989). In this study the authors tested a variety of NMDA receptor antagonists (including MK-801, PCP and ketamine) for signs of neuronal pathology upon repeat administration. The authors found that a dose of 40mg/kg of ketamine induced vacuole formation in cortical projection neurons resident in layers III and IV of the cingulate cortex of Sprague Dawley rats (indicative of pathology). However, such indicators of pathology were not present with lower doses of ketamine (5mg/kg, 10mg/kg and 20mg/kg) (Olney, Labruyere and Price, 1989).

1.10 Ketamine-induced disruption of astrocytes function and disrupted neural network activity

Astrocytes, which exist in both the grey and white matter of the brain, regulate neuronal network activity through neurotransmitter uptake, metabolism and volume transmission (McKenna, 2007; Albrecht *et al.*, 2010; Domingues, Taylor and Fern, 2010; Pascual *et al.*, 2012). Yet surprisingly I could only find one study which examined the role of astrocyte pathophysiology following repeat exposure to ketamine. In this study, Featherstone et al (2012), administered daily injections of 20mg/kg ketamine to mice for 14 days. Six months later, the authors found a persistent alteration in hippocampal theta activity which correlated with an increase in the number of glial-fibrillary acidic protein (GFAP) positive astrocytes in this area as well as a 50% decrease in the number of excitatory amino acid transporter 2 (EAAT2) positive cells. EAAT2 is predominately found in astrocytes throughout the brain, where it is responsible for 95% of glutamate uptake from the synapse (Danbolt, 2001; Huang and Bergles, 2004; Zhou and Danbolt, 2013, 2014). Given the fact that there is no extracellular degradation of glutamate in the brain (Danbolt, 2001; Zhou and Danbolt, 2014), I think that it is feasible to suggest that a reduction in EAAT2 expression in mice, given repeat ketamine, may contribute to increased extracellular glutamate levels in the hippocampus. This in turn would likely contribute to altered neural network oscillations and subsequent cognitive deficits in this brain region. Furthermore, as mentioned earlier, repeat ketamine administration also increases the level of extracellular glutamate in the prefrontal cortex (Zhang, Behrens and Lisman, 2008; Wang *et al.*, 2014). Hence, a similar scenario may occur in the prefrontal cortex; whereby astrocyte EAAT2 expression is decreased and glutamate uptake is impaired leading to increased extracellular glutamate and disrupted neural network oscillations that lead to cognitive deficits.

Regarding astrocyte modulation of neurotransmitter levels, it has recently been shown that astrocytes may modulate hippocampal tonic inhibition by releasing GABA via reverse transport (Héja *et al.*, 2009, 2012): Under enhanced network activity glutamate uptake by astrocytes appears to be coupled to the reversal of GABA transporters (GAT) -2/3, which in turn leads to GABA release through GAT and increased tonic inhibition. Moreover, recent findings from the Alzheimer disease field have shown that reactive

GFAP positive astrocytes may respond to hyperactivity within a neuronal network by up-regulating the synthesis and release of GABA (Jo *et al.*, 2014; Wu *et al.*, 2014). This increased release of GABA from astrocytes further exacerbated excitatory versus inhibitory imbalances present in the hippocampus, which in turn was associated with cognitive memory impairments. Alongside GABA release, astrocytes may also release glutamate which can aid synchronize neural activity in the hippocampus (Angulo *et al.*, 2004; Fellin *et al.*, 2004; Volterra and Meldolesi, 2005).

GABAergic disinhibition and excitatory versus inhibitory activity imbalances exist in rodent models of repeat ketamine administration. Hence, astroglia neurotransmission and its effects on neural network oscillations may be another line of enquiry worth investigating to further understand the cellular effects of repeat ketamine administration on the brain.

In summary, due to the key role astrocytes play in the control of extracellular neurotransmitter levels, via reuptake and release, and in turn the regulation of neural network oscillations, it is important to investigate these cell types more systematically in models of repeat ketamine administration to understand better what is driving structural, functional and cognitive changes seen in recreational ketamine users.

1.11 Microglia

As far as I am aware only one paper, so far, has looked at microglia in a repeat model of ketamine administration (Hou *et al.*, 2013). In this model mice were administered 100mg/kg of ketamine once daily for seven days and the microglia population in the prefrontal cortex was investigated histologically. Here the authors found no change in the number of Iba-1 positive microglia in the prefrontal cortex. However, the authors did not use a stringent unbiased stereological method to investigate differences in microglia number (Cotel *et al.*, 2015). Furthermore, they did not differentiate between resting and activated microglia, which serve different functions in the brain (Benarroch, 2013). Iba-1 is a good histological marker for identifying microglia; however, Iba-1 antibodies will bind to and illuminate both resting and active microglia (Laskaris *et al.*, 2015). If the researchers did not differentiate between these subtypes of microglia by

morphology and counted all the Iba-1 positive microglia they may have missed subtle changes in the ratio of resting: activated microglia. Such a scenario is evident in a PCP study conducted by Zhu et al (2014). In this study mice were administered 20mg/kg of PCP once daily for 14 days and changes to the number of microglia investigated in both the hippocampus and prefrontal cortex (Zhu *et al.*, 2014). The authors found no difference in the number of microglia in either the hippocampus or prefrontal cortex by stereological assessment (optical fractionator) of Iba-1 positive cells. However, they did find a significant increase in the number of CD11b positive reactive microglia in the prefrontal cortex. Hence, by investigating subtypes of microglia the authors were able to find a distinction between PCP treated mice and controls. Closer inspection of cellular sub-populations may therefore reveal important cellular changes in a disease model which otherwise may be accidently overlooked. Since ketamine is a derivative of PCP and acts in a similar manner to block the NMDA receptors (Morris, Cochran and Pratt, 2005; Blot, Bai and Otani, 2013; Steeds, Carhart-Harris and Stone, 2014), closer inspection of microglial sub-populations under repeat ketamine administration may also reveal changes in the ratio of resting: activated microglia.

1.12 Potential relevance to the neurobiology of schizophrenia

As described in the preceding sections, ketamine users can experience schizophrenia-like symptoms (Krystal *et al.*, 1994; Morgan, Mofeez, *et al.*, 2004; Muetzelfeldt *et al.*, 2008). Furthermore, ketamine may worsen symptoms in schizophrenic patients (Lahti, Holcomb, *et al.*, 1995; Lahti, Koffel, *et al.*, 1995; Lahti *et al.*, 2001) and such findings suggest that repeat ketamine users and schizophrenics may share underlying neurological changes which give rise to their symptoms. Indeed, as we have described, ketamine users and schizophrenic patients show similar structural, functional and biochemical changes in the brain(Steen, Hamer and Lieberman, 2005; Muñoz Maniega *et al.*, 2008; Pomarol-Clotet *et al.*, 2010; Brugger *et al.*, 2011; Liao *et al.*, 2011, 2012; Fusar-Poli *et al.*, 2012; Marsman *et al.*, 2013; Cooper *et al.*, 2014; Stone *et al.*, 2014; Reis Marques *et al.*, 2014).

On a cellular level, similar pathological changes have been reported in both rodent models of repeat ketamine use and post-mortem brain tissue from schizophrenic patients. Most notably, parvalbumin expression is reduced in the prefrontal cortex and hippocampus of both rodent models and schizophrenia patients (Beasley and Reynolds, 1997; Bitanihirwe *et al.*, 2009; Lewis *et al.*, 2012; Glausier, Fish and Lewis, 2014; Enwright *et al.*, 2016). These findings and those which show that ketamine may induce schizophrenia-like symptoms have helped contribute to the NMDA receptor hypothesis in schizophrenia (Stone, Morrison and Pilowsky, 2007; Howes, McCutcheon and Stone, 2015). This hypothesis suggests that the preferential inhibition of NMDA receptors on GABAergic interneurons in the cortex and hippocampus leads to disinhibition of glutamatergic projection neurons, and subsequently to impaired regulation of the activity of these projection neurons. This in turn is thought to cause desynchronous neural network activity which may give rise to altered cognition and psychopathology (Gonzalez-Burgos and Lewis, 2012; Anticevic *et al.*, 2013; Frohlich and Van Horn, 2014; Heckers and Konradi, 2014).

However as discussed, neural networks in the brain do not only consist of neurons but also astrocytes, oligodendrocytes, myelin and microglia. Furthermore, if any of these constituents (or different multiple combinations of these cell types) are disrupted or damaged then neuronal integrity and/or functional activity may become compromised. If this occurs, then desynchronous neural network activity usually results and cognitive abilities deteriorate.

The current literature suggests that alterations to myelin, oligodendrocytes, astrocytes and microglia may contribute to altered brain activity in schizophrenia and to the subsequent development of symptoms of the disorder. As covering the schizophrenia literature in detail is beyond the scope of this introduction, I will only highlight a few changes here. Furthermore, several in-depth reviews on glia and myelin in schizophrenia can be found in the literature (Davis *et al.*, 2003; Segal *et al.*, 2007; Schnieder and Dwork, 2011; Takahashi *et al.*, 2011; Xia *et al.*, 2014; Laskaris *et al.*, 2015; Müller *et al.*, 2015).

Reductions in gene expression in several oligodendrocyte and myelin-related genes have been found in the prefrontal cortex and hippocampus of schizophrenia patients. Genetic association studies also link oligodendrocyte and myelin-related genes to the aetiology of schizophrenia. Furthermore, analyses of post-mortem brain tissue from

schizophrenic patients have revealed changes in oligodendrocyte cell density in the prefrontal cortex as well as altered myelin architecture. Similarly, genetic association studies have found links between astrocyte-related genes (e.g. EAAT2 (Spangaro *et al.*, 2012; Mariachiara and Bramanti, 2014)) and the aetiology of schizophrenia. Altered astrocyte gene expression (e.g. increased GFAP, decreased EAAT2) has also been shown to change in the prefrontal cortex and hippocampus of schizophrenia patients. Moreover, increases in the number of reactive microglia have been found in the prefrontal cortex of schizophrenia patients which correlate with increased expression of pro-inflammatory cytokines, such as IL-6 (Potvin *et al.*, 2008; Beumer *et al.*, 2012; Pedrini *et al.*, 2012; Song *et al.*, 2013), found in the blood. It would appear then that some of the glial changes seen in schizophrenia patients, such as decreased EAAT2 expression in the hippocampus and increased IL-6 concentrations in the blood plasma, mimic similar changes seen in repeat ketamine users (Fan *et al.*, 2015) and rodent models (Behrens, Ali and Dugan, 2008; Featherstone *et al.*, 2012).

There is a concern here then that if people suffering from depression choose to self-medicate with ketamine, they may unwillingly cause further psychopathological, structural and functional changes to the brain reflective of changes seen in schizophrenia.

1.13 Limitations of rodent studies

Despite the clear potential for rodent models to provide informative data linking neuroimaging signals to their cellular correlates in the context of drug use and psychiatric disorders, it is important to acknowledge that this approach is not without limitations.

An obvious limitation, yet worth stating, is that the rodent brain is far simpler than the human brain, particularly when it comes to cortical anatomy. Another major issue in any rodent study of human drug use is modelling the dosage and timing of drug administration, in a way that most accurately reflects the quantity and pattern of use seen in humans. This is perhaps best exemplified by rodent studies on the effects of 3,4-methylenedioxymethamphetamine (MDMA) (Green *et al.*, 2012). Drug dosages taken

by humans may only be approximated for rodents. Ketamine users, for example take (on average) between 0.125g - 3g of ketamine per day/night (Wang *et al.*, 2013; Edward Roberts *et al.*, 2014). An 70kg person taking 1g of ketamine would equate to a dose of 14.3mg/kg and this is sufficient to induce pathological changes in the brain (Wang *et al.*, 2013). In rodents, similar doses of (16mg/kg – 30mg/kg) also induce noticeable pathological changes (Sun *et al.*, 2011; Featherstone *et al.*, 2012; Schobel, Chaudhury and Khan, 2013)(Robert E Featherstone et al., 2012; Schobel et al., 2013; Sun et al., 2011). Hence, although an approximation, studies using doses of ketamine within this range may be considered to have some relevance to doses ketamine users are exposed to.

In parallel to dosage issues, the route of drug administration in humans and rodents is different. The most common way in which people take ketamine is to inhale it as a powder (De Luca *et al.*, 2012), whereas the most common way to administer ketamine to rodents is via systemic intraperitoneal (IP) injection (Keilhoff *et al.*, 2004; Zhang, Behrens and Lisman, 2008; Kittelberger *et al.*, 2012; Featherstone *et al.*, 2014). These routes of administration will clearly lead to different pharmacokinetic profiles of drug absorption thus altering how quickly and how much of a drug reaches its target receptor in the brain and how quickly it is metabolized and cleared from the system. Nasal absorption of ketamine in humans allows for direct entry of the drug into the CNS and delays first-pass metabolism in the liver. To date however, no studies have examined the effect of intranasal ketamine in rodents. A further, more important and often underappreciated difference between rodents and humans is that the former metabolize drugs faster and thus the half-life of drugs is often considerably shorter in rodents (Lin and Lu, 1997; Reagan-Shaw, Nihal and Ahmad, 2008; D. Zhang *et al.*, 2012). Furthermore, differing proportions of active metabolites may induce different side-effects in humans and rodents, as is seen in the case of MDMA metabolism (Green *et al.*, 2012).

Accepting these limitations, one may suggest that the most robust and translational approach is in fact to combine results from parallel human and animal imaging studies to formulate conclusions on the effects of certain drugs on changes to the structure and function of the brain, as exemplified in the work of Schobel and colleagues (2013). Human studies can inform us of the changes which occur in the brains of drug users.

Comparison of these data to animal studies, provided that due care is given to dose, timing and route of drug administration has the potential to provide important information as to what changes in the human users may be specific to ketamine. Moreover, they offer tractable means to map the cellular mechanisms, which underlie and drive the observed neuroimaging signals.

1.14 Conclusion

MRI data from repeat ketamine users compared to poly-drug controls is limited to very few studies, but these provide important insights into the neural correlates of ketamine misuse. These studies highlight structural changes in white matter, bilateral decreases in frontal lobe grey matter volume and biochemical changes in the thalamus and frontal cortex in ketamine users. Current human neuroimaging methods, however, lack enough resolution to reveal the biological mechanism driving these morphological changes at the cellular level.

Furthermore, human imaging studies are subject to several confounding influences which may affect interpretation of the data. Whilst there is considerable literature from rodent models of repeat ketamine treatment; documenting detailed post-mortem cellular and molecular measurements, these studies have focused principally on neuronal changes. Only a few studies (Kim *et al.*, 2012; Schobel, Chaudhury and Khan, 2013) have combined these assessments with translational small animal MRI methods. There remains a clear gap in our understanding of the impact of ketamine on both myelination and glial cells, and how this contributes to altered brain structure and activity and ultimately disordered behaviour in terms of cognitive impairments and sub-threshold psychotic symptoms.

Chapter 2 Grey matter volume reductions in repeat ketamine users

2.1 Introduction

As discussed in chapter 1 (general introduction); over the last 10-12 years ketamine has been used as an "off-label" therapy for treating patients who are resistant to conventional anti-depressant medication (AKA: treatment-resistant depression) and has been proven highly effective (Zarate and Singh, 2006; DiazGranados *et al.*, 2010; Lapidus *et al.*, 2014). However, this type of therapy is not a "one-off" treatment, rather patients may require several ketamine infusions to keep their depressed symptoms at bay (Diamond et al, 2014; NY Ketamine Infusions LLC, 2018; Portland Ketamine Clinic, n.d.; Ketamine Health Centres, n.d.).

As repeat ketamine use, particularly when taken at recreational doses (higher than clinical doses) has been shown to cause psychotropic effects, functional, metabolic and structural changes in the brain, there remains a question as to how safe repeat use of ketamine is as a therapy (Feifel, 2016; Melvyn W Zhang, Harris and Ho, 2016; Short *et al.*, 2017; Singh *et al.*, 2017b). This concern is reinforced by the potential that patients will opt to self-medicate with "street" ketamine as a cheaper and more readily available substitute to ketamine infusions at a specialised clinic. If people choose to self-medicate then there is a risk that they will use higher doses more frequently than would be prescribed through a clinic, which could have long-term psychiatric and neurological consequences.

As such, it is important to understand what changes may occur in the brain under repeat ketamine use at higher than clinical doses and what the potential changes in brain structure may be.

In the literature, recreational repeat ketamine use has been shown to cause reductions in brain volume in the frontal cortex, as seen by MRI (Liao *et al.*, 2011; Wang *et al.*, 2013). However, so far only two studies have published such results. To ascertain whether these results are true of repeat ketamine use in general, and not just to a small number of people, independent studies are needed to replicate these results. Therefore, in this chapter I present my analysis on the effects of repeat ketamine use, on brain structure, in recreational ketamine users versus poly-drug control subjects, as seen by structural MRI (sMRI).

2.2 Experimental aims and hypotheses

a) Hypotheses

1. Repeat ketamine users will present with significant reductions in brain volume in the frontal cortex, striatum, brainstem and cerebellum as seen in previous studies (Liao *et al.*, 2011; Wang *et al.*, 2013)
2. Reductions in brain volume in ketamine users will correlate with greater amounts of ketamine taken and / or more frequent ketamine use and / or a longer history of ketamine use
3. Ketamine users will score worse on tests of psychological wellbeing as seen in previously published studies (Liao *et al.*, 2011; Edward Roberts *et al.*, 2014; Morgan *et al.*, 2014)
4.

b) Aims

1. To investigate the effects of repeat ketamine, use on brain structure between human ketamine users and poly-drug-user controls, by analysing MRI volumetric differences across the whole brain. To compare my results to those seen in previously published independent studies and see whether previous findings have been replicated
2. To assess whether there is any correlation between either; the amount of ketamine taken, the frequency of ketamine consumption or the years of ketamine use with any changes in brain volume
3. To assess whether there are differences in measures of psychological wellbeing between ketamine users and controls
4. To assess whether there is any correlation between the amount of ketamine taken, the frequency of ketamine consumption or the years of ketamine use with scores of psychological wellbeing

2.3 Materials and methods

a) Participants

Recruitment of participants was performed by Professor Celia Morgan, University College London.

48 participants were recruited for this study using a database of existing drug users at the clinical psychopharmacology unit, University College London (UCL), and via word of mouth. After giving informed consent, all participants were required to provide a self-report of their drug use history. Participants were also required to have no history of head injury, to be right handed and fluent in English.

Participants were grouped into two groups; ketamine users (participants that use ketamine at least three times per week) and poly-drug controls (participants with no history of regular ketamine use). I then matched groups for age, sex and education level. 6 participants were excluded that did not match these demographics. A further 6 participants were excluded as reliable MR images could not be obtained. This left 36 participants (17 ketamine users and 19 controls) from whom structural MR images were processed for analysis.

The study was approved by both the Imperial College Research Ethics Committee and the UCL Graduate School ethics committee. All participants were paid for their participation and travel.

b) Assessment of psychological wellbeing

All assessments of psychological wellbeing were performed by Fiona Pepper, King's College London.

Psychotic symptoms were assessed using the Comprehensive Assessment of At-Risk Mental State (CAARMS) abnormalities of thought content (bizarre + non-bizarre), abnormalities of perceptions and abnormalities of speech production subscales (Alison R Yung *et al.*, 2005). These subscales form part of a structured questionnaire used by psychiatrists to assess whether a person meets the threshold for a clinical diagnosis of a psychotic disorder. The threshold for a diagnosis is as follows:

- A severity score of 6 on the disorders of thought content severity subscale, 5 or 6 on the perceptual abnormalities subscale and/or 6 on the disorganized speech subscale.
- A frequency scale score of 4 or more on the disorders of thought content, perceptual abnormalities and /or disorganized speech subscales
- Psychotic symptoms present for longer than 1 week

The psychiatrist asks the participant questions and records their answers using a sliding scale. Psychotic symptoms are those symptoms experienced in episodes of psychosis and include but are not limited to; difficulty concentrating, depressed mood, disrupted sleep, anxiety, suspiciousness, withdrawal from family and friends, delusions, hallucinations, disorganised speech and suicidal thoughts or actions.

The Schizotypal Personality Questionnaire (SPQ) (Raine, 1991) was used to assess schizotypal symptoms using DSM-III-R criteria for schizotypal personality disorder, found in the third edition of the diagnostic and statistical manual for mental disorder (DSM). It is a 74-item questionnaire were each item is scored with a 1 or 0 depending on whether the participant answered yes or no, the higher the cumulative score for the participant the greater the schizotypal personality. Schizotypal symptoms include; strange thinking/behaviour, unusual beliefs, social discomfort, lack of emotion or inappropriate emotional responses, social anxiety and paranoia.

c) MRI acquisition

Acquisition of participant MR images was performed by Dr Emer Hughes, Imperial College London.

All participants underwent MR imaging on a Philips 3 Tesla *Intera* magnetic resonance scanner (Medical Systems, Best, The Netherlands), software release 2.1.3, equipped with a sensitivity encoding (SENSE) head volume coil located at the Robert Steiner Magnetic Imaging Center at The Hammersmith Hospital (London, UK). An initial localizer scan was performed followed by acquisition of a whole-brain T1-weighted 3-dimensional magnetisation prepared rapid gradient echo (3D-MPRAGE) image (repetition time (TR)= 9.6ms, echo time (TE)= 4.5 ms, flip angle 8°, slice thickness=1.2 mm, 0.94 mm× 0.94 mm in plane resolution, 150 slices) (Figure 1).

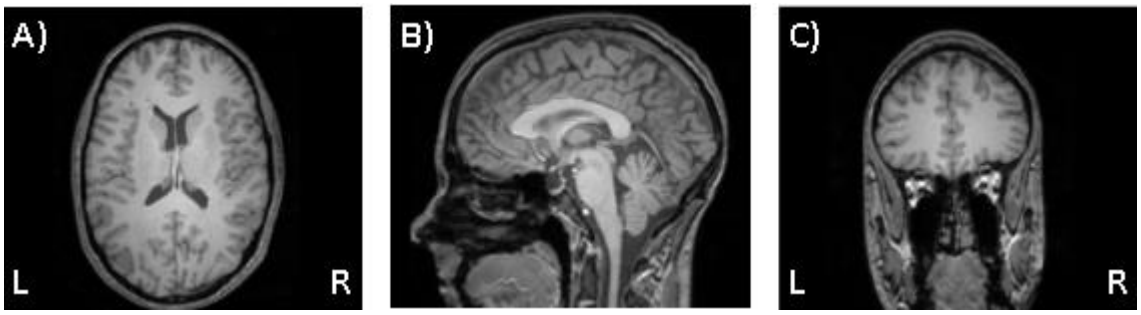

Figure 1. A representative T1-Weighted 3D-MPRAGE MR image from one of the study participants. A) Axial view. B) Sagital view. C) Coronal view.

d) *Freesurfer* MRI processing and analysis

Processing and analysis of MR images was then done using both a Region of Interest (ROI) based approach and a complimentary whole-brain voxel-wise approach.

An ROI based method of cortical reconstruction and volumetric segmentation was performed with the *Freesurfer* image analysis suite, which is documented and freely available for download online (*http://surfer.nmr.mgh.harvard.edu/*). The technical details of these procedures are described in many prior publications (Dale and Sereno, 1993; Dale, Fischl and Sereno, 1999; Fischl and Dale, 2000; Fischl, Liu and Dale, 2001; Fischl *et al.*, 2002, no date; Ségonne *et al.*, 2004; Fischl, Salat, *et al.*, 2004; Fischl, van der Kouwe, *et al.*, 2004; Han *et al.*, 2006; Jovicich *et al.*, 2006).

This processing includes motion correction and averaging of T1-weighted images to remove acquisition artefacts (Reuter, Rosas and Fischl, 2010), removal of non-brain tissue using a hybrid watershed/surface deformation procedure (Ségonne *et al.*, 2004). This is followed by automated Talairach transformation to align each MR image to a reference image before segmenting the subcortical white matter and deep grey matter volumetric structures into regions of interest (Fischl *et al.*, 2002; Fischl, Salat, *et al.*, 2004; Desikan *et al.*, 2006). Intensity normalization was then performed to improve the signal-noise ratio (Sled, Zijdenbos and Evans, 1998), followed by delineation of the cortical grey matter/white matter boundary and grey matter/cerebrospinal fluid border (Dale and Sereno, 1993; Fischl, Sereno and Dale, 1999; Fischl and Dale, 2000; Fischl, Liu and Dale, 2001; Segonne, Pacheco and Fischl, 2007). The cerebral cortex was then automatically split into regions of interest and cortical grey matter volume, cortical

thickness, cortical surface area, subcortical white matter volume and deep grey matter volume ROI measurements calculated (Fischl, van der Kouwe, *et al.*, 2004; Desikan *et al.*, 2006).

Multivariate general linear model (GLM) statistics were performed using *IBM SPSS statistics 22 to* determine group-level differences in individual cortical ROI volumes, thickness and surface area, as well as cortical volume (as a whole), subcortical grey and white matter volume. Total intracranial volume (TIV) was used as a covariate in statistical modelling of volume differences: there is natural biological variance in brain size across individuals, this means that for participants in each group whole brain volume will differ, as will the volume of each brain ROI. For example, participants with a larger brain are likely to also have a larger hippocampus and/or cortex. This difference is controlled by covarying for TIV in the GLM. Thus, variance in brain size can be excluded as a factor when interpreting any difference in brain ROI volume between groups. *Mathworks MATLAB R2014a* was used for false discovery rate (FDR) correction (q=0.05) of multiple comparisons (Genovese, Lazar and Nichols, 2002; Glickman, Rao and Schultz, 2014).

e) *CAT12 and SPM12* MRI processing and analysis

A whole-brain, voxel-wise tensor-based morphometry (TBM) analysis was implemented using the *Computational Anatomy Toolbox (CAT12)* plugin for *Statistical Parametric Mapping (SPM12)* software, to compliment and extend the ROI analysis. This software is documented and freely available for download online (*http://www.neuro.uni-jena.de/cat*). The technical details of this methodology are described in prior publications (J Ashburner and Friston, 2000; Good *et al.*, 2001; Tohka, Zijdenbos and Evans, 2004; Ashburner and Friston, 2005; Ashburner, 2007; Manjón *et al.*, 2010; Gaser and Dahnke, 2012; Malone *et al.*, 2015).

T1-weighted MR images were transformed (moved), using an affine registration, to ensure all images were approximately aligned within the same stereotaxic space. A non-linear transformation was then performed to register (move, stretch and adjust) the images to the Montreal Neurological Institute (MNI) 152 standard brain template. Logarithmic Jacobian (logJ) determinants were calculated from the inverse warp fields

in standard space. logJ determinants in this case are files which store information as to how each 3D voxel within an MR image has been distorted (moved, stretched and adjusted) to fit the MNI 152 brain template. Group-level comparisons of the logJ determinants reveal any volume differences between groups in specific voxels within the MR image. The logJ determinants were smoothed, with a 12mm full-width-at-half-maximal isotropic Gaussian kernel, to improve the signal-noise ratio before analysis. Multivariate GLM statistics were performed on logJ determinant images, with TIV as a covariate, to determine voxel-wise group-level differences in volume. FDR correction ($q<0.05$) was applied to correct for multiple comparisons.

f) Correlations

Partial correlations were performed in *IBM SPSS statistics 22* to investigate potential correlations between:

1. The amount of ketamine taken, the frequency of ketamine consumption or the years of ketamine use with the volume of the accumbens, caudate, cerebral cortex and cerebellar cortex, within ketamine users only. These partial correlations included additional covariables outlined in table 1.

Table 1. Partial correlations between measures of ketamine use and ROI brain volume

Variables	Co-varables
Ketamine - amount used (g per session)	Total intracranial volume (TIV)
Ketamine - frequency of use (days per month)	Alcohol - amount used (units per session)
Ketamine - years of use	Alcohol frequency of use (days per month)
Accumbens volume	Alcoho - years of use
Cerebral cortex volume	Cannabis - years of use
Cerebellar cortex volume	Ecstasy - years os use
	Cocaine - years of use
	Amphetamine - amount used (g per session)
	Amphetamine - frequency of use (days per month)
	Amphetamine - years of use
	Heroin - amount used (g per session)
	Heroin - frequency of use (days per month)
	Heroin - years of use

2. The amount of ketamine taken, the frequency of ketamine consumption or the years of ketamine use with scores of psychological wellbeing, within ketamine users only. These partial correlations included additional covariables outlined in table 2.

Table 2. Partial correlations between measures of ketamine use and psychological wellbeing

Variables	Co-varables
Ketamine - amount used (g per session)	Alcohol - amount used (units per session)
Ketamine - frequency of use (days per month)	Alcohol frequency of use (days per month)
Ketamine - years of use	Alcoho - years of use
CAARMS severity - abnormalities of thought content	Cannabis - years of use
CAARMS severity - perceptual abnormalities	Ecstasy - years os use
CAARMS frequency - abnormalities of thought content	Cocaine - years of use
CAARMS frequency - perceptual abnormalities	Amphetamine - amount used (g per session)
CAARMS frequency - abnormalities of speech production	Amphetamine - frequency of use (days per month)
SPQ - total score	Amphetamine - years of use
SPQ - cognitive and perceptual	Heroin - amount used (g per session)
SPQ - disorganisation	Heroin - frequency of use (days per month)
	Heroin - years of use

3. The volume of the accumbens, caudate, cerebral cortex and cerebellar cortex with scores of psychological wellbeing in ketamine users (table 3).

Table 3. Partial correlations between ROI brain volume and scores of psychological wellbeing

Variables	Co-variables
Accumbens volume	Total intracranial volume (TIV)
Cerebral cortex volume	
Cerebellar cortex volume	
CAARMS severity - abnormalities of thought content	
CAARMS severity - perceptual abnormalities	
CAARMS frequency - abnormalities of thought content	
CAARMS frequency - perceptual abnormalities	
CAARMS frequency - abnormalities of speech production	
SPQ - total score	
SPQ - cognitive and perceptual	
SPQ - disorganisation	

2.4 Results and discussion

a) Participant demographics and drug use

Amongst the 17 ketamine users the average amount of (self-reported) ketamine use per session was 4g. The average number of (self-reported) days per month ketamine was used was 17 days. Because participants were recruited by word of mouth and from a database of known drug users, I compared the use of other drugs, other than ketamine, between the two groups. I found that the number of alcohol users, nicotine users (i.e. cigarette smokers) and cannabis users were statistically well matched between groups (Table 4).

Table 4. Participant demographics and measures of drug use

Demographics	Poly-drug controls (n=19)	Ketamine users (n=17)	Test statistic	p-value
Age (mean ± SD)	25.5 ± 4.9	28.7 ± 5.1	t= -1.9	0.07
Gender (male / female)	13 / 6	12 / 5	x^2= 0.02	0.89
Years in education (mean ± SD)	16.8 ± 3.6	14.6 ± 3.5	t= -1.9	0.07
Ketamine Use				
Number of regular users	0	17	-	-
Amount used (g/session) (mean ± SD)	-	4 ± 3.4	-	-
Frequency (days/month) (mean ± SD)	-	17.4 ± 11.1	-	-
Other drugs used	n=	n=		
Alcohol	19	17	-	-
Tobacco (Cigarrete smoking)	16	16	x^2= 0.89	0.35
Cannabis	17	17	x^2= 1.90	0.17
Ecstasy	9	17	x^2= 12.4	0.00
Cocaine	9	16	x^2= 12.90	0.00
Amphetamine	5	16	x^2= 20.7	0.00
Heroin	0	6	-	-

However, the number of ecstasy, cocaine and amphetamine users was not statistically well matched (ecstasy; x^2=12.4, p<0.001. cocaine; x^2=12.9, p<0.001. amphetamine; x^2=20.7, p<0.001) and there were more ecstasy, cocaine and amphetamine users in the ketamine user group (ecstasy n=17, cocaine n=16, amphetamine n=16) than in the control group (ecstasy n=9, cocaine n=9, amphetamine n=5). In addition, 6 ketamine users also reported using heroin whereas none of the controls did (Table 4).

In addition to reporting what drugs they used, some participants also gave details as to the quantity of each drug used, the frequency of drug use and the number of years they had been taking the drug (Table 5). It is important to note here that not all participants gave these details for each drug used. However, analysing the data which was provided I discovered the following:

Alcohol

- Ketamine users drank more alcohol per session than controls (ketamine; 12 units, controls; 5 units, t=2.47, p=0.03).
- Ketamine users drank alcohol more frequently than controls (ketamine; 15 days per month, controls; 7 days per month, t=2.42, p=0.03)

- Ketamine users started drinking at an earlier age, as they had used alcohol for a greater number of years than controls (ketamine; 16 years, controls; 10 years, t=2.70, p=0.01)

Cannabis

- Ketamine users started using cannabis at an earlier age as they reported having used cannabis for a greater number of years than controls (ketamine; 14 years, controls; 8 years, t=3.35, p<0.001)

Ecstasy

- Ketamine users started using ecstasy at an earlier age as they reported having used ecstasy for a greater number of years than controls (ketamine; 10 years, controls; 5 years, t=3.17, p<0.001)

Cocaine

- Ketamine users started using cocaine at an earlier age as they reported having used cocaine for a greater number of years than controls (ketamine; 9 years, controls; 4 years, t=3.07, p=0.01)

For further details please see table 5.

It is important to note here that the participant data on the amount, frequency and duration of drug use is all self-report data, which is subject to estimates and errors in memory recall and therefore may not be entirely accurate. Unfortunately, this is an inherent problem with this type of data (Schacter, Guerin and St Jacques, 2011; Althubaiti, 2016).

However, if we accept that the self-report data was accurate then the two groups were not well matched for other drug use. This is unfortunately a limitation of this type of study and one which occurs frequently in the literature (Liao *et al.*, 2010, 2011, 2012; Stone *et al.*, 2012; Wang *et al.*, 2013; Edward Roberts *et al.*, 2014; Morgan *et al.*, 2014).

Table 5. Details of other drug use amongst participants who responded to further questions on the amount, frequency and length of use.

Other drugs ever used	Poly-drug controls (n=19)	Ketamine users (n=17)	Test statistic (t)	p-value
Alcohol	n = 19 of 19	n = 13 of 17		
Amount used (units per session)	5 ± 3	12 ± 10	2.47	0.03
Frequency (days per month)	7 ± 5	15 ± 11	2.42	0.03
Years of use	10 ± 6	16 ± 6	2.7	0.01
Tobacco (Cigarrete smoking)	n = 11 of 16	n = 14 of 16		
Amount used (cigarretes smoked per session)	8 ± 10	7 ± 6	0.26	0.80
Frequency (days per month)	21 ± 13	20 ± 12	0.31	0.76
Years of use	8 ± 8	14 ± 7	1.88	0.07
Cannabis	n = 7 of 17	n = 14 of 17		
Amount used (time taken to smoke 3.5g)	74 ± 131	12 ± 21	1.25	0.26
Frequency (days per month)	9 ± 12	20 ± 13	1.96	0.07
Years of use	8 ± 2	14 ± 6	3.35	0.00
Ecstasy	n = 5 of 9	n = 11 of 17		
Amount used (g per session)	0.37 ± 0.37	1.23 ± 2.93	0.96	0.36
Frequency (days per month)	1 ± 1	2 ± 1	1.64	0.13
Years of use	5 ± 3	10 ± 4	3.17	0.00
Cocaine	n = 5 of 9	n = 12 of 16		
Amount used (g per session)	0.69 ± 0.75	1.25 ± 1.09	1.23	0.24
Frequency (days per month)	3 ± 4	3 ± 3	0.20	0.85
Years of use	4 ± 2	9 ± 3	3.07	0.01
Amphetamine	n = 0 of 5	n = 11 of 16		
Amount used (g per session)	-	0.64 ± 0.53	-	-
Frequency (days per month)	-	4 ± 9	-	-
Years of use	-	11 ± 6	-	-
Heroin	n = 0	n = 4 of 6		
Amount used (g per session)	-	0.49 ± 0.37	-	-
Frequency (days per month)	-	2 ± 1	-	-
Years of use	-	7 ± 7	-	-

b) Grey matter volume reductions in ketamine users observed using *Freesurfer* ROI analysis

To investigate whether there were any group-level differences in brain structure I used the *Freesurfer* analysis suite to analyse brain volumes in distinct regions of interest (ROI). I first analysed 12 gross cortical grey matter, subcortical grey matter and subcortical white matter regions. I found that ketamine users had a significantly smaller cerebral cortex (ketamine; 540.95cm^3, controls; 572.91cm^3, F=7.14, p=0.01), smaller cerebellar cortex (ketamine; 121.95cm^3, controls; 131.01 cm^3, F=7.52, p=0.01), smaller nucleus accumbens (ketamine; 1.14 cm^3,controls; 1.24 cm^3, F= 10.47, p<0.001) and smaller caudate nucleus (ketamine; 7.34 cm^3, controls; 8.07 cm^3, F=7.31, p=0.01). For further

details see Table 6 and Figure 2 for an illustration of where these differences occur in the brain.

Table 6. Volume measurements from gross regions of interest in ketamine users and controls

Region of Interest	Poly-drug controls Mean (cm3)	SEM	Ketamine users Mean (cm3)	SEM	F-statistic	p-value	q-value	Percentage change in volume (%)	Cohen's d	
Accumbens	1.29	0.03	1.14	0.03	10.47	0.00	0.00	11.63	0.79	↓
Caudate	8.07	0.19	7.34	0.20	7.31	0.01	0.03	9.05	0.54	↓
Cerebral Cortex	572.91	8.19	540.95	8.66	7.14	0.01	0.03	5.58	0.36	↓
Cerebellum Cortex	131.01	2.26	121.95	2.39	7.52	0.01	0.03	6.92	0.56	↓
Pallidum	3.86	0.08	3.63	0.08	3.85	0.06	0.13	-	-	-
Putamen	12.55	0.25	11.96	0.26	2.65	0.11	0.20	-	-	-
Corpus Callosum	3.61	0.08	3.71	0.09	0.67	0.42	0.67	-	-	-
Thalamus	16.52	0.25	16.34	0.26	0.27	0.61	0.83	-	-	-
Cerebellum White Matter	34.07	0.74	34.53	0.78	0.18	0.67	0.83	-	-	-
Amygdala	3.42	0.06	3.44	0.07	0.07	0.79	0.83	-	-	-
Hippocampus	9.43	0.14	9.46	0.15	0.01	0.90	0.83	-	-	-
Cerebral White Matter	566.53	10.32	564.39	10.92	0.02	0.89	0.83	-	-	-

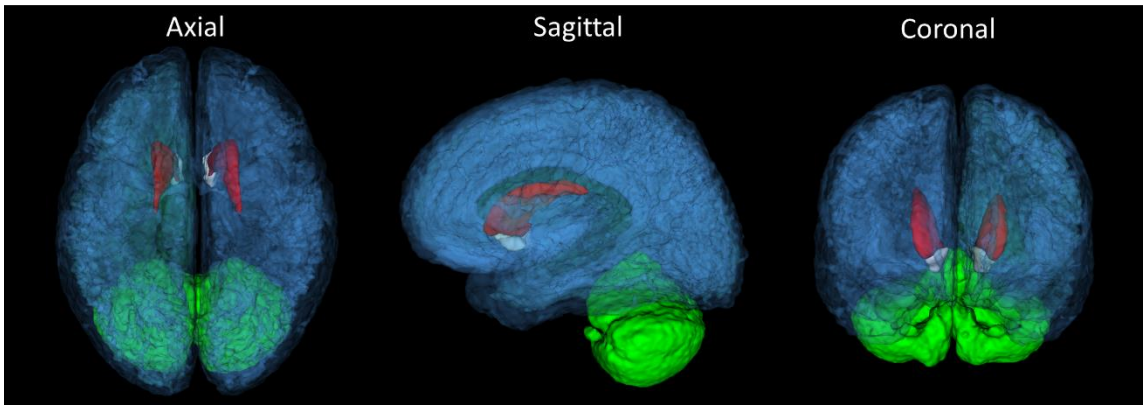

Figure 2. Transparent brain displaying significant gross volume differences between ketamine users and poly-drug controls. ROIs are shaded in the following colours: Cerebral cortices in blue, cerebellar cortices in green, caudate nuclei in white and nuclei accumbens in red.

Similar to published findings (Liao *et al.*, 2011; Wang *et al.*, 2013), my results show reductions in brain volume in the cerebral cortex and cerebellar cortex. In addition to what has been published previously, I also report reductions in brain volume in the nucleus accumbens and caudate nucleus of repeat ketamine users (Table 6).

The reduced cortical grey matter volumes present in ketamine users reported in the Liao et al (2011) study are specific to the superior frontal cortex and middle frontal cortex. In my study, to specifically locate in which region of the cortex volume reductions are situated, I used *Freesurfer* to sub-divide the cerebral cortex into its 34 constituent ROIs. I then analysed for group-level differences in volume measurements across all 34 ROIs.

After FDR multiple comparison correction (q≤0.05) I found significantly smaller volumes in ketamine users in 10 of 34 cortical ROIs (see table 7 for details):

- Inferior parietal cortex (ketamine; 26.67cm^3, controls; 31.73 cm^3, F=15.32, p<0.001)
- Temporal pole (ketamine; 4.55cm^3, controls; 5.08cm^3, F=11.52, p<0.001)
- Caudal middle frontal gyrus (ketamine; 13.78cm^3, controls; 16.19cm^3, F=9.06, p<0.001)
- Supramarginal gyrus (ketamine; 23.21cm^3, controls; 25.43cm^3, F=7.68, p=0.01)
- Paracentral gyrus (ketamine; 7.38cm^3, controls; 8.02cm^3, F=7.11, p=0.01)
- Middle temporal gyrus (ketamine; 24.06cm^3, controls; 26.02cm^3, F=5.81, p=0.02)
- Superior frontal gyrus (ketamine; 48.34cm^3, controls; 52.08cm^3, F=5.80, p=0.02)
- Isthmus of the cingulate cortex (ketamine; 4.84cm^3, controls; 5.31cm^3, F=5.34, p=0.03)
- Superior temporal gyrus (ketamine; 25.03cm^3, controls; 27.02cm^3, F=4.89, p=0.03)
- Banks of the superior temporal sulcus (ketamine; 5.51cm^3, controls 6.18cm^3, F=4.46, p=0.04)

Consistent with the study by Liao et al (2011) I found volume reductions in ketamine users in the superior frontal cortex and middle frontal cortex. Hence, I have reproduced similar findings to those in the literature in an independent cohort of ketamine users. This provides further evidence to support the hypothesis that repeat ketamine use alters brain structure in the frontal lobe. Furthermore, I have added new information to the field by showing that ketamine users also present with smaller volumes in regions of the parietal and temporal cortices (table 7). In summary, repeat ketamine use appears to alter brain structure in multiple cortical regions.

Table 7. Volume measurements for cortical ROIs from ketamine users and controls

Region of Interest	Poly-drug controls Mean (cm3)	SEM	Ketamine users Mean (cm3)	SEM	F-statistic	p-value	q-value	Percentage change in volume (%)	Cohen's d	
Inferior parietal cortex	31.73	0.71	27.67	0.75	15.32	0.00	0.00	12.80	1.31	↓
Temporal pole	5.08	0.11	4.55	0.11	11.52	0.00	0.00	10.51	1.13	↓
Caudal middle frontal gyrus	16.19	0.55	13.78	0.58	9.06	0.00	0.00	14.89	1.01	↓
Supramarginal gyrus	25.43	0.55	23.21	0.58	7.68	0.01	0.00	8.74	0.92	↓
Paracentral gyrus	8.02	0.17	7.38	0.18	7.11	0.01	0.00	8.08	0.88	↓
Middle temporal gyrus	26.02	0.56	24.06	0.59	5.81	0.02	0.00	7.55	0.81	↓
Superior frontal gyrus	52.08	1.06	48.34	1.13	5.80	0.02	0.00	7.18	0.81	↓
Isthmus - cingulate cortex	5.31	0.14	4.84	0.15	5.34	0.03	0.00	8.87	0.77	↓
Superior temporal gyrus	27.02	0.62	25.03	0.65	4.89	0.03	0.00	7.37	0.74	↓
Banks superior temporal sulcus	6.18	0.22	5.51	0.23	4.46	0.04	0.00	10.92	0.70	↓
Precuneus Cortex	20.79	0.45	19.47	0.48	3.93	0.06	0.00	-	-	-
Frontal pole	1.80	0.09	1.55	0.09	3.82	0.06	0.00	-	-	-
Rostral middle frontal gyrus	35.21	0.96	32.47	1.02	3.80	0.06	0.00	-	-	-
Fusiform gyrus	20.76	0.60	19.26	0.63	2.99	0.09	0.01	-	-	-
Rostral anterior cingulate gyrus	4.78	0.15	4.41	0.16	2.81	0.10	0.01	-	-	-
Inferior temporal gyrus	23.16	0.70	21.46	0.74	2.78	0.10	0.01	-	-	-
Medial orbital frontal cortex	10.00	0.31	9.27	0.33	2.57	0.12	0.01	-	-	-
Precentral gyrus	29.83	0.69	28.40	0.73	2.00	0.17	0.01	-	-	-
Superior parietal cortex	28.90	0.84	27.18	0.89	1.94	0.17	0.01	-	-	-
Cuneus cortex	5.29	0.16	5.58	0.17	1.63	0.21	0.01	-	-	-
Lateral orbito frontal cortex	16.03	0.39	15.33	0.42	1.49	0.23	0.01	-	-	-
Insula cortex	13.52	0.27	13.07	0.29	1.26	0.27	0.01	-	-	-
Postcentral gyrus	20.95	0.60	20.00	0.63	1.18	0.29	0.01	-	-	-
Transverse temporal cortex	2.34	0.09	2.20	0.10	1.07	0.31	0.01	-	-	-
Lingual gyrus	12.74	0.32	12.30	0.33	0.91	0.35	0.01	-	-	-
Pericalcarine cortex	3.55	0.11	3.70	0.12	0.82	0.37	0.02	-	-	-
Posterior-cingulate cortex	7.64	0.20	7.38	0.21	0.75	0.39	0.02	-	-	-
Caudal anterior-cingulate cortex	4.55	0.15	4.38	0.16	0.60	0.44	0.02	-	-	-
Pars opercularis	11.03	0.35	10.65	0.37	0.55	0.47	0.02	-	-	-
Pars orbitalis	5.41	0.16	5.26	0.16	0.47	0.50	0.02	-	-	-
Pars triangularis	8.69	0.33	8.89	0.35	0.19	0.67	0.02	-	-	-
Entorhinal cortex	3.89	0.11	3.94	0.12	0.09	0.77	0.02	-	-	-
Lateral occipital cortex	24.24	0.72	24.54	0.76	0.08	0.77	0.02	-	-	-
Parahippocampal gyrus	4.89	0.11	4.88	0.11	0.00	0.95	0.03	-	-	-

Cortical volume in *Freesurfer* is a combined measure of cortical thickness and cortical surface area. I was interested to see whether the cortical volume differences observed were due to changes in cortical thickness, surface area or a combination of the two. I found no significant differences in cortical thickness between the two groups across any of the 34 cortical ROIs (Table 8). However, I did find significant reductions in cortical surface area in ketamine users in 2 of 34 cortical ROIs (Table 9); in the temporal pole (ketamine; 7.22cm^2, controls; 8.22cm^2, F=13.22, p<0.001) and inferior parietal cortex (ketamine; 103.22cm^2, controls; 114.13cm^2, F=10.31, p<0.001). It would appear then that the smaller volumes found in the temporal pole and inferior parietal cortex of ketamine users are driven predominately by reductions in cortical surface area. Whereas, the smaller volumes in the caudal middle frontal gyrus, supramarginal gyrus, paracentral gyrus, middle temporal gyrus, superior frontal gyrus, isthmus of the cingulate cortex, superior temporal gyrus and banks of the superior temporal sulcus are likely due to a combination of reduced cortical thickness and smaller surface areas.

Table 8. Cortical thickness measurements from ketamine users and controls

Region of Interest	Poly-drug controls Mean (cm)	SEM	Ketamine users Mean (cm)	SEM	F-statistic	p-value	q-value
Rostral middle frontal gyrus	2.55	0.03	2.41	0.03	7.68	0.01	0.10
Transverse temporal cortex	2.35	0.06	2.13	0.06	7.10	0.01	0.10
Superior frontal gyrus	2.97	0.04	2.84	0.04	5.66	0.02	0.14
Pars opercularis	2.83	0.04	2.72	0.04	4.28	0.05	0.25
Caudal middle frontal gyrus	2.76	0.04	2.65	0.04	3.78	0.06	0.25
Precuneus Cortex	2.38	0.03	2.30	0.03	3.09	0.09	0.25
Medial orbital frontal cortex	2.72	0.05	2.60	0.05	2.90	0.10	0.25
Posterior-cingulate cortex	2.71	0.04	2.62	0.04	2.67	0.11	0.25
Temporal pole	3.96	0.06	4.10	0.06	2.54	0.12	0.25
Pars triangularis	2.77	0.04	2.67	0.05	2.39	0.13	0.25
Entorhinal cortex	3.40	0.06	3.54	0.07	2.33	0.14	0.25
Isthmus - cingulate cortex	2.71	0.04	2.62	0.04	2.18	0.15	0.25
Rostral anterior cingulate gyrus	3.09	0.06	2.97	0.06	2.03	0.16	0.25
Cuneus cortex	1.65	0.03	1.71	0.03	1.97	0.17	0.25
Inferior parietal cortex	2.54	0.04	2.47	0.04	1.65	0.21	0.29
Supramarginal gyrus	2.67	0.04	2.60	0.04	1.30	0.26	0.34
Superior parietal cortex	2.17	0.03	2.12	0.03	1.08	0.31	0.35
Precentral gyrus	2.56	0.04	2.49	0.04	1.07	0.31	0.35
Paracentral gyrus	2.34	0.04	2.28	0.04	1.01	0.32	0.35
Frontal pole	2.93	0.08	2.82	0.09	0.85	0.36	0.36
Insula cortex	3.17	0.04	3.11	0.04	0.84	0.37	0.36
Parahippocampal gyrus	2.80	0.06	2.87	0.06	0.64	0.43	0.39
Banks superior temporal sulcus	2.69	0.04	2.64	0.04	0.62	0.44	0.39
Caudal anterior-cingulate cortex	2.73	0.05	2.68	0.06	0.44	0.51	0.44
Pericalcarine cortex	1.37	0.02	1.39	0.02	0.41	0.53	0.44
Lateral orbito frontal cortex	2.92	0.04	2.89	0.04	0.23	0.63	0.50
Middle temporal gyrus	3.05	0.04	3.03	0.04	0.07	0.80	0.59
Pars orbitalis	2.93	0.06	2.91	0.06	0.05	0.83	0.59
Postcentral gyrus	2.02	0.03	2.02	0.03	0.03	0.85	0.59
Lateral occipital cortex	2.17	0.03	2.16	0.03	0.03	0.87	0.59
Fusiform gyrus	2.76	0.03	2.77	0.04	0.02	0.88	0.59
Superior temporal gyrus	2.92	0.04	2.91	0.05	0.01	0.93	0.59
Inferior temporal gyrus	2.92	0.04	2.92	0.04	0.00	0.97	0.59
Lingual gyrus	1.89	0.03	1.89	0.03	0.00	0.98	0.59

Table 9. Cortical surface area measurements from ketamine users and controls

Region of Interest	Poly-drug controls Mean (cm2)	SEM	Ketamine users Mean (cm2)	SEM	F-statistic	p-value	q-value	Percentage change in surface area (%)	Cohen's d	
Temporal pole	8.22	0.19	7.22	0.20	13.22	0.00	0.00	12.14	1.22	↓
Inferior parietal cortex	114.13	2.33	103.22	2.46	10.31	0.00	0.00	9.56	1.08	↓
Superior temporal gyrus	80.63	1.40	76.22	1.48	4.66	0.04	0.14	-	-	-
Banks superior temporal sulcus	23.71	0.75	21.44	0.79	4.37	0.04	0.14	-	-	-
Caudal middle frontal gyrus	51.76	1.65	47.00	1.74	3.93	0.06	0.17	-	-	-
Middle temporal gyrus	69.90	1.64	65.97	1.73	2.72	0.11	0.20	-	-	-
Inferior temporal gyrus	67.06	1.88	62.67	1.98	2.57	0.12	0.20	-	-	-
Fusiform gyrus	66.57	1.71	62.60	1.81	2.51	0.12	0.20	-	-	-
Transverse temporal cortex	8.77	0.26	9.35	0.28	2.22	0.15	0.20	-	-	-
Paracentral gyrus	32.13	0.72	30.61	0.76	2.12	0.15	0.20	-	-	-
Pars triangularis	27.55	1.03	29.72	1.09	2.07	0.16	0.20	-	-	-
Frontal pole	4.41	0.20	4.04	0.21	1.54	0.22	0.25	-	-	-
Entorhinal cortex	7.98	0.18	7.68	0.19	1.26	0.27	0.28	-	-	-
Superior parietal cortex	120.55	3.19	115.59	3.37	1.14	0.29	0.28	-	-	-
Supramarginal gyrus	87.48	2.53	83.76	2.68	1.02	0.32	0.28	-	-	-
Lingual gyrus	65.02	1.31	63.21	1.38	0.90	0.35	0.28	-	-	-
Postcentral gyrus	93.94	2.45	90.69	2.60	0.82	0.37	0.28	-	-	-
Lateral orbito frontal cortex	50.62	1.13	49.15	1.20	0.80	0.38	0.28	-	-	-
Lateral occipital cortex	104.01	2.18	106.83	2.31	0.78	0.38	0.28	-	-	-
Pericalcarine cortex	28.43	0.86	29.48	0.91	0.70	0.41	0.28	-	-	-
Isthmus - cingulate cortex	17.75	0.54	17.18	0.57	0.53	0.47	0.31	-	-	-
Rostral anterior cingulate gyrus	13.25	0.35	12.92	0.37	0.43	0.52	0.33	-	-	-
Posterior-cingulate cortex	25.74	0.69	26.33	0.73	0.34	0.56	0.34	-	-	-
Medial orbital frontal cortex	32.47	0.96	31.82	1.01	0.22	0.64	0.35	-	-	-
Precuneus Cortex	83.04	1.87	81.85	1.98	0.19	0.67	0.35	-	-	-
Pars opercularis	34.55	1.05	35.16	1.11	0.16	0.69	0.35	-	-	-
Parahippocampal gyrus	15.29	0.31	15.11	0.33	0.16	0.69	0.35	-	-	-
Precentral gyrus	108.14	2.30	106.93	2.43	0.13	0.72	0.35	-	-	-
Cuneus cortex	30.72	0.74	31.10	0.78	0.12	0.73	0.35	-	-	-
Insula cortex	42.55	0.81	42.34	0.86	0.03	0.86	0.38	-	-	-
Rostral middle frontal gyrus	121.12	3.53	120.26	3.73	0.03	0.87	0.38	-	-	-
Superior frontal gyrus	153.84	3.56	153.03	3.76	0.02	0.88	0.38	-	-	-
Pars orbitalis	14.70	0.41	14.77	0.43	0.01	0.91	0.38	-	-	-
Caudal anterior-cingulate cortex	14.89	0.53	14.81	0.56	0.01	0.92	0.38	-	-	-

Although I have been able to localise the reductions in cortical brain volume to specific cortical regions, such as the superior frontal cortex and middle frontal cortex, these regions are still relatively large; on the order of thousands of MRI voxels per region. It could be that within a given cortical ROI the volume difference observed only occurs in a subset of these thousands of voxels. Furthermore, although *Freeurfer* facilitates the subdivision of the cerebral cortex it does not do so for other gross brain regions, such as the cerebellar cortex.

To qualitatively assess in which voxels reductions in brain volume are, in ketamine users, I conducted a complimentary voxel-wise tensor-based morphometry (TBM) analysis.

c) Brain volume differences in repeat ketamine users and poly-drug controls; observed using voxel-wise TBM analysis

Whole brain voxel-wise TBM analysis of volume between ketamine users and controls did not reveal any significant differences after false discovery rate (FDR) correction for multiple statistical comparisons ($q \leq 0.05$). However, without FDR correction there were observable differences between groups ($p \leq 0.05$). The location of these (uncorrected) differences are summarised in table 10 and can be seen in Figure 3.

Table 10. Comparison of Freesurfer gross ROI volume differences and TBM (uncorrected) voxel-wise volume differences between ketamine users and controls

Region of Interest	ROI Analysis	Voxel Analysis
Accumbens	✓	✓
Caudate	✓	✓
Cerebellar cortex	✓	✓
Cerebral cortex	✓	✓
Cerebellar white matter	x	✓
Pallidum	x	✓
Corpus callosum	x	x
Amygdala	x	x
Cerebral white matter	x	x
Hippocampus	x	x
Putamen	x	x
Thalamus	x	x

Regions were significant ($p<0.05$) volume changes reside are highlighted in green. Regions were no significant changes reside are highlighted in red. Please note ROI results are FDR corrected at $q=0.05$, voxel-wise results are not.

However, as these results do not survive multiple comparison correction it is important not to overinterpret them, as there is a strong probability that these data may be false positives. The likely reasons for the results not surviving multiple comparison correction may be that the effect sizes are not large enough to survive FDR correction across hundreds of thousands of individual statistical tests (1 test per MRI voxel across > 500,000 voxels in an MR image of the human brain). This may be because the volumetric differences in each voxel were not large enough and/or the n number for each group was too small. On the contrary, the reason why positive results were seen in the

Freesurfer analysis is that significantly fewer individual statistical tests had to be corrected for multiple comparisons (*Freesurfer;* ≤ 34 individual tests, TBM; > 500,000 individual tests), which increases the likelihood that volume differences with smaller effect sizes (Cohens D ≈ 0.7 – 1.3) survive.

Unless otherwise stated, when I subsequently refer to volume differences between ketamine users and controls, I am referring to results obtained from my *Freesurfer* analysis.

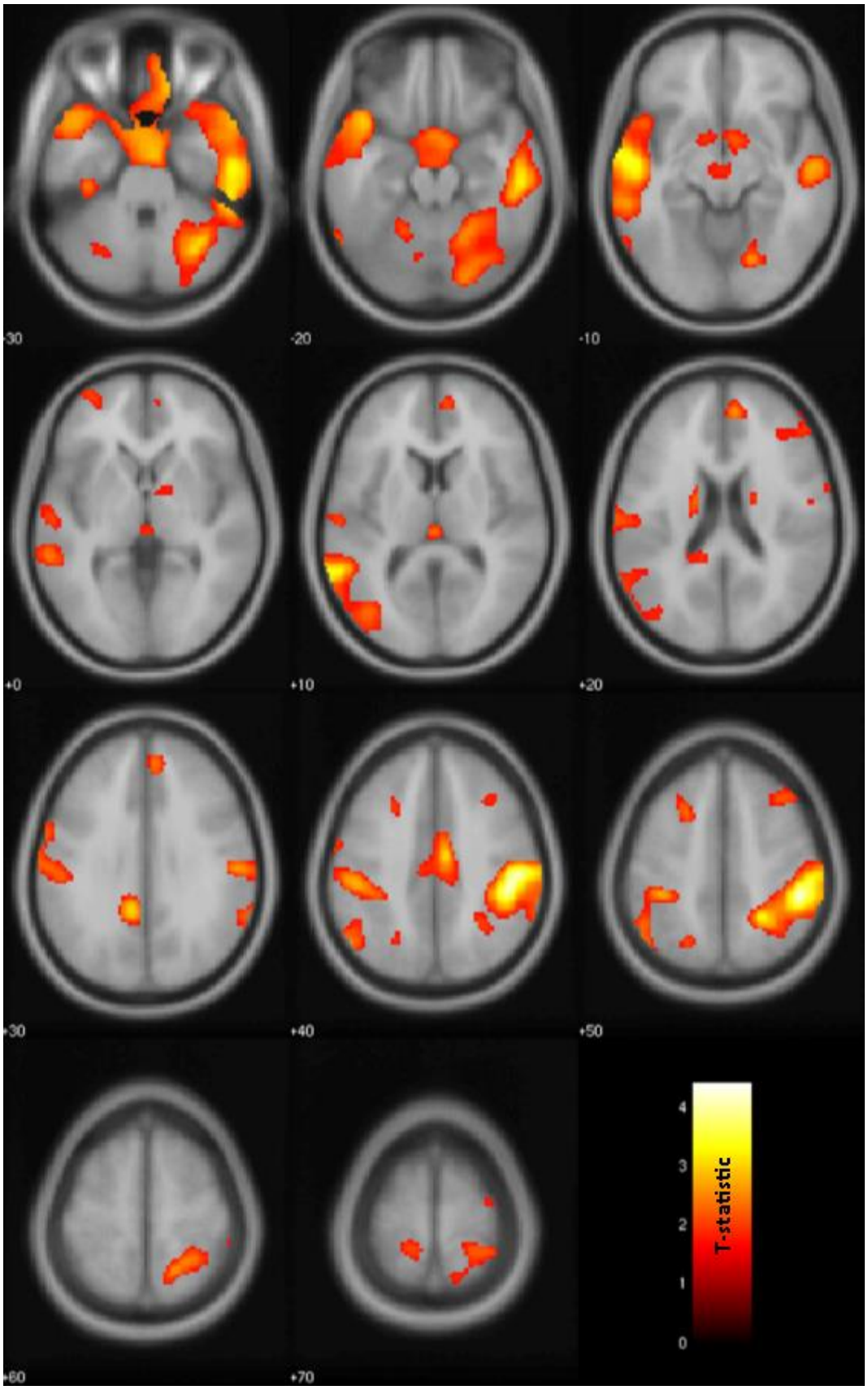

Figure 3. Axial brain slices displaying TBM analysis of volumetric differences between ketamine users and poly-drug controls. Smaller volumes in ketamine users are displayed in red. Numbers in the bottom left corner of each image indicate MNI z-coordinates. Data shown are thresholded at $p<0.05$ (uncorrected).

d) Increased sub-threshold psychotic symptoms and schizotypal personality in ketamine users

In addition to structural alterations and as was discussed in chapter 1 the literature shows that repeat ketamine users also present with disruptions in psychological wellbeing, compared to controls. Such differences include the presence of schizotypal symptoms, impaired executive function and dissociation (Liao *et al.*, 2011; Edward Roberts *et al.*, 2014; Morgan *et al.*, 2014).

In this study I analysed whether there were any differences in measures of psychological wellbeing between ketamine users and controls. Amongst data collected by collaborators were scores of psychiatric symptoms assessed using the comprehensive assessment of at-risk mental state (CAARMS) questionnaire (A.R. Yung *et al.*, 2005), as well as a score of schizotypal symptoms assessed using the schizotypal personality questionnaire (SPQ) (Raine, 1991).

In my analysis of CAARMS scores between groups I found that ketamine users scored significantly higher than controls in terms of the severity of abnormalities of thought content (ketamine; 2.5, controls; 0.4, $t=4.2$, $p<0.001$) and severity of perceptual abnormalities (ketamine; 3, controls; 1.6, $t=2.4$, $p=0.02$). Ketamine users also scored significantly higher than controls in terms of the frequency of abnormalities of thought content (ketamine; 3.4, controls; 0.25, $t= 4.8$, $p<0.001$), frequency of perceptual abnormalities (ketamine; 3.1, controls; 0.9, $t=3.9$, $p<0.001$) and frequency of abnormalities of speech production (ketamine; 2.6, controls; 0.7, $t=2.8$, $p<0.001$)

In summary, ketamine users scored significantly higher than controls on the CAARMS questionnaire. However, on average these scores were not great enough to reach the threshold for clinical diagnosis of psychosis. In other words, ketamine users have increased sub-threshold psychotic symptoms when compared to controls (Table 11).

Table 11. Measures of psychological wellbeing in ketamine users and controls

	Poly-drug controls (n=19)	Ketamine users (n=17)	Test statistic	p-value
Psychological wellbeing				
CAARMS severity	n = 19	n = 17		
- abnormalities of thought content	0.4 ± 0.7	2.5 ± 2	t= 4.2	0.00
- perceptual abnormalities	1.6 ± 1.8	3 ± 1.8	t= 2.4	0.02
- abnormalities of speech production	1.1 ± 1.5	2.2 ± 1.8	t= 1.9	0.06
CAARMS frequency	n = 16	n = 11		
- abnormalities of thought content	0.25 ± 0.58	3.4 ± 2.1	t= 4.8	0.00
- perceptual abnormalities	0.9 ± 1.5	3.1 ± 1.4	t= 3.9	0.00
- abnormalities of speech production	0.7 ± 1.5	2.6 ± 2	t= 2.8	0.01
SPQ	n = 18	n = 14		
- total score	11 ± 7.3	27.5 ± 20.6	t= 2.9	0.01
- cognitive and perceptual	2.6 ± 2.8	9.4 ± 8.7	t= 2.8	0.01
- interpersonal	4.4 ± 3.1	9.5 ± 9.3	t= 1.9	0.07
- disorganisation	4 ± 4.8	8.7 ± 5.2	t= 2.6	0.01

Ketamine users also scored higher on the SPQ compared to controls. The SPQ is a questionnaire designed to assess the extent of schizotypal symptoms. It is a 74 item questionnaire were each item is scored as a 1 or 0 depending on whether the participant answered yes or no, the higher the cumulative score the greater the schizotypal personality (Raine, 1991).

In my analysis of SPQ scores, ketamine users scored higher than controls on the SPQ cognitive and perceptual subscale (ketamine; 9.4, controls; 2.6, t=2.8, p=0.01), disorganized speech subscale (ketamine; 8.7, controls; 4, t=2.6, p=0.01) and total SPQ score (ketamine; 27.5, controls; 11, t=2.9, p= 0.01) (Table 11).

Hence, ketamine users have a stronger schizotypal personality than controls. Taken together with higher sub-threshold psychotic symptoms, ketamine users have a reduced level of psychological wellbeing compared to poly-drug controls.

As ketamine users, in this study, presented with reductions in brain volume and reductions in psychological wellbeing I decided to investigate whether there was any correlation between the two. I also decided to investigate whether there was any correlation between the amount, frequency and/or duration of ketamine use with either reduced brain volumes and/or reduced levels of psychological wellbeing.

e) Correlations between reduced brain volumes, psychological wellbeing and ketamine use metrics in ketamine users

To assess whether there was any correlation between smaller brain volumes and increased scores of psychological wellbeing I performed partial correlations in *SPSS*, for ketamine users only. I did so whilst covarying for TIV to control for variance in whole brain volume across individuals. I found no significant difference in any of the following:

		Volume			
		Nucleus accumbens	Caudate nucleus	Cerebral cortex	Cerebellar cortex
CAARMS severity					
Abnormalities of thought content	r	-0.03	0.12	-0.27	-0.22
	p	0.90	0.66	0.31	0.42
Perceptual abnormalities	r	-0.13	-0.06	-0.18	-0.01
	p	0.63	0.84	0.50	0.96
Abnormalities of speech production	r	0.04	0.05	0.12	-0.03
	p	0.89	0.87	0.67	0.91
CAARMS frequency					
Abnormalities of thought content	r	0.18	0.19	0.01	-0.50
	p	0.61	0.61	0.97	0.14
Perceptual abnormalities	r	0.37	0.24	0.23	0.20
	p	0.30	0.50	0.53	0.58
Abnormalities of speech production	r	0.53	0.14	0.60	0.30
	p	0.11	0.70	0.07	0.40
SPQ					
Total score	r	0.44	-0.13	0.23	0.12
	p	0.13	0.68	0.46	0.69
Cognitive and perceptual score	r	0.44	-0.12	0.27	0.05
	p	0.13	0.70	0.38	0.87
Disorganisation score	r	0.37	-0.28	0.35	0.26
	p	0.21	0.35	0.20	0.40

It would appear then that there is no relationship between reduced brain volumes and decreased psychological wellbeing in ketamine users. This could be because volume reductions and decreased psychological wellbeing, arising through repeat ketamine use, are both by-products of functional changes. Indeed, functional changes have been shown to correlate with altered psychological wellbeing in both single and repeat ketamine exposure (Honey *et al.*, 2004, 2008; Deakin *et al.*, 2008; De Simoni *et al.*, 2013; Doyle *et al.*, 2013b; Driesen *et al.*, 2013; Morgan *et al.*, 2014; Stone *et al.*, 2015). Or, it

could be that due to a low number of participants (ketamine users, n= 17), this study lacks the statistical power to detect any correlation. Conversely, in the study by Liao et al (2011) there were 44 ketamine users participating in the study and significant negative correlations were observed between the duration of ketamine use and decreased grey matter volumes.

Another explanation, however, is that the other drugs used by ketamine users are the main drivers / sole drivers of altered psychological wellbeing in ketamine users. To test this, I investigated whether metrics of ketamine use correlated with scores of psychological wellbeing. I found no significant correlations between the following:

		Amount of ketamine use (grams per session)	Frequency of ketamine use (days per month)
CAARMS severity			
Abnormalities of thought content	r	0.01	0.02
	p	0.99	0.95
Perceptual abnormalities	r	-0.03	-0.15
	p	0.90	0.57
Abnormalities of speech production	r	0.13	0.00
	p	0.63	0.99
CAARMS frequency			
Abnormalities of thought content	r	-0.22	0.53
	p	0.51	0.09
Perceptual abnormalities	r	0.28	0.30
	p	0.38	0.37
Abnormalities of speech production	r	0.02	0.01
	p	0.96	0.97
SPQ			
Total score	r	0.25	0.19
	p	0.41	0.54
Cognitive and perceptual score	r	0.46	0.34
	p	0.11	0.26
Disorganisation score	r	0.27	0.13
	p	0.37	0.67

Thus, there appears to be no relationship between either the frequency of ketamine use, or in the amount of ketamine use with the level of psychological wellbeing. As previously stated, the ketamine users in this study reported an average use of 4 ± 3.4g of ketamine per session. It might well be that if a certain threshold of ketamine use is met (e.g. 0.6g three times per week) psychological wellbeing will deteriorate, however,

this will then not worsen with greater quantities or more frequent use of ketamine (in a type of ceiling effect where a maximum perturbation is reached). Or again, it could be that due to a low number of participants (ketamine users, n= 17), this study lacks the statistical power to detect any correlation.

It might well be that pre-existing genetic and/or environmental factors are partly responsible for the difference in psychological wellbeing observed between ketamine users and controls. However, when I analysed self-report data regarding the number of participants who reported personal mental health problems, a family history of mental health problems, family history of alcoholism and/or a family history of drug abuse, I found no significant difference between groups:

- Personal mental health problems (ketamine users; 4, controls; 3, x^2= 0.34, p= 0.56)
- Family history of mental health problems (ketamine users; 5, controls; 5, x^2= 0.04, p= 0.84)
- Family history of alcoholism (ketamine users; 3, controls; 2, x^2= 0.38, p= 0.54)
- Family history of drug abuse (ketamine users; 7, controls; 3, x^2= 2.88, p= 0.09)

I think that it is more plausible that the other drugs used by ketamine users are partly, if not wholly, responsible for their reduced psychological wellbeing. Ketamine users in this study, compared to controls, had been users of alcohol, cannabis, ecstasy and cocaine for a greater number of years (Table 5). Ketamine users also reported drinking more alcohol, more frequently. This is an issue as evidence from the literature shows that the consumption of other drugs, such as alcohol, cannabis, ecstasy and cocaine can increase schizotypal personality, as measured by the SPQ (Van Dam, Earleywine and DiGiacomo, 2008a; Compton, Chien and Bollini, 2009; Fridberg *et al.*, 2011; Baskak *et al.*, 2012).

To determine whether other drug use was partly or wholly responsible for reduced psychological wellbeing I would have liked to correlate the frequency and amount of ketamine use (separately) with CAARMS scores and SPQ scores, whilst controlling for the frequency, amount and length (years of use) of other drug use. Unfortunately, however I lacked enough statistical power to do so. This was due to a small n number

(n=4). The reason for a small n number was that only ketamine users were tested (n=17). However, not all ketamine users were users of all other drugs. For example, only 6 users reported using heroin and only 4 of those gave further details as to the amount, frequency and length of heroin use. Therefore, I unfortunately cannot state whether other drug use is related to reduced psychological wellbeing in ketamine users, in this study.

My initial analysis showing a lack of a correlation between ketamine use and reduced psychological wellbeing raises doubts as to whether ketamine use correlates with structural changes observed. It is plausible that other drug use also influences the structural differences observed between ketamine users and controls.

As seen already, I cannot adequately control for other drug use metrics due to a low n number and lack of statistical power. Thus, I was unable to investigate any correlation between ketamine use and structural changes whilst controlling for other drug use. I was, however, able to correlate ketamine use with reductions in brain volume whilst only controlling for TIV. I found the following significant correlations:

- Negative correlation between the frequency of ketamine use and the volume of the cerebellar cortex ($r=-0.816$, $p<0.001$). i.e. the greater the frequency of ketamine use the smaller the volume of the cerebellum
- Negative correlation between the amount of ketamine use and the volume of the caudate nucleus ($r=-0.512$, $p=0.05$). i.e. the greater the amount of ketamine used the smaller the volume of the caudate nucleus.

The following correlations were not significant

- Frequency of ketamine use and volume of the nucleus accumbens ($r=0.39$, $p=0.15$), caudate nucleus ($r=0.19$, $p=0.50$) or cerebral cortex ($r=0.032$, $p= 0.91$
- Amount of ketamine use and volume of the nucleus accumbens ($r=0.45$, $p=0.10$), cerebral cortex ($r=0.33$, $p=0.24$) or cerebellar cortex ($r=-0.258$, $p=0.35$).

Although, I found two significant correlations between ketamine use and brain volume I cannot confidently state that the relationship is correct as it may be influenced using other drugs, which I was unable to control for. This is a concern reinforced by evidence in the literature linking other drug use to structural alterations in brain regions like those

assessed here. Examples include; frontal grey matter atrophy in alcoholism, frontal cortex volume and surface area reductions in poly-drug users (users of alcohol, cannabis, cocaine and amphetamine), cortical thinning in the frontal cortex, left middle temporal gyrus and right inferior parietal lobule in young adult cigarette smokers and smaller grey matter volume in the right prefrontal cortex and bilateral cingulate cortices in heroin users (Liu *et al.*, 2009; Kumra *et al.*, 2012; Grodin, Lin, C. a. Durkee, *et al.*, 2013; Li *et al.*, 2015; Pennington *et al.*, 2015).

Thus, although I have shown that there are reductions in volume in several brain regions, in ketamine users, I cannot confidently state that the results seen are due to repeat ketamine use alone. It could be that other drug use is contributing to the volume differences observed. This conclusion is not restricted to this study but can be extended to studies in the literature, the study by Liao et al (2011) on reduced prefrontal cortex grey matter in ketamine users being an example. In this study ketamine users were compared to healthy controls. Although subjects in both groups reported alcohol use only ketamine users reported using other drugs, including; ecstasy, marijuana, cocaine, amphetamines and heroin (Liao *et al.*, 2011). None of these drugs were controlled for in analysing structural differences between groups and therefore care should be taken when interpreting whether ketamine alone is responsible for the differences observed. This caution should also be extended to the DTI study and fMRI study by Liao et al (2010) and Liao et al (2012) which used the same cohort of study participants.

The difficulty in matching other drug use between ketamine users and control groups is one accepted in the literature and is common to research on recreational drug use (Morgan *et al.*, 2014). In future studies, a potential way around the issue of other drug use is to conduct studies with a larger number of participants, as well as obtaining details of the amounts, frequency and length of use of all other drugs used from all participants. This would allow for better matching of ketamine users to poly-drug controls and would facilitate the exclusion of participants who were outliers or did not match well for certain drug use. For example, if there were a greater number of participants within my study then I might be able to exclude ketamine users who also use heroin so that I get a better match between groups. Better matching of groups for other drug use would allow for more confident interpretations of structural differences observed. Furthermore, this would enable one to perform correlations between measures of ketamine use and

measures of volume change and scores of psychological wellbeing whilst controlling for other drug metrics. In turn, one could determine the extent to which other drug use was impacting on structural differences observed. In addition, with larger n numbers you would expect to see larger effect sizes (due to a smaller standard deviation from the mean). This would be useful for TBM analysis as changes with larger effect sizes are more likely to survive multiple comparison correction.

Having said all this, an alternative to increasing the number of study participants would be to study the effects of repeat ketamine administration in an environment free from other drug use. Hypothetically this would involve studying ketamine users who only used the drug ketamine (and no other drugs) and comparing them to healthy controls (who did not use any drugs). However, practically this scenario is not realistic as no group of people exist who only use ketamine, without using another drug. This does not mean however that we cannot study repeat ketamine administration in an environment free from other drug use and this is where studies in animal models, such as mice, can be used to study this.

By using mice to study the effects of repeat ketamine administration, on brain structure, one eradicates the problem of other drug use by simply administering only ketamine and no other drug to the mice. Additionally, by using mice one can regulate the amount, frequency and duration of drug administration to investigate whether these factors modulate brain structural alterations under ketamine. Moreover, comparable MRI techniques that have been used to study ketamine in humans can be used to study changes in mice. The benefit of this is it enables the comparison of results in mice to those seen in humans. This is also made possible as the gross anatomy of the mouse brain is like that of humans. For example, both mice and humans have bilateral cerebral cortices connected by a band of white matter (known as the corpus callosum), albeit of different complexity. The cerebral cortex in both species can also be split on a functional and anatomical basis into the frontal, parietal, temporal and occipital cortices; which run in the same sequence from the rostral end of the brain to the caudal end (Price, D. et al, (2011). Building Brains. John Wiley & Sons Incorporated; Hendelman, W., (2005). Atlas of Functional Neuroanatomy. Second Edition. CRC Press; Paxinos, G, and Franklin, K.B.J., (2001). The mouse brain in stereotaxic coordinates: Second Edition. Academic Press, New York.).

This is an approach which has been used successfully in laboratories to study ketamine (in the context of understanding the cellular mechanism of psychosis), schizophrenia pathology, antipsychotic drugs and neurodegenerative disease models (Lerch, Carroll, Dorr, *et al.*, 2008; Lerch, Carroll, Spring, *et al.*, 2008; Carroll *et al.*, 2011; Vernon *et al.*, 2012, 2014, 2011; Schobel, Chaudhury and Khan, 2013; Ellegood *et al.*, 2014; Portmann *et al.*, 2014; Harrison *et al.*, 2015; Holmes *et al.*, 2017; Lieberman *et al.*, 2018).

An additional benefit of using mice is that post-mortem investigations can be performed to determine the cellular and molecular correlates of brain structural changes observed using MRI.

f) Summary

In this chapter I was able to show that structural MR differences exist in the brains of repeat ketamine users versus poly-drug controls. Ketamine users have smaller cerebral cortices, cerebellar cortices, nucleus accumbens and caudate nuclei. I was also able to demonstrate that ketamine users present with significantly worse scores of psychological wellbeing. However, I did not find any significant correlations between the level of psychological wellbeing and reduced brain volumes in ketamine users.

Due to poor matching of other drug use between groups and thus poor statistical power, I was unable to correlate structural changes or scores of psychological wellbeing to the amount or frequency of ketamine use. Therefore, I am unable to confidently state that the group-level differences observed are due to ketamine alone.

One way to test the effects of repeat ketamine exposure on the brain is to study repeat ketamine administration in mice where the dose and frequency of ketamine administration can be controlled, and no other drugs are present. In the next chapter, I will present my study on mice which looks at the effects of repeat ketamine administration on brain structure and compares the results to changes seen in human ketamine users.

Chapter 3 The effects of repeat ketamine administration on mouse brain structure

3.1 Introduction

As discussed in Chapter 2, studies investigating the effects of chronic ketamine exposure on brain structure in human users suffer from potentially compromising factors including pre-existing genetic and environmental factors and the use of other psychotropic drugs. Such factors may influence the results seen regarding changes in brain structure and are extremely difficult to adequately control for. Furthermore, to my knowledge, there is no cohort of ketamine users with the same pre-existing genetic and environmental circumstances and who only take ketamine and no other recreational or psychotropic drug. This makes it very difficult to investigate the effects of repeat exposure to ketamine alone, in human users.

In contrast, it is possible to study the effects of repeat ketamine exposure without other confounding influences, upon brain structure in mice, using structural MRI and/or histological methods. The advantage of using mice, with homogenous genetics, identical environmental housing and controlled drug administration to investigate the effects of repeat ketamine administration is that one can be certain that any structural alterations observed are due solely to the drug that has been administered. Furthermore, post-mortem studies can be carried out on mice to assess the underlying cellular and molecular correlates of any observed MRI changes.

An example of where this approach has been effective, in the context of ketamine specifically, is in a study by Schobel et al (2013). In this study Schobel and colleagues measured cerebral blood flow (a marker of functional brain activity) and hippocampal volume in both mice (administered repeat doses of ketamine) and humans at high risk of developing psychosis. The authors found, in both mice and humans, increased cerebral blood flow to the hippocampus which predated structural atrophy in that brain region, and which in humans predicted a transition to psychosis. Furthermore, the authors were able, in mice, to show that an increase in extracellular glutamate, and a reduction in the number of parvalbumin positive GABAergic interneurons, was responsible for the increased cerebral blood flow in the hippocampus and which led to its subsequent atrophy. This study nicely demonstrates the use of MRI techniques in mice to investigate the cellular correlates which may be responsible for similar MR changes observed in humans. This approach has also been successful in studies

investigating schizophrenia pathology, the effects of antipsychotic drugs on brain structure and structural alterations in the brain which arise in neurodegeneration (Lerch, Carroll, Dorr, *et al.*, 2008; Lerch, Carroll, Spring, *et al.*, 2008; Carroll *et al.*, 2011; Vernon *et al.*, 2011, 2012, 2014; Harrison *et al.*, 2015; Holmes *et al.*, 2017; Lieberman *et al.*, 2018).

Taking inspiration from such studies, in this chapter I set out to investigate the effects of repeat ketamine administration on mouse brain volume, using structural MRI (sMRI). My aim was also to compare my findings to the differences previously reported in human repeat ketamine users, to understand better the potential influence of other drug use in results observed in human users; both in my study and in the literature.

As explained in chapter 1, another MRI technique for studying alterations in brain structure is diffusion tensor imaging (DTI). Although there was no DTI data to analyse from the ketamine users / poly-drug controls in chapter 2, there are two published DTI studies that report altered white matter structure in repeat ketamine users (Liao *et al.*, 2010; Edward Roberts *et al.*, 2014). In the first of these studies Liao et al (2010) found that ketamine users present with reduced fractional anisotropy (FA) values (i.e. altered brain structure) in the white matter underlying the frontal cortex and left tempero-parietal cortex, compared to healthy controls. These reductions in FA within the frontal cortex were negatively correlated with the estimated total ketamine consumption; the more ketamine consumed the greater the decrease in FA. However, in this study as in the study by Liao et al (2011), on the same participants, other drug use was not controlled for and it could be that the group-level differences observed are not due wholly (if at all) to ketamine consumption.

In a second study Roberts et al (2014) compared ketamine users to poly-drug controls and found reduced axial diffusivity (AD) (i.e. altered brain structure) in the white matter underlying the frontal, parietal and somatosensory cortices. However, in contrast to the Liao et al (2010) study, these changes could not be correlated to any ketamine use metrics.

It is important to note that these changes in DTI metrics may result from either pathological change at the cellular level (e.g. demyelination, axonal loss, oedema, inflammation), or neural plasticity (e.g. dendritic arborisation, axonal growth) (Zatorre,

Fields and Johansen-Berg, 2012; Stolp *et al.*, 2018). This is highlighted when considering changes in diffusion-based metrics such as fractional anisotropy, which may be the result of changes in myelin, membrane permeability, axonal number or size, or a combination of all of those factors (Zatorre, Fields and Johansen-Berg, 2012). To date, there are no published studies that report on the impact of repeat ketamine exposure on the mouse brain to complement the small body of human work in this area. Based on this, I decided to also use DTI to investigate the effects of repeat ketamine administration on mouse brain structure.

The general aim of this chapter then was to confirm whether repeat ketamine exposure alone is the driver of structural changes observed in the previous chapter and in the studies by Liao et al (2010), Liao et al (2011) and Roberts et al (2014). To achieve this, I investigated differences in brain structure between mice repeatedly administered ketamine and mice repeatedly administered saline.

I tested two different frequencies of ketamine administration: intermittent administration (mice received ketamine once every three days for thirty days) and daily administration (mice received ketamine once daily for fourteen consecutive days). The rationale for these dosing regimen was that in my study of human chronic ketamine users (Chapter 2) and in previously published studies (Liao *et al.*, 2010, 2011; Wang *et al.*, 2013; Edward Roberts *et al.*, 2014) ketamine users differed in their frequency of drug intake. In my study, for example, ketamine users on average used the drug 17±11 days of the month (Chapter 2, table 4). Hence, there are some users who use the drug intermittently, and others which use the drug almost (if not) daily. Because my human study lacked the statistical power and control to determine whether frequency of drug use had an impact on changes in brain structure, I decided to model this in my mouse experiments.

3.2 Experimental aims and hypotheses

a) Hypotheses

1. There will be differences in brain structure in mice repeatedly administered ketamine versus mice repeatedly administered saline in
    a. region of interest volume measurements
    b. TBM volume measurements
    c. FA, MD, AD and RD

b) Aims

1. To determine if there are differences in brain structure between mice repeatedly administered ketamine and mice administered saline, as assessed using MRI
    a. Region of interest measurements of brain volume
    b. Tensor based morphometry (TBM) measurements of brain volume
    c. DTI measures of fractional anisotropy (FA), mean diffusivity (MD), axial diffusivity (AD) and radial diffusivity (RD)
2. To determine whether the frequency of ketamine administration, in mice, modulates any structural differences observed
3. To qualitatively compare differences in brain volume in mice, repeatedly administered ketamine, to differences in brain volume found in repeat ketamine users
    a.

3.3 Materials and methods

a) Mice

Young adult (9-10-week-old) male, wild-type, C57BL/6J mice (Charles River, Harlow, UK) were housed in conventional metal top cages under a 12-hour light/dark cycle, 5 mice to a cage with free access to food and water. Young adult mice were chosen as this roughly matches the demographic of repeat ketamine users in human studies that have investigated the effects of ketamine on brain structure:

- Liao et al (2010,2011,2012); mean age of ketamine users was 26.9 ± 4.87 years, 33 of 41 participant were male
- Roberts et al (2014); mean age of ketamine users was 27 ± 6.74 years and the mean age of first use was 19.9 ± 6.27 years, 93% of study participants were male
- My study (chapter 2); mean age of ketamine users was 28.7 ± 5.11 years, 12 of 17 participants were male.

After a 10-day habituation period, mice were randomly assigned into ketamine and control treatment groups, and drug and vehicle injections began. All *in-vivo* experimental procedures were carried out in accordance with the Home Office Animal Scientific Procedures Act, United Kingdom, 1986.

b) Ketamine Administration

Human ketamine users differ in their frequency of drug use, for example, see Chapter 2 and previously published (Liao *et al.*, 2010, 2011; Wang *et al.*, 2013; Edward Roberts *et al.*, 2014). In my ketamine user dataset for example, the ketamine users were, on average, taking the drug 17 days a month. Hence, there are some individuals who use the drug intermittently and others that use the drug almost (if not) daily. Although my human study lacked the necessary statistical power to determine whether frequency of drug use had any impact on changes in brain structure, previous reports in the literature in larger samples suggest this is the case (Liao *et al.*, 2010). Taking these factors into account, I decided to test whether frequency of ketamine exposure had any impact on brain structure in my mouse experiments. I tested two different frequencies of ketamine administration; intermittent administration (mice received ketamine once every three

days for thirty days) and daily administration (mice received ketamine once daily for fourteen consecutive days).

Mice (n=60) were put into one of these two separate experiments; daily administration (DAY) or intermittent administration (INT). Within these experiments mice were randomly assigned into one of two groups; ketamine (KET) or saline (SAL), resulting in the following comparative groups: KET-DAY (n= 15) v SAL-DAY (n=15) in the daily experiment and KET-INT (n=15) v SAL-INT (n=15) in the intermittent experiment. Mice were administered intraperitoneal injections (i.p.) of either ketamine hydrochloride (ketamine) (Bio-Techne, Abingdon, UK) at 20mg/kg or 0.9% saline, respectively. KET-INT mice were given a single injection of ketamine at 20mg/kg and SAL-INT mice a single injection of 0.9% saline once every three days for thirty days (Figure 4). KET-DAY mice were given a single injection of ketamine and SAL-DAY mice a single injection of saline for 14 recurrent days (Figure 5).

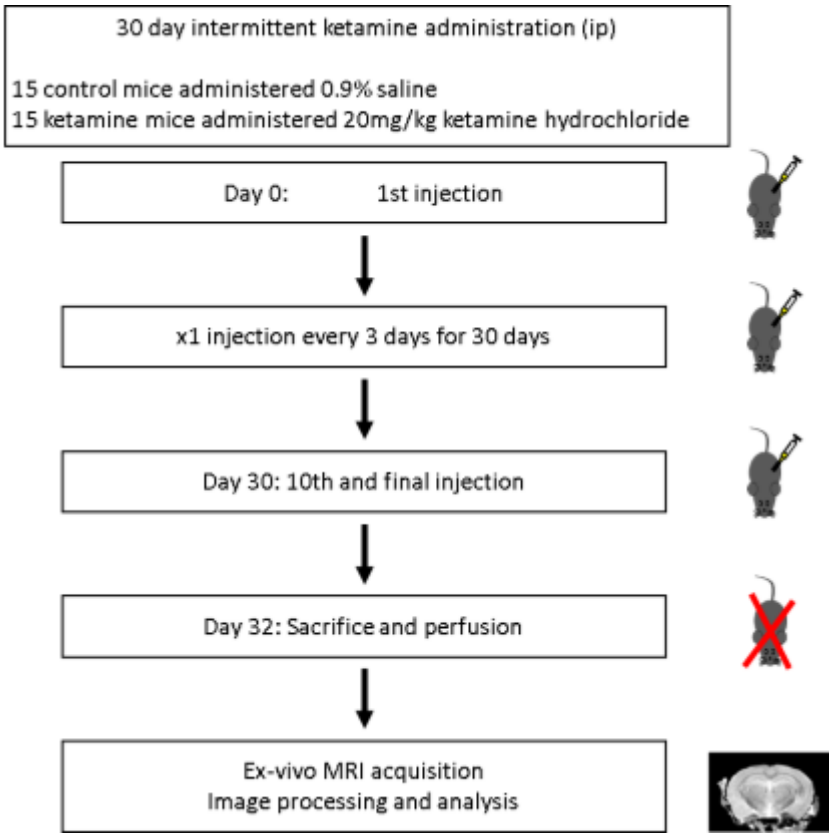

Figure 4. Experimental design for intermittent ketamine administration

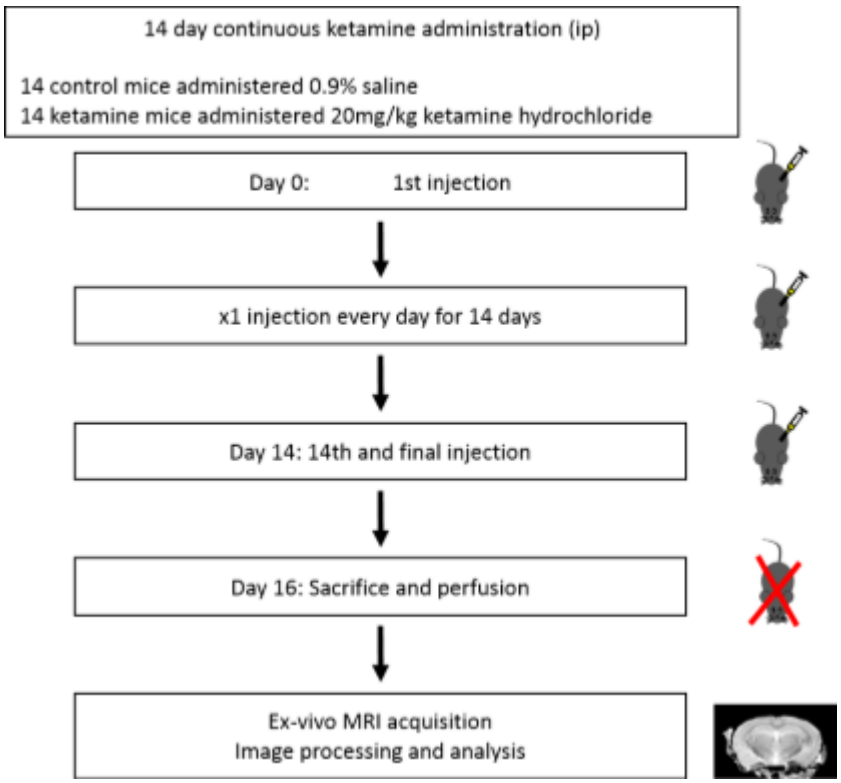

Figure 5. Experimental design for daily ketamine administration

My rationale for choosing a dose of 20mg/kg of ketamine was that a study assessing the effects of repeat ketamine administration in mice, similar to my intermittent experiment, found that a dose of 16-32mg/kg was both necessary and sufficient to induce pathological changes in brain structure, as seen by structural MR (Schobel, Chaudhury and Khan, 2013). These, changes mimicked those seen in a cohort of at-risk patients who transitioned to psychosis. As ketamine users present with sub-threshold levels of psychosis, I rationalised that doses of ketamine in mice, which lead to similar structural changes as seen in humans with psychosis, would be relevant. Furthermore, a study of repeat ketamine administration at 20mg/kg doses in mice aged 9-11 weeks, similar to my daily experiment, has shown long-lasting structural changes to the brain at the cellular level alongside prolonged changes in EEG (Featherstone *et al.*, 2012). Thus, it was my rationale that a 20mg/kg dose would be both necessary and sufficient to investigate potential changes in brain structure in mice repeatedly exposed to ketamine.

c) MRI preparation

Brains were prepared for *ex-vivo* MR image acquisition as per the method documented in Wood et al (2016) and Richetto et al (2016). *Ex-vivo* imaging was preferred to *in-vivo* imaging in order to obtain multiple MR images of the highest resolution possible (Lerch *et al.*, 2012). Moreover, my image acquisition lasted 12.5 hours and *in-vivo* imaging of mice for that length of time was not feasible as it would not have been ethical, healthy for the mice nor practical to keep mice under anaesthetic and in an MRI scanner for that length of time.

After the last injection and a subsequent two-day drug wash out period, mice were sacrificed via an overdose injection of sodium pentobarbital (13mg/10g bodyweight). Mice were then gravity perfused with phosphate buffered saline (PBS) (Sigma-Aldrich, UK), followed by perfusion with 4% paraformaldehyde (PFA) (Sigma-Aldrich, UK). The head was then removed, and skin and excess connective tissue removed, and the skull placed in 4% PFA for overnight fixation. The head was then stripped of the lower jaw and muscle tissue surrounding the skull before being transferred to PBS for 12-15 days, prior to *ex-vivo* MRI acquisition.

d) Ex-vivo MRI Acquisition, Processing and Analysis

A 7 Tesla horizontal small-bore magnet (Agilent Technologies Inc. Santa Clara, USA) and a quadrature volume radiofrequency coil (39 mm internal diameter, Rapid Biomedical GmbH) were used for all MRI acquisitions. Fixed brain samples were placed securely up to three at a time in an MR-compatible holder and immersed in proton-free susceptibility matching fluid (FluorinertTM FC-70; Sigma-Aldrich, UK) before image acquisition. The following were then acquired:

- T2-weighted 3D Fast Spin-Echo structural images of each mouse brain (matrix size= 256 x 256 x 256 with isotropic 112.5 µm voxels, TR= 3000 ms, TE= 40ms) (Figure 6)
- Diffusion tensor images from each mouse brain using a four shot Echo Planar Imaging (EPI) sequence (matrix size= 192 x 128 (40 slices), 150 x 225 x 500 µm

voxels, TR= 4000 ms, TE= 43ms), consisting of 30 diffusion directions with b= 2000 and four b = 0 images (δ/Δ = 4/16ms)

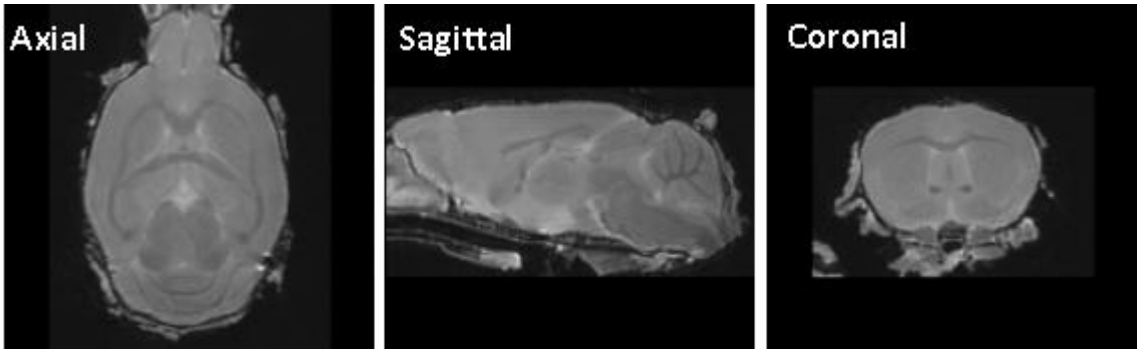

Figure 6. A representative T2-weighted MR image of a mouse brain taken from my study.

e) MRI processing of T2 structural images for volume analysis

MR images were then processed using a combination of *FSL* (Jenkinson *et al.*, 2012), *ANTs* (Avants *et al.*, 2011) and in-house C++ software utilizing the *ITK* library, available from https://github.com/spinicist/QUIT (Richetto *et al.*, 2016; Wood *et al.*, 2016). Multi-head scans were bias-field corrected (Tustison *et al.*, 2010) before being split into individual sample images and skull stripped.

A simple rigid registration was then performed between each subject image and the Dorr Atlas image (Dorr *et al.*, 2008) to ensure all subject images were approximately aligned with one another within the same 3D space. The Dorr atlas image is an average 3D image of 40 adult C57BL/6J mice (Dorr *et al.*, 2008).

An average study template image was then constructed using MR images from all the study animals (Avants *et al.*, 2010). One template was created from all intermittent treated mice and another was created from all daily treated mice, to analyse data in these separate experiments. These templates were then non-linearly registered (moved, stretched and adjusted) to the atlas image. All subject images from each respective experiment (daily or intermittent administration) were non-linearly registered to their respective study template. Logarithmic Jacobian (logJ) determinants were calculated from the inverse warp fields in standard space. logJ determinants in this case are files which store information as to how each 3D voxel in an MR image has been

distorted (moved, stretched ad adjusted) to fit the study template. The inverse transforms from the atlas to the study template and from the study template to each subject were applied to calculate the total brain volume and individual brain ROI volumes of each subject. ROIs match those found in the Dorr MR mouse brain atlas and encompass the entire mouse brain (Dorr *et al.*, 2008).

Or in more layman terms: What the above mouse MR pipeline does is take each T2 structural mouse brain image and split it into 62 ROIs; which incorporate the entire mouse brain. It then registers (moves/ rotates/ stretches and adjusts) each ROI, from individual mouse brain images, to the corresponding ROI from the study template (an average of all individual mouse brain images from each experiment). The way in which each ROI is registered is recorded in a file known as an inverse transform, from this file a measure of volume can be extracted for that specific ROI. Average volume measurements for each ROI from ketamine mice can then be compared to average volume measurements from saline mice. This comparison was performed for both my intermittent and daily experiments. Similarly, the logJ determinant file from each mouse was used to compare how each voxel, in each mouse brain, was distorted to match the study template. Comparing how each specific voxel in the mouse brain was distorted in each mouse gives an indirect measure of volume changes. In this way volume differences can be compared between ketamine treated mice and saline treated mice, at each voxel in the brain.

Multivariate GLM statistics were performed using *IBM SPSS statistics 22* to determine group-level differences in brain ROI volumes. Whole brain volume was used as a covariate and FDR correction (q=0.05) was applied, in *Mathworks MATLAB R2014a*, to correct for multiple comparisons. Voxel-wise group-level differences were determined using the Jacobian determinant images with permutation testing in *FSL randomise*, whole brain volume estimates were included as a covariate and multiple comparisons were FDR corrected (q=0.05).

f) DTI Processing and Analysis

DTI MR images were processed using a combination of *FSL* (Jenkinson *et al.*, 2012), ANTs (Avants *et al.*, 2011) and in-house C++ software utilizing the *ITK* library, available from

https://github.com/spinicist/QUIT (Richetto *et al.*, 2016; Wood *et al.*, 2016). *FSL topup* was used to remove distortion artefacts in the raw diffusion data (Andersson, Skare and Ashburner, 2003). DTI parameter maps for Mean Diffusivity (MD), Axial Diffusivity (AD), Radial Diffusivity (RD) and Fractional Anisotropy (FA) were calculated using *FSL dtifit*. The recorded rigid and non-linear registration transforms for aligning T2 structural scans were concatenated and applied to all DTI parameter maps to align them to the study template. All parameter maps were resampled to match the study template voxel size using a Gaussian interpolator (125µm full-width half-maximum).

Values from each DTI parameter map were calculated for each ROI in the Dorr atlas (Dorr *et al.*, 2008). Multivariate GLM statistics were then performed using *IBM SPSS statistics 22* to determine group-level differences in DTI parameter values for each ROI. Voxel-wise group-level differences, in each DTI parameter, were also analysed using permutation testing in *FSL randomise*. In both ROI and voxel-wise analyses multiple comparisons were FDR corrected (q=0.05) in *Mathworks MATLAB R2014a*.

3.4 Results and discussion

a) Region of interest volume differences in mice repeatedly administered ketamine versus saline

I used an atlas-based ROI method of analysis to determine group-level differences in regional brain volumes between mice repeatedly administered ketamine versus saline. To do so I used a combination of *FSL, ANTs* and in-house C++ software along with the Dorr atlas (Dorr *et al.*, 2008). From here on in I will refer to this combination of tools as the Mouse MR pipeline.

i) Intermittent experiment

Within the intermittent experiment I found significant volume differences in 3 of 62 ROIs at p≤0.05 and FDR q≤0.05 (Table 12). Ketamine mice had a significantly larger frontal lobe and stria medullaris and a significantly smaller fornix, compared to control mice:

- Frontal lobe: KET-INT; 57.42 ± 0.76 mm^3, SAL-INT; 56.31 ± 0.91 mm^3, F=13.19, p<0.001

- Stria medullaris: KET-INT; 0.98 ± 0.03 mm^3, SAL-INT; 0.94 ± 0.04 mm^3, F=9.68, p<0.001
- Fornix: KET-INT; 0.86 ± 0.03 mm^3, SAL-INT; 0.89 ± 0.03 mm^3, F=9.68, p<0.001

A greater volume of the cerebral cortex frontal lobe in KET-INT mice is a surprising initial finding as I expected to see a reduction in volume in this region, as analogously observed in human ketamine users (chapter 2)(Liao *et al.*, 2011; Wang *et al.*, 2013).

i) Daily experiment

Within the daily experiment I found no significant differences in volume between KET-DAY and SAL-DAY mice in any of the 62 ROIs (Table 13); after correcting for multiple comparisons (FDR q≤0.05). This is also a surprising result as I hypothesised that any volume difference observed in the intermittent experiment would be exacerbated in the daily experiment. My rationale being that a greater frequency of ketamine administration would be more damaging to the brain and result in greater atrophy.

Table 12. Region of interest volume measurments between KET-INT and SAL-INT mice.

Region of Interest	Saline mean (mm³)	SD	Ketamine mean (mm3)	SD	F statistic	p value	q value	Cohen's d	Percentage change (%)	
cerebral cortex frontal lobe	56.31	0.91	57.42	0.76	13.19	0.00	0.04	1.32	1.97	↑
fornix	0.89	0.03	0.86	0.03	9.71	0.00	0.05	1.00	-3.61	↓
stria medullaris	0.94	0.04	0.98	0.03	9.68	0.00	0.05	1.13	4.50	↑
interpedunclar nucleus	0.30	0.02	0.32	0.02	4.83	0.04	0.20	-	-	-
medial lemniscus or medial longitudinal fasciculus	3.28	0.11	3.18	0.15	4.76	0.04	0.20	-	-	-
arbor vita of cerebellum	11.87	0.35	11.64	0.37	4.75	0.04	0.20	-	-	-
superior olivary complex	1.06	0.09	1.12	0.08	4.55	0.04	0.20	-	-	-
cerebral cortex parieto-temporal lobe	100.81	1.12	101.95	1.90	3.98	0.06	0.22	-	-	-
striatum	26.50	0.47	26.21	0.47	3.44	0.07	0.26	-	-	-
pons	22.76	0.41	22.47	0.44	3.19	0.09	0.27	-	-	-
facial nerve (cranial nerve 7)	0.31	0.02	0.30	0.02	3.09	0.09	0.27	-	-	-
cerebral cortex entorhinal cortex	13.50	0.50	13.80	0.51	2.56	0.12	0.31	-	-	-
lateral ventricle	4.88	0.27	4.73	0.28	2.46	0.13	0.31	-	-	-
midbrain	18.07	0.31	17.88	0.39	2.30	0.14	0.31	-	-	-
medulla	35.23	1.50	34.18	2.24	2.27	0.14	0.31	-	-	-
cerebellar cortex	58.82	0.89	58.16	1.49	2.09	0.16	0.31	-	-	-
thalamus	23.14	0.50	23.36	0.51	1.40	0.25	0.40	-	-	-
superior colliculus	11.54	0.23	11.64	0.27	1.29	0.27	0.40	-	-	-
olfactory tubercle	4.92	0.14	4.86	0.15	1.22	0.28	0.40	-	-	-
periaqueductal grey	5.41	0.22	5.50	0.21	1.16	0.29	0.40	-	-	-
superior cerebellar peduncle	1.30	0.04	1.28	0.05	0.97	0.33	0.45	-	-	-
hippocampus	27.23	0.58	27.03	0.60	0.76	0.39	0.47	-	-	-
hypothalamus	14.46	0.46	14.57	0.36	0.61	0.44	0.47	-	-	-
fimbria	4.38	0.16	4.43	0.23	0.58	0.45	0.47	-	-	-
posterior commissure	0.19	0.01	0.18	0.02	0.57	0.46	0.47	-	-	-
pars posterior anterior commissure	0.59	0.03	0.60	0.04	0.56	0.46	0.47	-	-	-
cerebral peduncle	2.96	0.08	2.98	0.09	0.53	0.47	0.47	-	-	-
stria terminalis	1.25	0.03	1.26	0.05	0.45	0.51	0.48	-	-	-
nucleus accumbens	5.14	0.16	5.18	0.15	0.42	0.52	0.48	-	-	-
lateral septum	4.23	0.15	4.20	0.12	0.40	0.53	0.48	-	-	-
basal forebrain	6.95	0.25	6.90	0.22	0.35	0.56	0.48	-	-	-
fundus of striatum	0.26	0.02	0.25	0.02	0.28	0.60	0.50	-	-	-
corticospinal tract or pyramids	2.02	0.06	2.03	0.07	0.24	0.63	0.52	-	-	-
globus pallidus	3.69	0.14	3.71	0.14	0.11	0.74	0.59	-	-	-
subependymale zone or rhinocele	0.11	0.01	0.11	0.01	0.10	0.75	0.59	-	-	-
mammillary bodies	0.68	0.04	0.68	0.04	0.06	0.80	0.59	-	-	-
corpus callosum	22.75	0.47	22.80	0.59	0.06	0.81	0.59	-	-	-
middle cerebellar peduncle	1.52	0.05	1.51	0.08	0.05	0.82	0.59	-	-	-
olfactory bulbs	38.65	0.57	38.61	0.44	0.03	0.86	0.59	-	-	-
cerebral cortex occipital lobe	9.05	0.29	9.03	0.32	0.02	0.89	0.60	-	-	-
pre-para subiculum	3.08	0.13	3.07	0.13	0.01	0.93	0.62	-	-	-
internal capsule	3.48	0.06	3.48	0.13	0.00	1.00	0.62	-	-	-
cerebral aqueduct	0.63	0.06	0.68	0.05	6.93	0.01	0.13	-	-	-
cuneate nucleus	0.38	0.03	0.35	0.05	4.05	0.05	0.22	-	-	-
medial septum	1.62	0.08	1.58	0.06	2.22	0.15	0.31	-	-	-
pontine nucleus	0.93	0.09	0.88	0.08	2.07	0.16	0.31	-	-	-
inferior colliculus	7.79	0.30	7.93	0.26	1.91	0.18	0.32	-	-	-
lateral olfactory tract	1.71	0.06	1.68	0.05	1.88	0.18	0.32	-	-	-
optic tract	2.20	0.07	2.17	0.07	1.53	0.23	0.38	-	-	-
pars anterior anterior commissure	1.86	0.06	1.88	0.06	1.21	0.28	0.40	-	-	-
bed nucleus of stria terminalis	1.83	0.06	1.86	0.08	0.82	0.37	0.47	-	-	-
fasciculus retroflexus	0.42	0.02	0.43	0.02	0.77	0.39	0.47	-	-	-
dentate gyrus of hippocampus	5.07	0.14	5.12	0.18	0.62	0.44	0.47	-	-	-
habenular commissure	0.05	0.01	0.05	0.00	0.59	0.45	0.47	-	-	-
fourth ventricle	0.54	0.03	0.53	0.04	0.37	0.55	0.48	-	-	-
stratum granulosum of hippocampus	1.27	0.04	1.28	0.05	0.36	0.55	0.48	-	-	-
amygdala	19.21	0.38	19.15	0.65	0.06	0.81	0.59	-	-	-
inferior olivary complex	0.45	0.05	0.45	0.05	0.05	0.82	0.59	-	-	-
inferior cerebellar peduncle	1.12	0.09	1.13	0.06	0.04	0.84	0.59	-	-	-
third ventricle	1.79	0.05	1.79	0.13	0.00	0.96	0.62	-	-	-
mammilothalamic tract	0.39	0.01	0.39	0.02	0.00	0.97	0.62	-	-	-
ventral tegmental decussation	0.19	0.02	0.20	0.01	0.00	0.98	0.62	-	-	-
Summary regions										
Cerebral grey	324.01	1.87	326.35	2.95	6.54	0.02	0.02	0.95	0.72	↑
Cerebral White	42.34	0.57	42.49	0.75	0.37	0.55	0.10	-	-	-
Olfactory	45.38	0.56	45.26	0.47	0.40	0.53	0.10	-	-	-
Cerebellum	74.63	0.93	73.72	1.70	3.31	0.08	0.04	-	-	-
Ventricles	7.84	0.22	7.72	0.35	1.19	0.28	0.08	-	-	-
Brainstem	109.72	1.75	108.42	2.53	2.61	0.12	0.04	-	-	-

Table 13. Region of interest volume measurments between KET-DAY and SAL-DAY mice.

Region of Interest	Saline mean (mm^3)	SD	Ketamine mean (mm3)	SD	F statistic	p value	q value
corpus callosum	22.15	0.67	21.71	0.71	12.34	0.002	0.082
basal forebrain	6.69	0.28	6.91	0.27	8.39	0.008	0.164
cerebral cortex occipital lobe	9.27	0.37	8.95	0.45	5.91	0.023	0.246
arbor vita of cerebellum	11.60	0.42	11.29	0.48	5.18	0.032	0.262
olfactory tubercle	5.12	0.22	4.98	0.22	3.83	0.062	0.410
amygdala	19.00	0.76	19.36	0.74	3.57	0.070	0.410
pons	22.37	0.81	21.98	0.56	2.94	0.099	0.451
middle cerebellar peduncle	1.60	0.07	1.55	0.09	2.88	0.102	0.451
facial nerve (cranial nerve 7)	0.31	0.02	0.31	0.01	2.74	0.110	0.451
fimbria	4.07	0.24	4.17	0.22	2.44	0.131	0.476
lateral septum	4.16	0.36	4.29	0.27	1.62	0.215	0.529
cerebellar cortex	57.87	1.98	57.25	1.71	1.45	0.239	0.529
pre-para subiculum	2.85	0.14	2.79	0.12	1.44	0.242	0.529
stria medullaris	0.90	0.04	0.88	0.06	1.42	0.244	0.529
lateral olfactory tract	1.71	0.06	1.68	0.08	1.32	0.261	0.529
inferior cerebellar peduncle	1.20	0.07	1.17	0.06	1.28	0.268	0.529
superior colliculus	11.50	0.52	11.60	0.39	1.11	0.302	0.529
cerebral cortex parieto-temporal lobe	100.46	3.90	100.80	3.08	1.02	0.322	0.529
pontine nucleus	0.89	0.08	0.85	0.09	1.02	0.323	0.529
internal capsule	3.36	0.11	3.32	0.13	0.90	0.351	0.545
cerebral peduncle	2.92	0.13	2.95	0.12	0.85	0.367	0.545
lateral ventricle	4.64	0.57	4.78	0.49	0.81	0.377	0.545
striatum	26.26	1.01	26.07	0.83	0.73	0.402	0.545
hypothalamus	13.83	0.73	13.96	0.45	0.64	0.431	0.545
periaqueductal grey	5.41	0.21	5.47	0.26	0.62	0.439	0.545
globus pallidus	3.70	0.13	3.72	0.14	0.57	0.457	0.551
bed nucleus of stria terminalis	1.70	0.09	1.68	0.09	0.53	0.473	0.552
cerebral cortex entorhinal cortex	13.72	0.66	13.81	0.45	0.50	0.485	0.552
pars anterior anterior commissure	1.70	0.09	1.68	0.06	0.43	0.520	0.553
hippocampus	27.46	0.79	27.28	1.15	0.41	0.526	0.553
mammillary bodies	0.57	0.09	0.59	0.06	0.35	0.560	0.560
olfactory bulbs	37.95	1.59	38.09	0.92	0.26	0.614	0.560
ventral tegmental decussation	0.16	0.02	0.16	0.02	0.25	0.619	0.560
thalamus	22.58	0.96	22.46	0.74	0.23	0.636	0.560
superior cerebellar peduncle	1.24	0.06	1.23	0.04	0.22	0.645	0.560
cerebral cortex frontal lobe	54.62	1.50	54.76	1.88	0.21	0.648	0.560
midbrain	17.57	0.70	17.61	0.55	0.20	0.656	0.560
corticospinal tract or pyramids	1.99	0.15	2.01	0.10	0.14	0.711	0.594
interpedunclar nucleus	0.32	0.03	0.32	0.02	0.13	0.725	0.594
medulla	34.11	3.18	34.35	1.96	0.11	0.743	0.597
mammilothalamic tract	0.35	0.02	0.35	0.03	0.06	0.807	0.636
nucleus accumbens	5.13	0.28	5.13	0.20	0.01	0.943	0.657
fornix	0.82	0.05	0.82	0.03	0.00	0.988	0.657
medial lemniscus or medial longitudinal fasciculus	3.07	0.24	3.06	0.17	0.00	0.991	0.657
optic tract	2.08	0.09	2.07	0.08	0.00	0.995	0.657
fasciculus retroflexus	0.38	0.02	0.36	0.02	5.80	0.024	0.246
subependymale zone or rhinocele	0.10	0.01	0.10	0.01	2.28	0.143	0.476
third ventricle	1.64	0.09	1.68	0.10	2.20	0.151	0.476
fundus of striatum	0.25	0.02	0.26	0.02	1.34	0.258	0.529
cuneate nucleus	0.34	0.05	0.36	0.05	1.11	0.302	0.529
medial septum	1.60	0.11	1.57	0.07	1.07	0.310	0.529
cerebral aqueduct	0.70	0.04	0.68	0.08	0.73	0.401	0.545
habenular commissure	0.04	0.01	0.04	0.01	0.64	0.430	0.545
posterior commissure	0.15	0.01	0.16	0.01	0.45	0.511	0.553
superior olivary complex	1.06	0.07	1.04	0.07	0.31	0.581	0.560
stria terminalis	1.19	0.05	1.20	0.06	0.21	0.651	0.560
fourth ventricle	0.50	0.02	0.51	0.05	0.05	0.830	0.642
pars posterior anterior commissure	0.59	0.04	0.59	0.03	0.04	0.848	0.643
dentate gyrus of hippocampus	5.11	0.18	5.12	0.28	0.02	0.880	0.655
inferior olivary complex	0.42	0.11	0.42	0.08	0.01	0.904	0.657
stratum granulosum of hippocampus	1.30	0.07	1.30	0.10	0.01	0.916	0.657
inferior colliculus	7.43	0.44	7.41	0.39	0.00	0.962	0.657
Summary Regions							
Cerebral grey	320.28	10.28	320.78	9.17	0.81	0.375	-
Cerebral White	40.70	1.23	40.31	1.23	2.55	0.123	-
Olfactory	44.88	1.72	44.84	1.08	0.00	0.978	-
Cerebellum	73.49	2.39	72.48	2.21	2.85	0.104	-
Ventricles	7.48	0.60	7.65	0.49	1.21	0.282	-
Brainstem	106.95	4.61	106.94	3.25	0.02	0.878	-

b) Volume differences between mice repeatedly administered ketamine versus saline, as seen by TBM analysis

In chapter 2, I first analysed volume differences between ketamine users and controls using a region of interest approach. I then performed a complimentary TBM analysis to specifically locate where, in each region, volume changes were. I used a similar approach in this chapter when analysing my mouse MR data. From my ROI analysis of volume differences between KET-INT and SAL-INT mice I found KET-INT mice to have a significantly larger frontal lobe. To specifically locate in which voxels of the frontal lobe this difference was I performed a whole-brain voxel by voxel TBM analysis.

i) Intermittent experiment

Within the intermittent experiment I found significant qualitative, group-level volume differences in voxels spanning multiple brain regions (Figure 7). A summary of which regions contain voxels with a significant difference in volume can be found in Table 14.

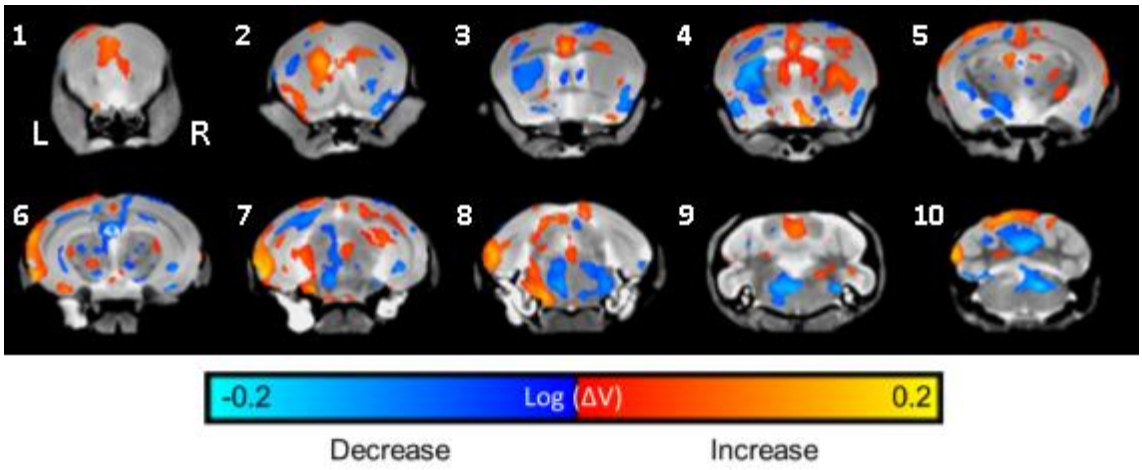

Figure 7. Coronal brain slices displaying TBM analysis of volumetric differences between KET-INT and SAL-INT mice**.** Smaller volumes in KET-INT mice are displayed in blue. Larger volumes in KET-INT mice are displayed in red. Data shown are thresholded at $p<0.05$, FDR corrected at $q=0.05$. L = Left, R = Right.

Of the 62 ROIs previously analysed 42 contain voxels that either show a larger volume (red blobs) or a smaller volume (blue blobs) in KET-INT mice. Some regions, such as the hippocampus, show both larger volumes in a cluster of voxels (left hippocampus) and

smaller volumes in another subset of voxels (right hippocampus) (panel 7, Figure 7). Unilateral differences in volume can also be seen in clusters of voxels in other brain regions. For example, within the parietal lobe (panel 4, Figure 7) a cluster of voxels in the lower cortical layers of the left cortex show smaller volumes in KET-INT mice, whereas in the upper layers of the left cortex there is a cluster of voxels depicting larger volumes. Furthermore, this pattern is reversed in the right hemisphere of the parietal cortex (panel 4, Figure 7); a cluster of voxels in the lower cortical layers depict larger volumes and a cluster of voxels in the upper layers depict smaller volumes. Such converse changes across the parietal lobe and hippocampus might explain why no overall difference in volume were seen at the ROI level; as the sum of voxels depicting smaller volumes cancels out the sum of voxels depicting larger volumes.

Looking more closely at the frontal lobe we can see that a small cluster of voxels, depicting a larger volume in KET-INT mice, is responsible for an overall larger volume in KET-INT mice at the ROI level.

Overall ketamine is having a widespread effect on volume across the brain when given intermittently.

Table 14. ROI analysis versus voxel-wise analysis for volumetric differences in the intermittent experiment. Regions where significant ($p<0.05$, FDR $q<0.05$) volume changes reside are highlighted in green. Regions where no significant changes reside are highlighted in red.

Region of Interest	ROI analysis	Voxel Analysis
cerebral cortex frontal lobe	✓	✓
fornix	✓	✓
stria medullaris	✓	✓
interpeduncular nucleus	x	✓
medial lemniscus or medial longitudinal fasciculus	x	✓
arbor vita of cerebellum	x	✓
superior olivary complex	x	✓
cerebral cortex parieto-temporal lobe	x	✓
striatum	x	✓
pons	x	✓
facial nerve (cranial nerve 7)	x	✓
cerebral cortex entorhinal cortex	x	✓
lateral ventricle	x	✓
midbrain	x	✓
medulla	x	✓
cerebellar cortex	x	✓
thalamus	x	✓
superior colliculus	x	✓
olfactory tubercle	x	✓
periaqueductal grey	x	✓
superior cerebellar peduncle	x	✓
hippocampus	x	✓
hypothalamus	x	✓
fimbria	x	✓
posterior commissure	x	✓
pars posterior anterior commissure	x	✓
cerebral peduncle	x	✓
stria terminalis	x	✓
nucleus accumbens	x	✓
lateral septum	x	✓
basal forebrain	x	✓
fundus of striatum	x	✓
corticospinal tract or pyramids	x	✓
globus pallidus	x	✓
subependymale zone or rhinocele	x	✓
mammillary bodies	x	✓
corpus callosum	x	✓
middle cerebellar peduncle	x	✓
olfactory bulbs	x	✓
cerebral cortex occipital lobe	x	✓
pre-para subiculum	x	✓
internal capsule	x	✓
cerebral aqueduct	x	x
cuneate nucleus	x	x
medial septum	x	x
pontine nucleus	x	x
inferior colliculus	x	x
lateral olfactory tract	x	x
optic tract	x	x
pars anterior anterior commissure	x	x
bed nucleus of stria terminalis	x	x
fasciculus retroflexus	x	x
dentate gyrus of hippocampus	x	x
habenular commissure	x	x
fourth ventricle	x	x
stratum granulosum of hippocampus	x	x
amygdala	x	x
inferior olivary complex	x	x
inferior cerebellar peduncle	x	x
third ventricle	x	x
mammilothalamic tract	x	x
ventral tegmental decussation	x	x

ii) Daily administration

In contrast to the atlas-based analysis, voxel-wise TBM analysis revealed significant differences in volume between KET-DAY and SAL-DAY mice in multiple brain regions (Figure 8). A summary of which regions contain voxels with a significant difference in volume can be found in Table 15.

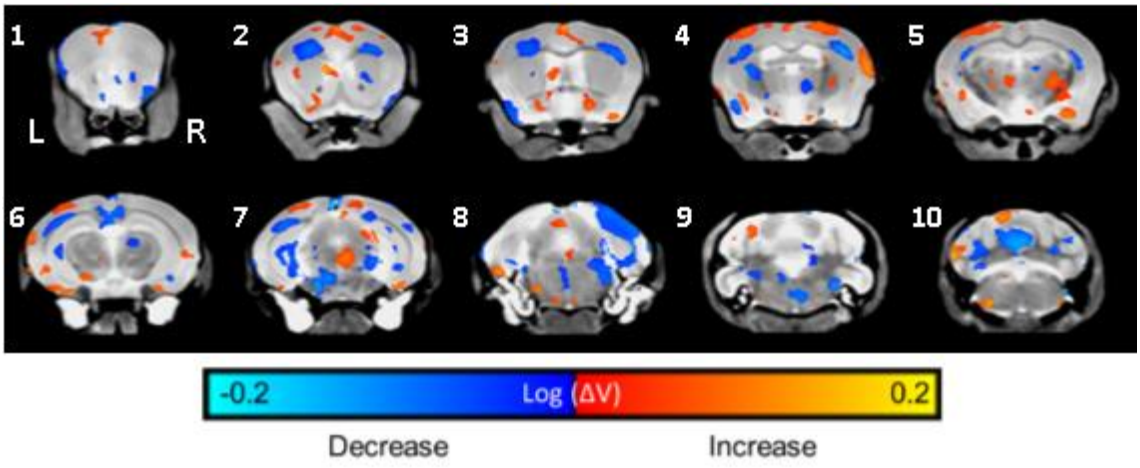

Figure 8. Coronal brain slices displaying TBM analysis of volumetric differences between KET-DAY and SAL-DAY mice**. S**maller volumes in KET mice are displayed in blue. Larger volumes in KET mice are displayed in red. Data shown are thresholded at $p<0.05$, FDR corrected at $q=0.05$. L = Left, R = Right.

Of the 62 ROIs previously analysed 45 contain voxels that show a significant difference in volume. There are some bilateral differences in volume between KET-DAY and SAL-INT mice. For example, there is a bilateral decrease in volume in the corpus callosum (panels 2-4, Figure 8). There is also a bilateral increase in volume in voxels of the upper layers of the parietal cortex (panel 4, Figure 8). Overall, like the intermittent experiment, there is a widespread effect on brain volume in KET-DAY mice.

Table 15. ROI analysis versus voxel-wise analysis for volumetric differences in the daily experiment. Regions where significant ($p<0.05$, FDR $q<0.05$) volume changes reside are highlighted in green. Regions where no significant changes reside are highlighted in red.

Region of interest	ROI analysis	Voxel Analysis
amygdala	X	✔
arbor vita of cerebellum	X	✔
basal forebrain	X	✔
bed nucleus of stria terminalis	X	✔
cerebellar cortex	X	✔
cerebral cortex entorhinal cortex	X	✔
cerebral cortex frontal lobe	X	✔
cerebral cortex occipital lobe	X	✔
cerebral cortex parieto-temporal lobe	X	✔
cerebral peduncle	X	✔
corpus callosum	X	✔
corticospinal tract or pyramids	X	✔
facial nerve (cranial nerve 7)	X	✔
fimbria	X	✔
fornix	X	✔
globus pallidus	X	✔
hippocampus	X	✔
hypothalamus	X	✔
inferior cerebellar peduncle	X	✔
internal capsule	X	✔
interpedunclar nucleus	X	✔
lateral olfactory tract	X	✔
lateral septum	X	✔
lateral ventricle	X	✔
mammillary bodies	X	✔
mammilothalamic tract	X	✔
medial lemniscus or medial longitudinal fasciculus	X	✔
medulla	X	✔
midbrain	X	✔
middle cerebellar peduncle	X	✔
nucleus accumbens	X	✔
olfactory bulbs	X	✔
olfactory tubercle	X	✔
optic tract	X	✔
pars anterior anterior commissure	X	✔
periaqueductal grey	X	✔
pons	X	✔
pontine nucleus	X	✔
pre-para subiculum	X	✔
stria medullaris	X	✔
striatum	X	✔
superior cerebellar peduncle	X	✔
superior colliculus	X	✔
thalamus	X	✔
ventral tegmental decussation	X	✔
cerebral aqueduct	X	X
cuneate nucleus	X	X
dentate gyrus of hippocampus	X	X
fasciculus retroflexus	X	X
fourth ventricle	X	X
fundus of striatum	X	X
habenular commissure	X	X
inferior colliculus	X	X
inferior olivary complex	X	X
medial septum	X	X
pars posterior anterior commissure	X	X
posterior commissure	X	X
stratum granulosum of hippocampus	X	X
stria terminalis	X	X
subependymale zone or rhinocele	X	X
superior olivary complex	X	X
third ventricle	X	X

iii) Comparing results across daily and intermittent experiments

In both the daily and intermittent experiments ketamine has altered brain volume across multiple voxels in multiple brain regions. Some regions contain similar clusters of voxels depicting the same direction of change in volume, for example:

- Frontal cortex; in both experiments there are voxels within and next to the prefrontal cortex which depict an increase in volume in mice given ketamine. This cluster of voxels is larger in KET-INT mice and spans more of the prefrontal cortex and motor cortex (panel 1, Figure 7) than in KET-DAY mice (panel 1, Figure 8)
- Parietal cortex; in both experiments there are voxels within the upper layers of the parietal cortex (more so in the left hemisphere of the somatosensory areas) that depict larger volumes in both KET-INT mice (panels 4&5, Figure 7) and KET-DAY mice (panels 4&5, Figure 8)
- Cerebellar cortex; in both experiments there are voxels within the cerebellar cortex that show a smaller volume within mice given ketamine (panel 10 Figure 7 and panel 10 Figure 8). The cluster size is roughly equal in both experiments.

These data suggest that repeat ketamine exposure has common effects on brain structure regardless of the interval of repeat administration, which suggests that these changes may be driven by similar cellular and molecular mechanisms. However, there are also clusters of voxels in the same anatomical, location across both experiments, which show opposite changes in volume in mice given ketamine. For example, in the corpus callosum of KET-INT mice there is an increase in volume (panel 2, Figure 7), whereas in KET-DAY mice there is a decrease in volume (panel 2, Figure 8). This would suggest that the interval of repeat ketamine administration has different effects on brain structure which might arise through different cellular and molecular mechanisms. Moreover, there are also structural changes present in the intermittent experiment that are not present in the daily experiment and vice-versa. Examples include;

- A large cluster of voxels in the left striatum of KET-INT mice that displays a significant reduction in volume (panel 3, Figure 7), which is not present in KET-DAY mice.

- A large cluster of voxels in the right visual cortex of KET-DAY mice that displays a significant reduction in volume (panel 8, Figure 8), which is not present in KET-INT mice.

c) Comparing the effects on brain volume of repeat ketamine administration in mice to repeat ketamine use in humans

Consistent with and extending the published findings of Liao et al (2011) and Wang et al (2013), the data presented in chapter 2 of this thesis provides evidence that repeat ketamine use in humans results in significant reductions in brain volume in the cerebral cortex, cerebellum and caudate/putamen (i.e. striatum). In the subsequent section, I compare these volume changes to those observed in mice exposed to both daily and intermittent ketamine administration.

i) Cerebral cortex

Data presented in chapter 2 of this thesis suggests that chronic ketamine users present with a smaller cerebral cortex, specifically in the frontal lobe; superior frontal cortex and middle frontal cortex, consistent with published data (Liao *et al.*, 2011; Wang *et al.*, 2013). However, in contrast to these data, in my mouse ketamine experiments I did not find any general reduction in cortical volume. The atlas-based segmentation data suggested that mice exposed to ketamine intermittently (KET-INT), but not daily (KET-DAY), have a significantly larger frontal lobe. The TBM analysis of structural MR images from both KET-INT and KET-DAY mice, which has increased sensitivity, extends this to reveal clusters of voxels with significantly increased volume in the prefrontal cortex (PFC; panel 1 Figure 7 and panel 1 Figure 8), supplementary motor area (panels 4-6 Figure 7 and panels 4-6 Figure 8), anterior cingulate cortex (ACC; panel 3 Figure 7 and panel 3 Figure 8), visual cortex and auditory cortex (panels 6&7 Figure 7 and panels 6&7 Figure 8). Thus, at the level of the frontal lobe, the impact of ketamine exposure in humans and mice appears to be completely opposite. It is important to note however, that the TBM analysis also reveals sparse, but statistically significant clusters of voxels in the somatosensory cortex, motor cortex, insular cortex, piriform cortex and visual cortex with reduced volume in both KET-INT and KET-DAY mice.

Overall then, with regards to the impact of repeat ketamine exposure, there are both similarities and differences across the two species. The mechanism by which these different changes arise is for the moment unclear and species-specific effects are possible and cannot be definitively excluded.

It is conceivable, however, that these differences, particularly in the frontal lobe are the by-product of additional drug use in human ketamine users. I hypothesize that heavy and frequent use of multiple psychotropic drugs by ketamine users is having a detrimental effect on the frontal lobe leading to cerebral atrophy. Indeed, in the study by Liao (2011), the data were not controlled for smoking status and there is evidence to suggest that smoking directly impacts on brain volume (Li *et al.*, 2015; Peng *et al.*, 2018).

ii) Cerebellum

Data published by Wang et al (2013), report cerebellar atrophy in ketamine users compared to a small number of non-poly drug users as controls. Controlling (insofar as possible) for poly-drug use, my own data in chapter 2, confirms that ketamine users have a significantly reduced volume of the cerebellar cortex, as compared to poly-drug controls. Atlas based segmentation of the mouse ketamine data, did not find any significant differences in the total volume of the cerebellar cortex in either KET-INT or KET-DAY mice, compared to vehicle controls. In contrast, the more sensitive TBM analysis revealed that both KET-INT and KET-DAY mice have clusters of voxels with significantly reduced volume in cerebellar cortex lobules 4 and 5 (panel 10 Figure 7 and panel 10 Figure 8). Notably, this analysis also revealed clusters of voxels with significant volume increases in both KET-INT and KET-DAY mice in lobule 6 of the cerebellar cortex. These contradictory effects in the mouse TBM data therefore likely explain the lack of overall differences in total cerebellar cortex volume. These data also suggest that repeat ketamine exposure has both common and distinct effects on the volume of the cerebellum across species, as revealed by the greater sensitivity and higher resolution of the mouse data.

iii) Striatum

Like in the cerebellum, Wang et al (2013) reported evidence for atrophy of the striatum of ketamine users. My own data on ketamine users also provides evidence for decreased

volume of the nucleus accumbens and caudate nucleus (Chapter 2) as compared to poly-drug controls. Atlas-based segmentation analysis revealed that neither the volumes of the striatum nor the nucleus accumbens were significantly different to vehicle controls in both KEY-INT and KET-DAY exposed mice. Again however, the more sensitive TBM analyses of these datasets revealed clusters of voxels with reduced volume in the left striatum of both KET-INT and KET-DAY mice, as compared to vehicle controls. These, at least qualitatively, appear to be largest in the KET-INT exposed mice. However, it is also worth noting that TBM analysis revealed small clusters of voxels with increased volume in the left nucleus accumbens of both KET-INT and KET-DAY mice as compared to vehicle controls.

d) Region of interest analysis of DTI differences in mice repeatedly given ketamine or saline

As discussed in chapter 1 and the introduction to this chapter, DTI is used to measure structural changes in the brain by measuring the diffusion of water through neural tissue (Le Bihan *et al.*, 2001). MD is a measure of the mean rate of water diffusion in a given locus in all directions. AD is a measure of water diffusion parallel to the orientation of axons and white matter fibres. RD is a measure of the diffusion of water orthogonal to the orientation of axons and white matter fibres. FA is a measure of the preferential diffusion of water molecules in each direction. Values of FA range from 0 (isotropic diffusion) to 1 (anisotropic diffusion). Differences in any of these parameters between ketamine and saline mice would suggest a difference in the cellular composition of neural tissue in that given region of the brain.

Using the mouse MR pipeline, I split each of the DTI scans into the following DTI parameter maps; FA, MD, RD and AD. Differences in any of these parameters between ketamine and saline mice would be predicted to suggest a difference in the cellular composition of neural tissue in that given position within the brain, which may be more sensitive than volumetric changes alone.

I first used the MR pipeline to extract values of FA, MD, AD and RD for each of the 62 ROIs comprising the Dorr atlas (Dorr *et al.*, 2008), from parameter maps from every mouse in my daily and intermittent experiments. I then compared average values for

each DTI parameter between KET-INT and SAL-INT mice and between KET-DAY and SAL-DAY mice.

i) Mean diffusivity (MD)

I first compared average values of MD in KET-INT mice versus SAL-INT mice. I found no significant differences in any of the 62 ROIs (Figure 9 and Table 16).

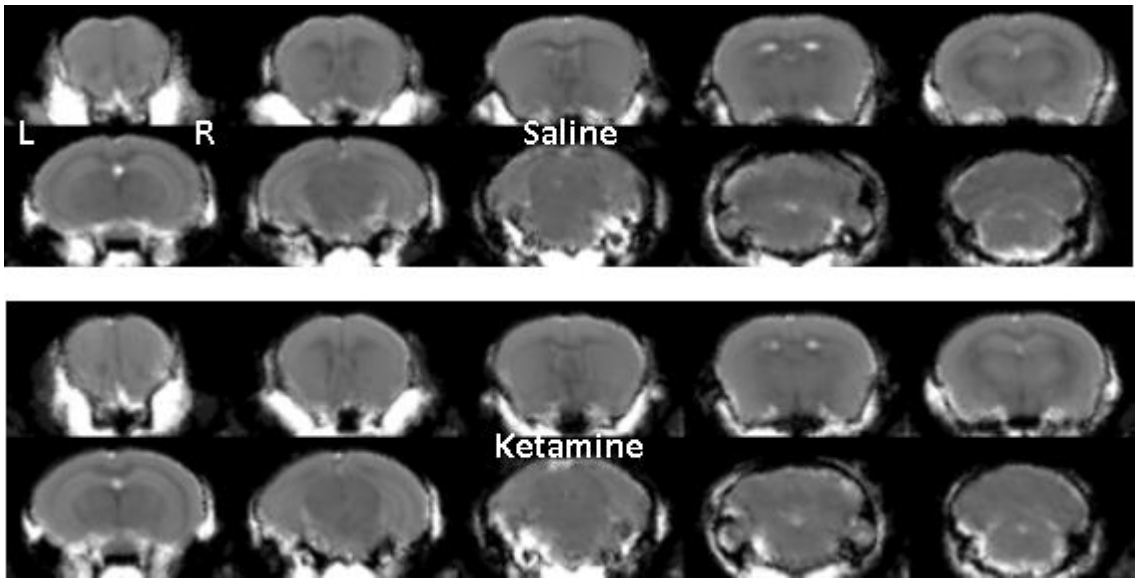

Figure 9. Coronal sections of group mean MD images from KET-INT and SAL-INT mice. L= left, R= Right.

Next, I compared average MD values between KET-DAY and SAL-DAY mice. I found significant reductions, at $p \leq 0.05$ and FDR $q \leq 0.05$, in MD in 24 of 62 ROIs (Figure 10 and Table 17). Of these 10 were grey matter ROIs; entorhinal cortex, parieto-temporal lobe, frontal lobe, inferior olivary complex, superior olivary complex, interpeduncular nucleus, pontine nucleus, superior colliculus, midbrain and amygdala. A further 13 were white matter ROIs; arbor vita of the cerebellum, inferior cerebellar peduncle, corpus callosum, fimbria, fornix, optic tract, mammillothalamic tract, stria medullaris, fasciculus retroflexus, cerebral peduncle, medial lemniscus, facial nerve and lateral septum. The remaining ROI showing a significant difference in MD between groups was the fourth ventricle.

Of the 13 white matter ROIs which displayed a significant decrease in MD, 2 were in the cerebellum; arbor vita of the cerebellum and the inferior cerebellar peduncle. These two changes resulted in an overall decrease in MD in the cerebellum (KET-DAY; 3.18 ± 0.24 mm^2s^{-1}, SAL-DAY; 3.40 ± 0.16 mm^2s^{-1}, t=2.82, p=0.01).

Table 16. Region of interest differences in mean diffusivity (MD) between KET-INT and SAL-INT mice.

Region of Interest	Saline mean ($mm^2 s^{-1}$)	SD	Ketamine mean ($mm^2 s^{-1}$)	SD	T statistic	p value	q value
inferior cerebellar peduncle	3.33	0.35	3.78	0.60	-2.48	0.021	0.318
cerebral peduncle	3.86	0.38	3.43	0.56	2.44	0.022	0.318
optic tract	3.55	0.48	3.14	0.46	2.35	0.026	0.318
superior olivary complex	3.71	0.80	4.47	1.05	-2.23	0.035	0.318
amygdala	3.82	0.40	3.55	0.27	2.16	0.041	0.318
cuneate nucleus	3.11	0.14	3.23	0.17	-2.13	0.042	0.318
medial septum	3.21	0.50	2.85	0.48	2.02	0.053	0.344
olfactory tubercle	4.09	0.75	3.60	0.64	1.90	0.068	0.367
cerebral cortex frontal lobe	3.51	0.18	3.35	0.28	1.79	0.087	0.367
facial nerve (cranial nerve 7)	3.20	0.44	3.52	0.55	-1.76	0.089	0.367
cerebral cortex parieto-temporal lobe	3.38	0.19	3.25	0.24	1.65	0.110	0.416
cerebral cortex entorhinal cortex	3.19	0.55	3.58	0.76	-1.60	0.122	0.426
basal forebrain	3.22	0.41	2.99	0.41	1.53	0.137	0.442
stria terminalis	2.86	0.21	2.74	0.22	1.49	0.148	0.442
superior cerebellar peduncle	3.00	0.36	2.85	0.21	1.39	0.178	0.442
fimbria	2.87	0.21	2.77	0.18	1.33	0.195	0.442
corpus callosum	3.14	0.21	3.03	0.24	1.33	0.195	0.442
interpedunclar nucleus	3.25	0.40	3.02	0.60	1.25	0.221	0.442
striatum	3.21	0.22	3.10	0.24	1.24	0.224	0.442
globus pallidus	3.03	0.23	2.93	0.23	1.21	0.238	0.442
inferior olivary complex	6.07	1.95	5.24	1.89	1.20	0.242	0.442
midbrain	3.05	0.30	2.91	0.34	1.16	0.254	0.442
nucleus accumbens	3.21	0.23	3.10	0.28	1.14	0.263	0.442
hypothalamus	2.95	0.36	2.80	0.36	1.11	0.278	0.451
fundus of striatum	3.16	0.29	3.04	0.33	1.05	0.304	0.461
pars posterior anterior commissure	3.01	0.28	2.90	0.28	1.04	0.306	0.461
hippocampus	3.46	0.19	3.39	0.21	1.02	0.315	0.461
thalamus	3.02	0.19	2.96	0.19	0.94	0.356	0.505
pars anterior anterior commissure	3.15	0.23	3.06	0.29	0.89	0.381	0.524
lateral septum	2.87	0.23	2.80	0.23	0.80	0.432	0.563
olfactory bulbs	3.18	0.17	3.14	0.21	0.66	0.515	0.600
internal capsule	2.89	0.25	2.84	0.20	0.59	0.561	0.608
stria medullaris	2.94	0.34	2.89	0.17	0.56	0.578	0.608
pons	3.36	0.42	3.44	0.48	-0.48	0.634	0.640
cerebral aqueduct	2.71	0.29	2.77	0.51	-0.41	0.683	0.674
cerebellar cortex	2.84	0.08	2.86	0.14	-0.31	0.756	0.720
medulla	3.57	0.32	3.53	0.38	0.26	0.799	0.720
corticospinal tract or pyramids	3.99	0.66	4.06	0.82	-0.24	0.811	0.720
mammillary bodies	3.65	0.55	3.69	0.50	-0.19	0.848	0.720
superior colliculus	2.89	0.21	2.87	0.21	0.17	0.868	0.720
arbor vita of cerebellum	3.02	0.16	3.01	0.18	0.14	0.887	0.720
periaqueductal grey	2.82	0.28	2.81	0.28	0.10	0.917	0.720
cerebral cortex occipital lobe	2.97	0.46	2.99	0.43	-0.10	0.921	0.720
subependymale zone or rhinocele	3.24	0.28	3.25	0.47	-0.08	0.935	0.720
middle cerebellar peduncle	3.66	0.68	3.67	0.58	-0.04	0.970	0.722
third ventricle	3.00	0.41	2.77	0.29	1.80	0.084	0.367
lateral ventricle	3.26	0.53	3.02	0.38	1.41	0.170	0.442
bed nucleus of stria terminalis	2.81	0.24	2.68	0.28	1.33	0.194	0.442
fourth ventricle	3.18	0.41	3.35	0.41	-1.17	0.252	0.442
dentate gyrus of hippocampus	3.29	0.26	3.22	0.19	0.76	0.455	0.563
ventral tegmental decussation	2.81	0.31	2.72	0.38	0.75	0.461	0.563
medial lemniscus or medial longitudinal fasciculus	3.72	0.61	3.54	0.65	0.75	0.462	0.563
pontine nucleus	3.59	0.76	3.78	0.69	-0.73	0.471	0.563
fornix	2.88	0.32	2.81	0.35	0.59	0.561	0.608
pre-para subiculum	3.21	0.39	3.14	0.25	0.58	0.569	0.608
mammilothalamic tract	3.03	0.31	2.98	0.24	0.55	0.589	0.608
fasciculus retroflexus	2.84	0.21	2.82	0.27	0.29	0.777	0.720
inferior colliculus	2.94	0.20	2.96	0.15	-0.23	0.818	0.720
posterior commissure	2.59	0.23	2.57	0.17	0.20	0.843	0.720
lateral olfactory tract	3.43	0.60	3.46	0.63	-0.12	0.904	0.720
habenular commissure	4.00	1.55	4.03	0.71	-0.06	0.952	0.721
stratum granulosum of hippocampus	3.31	0.23	3.31	0.15	-0.01	0.989	0.724
Summary Regions							
Cerebral grey	3.22	0.22	3.14	0.24	1.05	0.304	-
Cerebral White	3.11	0.32	3.00	0.27	1.05	0.303	-
Olfactory	3.49	0.37	3.36	0.39	0.89	0.382	-
Cerebellum	3.17	0.23	3.23	0.29	-0.66	0.516	-
Ventricles	3.04	0.38	2.98	0.37	0.43	0.671	-
Brainstem	3.47	0.33	3.47	0.41	-0.01	0.991	-

Table 17. Region of interest differences in mean diffusivity (MD) between KET-DAY and SAL-DAY mice.

Region of Interest	Saline mean ($mm^2 s^{-1}$)	SD	Ketamine mean ($mm^2 s^{-1}$)	SD	T statistic	p value	q value	Cohen's d	Percentage change (%)	
inferior olivary complex	3.52	0.25	3.22	0.16	3.56	0.00	0.00	1.43	-8.53	↓
arbor vita of cerebellum	3.13	0.39	2.69	0.25	3.30	0.00	0.00	1.34	-13.92	↓
cerebral cortex entorhinal cortex	3.23	0.20	2.98	0.21	3.13	0.00	0.00	1.22	-7.80	↓
interpedunclar nucleus	3.44	0.25	3.14	0.24	3.08	0.01	0.00	1.22	-8.77	↓
mammilothalamic tract	3.40	0.20	3.15	0.22	3.01	0.01	0.00	1.19	-7.41	↓
pontine nucleus	3.34	0.16	3.12	0.21	3.00	0.01	0.00	1.18	-6.77	↓
cerebral cortex parieto-temporal lobe	3.55	0.31	3.18	0.32	2.89	0.01	0.00	1.17	-10.39	↓
cerebral cortex frontal lobe	3.24	0.18	3.01	0.21	2.87	0.01	0.00	1.18	-6.99	↓
medial lemniscus or medial longitudinal fasciculus	3.34	0.21	3.11	0.20	2.82	0.01	0.00	1.21	-6.84	↓
superior colliculus	3.59	0.20	3.35	0.25	2.76	0.01	0.00	1.06	-6.92	↓
fimbria	3.39	0.32	3.06	0.27	2.75	0.01	0.00	1.11	-9.61	↓
inferior cerebellar peduncle	3.34	0.22	3.08	0.26	2.70	0.01	0.00	1.08	-7.87	↓
fornix	3.18	0.17	3.00	0.17	2.58	0.02	0.01	1.06	-5.54	↓
midbrain	3.78	0.35	3.45	0.30	2.53	0.02	0.01	1.01	-8.75	↓
facial nerve (cranial nerve 7)	3.30	0.19	3.13	0.19	2.27	0.03	0.01	0.89	-5.20	↓
stria medullaris	3.47	0.55	3.06	0.32	2.25	0.04	0.01	0.91	-11.77	↓
amygdala	3.43	0.25	3.23	0.18	2.22	0.04	0.01	0.92	-5.66	↓
cerebral peduncle	3.34	0.23	3.16	0.18	2.21	0.04	0.01	0.87	-5.48	↓
corpus callosum	3.70	0.19	3.49	0.28	2.20	0.04	0.01	0.88	-5.61	↓
superior olivary complex	3.25	0.21	3.05	0.27	2.14	0.04	0.01	0.83	-6.30	↓
fasciculus retroflexus	3.22	0.19	3.06	0.19	2.09	0.05	0.01	0.84	-4.98	↓
optic tract	3.13	0.28	2.93	0.21	2.09	0.05	0.01	0.81	-6.55	↓
lateral septum	3.79	0.33	3.52	0.32	2.07	0.05	0.01	0.83	-7.15	↓
fourth ventricle	3.31	0.20	3.15	0.19	2.03	0.05	0.01	0.82	-4.76	↓
inferior colliculus	3.60	0.19	3.45	0.18	2.02	0.06	0.01	-	-	-
stria terminalis	3.21	0.18	3.08	0.15	1.99	0.06	0.01	-	-	-
basal forebrain	3.56	0.27	3.34	0.27	1.97	0.06	0.01	-	-	-
mammilary bodies	5.13	0.78	4.48	1.06	1.75	0.09	0.01	-	-	-
internal capsule	4.18	0.36	3.90	0.43	1.71	0.10	0.01	-	-	-
fundus of striatum	3.93	0.40	3.67	0.39	1.64	0.11	0.01	-	-	-
bed nucleus of stria terminalis	3.36	0.25	3.22	0.20	1.54	0.14	0.02	-	-	-
striatum	3.30	0.20	3.20	0.13	1.53	0.14	0.02	-	-	-
medial septum	3.28	0.27	3.12	0.30	1.48	0.15	0.02	-	-	-
middle cerebellar peduncle	3.56	0.35	3.32	0.46	1.45	0.16	0.02	-	-	-
dentate gyrus of hippocampus	3.51	0.23	3.38	0.19	1.44	0.17	0.02	-	-	-
pons	2.97	0.86	3.36	0.40	-1.43	0.17	0.02	-	-	-
corticospinal tract or pyramids	4.03	0.66	3.73	0.41	1.36	0.19	0.02	-	-	-
posterior commissure	4.00	2.03	5.11	2.11	-1.35	0.19	0.02	-	-	-
pars posterior anterior commissure	3.86	0.85	3.51	0.47	1.23	0.24	0.02	-	-	-
olfactory tubercle	3.82	0.58	3.52	0.72	1.15	0.26	0.03	-	-	-
hypothalamus	3.58	0.20	3.49	0.16	1.13	0.27	0.03	-	-	-
habenular commissure	3.25	0.45	3.42	0.26	-1.13	0.27	0.03	-	-	-
superior cerebellar peduncle	3.73	0.28	3.62	0.32	0.96	0.35	0.03	-	-	-
pars anterior anterior commissure	4.79	1.26	4.37	1.04	0.91	0.37	0.03	-	-	-
cerebellar cortex	3.27	0.23	3.18	0.26	0.87	0.39	0.03	-	-	-
medulla	3.44	0.88	3.18	0.62	0.85	0.40	0.03	-	-	-
nucleus accumbens	3.82	0.37	3.70	0.43	0.73	0.47	0.04	-	-	-
hippocampus	3.61	0.20	3.68	0.32	-0.68	0.51	0.04	-	-	-
stratum granulosum of hippocampus	3.75	0.50	3.66	0.32	0.52	0.61	0.05	-	-	-
olfactory bulbs	3.60	0.35	3.51	0.51	0.51	0.62	0.05	-	-	-
globus pallidus	3.50	0.42	3.57	0.29	-0.47	0.65	0.05	-	-	-
subependymale zone or rhinocele	3.93	1.04	3.80	0.67	0.35	0.73	0.05	-	-	-
third ventricle	3.03	0.24	3.05	0.11	-0.34	0.74	0.05	-	-	-
pre-para subiculum	3.56	0.21	3.52	0.35	0.31	0.76	0.05	-	-	-
cerebral cortex occipital lobe	3.87	0.41	3.84	0.42	0.18	0.86	0.06	-	-	-
thalamus	3.99	0.51	3.95	0.54	0.18	0.86	0.06	-	-	-
ventral tegmental decussation	3.15	0.21	3.16	0.34	-0.12	0.91	0.06	-	-	-
periaqueductal grey	3.07	0.30	3.06	0.30	0.05	0.96	0.06	-	-	-
lateral ventricle	3.42	0.22	3.26	0.18	2.00	0.06	0.01	-	-	-
cerebral aqueduct	3.10	0.16	3.06	0.15	0.73	0.47	0.04	-	-	-
lateral olfactory tract	3.38	0.28	3.31	0.22	0.69	0.50	0.04	-	-	-
cuneate nucleus	3.70	0.45	3.77	0.58	-0.35	0.73	0.05	-	-	-
Summary Regions										
Cerebral grey	3.65	0.19	3.49	0.25	1.79	0.09	0.00	-	-	-
Cerebral White	3.58	0.33	3.45	0.25	1.08	0.29	0.00	-	-	-
Olfactory	3.68	0.29	3.54	0.32	1.19	0.25	0.00	-	-	-
Cerebellum	3.40	0.16	3.18	0.24	2.82	0.01	0.00	1.08	-6.65	↓
Ventricles	3.22	0.17	3.13	0.15	1.34	0.19	0.00	-	-	-
Brainstem	3.43	0.21	3.28	0.21	1.78	0.09	0.00	-	-	-

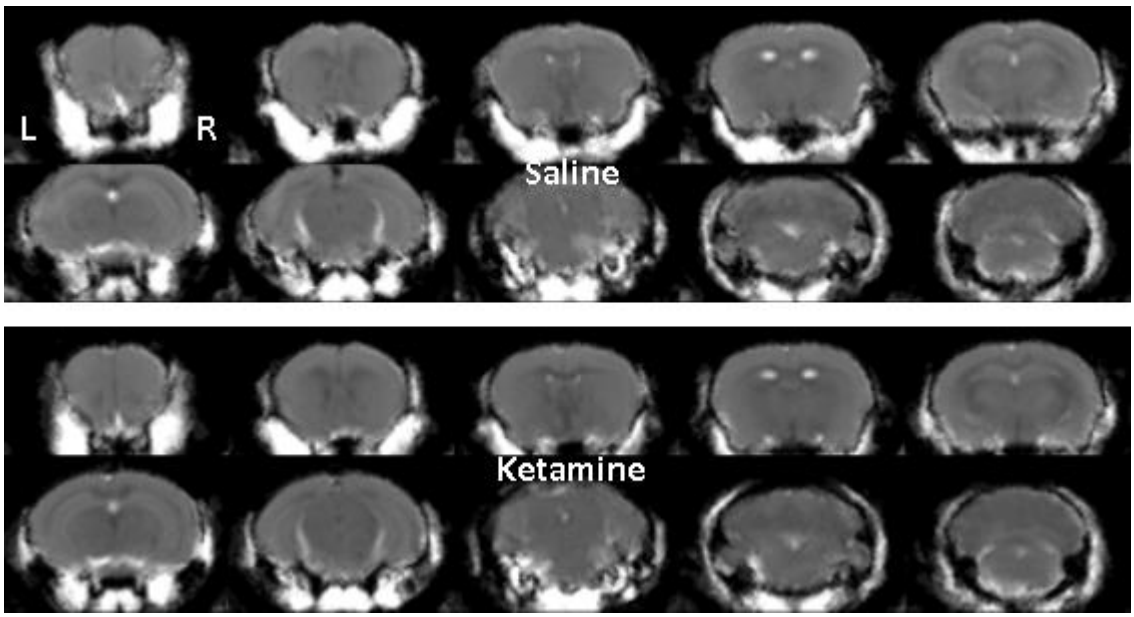

Figure 10. Coronal sections of group mean MD images from KET-DAY and SAL-DAY mice. L= left, R= Right.

ii) Axial diffusivity (AD)

Next, I compared average AD values between KET-INT and SAL-INT mice. I found no significant difference in AD in any of the 62 ROIs (Figure 11 and Table 18).

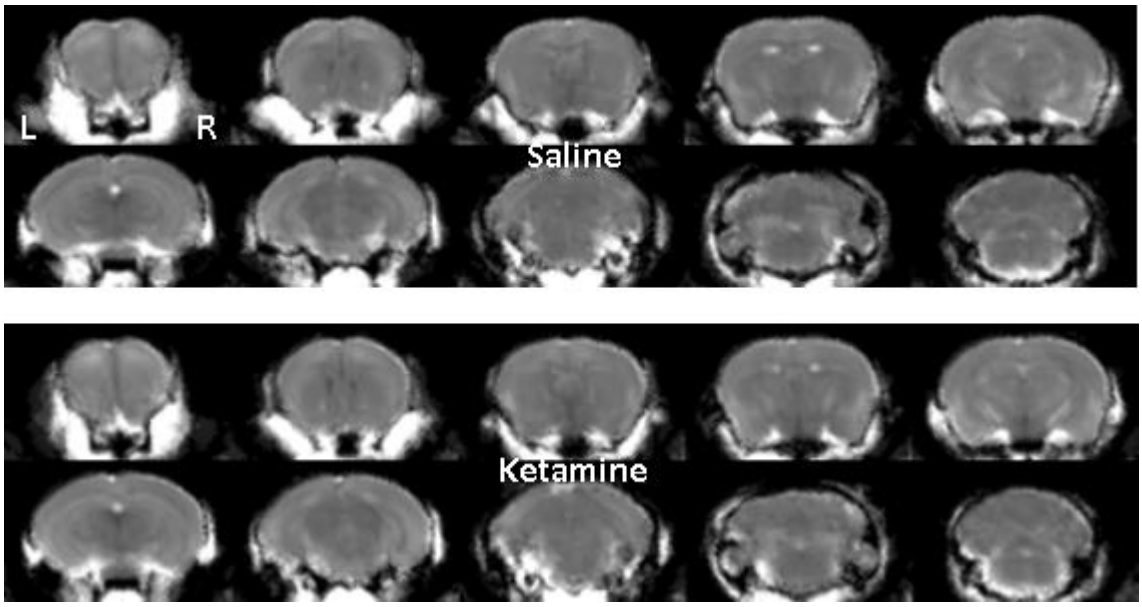

Figure 11. Coronal sections of group mean MD images from KET-INT and SAL-INT mice. L= left, R= Right.

Table 18. Region of interest differences in axial diffusivity (AD) between KET-INT and SAL-INT mice.

Region of Interest	Saline mean ($mm^2 s^{-1}$)	SD	Ketamine mean ($mm^2 s^{-1}$)	SD	T statistic	p value	q value
superior olivary complex	4.60	0.86	5.45	1.16	-2.87	0.008	0.111
facial nerve (cranial nerve 7)	3.75	0.51	4.14	0.61	-2.36	0.027	0.146
inferior cerebellar peduncle	4.53	0.50	4.86	0.63	-1.80	0.086	0.146
cerebral aqueduct	3.23	0.31	3.25	0.53	-1.53	0.139	0.146
cerebral cortex entorhinal cortex	3.86	0.60	4.32	0.84	-1.52	0.141	0.146
pons	4.30	0.46	4.37	0.54	-1.45	0.162	0.146
cuneate nucleus	3.77	0.25	4.08	0.26	-1.41	0.179	0.146
periaqueductal grey	3.50	0.34	3.44	0.36	-1.19	0.251	0.146
superior colliculus	3.46	0.26	3.44	0.27	-1.15	0.269	0.146
cerebellar cortex	3.52	0.11	3.53	0.16	-1.12	0.279	0.146
mammillary bodies	4.26	0.63	4.43	0.56	-1.10	0.283	0.146
medulla	4.44	0.41	4.41	0.47	-1.10	0.286	0.146
arbor vita of cerebellum	3.80	0.19	3.80	0.20	-1.09	0.292	0.146
stria medullaris	3.69	0.40	3.65	0.24	-1.07	0.300	0.146
inferior olivary complex	7.17	2.34	6.42	2.21	1.04	0.308	0.146
corticospinal tract or pyramids	5.15	0.78	5.18	0.99	-1.03	0.312	0.146
hippocampus	4.36	0.25	4.27	0.29	-0.87	0.399	0.146
olfactory bulbs	4.01	0.21	3.95	0.27	-0.86	0.403	0.146
striatum	3.90	0.30	3.76	0.32	-0.84	0.414	0.146
nucleus accumbens	3.95	0.31	3.79	0.37	-0.82	0.422	0.146
thalamus	3.86	0.27	3.77	0.29	-0.82	0.426	0.146
pars posterior anterior commissure	3.75	0.37	3.59	0.38	-0.81	0.432	0.146
superior cerebellar peduncle	3.91	0.45	3.76	0.32	-0.74	0.471	0.146
internal capsule	4.14	0.32	4.00	0.36	-0.71	0.487	0.146
cerebral cortex occipital lobe	3.66	0.49	3.61	0.47	-0.69	0.500	0.146
midbrain	3.91	0.41	3.74	0.48	-0.67	0.511	0.146
cerebral cortex parieto-temporal lobe	4.10	0.24	3.90	0.30	-0.67	0.511	0.146
corpus callosum	4.10	0.27	4.01	0.32	-0.67	0.514	0.146
hypothalamus	3.85	0.40	3.64	0.45	-0.66	0.520	0.146
cerebral cortex frontal lobe	4.29	0.23	4.07	0.35	-0.65	0.525	0.146
fimbria	3.93	0.25	3.87	0.24	-0.63	0.540	0.146
globus pallidus	4.14	0.34	4.00	0.34	-0.61	0.554	0.147
basal forebrain	4.10	0.49	3.76	0.55	-0.50	0.621	0.155
stria terminalis	3.96	0.27	3.85	0.32	-0.49	0.631	0.155
interpedunclar nucleus	4.14	0.48	3.85	0.76	-0.48	0.638	0.155
amygdala	4.88	0.46	4.56	0.37	-0.37	0.717	0.171
cerebral peduncle	5.48	0.51	4.95	0.70	0.28	0.779	0.183
optic tract	4.83	0.58	4.21	0.70	0.12	0.905	0.208
olfactory tubercle	5.21	0.90	4.51	0.95	0.04	0.968	0.219
medial septum	4.12	0.61	3.67	0.63	0.00	0.999	0.223
fourth ventricle	3.82	0.47	4.00	0.48	-2.01	0.059	0.146
pontine nucleus	4.59	0.92	4.80	0.84	-1.64	0.114	0.146
inferior colliculus	3.59	0.25	3.60	0.20	-1.24	0.233	0.146
stratum granulosum of hippocampus	3.99	0.28	4.00	0.20	-1.21	0.247	0.146
pre-para subiculum	3.81	0.45	3.73	0.28	-1.08	0.299	0.146
fasciculus retroflexus	3.51	0.29	3.46	0.35	-1.06	0.306	0.146
subependymale zone or rhinocele	4.28	0.35	4.25	0.50	-1.04	0.311	0.146
dentate gyrus of hippocampus	4.01	0.33	3.89	0.26	-1.01	0.326	0.146
mammilothalamic tract	3.86	0.39	3.80	0.33	-1.01	0.328	0.146
posterior commissure	3.27	0.27	3.16	0.27	-1.01	0.329	0.146
fornix	3.66	0.41	3.64	0.43	-0.99	0.338	0.146
habenular commissure	4.50	1.73	4.57	0.77	-0.96	0.348	0.146
lateral olfactory tract	4.25	0.70	4.27	0.72	-0.93	0.360	0.146
middle cerebellar peduncle	5.01	0.68	5.01	0.54	-0.87	0.397	0.146
medial lemniscus or medial longitudinal fasciculus	4.73	0.76	4.52	0.79	-0.86	0.400	0.146
lateral septum	3.69	0.32	3.60	0.34	-0.83	0.421	0.146
fundus of striatum	3.89	0.43	3.82	0.40	-0.80	0.435	0.146
pars anterior anterior commissure	4.06	0.28	3.92	0.37	-0.77	0.452	0.146
bed nucleus of stria terminalis	3.48	0.33	3.34	0.36	-0.68	0.504	0.146
ventral tegmental decussation	3.77	0.43	3.58	0.53	-0.64	0.527	0.146
lateral ventricle	4.17	0.60	3.88	0.46	-0.55	0.593	0.155
third ventricle	3.58	0.45	3.31	0.33	-0.53	0.604	0.155
Summary Regions							
Cerebral grey	4.01	0.28	3.90	0.30	-0.85	0.408	-
Cerebral White	4.05	0.40	3.91	0.36	-0.72	0.481	-
Olfactory	4.44	0.43	4.25	0.49	-0.74	0.469	-
Cerebellum	4.15	0.26	4.19	0.32	-1.21	0.245	-
Ventricles	3.70	0.43	3.61	0.42	-1.19	0.251	-
Brainstem	4.32	0.41	4.33	0.49	-1.17	0.258	-

I then compared average AD values between KET-DAY and SAL-DAY mice. I found significant reductions in AD in 20 of 62 ROIs in KET-DAY mice (Figure 12, Table 19). Each of these 20 ROIs also displayed significant reductions in MD in KET-DAY mice. In total, 9 of the 20 ROIs were in the grey matter; entorhial cortex, parieto-temporal lobe, frontal lobe, inferior olivary comples, superior olivary complex, interpendunclar necleus, pontine nucleus, midbrain and amygdala. Additionally, 10 of the regions were in the white matter; arbor vita of the cerebelum, inferior cerebellar peduncle, fimbria, fornix, mammilothalamic tract, stria medullaris, fasiculus retroflexus, cerebral peduncle, medial lemniscus and facial nerve. The last ROI displaying a significant reduction in AD in KET-DAY mice was the fourth ventricle.

Again, there was a significant decrease in AD in 2 ROIs within the cerebellum; arbor vita of the cerebellum and inferior cerebellar peduncle, thus there was an overall decrease in AD within the cerebellum (KET-DAY; 4.04 ± 0.29 mm^2s^{-1}, SAL-DAY; 4.34 ± 0.21 mm^2s^{-1}, t=2.91, p=0.01).

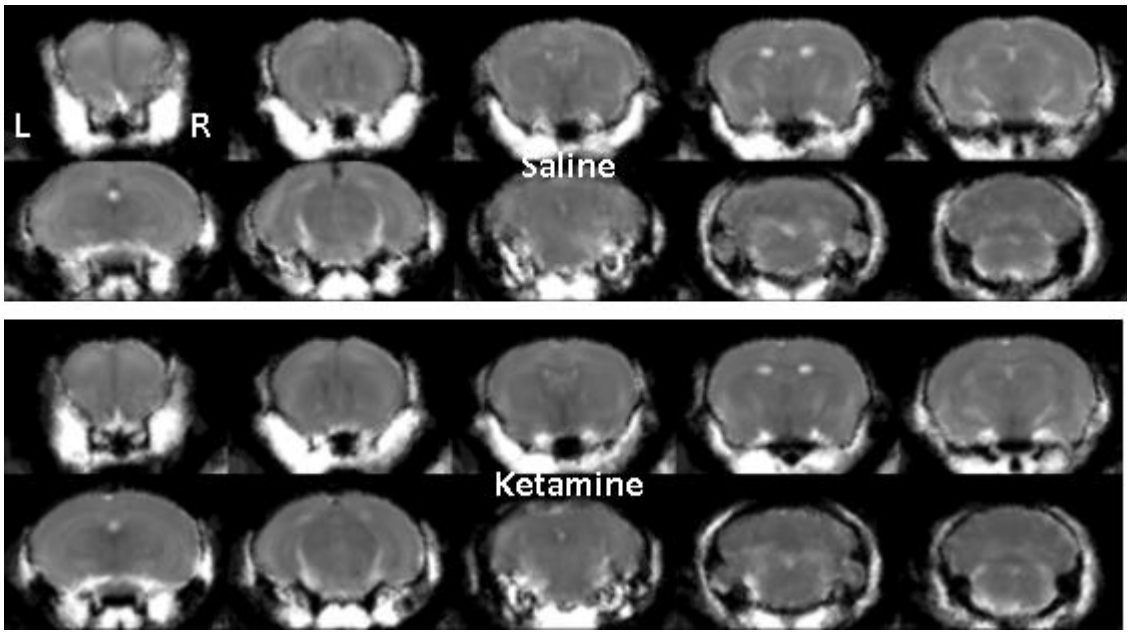

Figure 12. Coronal sections of group mean MD images from KET-INT and SAL-INT mice. L= left, R= Right.

Table 19. Region of interest differences in axial diffusivity (AD) between KET-DAY and SAL-DAY mice.

Region of Interest	Saline mean ($mm^2 s^{-1}$)	SD	Ketamine mean ($mm^2 s^{-1}$)	SD	T statistic	p-value	q-value	Cohen's d	Percentage change (%)	
inferior olivary complex	4.29	0.32	3.89	0.22	3.60	0.00	0.00	1.46	-9.32	↓
cerebral cortex entorhinal cortex	4.22	0.24	3.86	0.28	3.42	0.00	0.00	1.38	-8.36	↓
mammilothalamic tract	4.13	0.21	3.82	0.25	3.35	0.00	0.00	1.34	-7.54	↓
arbor vita of cerebellum	3.87	0.55	3.28	0.33	3.19	0.01	0.00	1.30	-15.17	↓
cerebral cortex parieto-temporal lobe	4.70	0.35	4.27	0.38	2.99	0.01	0.00	1.18	-9.16	↓
interpedunclar nucleus	4.36	0.35	3.97	0.31	2.95	0.01	0.00	1.18	-9.01	↓
inferior cerebellar peduncle	4.27	0.27	3.95	0.32	2.69	0.01	0.01	1.08	-7.43	↓
pontine nucleus	4.35	0.24	4.08	0.27	2.59	0.02	0.01	1.06	-6.06	↓
medial lemniscus or medial longitudinal fasciculus	4.37	0.26	4.12	0.25	2.47	0.02	0.01	0.98	-5.74	↓
cerebral cortex frontal lobe	4.50	0.21	4.24	0.32	2.47	0.02	0.01	0.96	-5.92	↓
cerebral peduncle	4.13	0.30	3.86	0.23	2.46	0.02	0.01	1.01	-6.37	↓
fornix	4.18	0.22	3.96	0.24	2.43	0.02	0.01	0.96	-5.30	↓
midbrain	4.86	0.45	4.47	0.36	2.36	0.03	0.01	0.96	-7.96	↓
fourth ventricle	4.21	0.24	3.98	0.25	2.35	0.03	0.01	0.94	-5.39	↓
stria medullaris	4.28	0.62	3.80	0.41	2.26	0.04	0.01	0.91	-11.18	↓
fimbria	4.17	0.36	3.87	0.33	2.18	0.04	0.01	0.87	-7.18	↓
fasciculus retroflexus	4.11	0.26	3.89	0.25	2.14	0.04	0.01	0.86	-5.35	↓
amygdala	4.29	0.29	4.06	0.24	2.15	0.04	0.01	0.86	-5.44	↓
facial nerve (cranial nerve 7)	4.12	0.25	3.90	0.25	2.14	0.04	0.01	0.88	-5.24	↓
superior olivary complex	4.47	0.28	4.19	0.38	2.13	0.04	0.01	0.84	-6.32	↓
optic tract	3.81	0.33	3.57	0.28	1.99	0.06	0.01	-	-	-
striatum	4.61	0.25	4.42	0.24	1.97	0.06	0.01	-	-	-
superior colliculus	4.66	0.33	4.39	0.35	1.97	0.06	0.01	-	-	-
corpus callosum	4.64	0.23	4.40	0.36	1.94	0.07	0.01	-	-	-
lateral septum	4.56	0.39	4.27	0.36	1.86	0.08	0.01	-	-	-
medial septum	4.04	0.32	3.81	0.34	1.79	0.09	0.01	-	-	-
basal forebrain	4.45	0.36	4.20	0.35	1.78	0.09	0.01	-	-	-
mammillary bodies	5.83	0.82	5.15	1.09	1.77	0.09	0.01	-	-	-
internal capsule	5.16	0.43	4.83	0.52	1.73	0.10	0.01	-	-	-
stria terminalis	4.04	0.21	3.91	0.20	1.70	0.10	0.01	-	-	-
middle cerebellar peduncle	4.43	0.35	4.15	0.49	1.64	0.11	0.01	-	-	-
bed nucleus of stria terminalis	4.05	0.26	3.90	0.24	1.44	0.16	0.01	-	-	-
posterior commissure	4.80	2.19	6.05	2.29	-1.39	0.18	0.01	-	-	-
cerebellar cortex	4.18	0.34	4.00	0.30	1.35	0.19	0.01	-	-	-
corticospinal tract or pyramids	5.14	0.80	4.80	0.54	1.23	0.23	0.02	-	-	-
pars posterior anterior commissure	4.87	0.91	4.50	0.55	1.23	0.23	0.02	-	-	-
inferior colliculus	4.43	0.24	4.32	0.26	1.09	0.29	0.02	-	-	-
olfactory tubercle	4.76	0.67	4.44	0.81	1.07	0.30	0.02	-	-	-
hypothalamus	4.50	0.26	4.41	0.20	1.04	0.31	0.02	-	-	-
habenular commissure	4.18	0.54	4.37	0.37	-1.01	0.33	0.02	-	-	-
medulla	3.98	0.93	3.67	0.66	0.96	0.35	0.02	-	-	-
dentate gyrus of hippocampus	4.48	0.29	4.38	0.20	0.95	0.35	0.02	-	-	-
superior cerebellar peduncle	4.96	0.31	4.84	0.37	0.87	0.39	0.02	-	-	-
pars anterior anterior commissure	5.85	1.50	5.42	1.27	0.76	0.45	0.03	-	-	-
pons	3.97	0.88	4.18	0.38	-0.74	0.47	0.03	-	-	-
nucleus accumbens	4.75	0.40	4.63	0.49	0.67	0.51	0.03	-	-	-
olfactory bulbs	4.52	0.41	4.39	0.60	0.62	0.54	0.03	-	-	-
stratum granulosum of hippocampus	4.83	0.58	4.71	0.40	0.56	0.58	0.03	-	-	-
ventral tegmental decussation	4.06	0.22	4.13	0.45	-0.54	0.60	0.03	-	-	-
pre-para subiculum	4.64	0.23	4.56	0.47	0.53	0.61	0.03	-	-	-
subependymale zone or rhinocele	4.92	1.22	4.75	0.77	0.41	0.69	0.04	-	-	-
periaqueductal grey	3.96	0.40	4.01	0.42	-0.31	0.76	0.04	-	-	-
thalamus	5.14	0.56	5.09	0.61	0.22	0.83	0.04	-	-	-
cerebral cortex occipital lobe	4.78	0.54	4.74	0.52	0.19	0.85	0.04	-	-	-
third ventricle	3.89	0.22	3.90	0.16	-0.13	0.90	0.04	-	-	-
hippocampus	4.52	0.19	4.51	0.36	0.13	0.90	0.04	-	-	-
globus pallidus	4.77	0.40	4.78	0.39	-0.09	0.93	0.04	-	-	-
lateral ventricle	4.22	0.24	4.03	0.22	2.02	0.06	0.01	-	-	-
fundus of striatum	4.85	0.48	4.57	0.46	1.51	0.14	0.01	-	-	-
lateral olfactory tract	4.54	0.32	4.37	0.24	1.46	0.16	0.01	-	-	-
cerebral aqueduct	3.79	0.16	3.73	0.17	0.87	0.39	0.02	-	-	-
cuneate nucleus	4.62	0.48	4.72	0.61	-0.44	0.66	0.03	-	-	-
Summary Regions										
Cerebral grey	4.63	0.22	4.43	0.32	1.82	0.08	0.00	-	-	-
Cerebral White	4.45	0.38	4.30	0.30	1.09	0.29	0.01	-	-	-
Olfactory	4.68	0.35	4.49	0.36	1.37	0.18	0.00	-	-	-
Cerebellum	4.34	0.21	4.04	0.29	2.91	0.01	0.00	1.18	-6.81	↓
Ventricles	4.03	0.18	3.91	0.18	1.57	0.13	0.00	-	-	-
Brainstem	4.38	0.26	4.19	0.27	1.76	0.09	0.00	-	-	-

iii) Radial diffusivity

As with measures of MD and AD, I found no significant differences in RD between KET-INT and SAL-INT mice (Figure 13 and table 20).

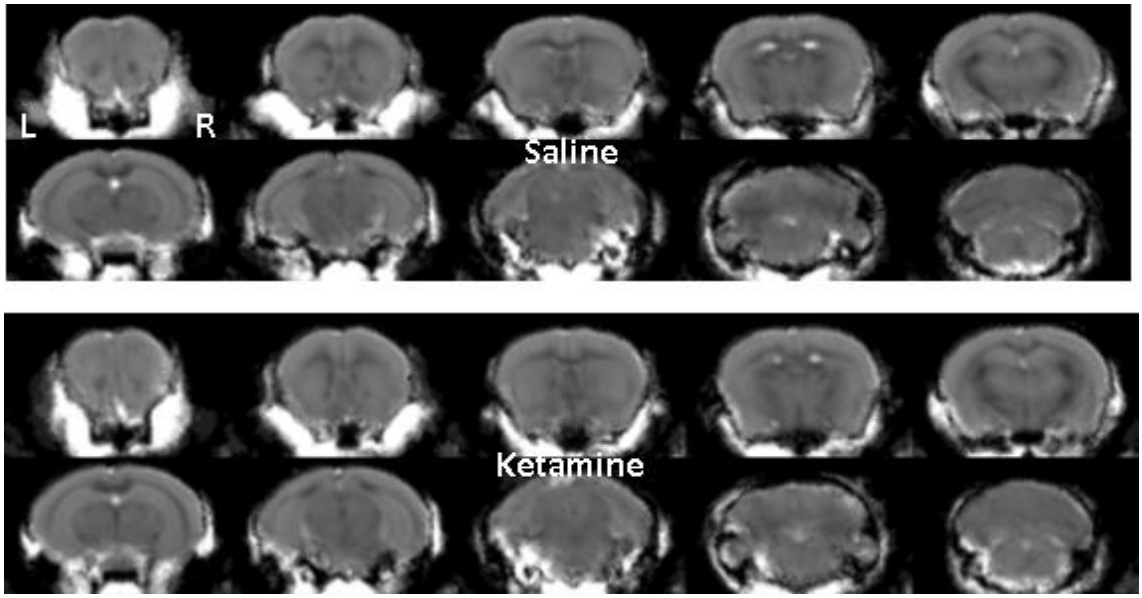

Figure 13. Coronal sections of group mean MD images from KET-INT and SAL-INT mice. L= left, R= Right.

However, I did find significant differences in RD in 24 of 62 ROIs when comparing KET-DAY mice to SAL-DAY mice (Table 21 and Figure 14).Of these 24 regions, 21 also displayed a significant reduction in MD in KET-INT mice as follows; entorhinal cortex, parieto-temporal lobe, frontal lobe, inferior olivary complex, superior olivary complex, interpeduncular nucleus, pontine nucleus, superior colliculus, midbrain, amygdala, arbor vita of the cerebellum, inferior cerebellar peduncle, corpus callosum, fimbria, fornix, optic tract, mammillothalamic tract, stria medullaris, medial lemniscus, facial nerve and lateral septum. Additionally, the following regions displayed significant reductions in RD; inferior colliculus, stria terminalis and basal forebrain.

Again, as with MD and AD results KET-DAY mice displayed significantly reduced RD in the cerebellum (KET-DAY; 2.74 ± 0.21 mm^2s^{-1}, SAL-DAY; 2.94 ± 0.13 mm^2s^{-1}, t=2.73, p=0.01)

Table 20. Region of interest differences in radial diffusivity (RD) between KET-INT and SAL-INT mice.

Region of Interest	Saline mean ($mm^2 s^{-1}$)	SD	Ketamine mean ($mm^2 s^{-1}$)	SD	T statistic	p value	q value
amygdala	3.29	0.37	3.05	0.23	2.15	0.042	0.405
arbor vita of cerebellum	2.63	0.15	2.62	0.17	0.25	0.805	0.723
basal forebrain	2.78	0.38	2.60	0.34	1.34	0.192	0.410
bed nucleus of stria terminalis	2.48	0.20	2.36	0.25	1.50	0.146	0.410
cerebellar cortex	2.50	0.07	2.52	0.13	-0.45	0.659	0.658
cerebral aqueduct	2.44	0.29	2.53	0.50	-0.58	0.571	0.645
cerebral cortex entorhinal cortex	2.86	0.52	3.20	0.73	-1.50	0.146	0.410
cerebral cortex frontal lobe	3.11	0.16	2.99	0.24	1.60	0.123	0.410
cerebral cortex occipital lobe	2.63	0.46	2.68	0.42	-0.31	0.759	0.697
cerebral cortex parieto-temporal lobe	3.02	0.18	2.92	0.21	1.37	0.183	0.410
cerebral peduncle	3.06	0.34	2.68	0.50	2.42	0.023	0.405
corpus callosum	2.66	0.18	2.54	0.21	1.72	0.098	0.405
corticospinal tract or pyramids	3.42	0.61	3.50	0.74	-0.34	0.736	0.697
cuneate nucleus	2.78	0.11	2.80	0.14	-0.54	0.594	0.645
dentate gyrus of hippocampus	2.93	0.23	2.89	0.16	0.52	0.610	0.647
facial nerve (cranial nerve 7)	2.92	0.41	3.21	0.52	-1.70	0.102	0.405
fimbria	2.34	0.20	2.22	0.16	1.76	0.090	0.405
fundus of striatum	2.79	0.24	2.65	0.32	1.38	0.180	0.410
globus pallidus	2.48	0.18	2.40	0.18	1.28	0.212	0.410
hippocampus	3.02	0.16	2.95	0.17	1.12	0.273	0.472
hypothalamus	2.50	0.34	2.38	0.31	0.94	0.358	0.557
inferior cerebellar peduncle	2.73	0.31	3.24	0.59	-2.89	0.009	0.405
inferior olivary complex	5.52	1.76	4.65	1.74	1.37	0.180	0.410
internal capsule	2.27	0.22	2.26	0.14	0.08	0.937	0.742
interpedunclar nucleus	2.81	0.37	2.60	0.53	1.25	0.223	0.410
lateral septum	2.46	0.19	2.40	0.18	0.77	0.447	0.603
mammillary bodies	3.34	0.52	3.31	0.48	0.16	0.872	0.727
medial septum	2.75	0.45	2.44	0.41	2.02	0.053	0.405
medulla	3.13	0.29	3.09	0.34	0.31	0.761	0.697
midbrain	2.62	0.25	2.50	0.28	1.27	0.215	0.410
middle cerebellar peduncle	2.99	0.70	3.00	0.61	-0.05	0.962	0.742
nucleus accumbens	2.84	0.19	2.76	0.24	1.00	0.328	0.528
olfactory bulbs	2.77	0.15	2.73	0.18	0.70	0.492	0.627
olfactory tubercle	3.53	0.70	3.15	0.50	1.69	0.104	0.405
optic tract	2.91	0.46	2.61	0.35	1.99	0.058	0.405
pars anterior anterior commissure	2.69	0.22	2.63	0.26	0.66	0.517	0.635
pars posterior anterior commissure	2.64	0.23	2.56	0.24	0.90	0.374	0.563
periaqueductal grey	2.47	0.25	2.49	0.24	-0.13	0.895	0.727
pons	2.89	0.40	2.97	0.45	-0.54	0.592	0.645
stria medullaris	2.57	0.31	2.51	0.14	0.69	0.497	0.627
stria terminalis	2.31	0.20	2.19	0.19	1.71	0.098	0.405
striatum	2.86	0.19	2.78	0.20	1.25	0.223	0.410
subependymale zone or rhinocele	2.72	0.25	2.75	0.46	-0.22	0.829	0.727
superior cerebellar peduncle	2.55	0.31	2.40	0.16	1.65	0.114	0.410
superior colliculus	2.60	0.18	2.59	0.19	0.12	0.903	0.727
superior olivary complex	3.26	0.77	3.98	1.01	-2.20	0.037	0.405
thalamus	2.60	0.15	2.55	0.15	1.01	0.323	0.528
fasciculus retroflexus	2.50	0.18	2.49	0.23	0.13	0.896	0.727
fornix	2.49	0.29	2.39	0.32	0.88	0.387	0.565
fourth ventricle	2.86	0.38	3.03	0.38	-1.23	0.228	0.410
habenular commissure	3.75	1.46	3.75	0.69	-0.02	0.985	0.742
inferior colliculus	2.62	0.18	2.64	0.13	-0.36	0.722	0.697
lateral olfactory tract	3.02	0.56	3.05	0.58	-0.16	0.872	0.727
lateral ventricle	2.80	0.50	2.59	0.34	1.36	0.186	0.410
mammilothalamic tract	2.61	0.27	2.56	0.20	0.58	0.570	0.645
medial lemniscus or medial longitudinal fasciculus	3.21	0.55	3.06	0.58	0.76	0.452	0.603
pontine nucleus	3.09	0.69	3.27	0.63	-0.77	0.448	0.603
posterior commissure	2.25	0.22	2.28	0.14	-0.44	0.662	0.658
pre-para subiculum	2.91	0.36	2.85	0.23	0.57	0.574	0.645
stratum granulosum of hippocampus	2.96	0.20	2.97	0.13	-0.03	0.979	0.742
third ventricle	2.71	0.39	2.49	0.28	1.76	0.090	0.405
ventral tegmental decussation	2.34	0.26	2.29	0.31	0.47	0.644	0.658
Summary Regions							
Cerebral grey	2.83	0.19	2.76	0.20	1.03	0.314	-
Cerebral White	2.65	0.29	2.55	0.22	1.02	0.315	-
Olfactory	3.01	0.33	2.92	0.35	0.71	0.484	-
Cerebellum	2.68	0.22	2.75	0.28	-0.80	0.432	-
Ventricles	2.70	0.36	2.66	0.35	0.34	0.737	-
Brainstem	3.04	0.29	3.04	0.37	0.02	0.983	-

Table 21. Region of interest differences in radial diffusivity (RD) between KET-DAY and SAL-DAY mice.

Region of Interest	Saline mean ($mm^2 s^{-1}$)	SD	Ketamine mean ($mm^2 s^{-1}$)	SD	T statistic	p value	q value	Cohen's d	Percentage change (%)	
inferior olivary complex	3.14	0.21	2.89	0.14	3.37	0.00	0.00	1.40	-7.88	↓
superior colliculus	3.06	0.17	2.82	0.21	3.15	0.00	0.00	1.26	-7.81	↓
interpedunclar nucleus	2.98	0.21	2.72	0.20	3.11	0.00	0.00	1.27	-8.62	↓
arbor vita of cerebellum	2.76	0.34	2.40	0.21	3.17	0.01	0.01	1.27	-13.07	↓
fimbria	3.00	0.31	2.66	0.24	3.04	0.01	0.01	1.23	-11.29	↓
pontine nucleus	2.84	0.14	2.63	0.20	3.02	0.01	0.01	1.22	-7.29	↓
cerebral cortex frontal lobe	2.61	0.18	2.40	0.16	3.01	0.01	0.01	1.23	-7.94	↓
medial lemniscus or medial longitudinal fasciculus	2.82	0.19	2.60	0.18	2.96	0.01	0.01	1.19	-7.67	↓
cerebral cortex parieto-temporal lobe	2.97	0.30	2.63	0.31	2.78	0.01	0.01	1.11	-11.45	↓
cerebral cortex entorhinal cortex	2.74	0.19	2.54	0.18	2.77	0.01	0.01	1.08	-7.40	↓
mammilothalamic tract	3.04	0.20	2.82	0.20	2.73	0.01	0.01	1.10	-7.27	↓
inferior cerebellar peduncle	2.87	0.21	2.64	0.24	2.62	0.02	0.01	1.02	-8.21	↓
midbrain	3.24	0.31	2.93	0.28	2.60	0.02	0.01	1.05	-9.40	↓
inferior colliculus	3.19	0.17	3.02	0.16	2.59	0.02	0.01	1.03	-5.32	↓
fornix	2.67	0.16	2.52	0.15	2.48	0.02	0.01	0.97	-5.62	↓
facial nerve (cranial nerve 7)	2.90	0.16	2.75	0.16	2.32	0.03	0.02	0.94	-5.09	↓
corpus callosum	3.23	0.18	3.04	0.24	2.32	0.03	0.02	0.90	-6.04	↓
amygdala	2.99	0.23	2.82	0.16	2.22	0.04	0.02	0.86	-5.89	↓
lateral septum	3.41	0.31	3.14	0.30	2.18	0.04	0.02	0.89	-7.83	↓
stria medullaris	3.07	0.51	2.69	0.29	2.22	0.04	0.02	0.92	-12.16	↓
stria terminalis	2.80	0.17	2.67	0.13	2.16	0.04	0.02	0.86	-4.64	↓
optic tract	2.79	0.25	2.61	0.17	2.16	0.04	0.02	0.84	-6.69	↓
superior olivary complex	2.65	0.18	2.48	0.22	2.13	0.04	0.02	0.85	-6.33	↓
basal forebrain	3.11	0.23	2.91	0.24	2.08	0.05	0.02	0.85	-6.33	↓
fasciculus retroflexus	2.78	0.17	2.65	0.16	1.99	0.06	0.02	-	-	-
cerebral peduncle	2.95	0.22	2.80	0.16	1.91	0.07	0.03	-	-	-
mammillary bodies	4.77	0.77	4.14	1.05	1.73	0.10	0.03	-	-	-
fundus of striatum	3.47	0.37	3.22	0.36	1.70	0.10	0.03	-	-	-
dentate gyrus of hippocampus	3.02	0.20	2.88	0.20	1.69	0.10	0.03	-	-	-
internal capsule	3.69	0.34	3.44	0.40	1.67	0.11	0.03	-	-	-
pons	2.48	0.89	2.95	0.47	-1.66	0.12	0.04	-	-	-
bed nucleus of stria terminalis	3.01	0.25	2.87	0.18	1.53	0.14	0.04	-	-	-
corticospinal tract or pyramids	3.47	0.59	3.19	0.35	1.44	0.17	0.05	-	-	-
middle cerebellar peduncle	3.12	0.35	2.91	0.44	1.35	0.19	0.05	-	-	-
posterior commissure	3.59	1.96	4.64	2.03	-1.32	0.20	0.05	-	-	-
medial septum	2.90	0.26	2.77	0.28	1.25	0.22	0.06	-	-	-
pars posterior anterior commissure	3.35	0.83	3.02	0.44	1.22	0.24	0.06	-	-	-
habenular commissure	2.78	0.41	2.94	0.23	-1.19	0.25	0.06	-	-	-
olfactory tubercle	3.35	0.54	3.07	0.67	1.18	0.25	0.06	-	-	-
hypothalamus	3.11	0.17	3.04	0.14	1.12	0.27	0.06	-	-	-
hippocampus	3.16	0.23	3.27	0.31	-1.05	0.30	0.07	-	-	-
pars anterior anterior commissure	4.27	1.14	3.85	0.93	1.00	0.33	0.08	-	-	-
superior cerebellar peduncle	3.12	0.27	3.00	0.31	0.97	0.34	0.08	-	-	-
striatum	2.65	0.20	2.59	0.13	0.85	0.41	0.09	-	-	-
medulla	3.17	0.85	2.93	0.60	0.80	0.43	0.09	-	-	-
nucleus accumbens	3.34	0.36	3.23	0.40	0.74	0.46	0.10	-	-	-
globus pallidus	2.87	0.46	2.97	0.29	-0.61	0.55	0.11	-	-	-
stratum granulosum of hippocampus	3.21	0.46	3.13	0.28	0.49	0.63	0.12	-	-	-
third ventricle	2.59	0.26	2.63	0.09	-0.47	0.64	0.12	-	-	-
cerebellar cortex	2.81	0.20	2.77	0.25	0.44	0.67	0.13	-	-	-
olfactory bulbs	3.14	0.34	3.07	0.47	0.44	0.67	0.13	-	-	-
periaqueductal grey	2.62	0.25	2.58	0.25	0.33	0.75	0.13	-	-	-
subependymale zone or rhinocele	3.43	0.95	3.33	0.63	0.31	0.76	0.13	-	-	-
cerebral cortex occipital lobe	3.42	0.36	3.39	0.38	0.18	0.86	0.14	-	-	-
ventral tegmental decussation	2.69	0.21	2.67	0.30	0.15	0.88	0.14	-	-	-
thalamus	3.41	0.50	3.38	0.51	0.15	0.88	0.14	-	-	-
pre-para subiculum	3.02	0.22	3.01	0.31	0.14	0.89	0.14	-	-	-
lateral ventricle	3.03	0.21	2.88	0.17	1.97	0.06	0.02	-	-	-
fourth ventricle	2.86	0.18	2.74	0.17	1.77	0.09	0.03	-	-	-
cerebral aqueduct	2.76	0.15	2.72	0.14	0.64	0.53	0.11	-	-	-
cuneate nucleus	3.23	0.45	3.30	0.57	-0.31	0.76	0.13	-	-	-
lateral olfactory tract	2.80	0.26	2.78	0.22	0.22	0.83	0.14	-	-	-
Summary Regions										
Cerebral grey	3.16	0.19	3.02	0.22	1.74	0.10	0.01	-	-	-
Cerebral White	3.14	0.31	3.03	0.23	1.07	0.30	0.01	-	-	-
Olfactory	3.18	0.26	3.06	0.30	1.06	0.30	0.01	-	-	-
Cerebellum	2.94	0.13	2.74	0.21	2.73	0.01	0.00	1.15	-6.57	↓
Ventricles	2.81	0.16	2.74	0.13	1.16	0.26	0.01	-	-	-
Brainstem	2.96	0.19	2.83	0.19	1.77	0.09	0.01	-	-	-

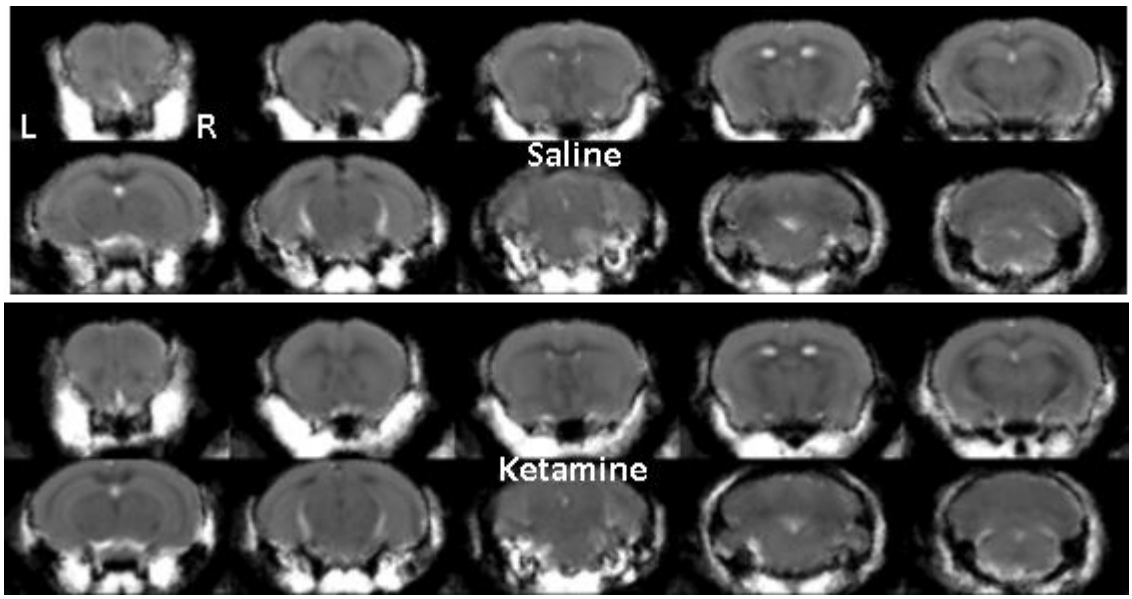

Figure 14. Coronal sections of group mean MD images from KET-DAY and SAL-DAY mice. L= left, R= Right.

iv) Comparing reductions in MD, AD and RD in KET-DAY mice

In the KET-DAY mice, of the 24 ROIs which showed significant reductions in MD, a total of 17 also presented with significant reductions in both AD and RD; entorhinal cortex, parieto-temporal lobe, frontal lobe, inferior olivary complex, superior olivary complex, interpeduncular nucleus, pontine nucleus, superior colliculus, midbrain, amygdala, arbor vita of the cerebellum, inferior cerebellar peduncle, fimbria, fornix, mammillothalamic tract, medial lemniscus, and facial nerve.

These data (decreased MD, AD and RD) suggest that water diffusion is restricted in all directions in these brain regions following repeat daily ketamine exposure. It may be hypothesised that these DTI changes could reflect alterations in common cellular compartments, although since both grey and white matter regions are present, this requires a detailed post-mortem investigation of both tissue types to confirm. Such a general reduction in water diffusion may suggest a physical block or barrier that hinders tissue water diffusion. This could reflect an increase in cell number, or an increase in the amount of sub-cellular structures in the neuropil, with many more cellular possibilities including dendritic branching, an increased number of glial ramifications, increased myelination, or a change in the amount and/or orientation of the cerebral vasculature (Alexander *et al.*, 2007; Beaulieu, 2009; Zatorre, Fields and Johansen-Berg, 2012; Aung, Mar and Benzinger, 2013; Stolp *et al.*, 2018).

Of the remaining 7 ROIs displaying a reduction in MD, 3 also displayed a reduction in AD; the cerebral peduncle, fasciculus retroflexus and fourth ventricle. Except for the fourth ventricle, these changes may be interpreted to suggest restricted water diffusion along axons or white matter tracts, possibly due to changes in either axonal or myelin thickness, and/or the density of myelin and axons, as well as a change in cell density, number and/or morphology (Alexander *et al.*, 2007; Beaulieu, 2009; Zatorre, Fields and Johansen-Berg, 2012; Aung, Mar and Benzinger, 2013; Stolp *et al.*, 2018).

The remaining 4 regions displaying decreases in MD also displayed decreases in RD; namely the stria medullaris, corpus callosum, optic tract and lateral septum. These data suggest restricted water diffusion across axons and white matter in these regions possibly due to changes in myelin content and/or structural organisation (Alexander *et al.*, 2007; Beaulieu, 2009; Aung, Mar and Benzinger, 2013).

Importantly, each of these possible cellular correlates may not be mutually exclusive and may occur concurrently, thus detailed post-mortem studies are required to establish which of these cellular processes is driving the effects of ketamine.

v) Fractional anisotropy (FA).

Unlike for MD, AD and RD, I found significant differences in FA between KET-INT and SAL-INT mice in 17 ROIs (Figure 15 and Table 22). 10 of these ROIs displayed significant increases in FA, both in the grey matter; cuneate nucleus, mammillary bodies, inferior olivary complex, entorhinal cortex, and the white matter; fimbria, facial nerve, corpus callosum, cerebral peduncle and ventral tegmental decussation. 7 ROI displayed significant reductions in FA, again these were both in the grey matter; parieto-temporal lobe, frontal lobe, occipital lobe, midbrain, interpeduncular nucleus, dentate gyrus of the hippocampus, and in the white matter; inferior cerebellar peduncle.

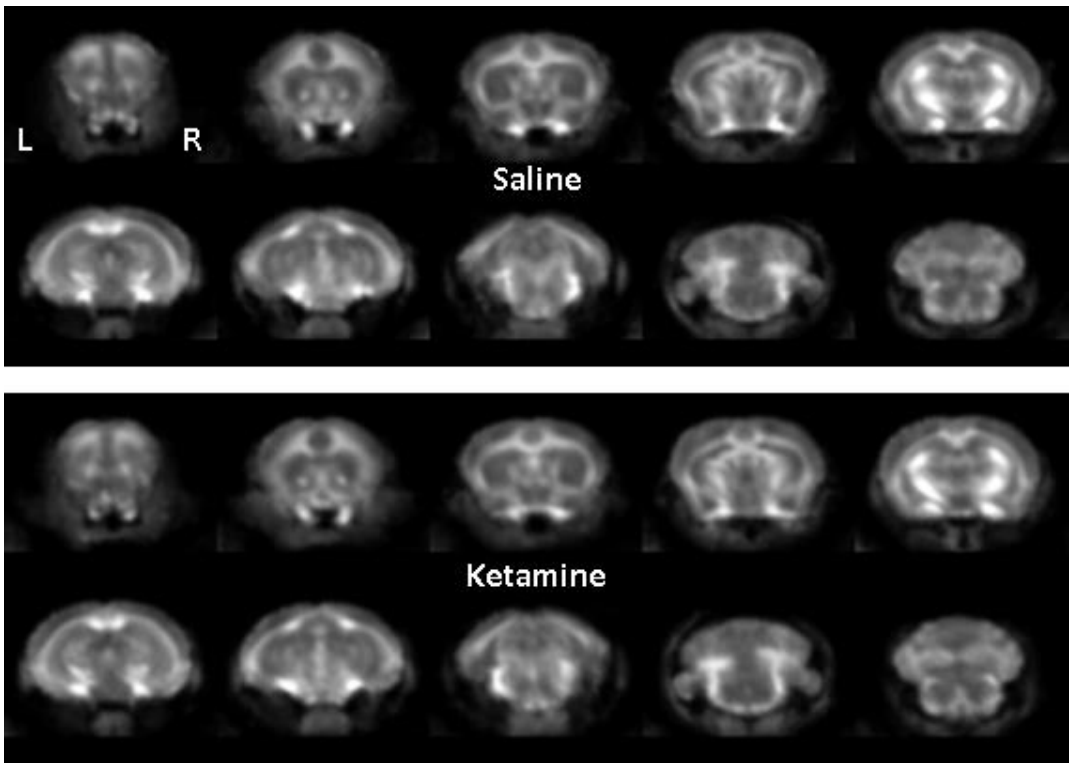

Figure 15. Coronal sections of group mean FA images from KET-INT and SAL-INT mice. L= left, R= Right.

Table 22. Region of interest differences in fractional anisotropy (FA) between KET-INT and SAL-INT mice.

Region of Interest	Saline mean	SD	Ketamine mean	SD	T statistic	p value	q value	Cohen's d	Percentage change (%)	
cuneate nucleus	0.20	0.03	0.25	0.03	-4.83	0.00	0.00	1.67	24.32	↑
fimbria	0.33	0.02	0.36	0.02	-3.57	0.00	0.00	1.50	6.53	↑
facial nerve (cranial nerve 7)	0.16	0.02	0.18	0.02	-3.41	0.00	0.00	1.00	12.98	↑
periaqueductal grey	0.25	0.01	0.26	0.01	-3.34	0.00	0.00	1.00	4.25	↑
mammillary bodies	0.18	0.02	0.21	0.03	-3.19	0.00	0.00	1.18	16.72	↑
cerebral cortex parieto-temporal lobe	0.20	0.01	0.18	0.01	3.15	0.00	0.00	2.00	-7.95	↓
corpus callosum	0.29	0.02	0.31	0.02	-3.01	0.01	0.00	1.00	6.17	↑
cerebral cortex frontal lobe	0.21	0.01	0.20	0.01	2.84	0.01	0.00	1.00	-5.35	↓
midbrain	0.25	0.01	0.23	0.02	2.59	0.02	0.00	1.26	-6.33	↓
interpedunclar nucleus	0.23	0.01	0.22	0.01	2.54	0.02	0.00	1.00	-5.80	↓
inferior cerebellar peduncle	0.31	0.05	0.28	0.03	2.48	0.02	0.00	0.73	-11.08	↓
cerebral peduncle	0.36	0.02	0.39	0.03	-2.34	0.03	0.00	1.18	6.43	↑
cerebral cortex occipital lobe	0.20	0.02	0.18	0.02	2.31	0.03	0.00	1.00	-8.97	↓
inferior olivary complex	0.15	0.06	0.20	0.07	-2.28	0.03	0.00	0.77	37.25	↑
cerebral cortex entorhinal cortex	0.16	0.02	0.18	0.03	-2.17	0.04	0.00	0.78	12.67	↑
ventral tegmental decussation	0.19	0.01	0.20	0.02	-2.13	0.04	0.00	0.63	6.36	↑
dentate gyrus of hippocampus	0.21	0.01	0.20	0.01	2.02	0.05	0.00	1.00	-4.94	↓
internal capsule	0.37	0.02	0.36	0.03	1.87	0.07	0.00	-	-	-
fundus of striatum	0.22	0.03	0.24	0.04	-1.83	0.08	0.00	-	-	-
nucleus accumbens	0.22	0.01	0.21	0.01	1.80	0.08	0.00	-	-	-
superior cerebellar peduncle	0.28	0.02	0.29	0.02	-1.78	0.09	0.00	-	-	-
fornix	0.25	0.02	0.26	0.02	-1.76	0.09	0.00	-	-	-
basal forebrain	0.25	0.02	0.24	0.02	1.74	0.09	0.00	-	-	-
superior olivary complex	0.22	0.05	0.24	0.04	-1.67	0.11	0.00	-	-	-
pontine nucleus	0.24	0.04	0.26	0.06	-1.36	0.19	0.00	-	-	-
subependymale zone or rhinocele	0.30	0.02	0.28	0.04	1.34	0.19	0.00	-	-	-
lateral olfactory tract	0.18	0.02	0.19	0.03	-1.31	0.20	0.00	-	-	-
olfactory tubercle	0.23	0.03	0.22	0.02	1.31	0.20	0.00	-	-	-
bed nucleus of stria terminalis	0.23	0.02	0.23	0.02	-1.29	0.21	0.00	-	-	-
striatum	0.21	0.01	0.20	0.01	1.24	0.23	0.00	-	-	-
inferior colliculus	0.21	0.01	0.21	0.01	1.21	0.24	0.00	-	-	-
pons	0.24	0.01	0.25	0.01	-1.18	0.25	0.00	-	-	-
hippocampus	0.24	0.01	0.25	0.01	-1.14	0.26	0.00	-	-	-
stria medullaris	0.24	0.01	0.25	0.01	-1.03	0.31	0.00	-	-	-
cerebral aqueduct	0.20	0.01	0.21	0.01	-1.00	0.32	0.00	-	-	-
fasciculus retroflexus	0.22	0.02	0.22	0.02	0.95	0.35	0.00	-	-	-
stria terminalis	0.35	0.02	0.36	0.03	-0.91	0.37	0.00	-	-	-
olfactory bulbs	0.22	0.01	0.22	0.01	0.88	0.39	0.00	-	-	-
arbor vita of cerebellum	0.24	0.02	0.25	0.01	-0.78	0.44	0.01	-	-	-
pars posterior anterior commissure	0.23	0.02	0.22	0.02	0.78	0.44	0.01	-	-	-
optic tract	0.30	0.02	0.29	0.02	0.75	0.46	0.01	-	-	-
habenular commissure	0.14	0.03	0.14	0.02	-0.73	0.47	0.01	-	-	-
hypothalamus	0.27	0.02	0.27	0.01	0.65	0.52	0.01	-	-	-
corticospinal tract or pyramids	0.23	0.04	0.24	0.05	-0.64	0.53	0.01	-	-	-
medulla	0.26	0.02	0.27	0.01	-0.64	0.53	0.01	-	-	-
pars anterior anterior commissure	0.27	0.03	0.26	0.02	0.63	0.54	0.01	-	-	-
amygdala	0.25	0.01	0.25	0.01	-0.48	0.63	0.01	-	-	-
cerebellar cortex	0.21	0.01	0.21	0.01	0.48	0.63	0.01	-	-	-
superior colliculus	0.20	0.01	0.20	0.01	-0.38	0.70	0.01	-	-	-
middle cerebellar peduncle	0.33	0.06	0.34	0.06	-0.37	0.71	0.01	-	-	-
pre-para subiculum	0.19	0.01	0.19	0.01	0.31	0.76	0.01	-	-	-
medial lemniscus or medial longitudinal fasciculus	0.26	0.02	0.26	0.02	-0.27	0.79	0.01	-	-	-
medial septum	0.27	0.02	0.27	0.02	0.26	0.80	0.01	-	-	-
posterior commissure	0.23	0.01	0.23	0.01	-0.20	0.84	0.01	-	-	-
thalamus	0.26	0.01	0.26	0.02	0.14	0.89	0.01	-	-	-
globus pallidus	0.33	0.02	0.33	0.02	0.12	0.91	0.01	-	-	-
fourth ventricle	0.29	0.02	0.28	0.02	1.23	0.23	0.00	-	-	-
third ventricle	0.22	0.01	0.22	0.01	1.07	0.30	0.00	-	-	-
lateral septum	0.27	0.01	0.27	0.02	1.04	0.31	0.00	-	-	-
lateral ventricle	0.28	0.02	0.27	0.02	0.23	0.82	0.01	-	-	-
mammilothalamic tract	0.26	0.02	0.26	0.02	-0.14	0.89	0.01	-	-	-
stratum granulosum of hippocampus	0.20	0.01	0.20	0.01	0.07	0.94	0.01	-	-	-
Summary Regions										
Cerebral grey	0.23	0.01	0.23	0.01	0.12	0.91	0.05	-	-	-
Cerebral White	0.28	0.01	0.28	0.01	-1.02	0.32	0.02	-	-	-
Olfactory	0.23	0.01	0.23	0.01	1.10	0.28	0.02	-	-	-
Cerebellum	0.28	0.02	0.27	0.02	0.37	0.72	0.04	-	-	-
Ventricles	0.25	0.01	0.24	0.01	1.19	0.24	0.02	-	-	-
Brainstem	0.22	0.01	0.23	0.01	-2.49	0.02	0.01	1.00	5.62	↑

I next investigated whether there were any differences in FA between KET-DAY and SAL-DAY mice. I found 6 regions displaying significant increases in FA (Figure 16 and Table 23); dentate gyrus of the hippocampus, fimbria, stratum granulosum of the hippocampus, lateral septum, inferior colliculus and medial lemniscus. Of these 6 regions, 3 also displayed significant reductions in MD in KET-DAY mice; fimbria, lateral septum and media lemniscus. Furthermore, the inferior colliculus also displayed a significant reduction in RD in KET-DAY mice.

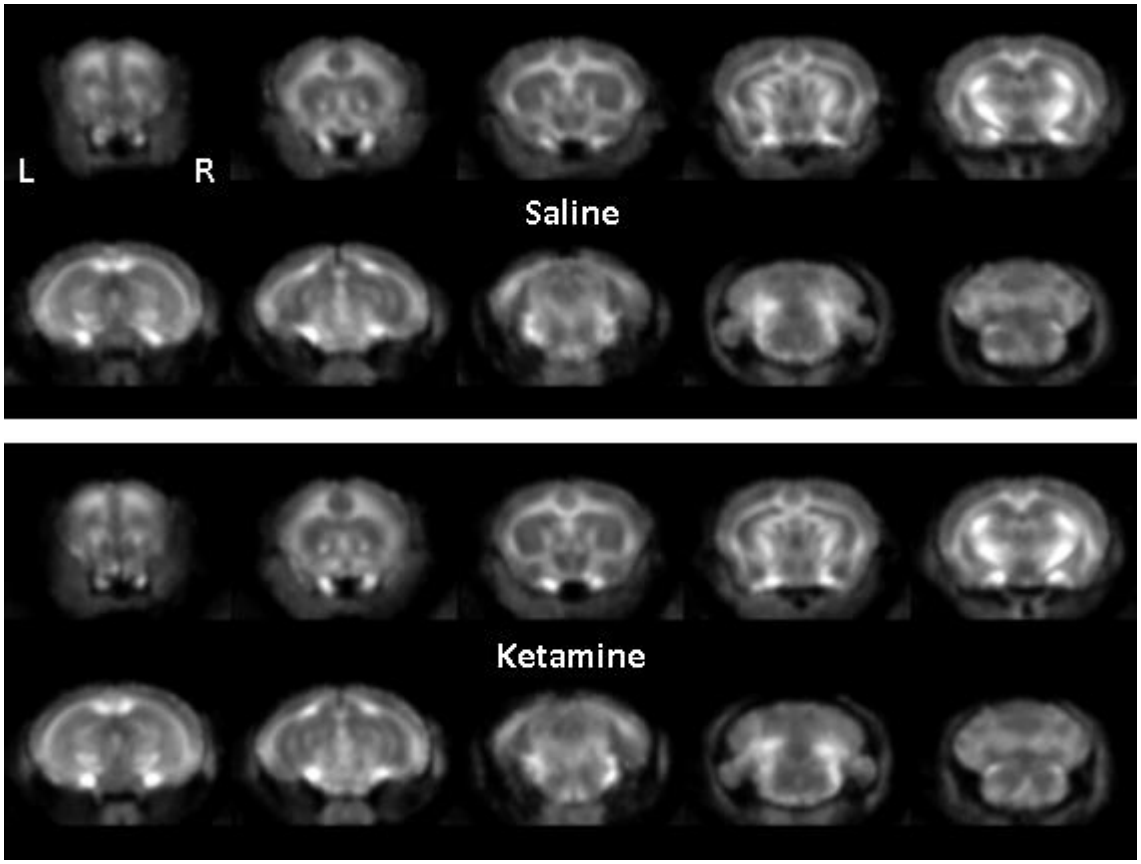

Figure 16. Coronal sections of group mean FA images from KET-DAY and SAL-DAY mice. L= left, R= Right.

Comparing differences between daily and intermittent administration of ketamine revealed a common reduction in FA in the fimbria of mice exposed to either intermittent or daily ketamine. In contrast, whilst there were significant increases in FA in the dentate gyrus of KET-DAY mice, there was a significant decrease in FA in the same region in KET-INT mice, highlighting a clearly distinct effect as a function of the frequency of ketamine exposure.

Table 23. Region of interest differences in fractional anisotropy (FA) between KET-DAY and SAL-DAY mice.

Region of Interest	Saline mean	Saline SD	Ketamine mean	Ketamine SD	T statistic	p value	q value	Cohen's d	Percentage change (%)	
dentate gyrus of hippocampus	0.25	0.01	0.28	0.02	-4.08	0.00	0.00	1.90	9.73	↑
fimbria	0.22	0.02	0.25	0.02	-3.63	0.00	0.00	1.50	11.40	↑
stratum granulosum of hippocampus	0.25	0.02	0.27	0.01	-2.52	0.02	0.04	1.26	6.61	↑
lateral septum	0.20	0.02	0.21	0.01	-2.38	0.03	0.04	0.63	7.17	↑
inferior colliculus	0.22	0.02	0.24	0.02	-2.22	0.04	0.04	1.00	7.91	↑
medial lemniscus or medial longitudinal fasciculus	0.29	0.02	0.31	0.02	-2.15	0.04	0.04	1.00	4.90	↑
pars anterior anterior commissure	0.17	0.04	0.21	0.04	-1.99	0.06	0.05	-	-	-
lateral olfactory tract	0.32	0.02	0.30	0.02	1.88	0.07	0.05	-	-	-
hippocampus	0.23	0.02	0.22	0.02	1.86	0.08	0.05	-	-	-
arbor vita of cerebellum	0.19	0.05	0.17	0.02	1.82	0.09	0.05	-	-	-
fundus of striatum	0.23	0.02	0.24	0.02	-1.76	0.09	0.05	-	-	-
pons	0.27	0.10	0.21	0.08	1.76	0.09	0.05	-	-	-
inferior olivary complex	0.20	0.02	0.18	0.01	1.72	0.10	0.05	-	-	-
fourth ventricle	0.26	0.01	0.25	0.01	1.67	0.11	0.05	-	-	-
corticospinal tract or pyramids	0.25	0.02	0.26	0.01	-1.65	0.12	0.05	-	-	-
superior cerebellar peduncle	0.29	0.03	0.31	0.03	-1.51	0.14	0.05	-	-	-
cerebellar cortex	0.26	0.03	0.24	0.02	1.44	0.17	0.05	-	-	-
olfactory tubercle	0.25	0.02	0.26	0.02	-1.43	0.17	0.05	-	-	-
cerebral cortex frontal lobe	0.35	0.02	0.36	0.02	-1.43	0.17	0.05	-	-	-
cerebral cortex occipital lobe	0.20	0.02	0.21	0.02	-1.42	0.17	0.05	-	-	-
corpus callosum	0.23	0.01	0.24	0.01	-1.41	0.17	0.05	-	-	-
medial septum	0.23	0.01	0.22	0.02	1.34	0.19	0.05	-	-	-
nucleus accumbens	0.20	0.02	0.21	0.02	-1.33	0.20	0.05	-	-	-
periaqueductal grey	0.27	0.02	0.28	0.01	-1.30	0.21	0.05	-	-	-
cuneate nucleus	0.24	0.03	0.25	0.03	-1.28	0.21	0.05	-	-	-
cerebral cortex parieto-temporal lobe	0.29	0.02	0.30	0.02	-1.24	0.23	0.05	-	-	-
superior colliculus	0.27	0.03	0.29	0.02	-1.16	0.26	0.06	-	-	-
pontine nucleus	0.27	0.02	0.28	0.03	-1.09	0.29	0.06	-	-	-
cerebral cortex entorhinal cortex	0.28	0.02	0.28	0.02	0.98	0.34	0.07	-	-	-
olfactory bulbs	0.23	0.02	0.23	0.01	-0.99	0.34	0.07	-	-	-
stria terminalis	0.25	0.01	0.25	0.01	-0.91	0.37	0.07	-	-	-
mammilothalamic tract	0.20	0.02	0.19	0.01	0.89	0.39	0.07	-	-	-
subependymale zone or rhinocele	0.23	0.04	0.24	0.03	-0.86	0.40	0.07	-	-	-
pars posterior anterior commissure	0.25	0.03	0.26	0.02	-0.85	0.41	0.07	-	-	-
fornix	0.29	0.02	0.30	0.01	-0.84	0.41	0.07	-	-	-
midbrain	0.27	0.02	0.27	0.02	-0.82	0.42	0.07	-	-	-
interpedunclar nucleus	0.22	0.02	0.22	0.01	0.78	0.45	0.07	-	-	-
lateral ventricle	0.22	0.01	0.23	0.01	-0.76	0.46	0.07	-	-	-
striatum	0.35	0.03	0.34	0.03	0.74	0.47	0.07	-	-	-
internal capsule	0.23	0.02	0.23	0.01	-0.66	0.52	0.08	-	-	-
mammillary bodies	0.14	0.02	0.15	0.02	-0.64	0.53	0.08	-	-	-
medulla	0.17	0.02	0.16	0.01	0.64	0.53	0.08	-	-	-
amygdala	0.23	0.02	0.24	0.01	-0.61	0.55	0.08	-	-	-
cerebral peduncle	0.22	0.03	0.22	0.01	0.60	0.56	0.08	-	-	-
basal forebrain	0.25	0.02	0.25	0.01	-0.58	0.57	0.08	-	-	-
inferior cerebellar peduncle	0.26	0.02	0.27	0.02	-0.53	0.60	0.08	-	-	-
pre-para subiculum	0.26	0.02	0.26	0.02	0.51	0.62	0.08	-	-	-
middle cerebellar peduncle	0.25	0.02	0.25	0.02	-0.50	0.62	0.08	-	-	-
cerebral aqueduct	0.21	0.01	0.20	0.01	0.47	0.64	0.08	-	-	-
globus pallidus	0.29	0.05	0.28	0.04	0.47	0.64	0.08	-	-	-
habenular commissure	0.26	0.03	0.26	0.03	0.43	0.67	0.08	-	-	-
facial nerve (cranial nerve 7)	0.23	0.01	0.23	0.01	0.38	0.71	0.08	-	-	-
stria medullaris	0.24	0.02	0.23	0.02	0.37	0.71	0.08	-	-	-
posterior commissure	0.20	0.07	0.21	0.09	-0.31	0.76	0.09	-	-	-
fasciculus retroflexus	0.27	0.02	0.27	0.02	0.28	0.79	0.09	-	-	-
bed nucleus of stria terminalis	0.20	0.03	0.21	0.01	-0.24	0.81	0.09	-	-	-
optic tract	0.21	0.01	0.21	0.02	0.23	0.82	0.09	-	-	-
hypothalamus	0.24	0.02	0.24	0.01	0.03	0.97	0.10	-	-	-
ventral tegmental decussation	0.27	0.02	0.28	0.01	-1.86	0.08	0.05	-	-	-
superior olivary complex	0.32	0.02	0.33	0.02	-1.31	0.20	0.05	-	-	-
third ventricle	0.27	0.04	0.26	0.01	0.92	0.38	0.07	-	-	-
thalamus	0.27	0.04	0.27	0.03	-0.11	0.91	0.10	-	-	-
Summary Regions										
Cerebral grey	0.25	0.01	0.25	0.01	-0.80	0.43	-	-	-	-
Cerebral White	0.23	0.01	0.24	0.01	-1.45	0.16	-	-	-	-
Olfactory	0.26	0.02	0.26	0.01	-0.58	0.57	-	-	-	-
Cerebellum	0.25	0.01	0.25	0.01	0.92	0.37	-	-	-	-
Ventricles	0.24	0.02	0.23	0.01	0.98	0.34	-	-	-	-
Brainstem	0.25	0.01	0.25	0.01	-0.70	0.49	-	-	-	-

e) Voxel-based analysis of DTI parameter maps; MD, AD, RD and FA

To complement and extend the atlas based analysis, I next analysed the DTI parameter maps on a voxel by voxel basis. Like the TBM analysis in which I extracted volume measurements from each voxel in each mouse brain image, using the MR mouse pipeline I was also able to extract measures of MD, AD, RD and FA from each voxel of my DTI parameter maps from all animals in my two experiments. I was then able to compare average vales between KET-INT and SAL-INT mice and between KET-DAY and SAL-DAY mice.

i) Daily ketamine administration (MD, AD and RD)

As I found significant decreases in MA, AD and RD in multiple brain regions in KET-DAY mice I decided to first analyse these parameter maps in a voxel by voxel manner. This analysis revealed several voxel clusters with significant ($p \leq 0.05$ and FDR $q \leq 0.05$) decreases in MD, AD and RD, spanning multiple brain regions which map onto those identified by the atlas-based analysis (Figures 17-19 respectively).

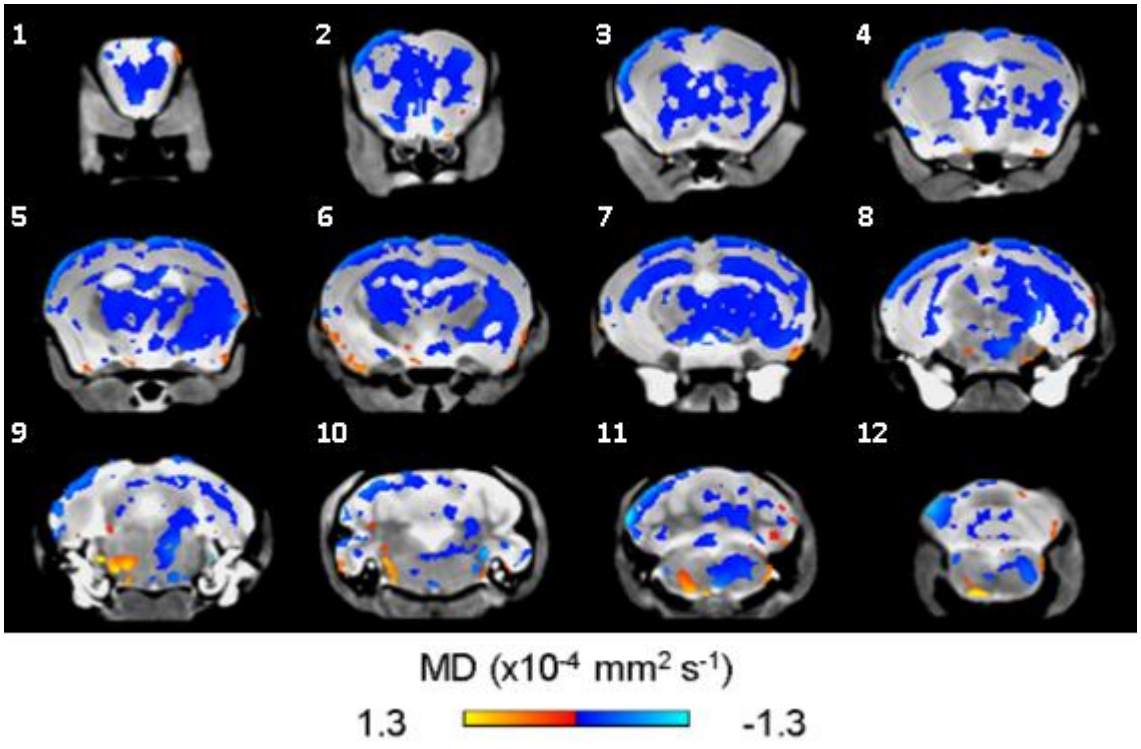

Figure 17. Coronal brain slices displaying mean diffusivity (MD) differences between KET-DAY and SAL-DAY mice**.** Smaller MD in KET-DAY mice are displayed in blue. Larger MD in KET-DAY mice are displayed in red. Data shown are thresholded at $p<0.05$, FDR corrected at $q=0.05$.

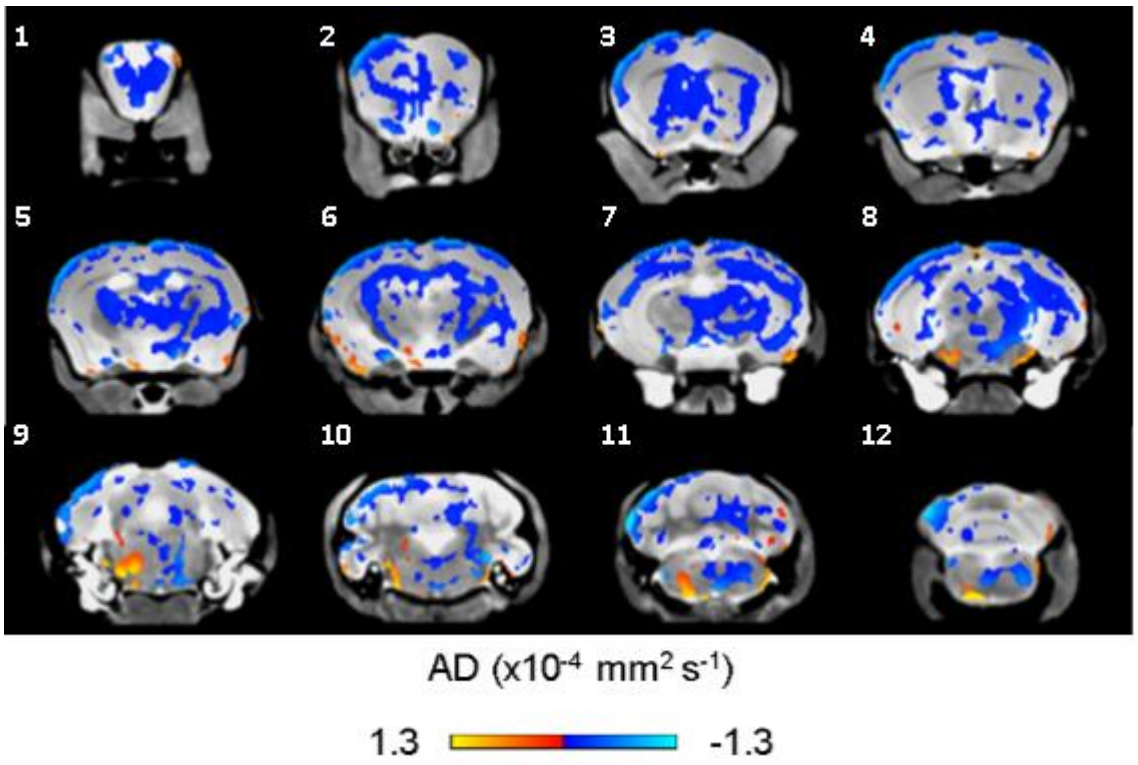

Figure 18. Coronal brain slices displaying axial diffusivity (AD) differences between KET-DAY and SAL-DAY mice**.** Smaller AD in KET-DAY mice are displayed in blue. Larger AD in KET-DAY mice are displayed in red. Data shown are thresholded at $p<0.05$, FDR corrected at $q=0.05$.

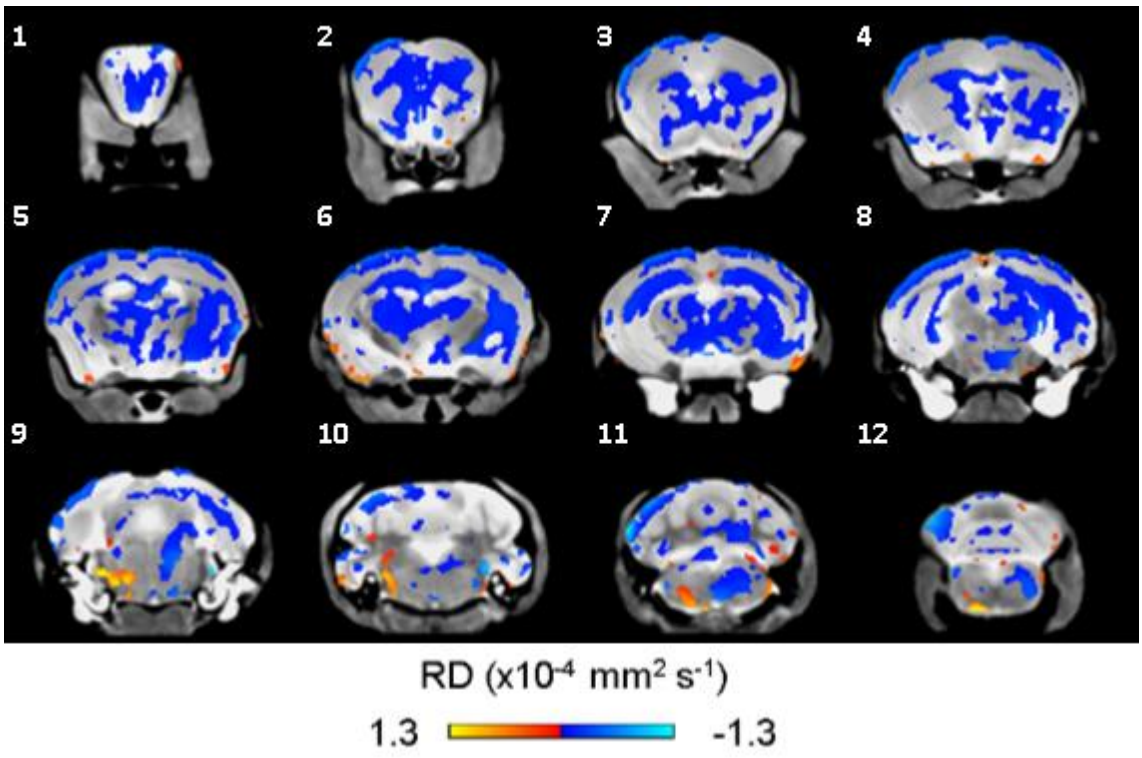

Figure 19. Coronal brain slices displaying radial diffusivity (RD) differences between KET-DAY and SAL-DAY mice**.** Smaller RD in KET-DAY mice are displayed in blue. Larger RD in KET-DAY mice are displayed in red. Data shown are thresholded at $p<0.05$, FDR corrected at $q=0.05$.

59 of 62 previously assessed brain regions displayed voxel clusters with significant decreases in MD (table 24), 60 of 62 previously analysed ROIs displayed voxel clusters with significant decreases in AD (Table 25) and 59 of 62 brain regions displayed voxel clusters with significant decreases in RD (Table 26).

In general, the differences in MD, AD and RD between KET-DAY and SAL-DAY mice are very extensive, particularly within the frontal cortex, basal ganglia, hippocampus, thalamus, ventral midbrain and most major white matter tracts. Thus, daily repeat ketamine administration clearly has a profound effect on mouse brain microstructure.

ii) Interittent ketamine administration (MD, AD and RD)

Although I did not find any significant differences in MD, AD and RD in my ROI analysis of KET-INT mice, I analysed this dataset for voxel-level differences in these parameters, based on the increased sensitivity of this method, including the ability to reveal whether there may be both increases and decreases in these parameters within a given ROI. This is important, since the atlas ROI are large and interpolate the signal to an average across all voxels contained in the ROI. Hence, if there are differential effects within a given ROI, these will not be seen and will likely average out to no net change. Furthermore, since the analysis is conducted on a per voxel basis, rather than a global average of the ROI, it is inherently more sensitive to detect subtle perturbations of brain structure.

It is not surprising therefore that a voxel-wise analysis of the DTI data revealed significant ($p \leq 0.05$ and FDR $q \leq 0.05$) differences in MD, AD and RD in clusters of voxels across multiple brain regions (Figures 20-22 respectively).

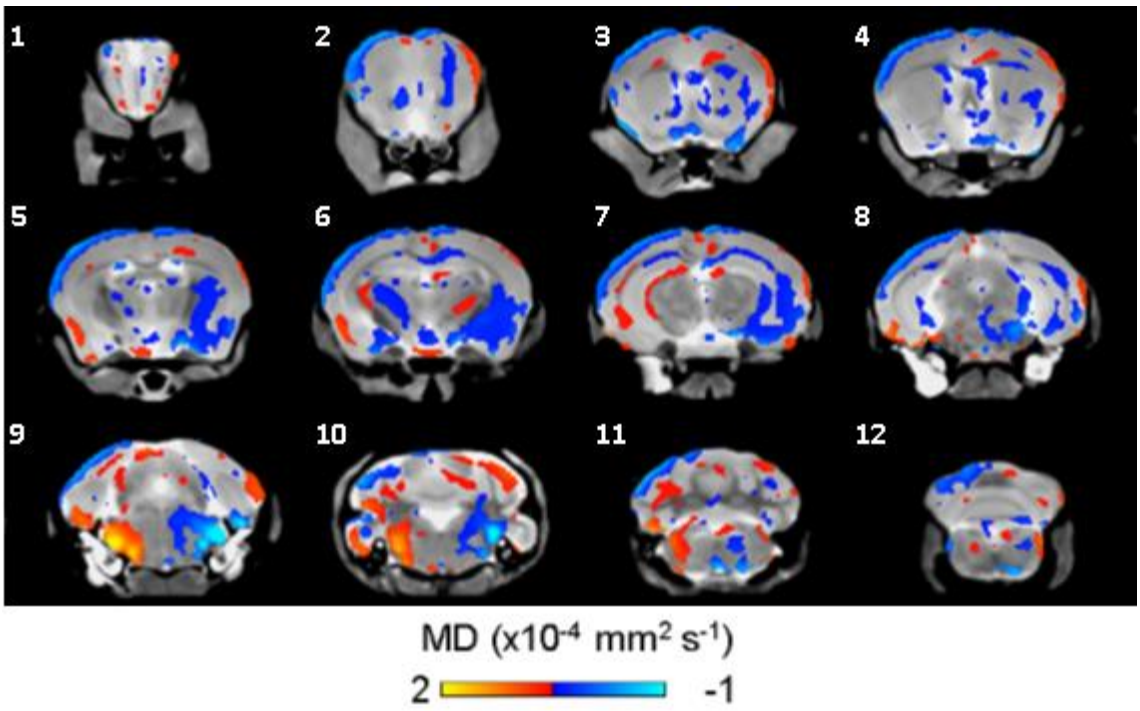

Figure 20. Coronal brain slices displaying mean diffusivity (MD) differences between KET-INT and SAL-INT mice**.** Smaller MD in KET-INT mice are displayed in blue. Larger MD in KET-INT mice are displayed in red. Data shown are thresholded at p<0.05, FDR corrected at q=0.05.

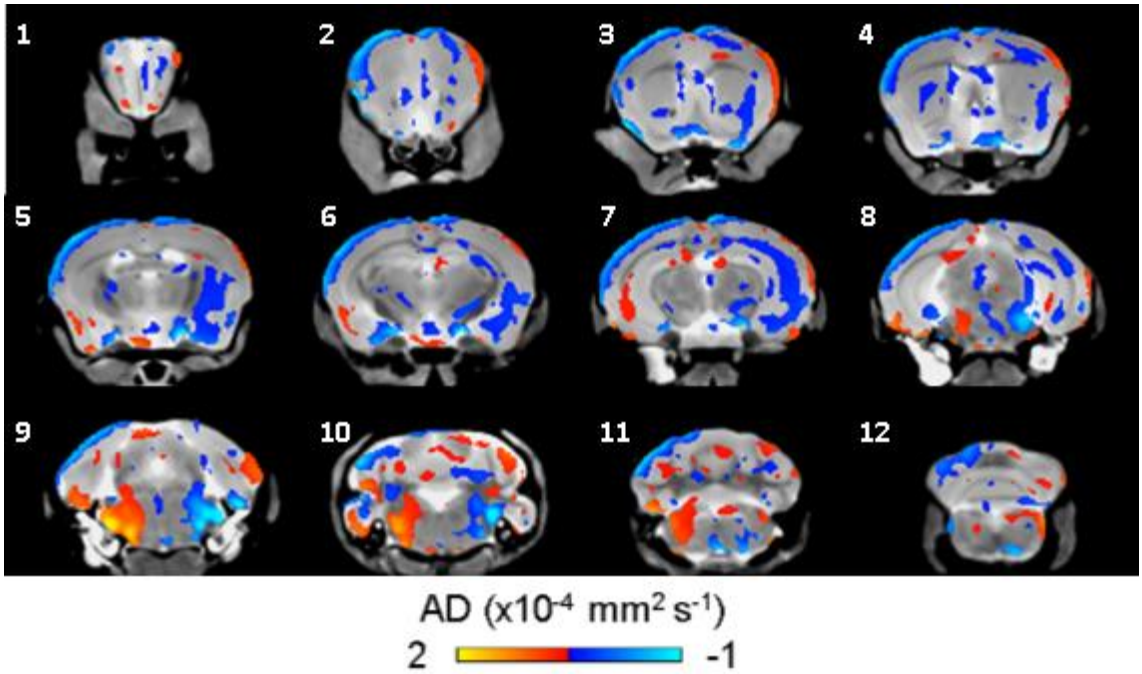

Figure 21. Coronal brain slices displaying axial diffusivity (AD) differences between KET-INT and SAL-INT mice**.** Smaller AD in KET-INT mice are displayed in blue. Larger AD in KET-INT mice are displayed in red. Data shown are thresholded at p<0.05, FDR corrected at q=0.05.

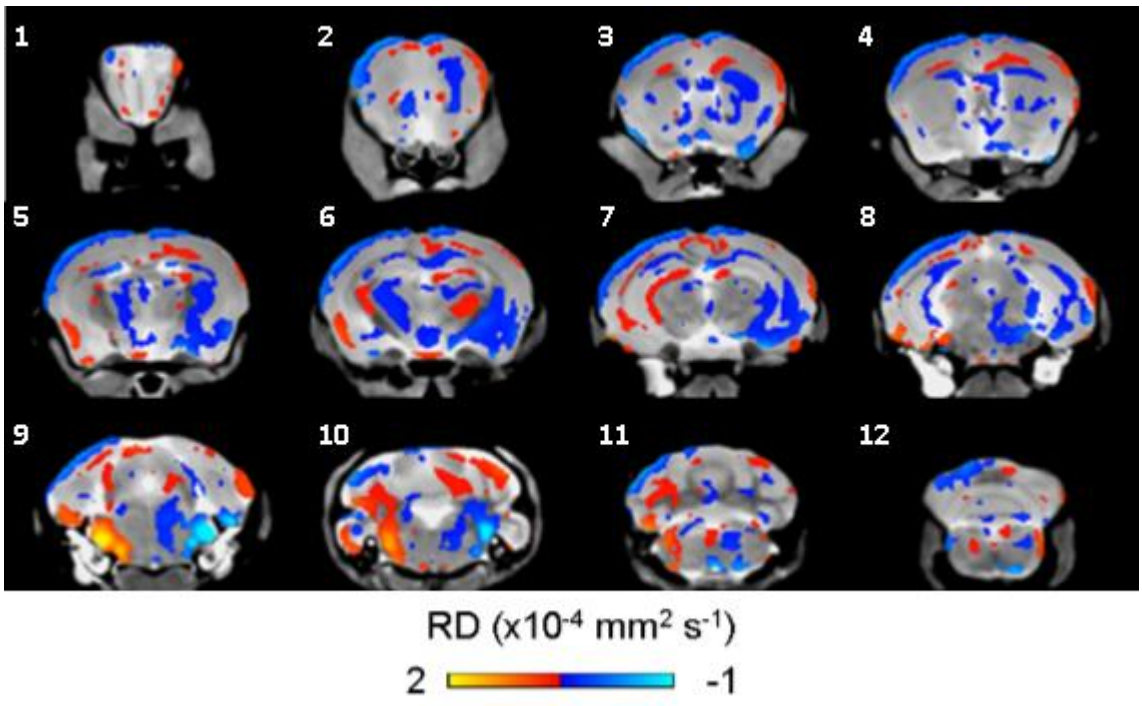

Figure 22. Coronal brain slices displaying radial diffusivity (RD) differences between KET-INT and SAL-INT mice**.** Smaller RD in KET-INT mice are displayed in blue. Larger AD in KET-INT mice are displayed in red. Data shown are thresholded at $p<0.05$, FDR corrected at $q=0.05$.

45 of 62 previously assessed brain regions displayed voxel clusters with significant differences in MD (Table 27), 40 of 62 previously analysed ROIs displayed voxel clusters with significant decreases in AD (Table 28) and 47 of 62 brain regions displayed voxel clusters with significant decreases in RD (Table 29).

Unlike in KET-DAY mice, decreases in MD, AD and RD in KET-INT mice are clearly much more restricted and the size of the voxel clusters is noticeably smaller. Furthermore, unlike in KET-DAY mice, where the effects on, MD, AD and RD reflect a rather common, almost global decrease, the KET-INT mice appears to show a balance between both increases and decreases in MD, AD and RD in KET-INT mice, which often overlap within a specified ROI and may be lateralised, rather than bilateral. These factors likely combine to explain the overall lack of significance in the atlas data for the KET-INT dataset, and highlight the power of voxel-wise analysis to complement and extend the atlas-based analysis.

For example, regions displaying clusters of voxels with bilateral decreases in MD, AD and RD in KET-INT mice included the cerebral cortex (frontal, parietal, temporal and occipital lobes) where decreases were more widespread in the left hemisphere of each

region, the corpus callosum, where decreases were more pronounced in the right hemisphere and the amygdala, where decreases were more pronounced in the right hemisphere (panel 6 in Figures 20-22).

Similarly, there are examples of regions displaying clusters of voxels with unilateral decreases in MD, AD and RD in KET-INT mice including the left striatum (panel 4 in Figures 20-22), right hippocampus (panel 7 in Figures 20-22) and left lobule of the cerebellar cortex (panels 11&12 in Figures 20-22). Examples of regions displaying clusters of voxels with unilateral increases in MD, AD and RD in KET-INT mice include the left piriform cortex (panels 5&6 in Figures 20-22), right thalamus (panel 6 in Figures 20-22), left amygdala (panel 7 in Figures 20-22) and right lobule of the cerebellar cortex (panels 10&11 in Figures 20-22).

Despite these differences, it is notable that several brain regions in both KET-DAY and KET-INT mice show similar directional changes in MD, AD and RD, albeit of lower magnitude in the KET-INT mice. Examples include significant decreases in MD, AD and RD within the cerebral cortex (particularly in the upper layers of the left hemisphere) and in the corpus callosum. As mentioned above, the clusters of voxels displaying these decreases do however appear smaller and less widespread in KET-INT mice compared to KET-DAY mice.

Table 24. Region of interest analysis versus voxel-wise analysis for mean diffusivity (MD) differences in the daily experiment. Regions where significant ($p<0.05$, FDR $q< 0.05$) changes reside are highlighted in green. Regions where no significant changes reside are highlighted in red.

Region of interest	ROI analysis	Voxel Analysis
amygdala	✔	✔
arbor vita of cerebellum	✔	✔
basal forebrain	✔	✔
cerebral cortex entorhinal cortex	✔	✔
cerebral cortex frontal lobe	✔	✔
cerebral cortex parieto-temporal lobe	✔	✔
cerebral peduncle	✔	✔
corpus callosum	✔	✔
facial nerve (cranial nerve 7)	✔	✔
fasciculus retroflexus	✔	✔
fimbria	✔	✔
fornix	✔	✔
fourth ventricle	✔	✔
fundus of striatum	✔	✔
inferior cerebellar peduncle	✔	✔
inferior colliculus	✔	✔
inferior olivary complex	✔	✔
internal capsule	✔	✔
lateral septum	✔	✔
lateral ventricle	✔	✔
mammillary bodies	✔	✔
mammilothalamic tract	✔	✔
medial lemniscus or medial longitudinal fasciculus	✔	✔
medial septum	✔	✔
middle cerebellar peduncle	✔	✔
olfactory tubercle	✔	✔
pontine nucleus	✔	✔
stria terminalis	✔	✔
superior colliculus	✔	✔
superior olivary complex	✔	✔
bed nucleus of stria terminalis	X	✔
cerebellar cortex	X	✔
cerebral cortex occipital lobe	X	✔
corticospinal tract or pyramids	X	✔
dentate gyrus of hippocampus	X	✔
globus pallidus	X	✔
habenular commissure	X	✔
hippocampus	X	✔
hypothalamus	X	✔
interpeduncular nucleus	X	✔
medulla	X	✔
midbrain	X	✔
nucleus accumbens	X	✔
olfactory bulbs	X	✔
optic tract	X	✔
pars anterior anterior commissure	X	✔
pars posterior anterior commissure	X	✔
periaqueductal grey	X	✔
pons	X	✔
posterior commissure	X	✔
pre-para subiculum	X	✔
stratum granulosum of hippocampus	X	✔
stria medullaris	X	✔
striatum	X	✔
subependymale zone or rhinocele	X	✔
superior cerebellar peduncle	X	✔
thalamus	X	✔
third ventricle	X	✔
ventral tegmental decussation	X	✔
cerebral aqueduct	X	X
cuneate nucleus	X	X
lateral olfactory tract	X	X

Table 25. Region of interest analysis versus voxel-wise analysis for axial diffusivity (AD) differences in the daily experiment. Regions where significant ($p<0.05$, FDR $q< 0.05$) changes reside are highlighted in green. Regions where no significant changes reside are highlighted in red.

Region of interest	ROI analysis	Voxel Analysis
amygdala	✔	✔
arbor vita of cerebellum	✔	✔
basal forebrain	✔	✔
cerebral cortex entorhinal cortex	✔	✔
cerebral cortex frontal lobe	✔	✔
cerebral cortex parieto-temporal lobe	✔	✔
cerebral peduncle	✔	✔
corpus callosum	✔	✔
facial nerve (cranial nerve 7)	✔	✔
fasciculus retroflexus	✔	✔
fimbria	✔	✔
fornix	✔	✔
inferior cerebellar peduncle	✔	✔
inferior olivary complex	✔	✔
internal capsule	✔	✔
interpeduncular nucleus	✔	✔
lateral septum	✔	✔
mammillary bodies	✔	✔
mammilothalamic tract	✔	✔
medial lemniscus or medial longitudinal fasciculus	✔	✔
medial septum	✔	✔
middle cerebellar peduncle	✔	✔
olfactory tubercle	✔	✔
pontine nucleus	✔	✔
superior colliculus	✔	✔
superior olivary complex	✔	✔
fourth ventricle	✔	✔
fundus of striatum	✔	✔
lateral olfactory tract	✔	✔
lateral ventricle	✔	✔
bed nucleus of stria terminalis	X	✔
cerebellar cortex	X	✔
cerebral cortex occipital lobe	X	✔
corticospinal tract or pyramids	X	✔
dentate gyrus of hippocampus	X	✔
globus pallidus	X	✔
habenular commissure	X	✔
hippocampus	X	✔
hypothalamus	X	✔
inferior colliculus	X	✔
medulla	X	✔
midbrain	X	✔
nucleus accumbens	X	✔
olfactory bulbs	X	✔
optic tract	X	✔
pars anterior anterior commissure	X	✔
pars posterior anterior commissure	X	✔
periaqueductal grey	X	✔
pons	X	✔
posterior commissure	X	✔
pre-para subiculum	X	✔
stratum granulosum of hippocampus	X	✔
stria medullaris	X	✔
stria terminalis	X	✔
striatum	X	✔
subependymale zone or rhinocele	X	✔
superior cerebellar peduncle	X	✔
thalamus	X	✔
third ventricle	X	✔
ventral tegmental decussation	X	✔
cerebral aqueduct	X	X
cuneate nucleus	X	X

Table 26. Region of interest analysis versus voxel-wise analysis for radial diffusivity (RD) differences in the daily experiment. Regions where significant ($p<0.05$, FDR $q< 0.05$) changes reside are highlighted in green. Regions where no significant changes reside are highlighted in red.

Region of interest	ROI analysis	Voxel Analysis
amygdala	✔	✔
arbor vita of cerebellum	✔	✔
basal forebrain	✔	✔
cerebral cortex entorhinal cortex	✔	✔
cerebral cortex frontal lobe	✔	✔
cerebral cortex parieto-temporal lobe	✔	✔
cerebral peduncle	✔	✔
corpus callosum	✔	✔
facial nerve (cranial nerve 7)	✔	✔
fasciculus retroflexus	✔	✔
fimbria	✔	✔
fornix	✔	✔
fourth ventricle	✔	✔
fundus of striatum	✔	✔
inferior cerebellar peduncle	✔	✔
inferior colliculus	✔	✔
inferior olivary complex	✔	✔
internal capsule	✔	✔
interpeduncular nucleus	✔	✔
lateral septum	✔	✔
lateral ventricle	✔	✔
mammillary bodies	✔	✔
mammilothalamic tract	✔	✔
medial lemniscus or medial longitudinal fasciculus	✔	✔
medial septum	✔	✔
middle cerebellar peduncle	✔	✔
olfactory tubercle	✔	✔
pontine nucleus	✔	✔
stria medullaris	✔	✔
stria terminalis	✔	✔
superior colliculus	✔	✔
superior olivary complex	✔	✔
bed nucleus of stria terminalis	X	✔
cerebellar cortex	X	✔
cerebral cortex occipital lobe	X	✔
corticospinal tract or pyramids	X	✔
dentate gyrus of hippocampus	X	✔
globus pallidus	X	✔
habenular commissure	X	✔
hippocampus	X	✔
hypothalamus	X	✔
medulla	X	✔
midbrain	X	✔
nucleus accumbens	X	✔
olfactory bulbs	X	✔
optic tract	X	✔
pars anterior anterior commissure	X	✔
pars posterior anterior commissure	X	✔
periaqueductal grey	X	✔
pons	X	✔
posterior commissure	X	✔
pre-para subiculum	X	✔
stratum granulosum of hippocampus	X	✔
striatum	X	✔
subependymale zone or rhinocele	X	✔
superior cerebellar peduncle	X	✔
thalamus	X	✔
third ventricle	X	✔
ventral tegmental decussation	X	✔
cerebral aqueduct	X	X
cuneate nucleus	X	X
lateral olfactory tract	X	X

Table 27. Region of interest analysis versus voxel-wise analysis for mean diffusivity (MD) differences in the intermittent experiment. Regions where significant ($p<0.05$, FDR $q< 0.05$) changes reside are highlighted in green. Regions where no significant changes reside are highlighted in red.

Region of interest	ROI analysis	Voxel Analysis
amygdala	x	✔
arbor vita of cerebellum	x	✔
basal forebrain	x	✔
cerebellar cortex	x	✔
cerebral aqueduct	x	✔
cerebral cortex entorhinal cortex	x	✔
cerebral cortex frontal lobe	x	✔
cerebral cortex occipital lobe	x	✔
cerebral cortex parieto-temporal lobe	x	✔
cerebral peduncle	x	✔
corpus callosum	x	✔
corticospinal tract or pyramids	x	✔
cuneate nucleus	x	✔
facial nerve (cranial nerve 7)	x	✔
fimbria	x	✔
fundus of striatum	x	✔
globus pallidus	x	✔
hippocampus	x	✔
hypothalamus	x	✔
inferior cerebellar peduncle	x	✔
inferior olivary complex	x	✔
internal capsule	x	✔
interpedunclar nucleus	x	✔
lateral septum	x	✔
mammillary bodies	x	✔
medial septum	x	✔
medulla	x	✔
midbrain	x	✔
middle cerebellar peduncle	x	✔
nucleus accumbens	x	✔
olfactory bulbs	x	✔
olfactory tubercle	x	✔
optic tract	x	✔
pars anterior anterior commissure	x	✔
pars posterior anterior commissure	x	✔
periaqueductal grey	x	✔
pons	x	✔
stria medullaris	x	✔
stria terminalis	x	✔
striatum	x	✔
subependymale zone or rhinocele	x	✔
superior cerebellar peduncle	x	✔
superior colliculus	x	✔
superior olivary complex	x	✔
thalamus	x	✔
bed nucleus of stria terminalis	x	x
dentate gyrus of hippocampus	x	x
fasciculus retroflexus	x	x
fornix	x	x
fourth ventricle	x	x
habenular commissure	x	x
inferior colliculus	x	x
lateral olfactory tract	x	x
lateral ventricle	x	x
mammilothalamic tract	x	x
medial lemniscus or medial longitudinal fasciculus	x	x
pontine nucleus	x	x
posterior commissure	x	x
pre-para subiculum	x	x
stratum granulosum of hippocampus	x	x
third ventricle	x	x
ventral tegmental decussation	x	x

Table 28. Region of interest analysis versus voxel-wise analysis for axial diffusivity (AD) differences in the intermittent experiment. Regions where significant ($p<0.05$, FDR $q< 0.05$) changes reside are highlighted in green. Regions where no significant changes reside are highlighted in red.

Region of interest	ROI analysis	Voxel Analysis
amygdala	x	✔
arbor vita of cerebellum	x	✔
basal forebrain	x	✔
cerebellar cortex	x	✔
cerebral aqueduct	x	✔
cerebral cortex entorhinal cortex	x	✔
cerebral cortex frontal lobe	x	✔
cerebral cortex occipital lobe	x	✔
cerebral cortex parieto-temporal lobe	x	✔
cerebral peduncle	x	✔
corpus callosum	x	✔
corticospinal tract or pyramids	x	✔
cuneate nucleus	x	✔
facial nerve (cranial nerve 7)	x	✔
fimbria	x	✔
globus pallidus	x	✔
hippocampus	x	✔
hypothalamus	x	✔
inferior cerebellar peduncle	x	✔
inferior olivary complex	x	✔
internal capsule	x	✔
interpedunclar nucleus	x	✔
mammillary bodies	x	✔
medial septum	x	✔
medulla	x	✔
midbrain	x	✔
nucleus accumbens	x	✔
olfactory bulbs	x	✔
olfactory tubercle	x	✔
optic tract	x	✔
pars posterior anterior commissure	x	✔
periaqueductal grey	x	✔
pons	x	✔
stria medullaris	x	✔
stria terminalis	x	✔
striatum	x	✔
superior cerebellar peduncle	x	✔
superior colliculus	x	✔
superior olivary complex	x	✔
thalamus	x	✔
bed nucleus of stria terminalis	x	x
dentate gyrus of hippocampus	x	x
fasciculus retroflexus	x	x
fornix	x	x
fourth ventricle	x	x
fundus of striatum	x	x
habenular commissure	x	x
inferior colliculus	x	x
lateral olfactory tract	x	x
lateral septum	x	x
lateral ventricle	x	x
mammilothalamic tract	x	x
medial lemniscus or medial longitudinal fasciculus	x	x
middle cerebellar peduncle	x	x
pars anterior anterior commissure	x	x
pontine nucleus	x	x
posterior commissure	x	x
pre-para subiculum	x	x
stratum granulosum of hippocampus	x	x
subependymale zone or rhinocele	x	x
third ventricle	x	x
ventral tegmental decussation	x	x

Table 29. Region of interest analysis versus voxel-wise analysis for radial diffusivity (RD) differences in the intermittent experiment. Regions where significant ($p<0.05$, FDR $q< 0.05$) changes reside are highlighted in green. Regions where no significant changes reside are highlighted in red.

Region of interest	ROI analysis	Voxel Analysis
amygdala	x	✔
arbor vita of cerebellum	x	✔
basal forebrain	x	✔
bed nucleus of stria terminalis	x	✔
cerebellar cortex	x	✔
cerebral aqueduct	x	✔
cerebral cortex entorhinal cortex	x	✔
cerebral cortex frontal lobe	x	✔
cerebral cortex occipital lobe	x	✔
cerebral cortex parieto-temporal lobe	x	✔
cerebral peduncle	x	✔
corpus callosum	x	✔
corticospinal tract or pyramids	x	✔
cuneate nucleus	x	✔
dentate gyrus of hippocampus	x	✔
facial nerve (cranial nerve 7)	x	✔
fimbria	x	✔
fundus of striatum	x	✔
globus pallidus	x	✔
hippocampus	x	✔
hypothalamus	x	✔
inferior cerebellar peduncle	x	✔
inferior olivary complex	x	✔
internal capsule	x	✔
interpedunclar nucleus	x	✔
lateral septum	x	✔
mammillary bodies	x	✔
medial septum	x	✔
medulla	x	✔
midbrain	x	✔
middle cerebellar peduncle	x	✔
nucleus accumbens	x	✔
olfactory bulbs	x	✔
olfactory tubercle	x	✔
optic tract	x	✔
pars anterior anterior commissure	x	✔
pars posterior anterior commissure	x	✔
periaqueductal grey	x	✔
pons	x	✔
stria medullaris	x	✔
stria terminalis	x	✔
striatum	x	✔
subependymale zone or rhinocele	x	✔
superior cerebellar peduncle	x	✔
superior colliculus	x	✔
superior olivary complex	x	✔
thalamus	x	✔
fasciculus retroflexus	x	x
fornix	x	x
fourth ventricle	x	x
habenular commissure	x	x
inferior colliculus	x	x
lateral olfactory tract	x	x
lateral ventricle	x	x
mammilothalamic tract	x	x
medial lemniscus or medial longitudinal fasciculus	x	x
pontine nucleus	x	x
posterior commissure	x	x
pre-para subiculum	x	x
stratum granulosum of hippocampus	x	x
third ventricle	x	x
ventral tegmental decussation	x	x

iii) FA differences in both daily and intermittent experiments

In KET-INT mice I found widespread significant differences in FA, compared to controls (Figure 23). For example, there were significant bilateral decreases in FA in clusters of voxels in the cerebral cortex; frontal, parietal, temporal and occipital lobes. There were significant bilateral increases in FA in the corpus callosum (panels 3-7, Figure 23), lower cortical layers of the frontal lobe (panel 2, Figure 23) and hippocampus (panel 8, Figure 23). There were also unilateral decreases in FA in voxel clusters of the right insular cortex (panel 3, Figure 23), left thalamus (panel 6, Figure 23), right internal capsule (panel 6, Figure 23) and right medial cerebellar nucleus (panel 11, Figure 23). Furthermore, there were unilateral decreases in FA in the left medial cerebellar nucleus (panel 11, Figure 23).

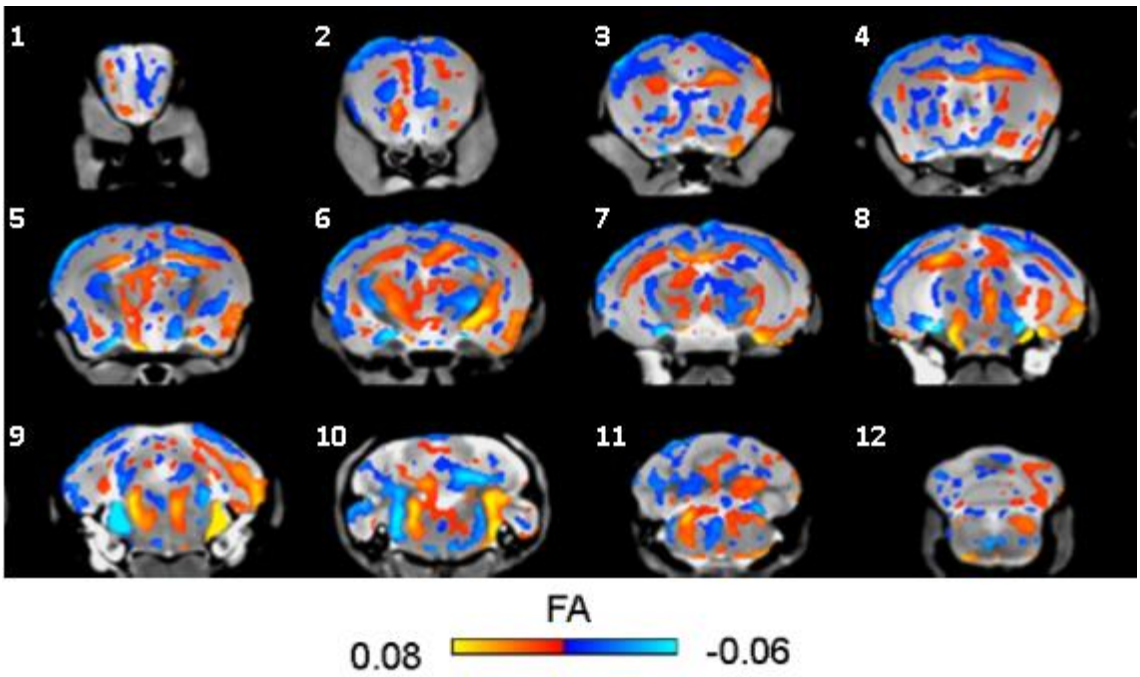

Figure 23. Coronal brain slices displaying fractional anisotropy (FA) differences between KET-INT and SAL-INT mice**.** Smaller FA in KET-INT mice are displayed in blue. Larger FA in KET-INT mice are displayed in red. Data shown are thresholded at $p<0.05$, FDR corrected at $q=0.05$.

For a comparison between where significant differences in FA are located, in KET-INT mice, from my ROI analysis and voxel-wise analysis please see Table 30.

Table 30. Region of interest analysis versus voxel-wise analysis for fractional anisotropy (FA) differences in the intermittent experiment. Regions where significant ($p<0.05$, FDR $q< 0.05$) changes reside are highlighted in green. Regions where no significant changes reside are highlighted in red.

Region of interest	ROI analysis	Voxel Analysis
cerebral cortex frontal lobe	✔	✔
cerebral cortex occipital lobe	✔	✔
cerebral cortex parieto-temporal lobe	✔	✔
cerebral peduncle	✔	✔
corpus callosum	✔	✔
cuneate nucleus	✔	✔
facial nerve (cranial nerve 7)	✔	✔
fimbria	✔	✔
inferior cerebellar peduncle	✔	✔
inferior olivary complex	✔	✔
mammillary bodies	✔	✔
midbrain	✔	✔
periaqueductal grey	✔	✔
interpedunclar nucleus	✔	✔
ventral tegmental decussation	✔	✔
amygdala	x	✔
arbor vita of cerebellum	x	✔
basal forebrain	x	✔
bed nucleus of stria terminalis	x	✔
cerebellar cortex	x	✔
cerebral aqueduct	x	✔
cerebral cortex entorhinal cortex	x	✔
corticospinal tract or pyramids	x	✔
dentate gyrus of hippocampus	x	✔
fasciculus retroflexus	x	✔
fornix	x	✔
fundus of striatum	x	✔
globus pallidus	x	✔
habenular commissure	x	✔
hippocampus	x	✔
hypothalamus	x	✔
inferior colliculus	x	✔
internal capsule	x	✔
lateral olfactory tract	x	✔
medial lemniscus or medial longitudinal fasciculus	x	✔
medial septum	x	✔
medulla	x	✔
middle cerebellar peduncle	x	✔
nucleus accumbens	x	✔
olfactory bulbs	x	✔
olfactory tubercle	x	✔
optic tract	x	✔
pars anterior anterior commissure	x	✔
pars posterior anterior commissure	x	✔
pons	x	✔
pontine nucleus	x	✔
posterior commissure	x	✔
pre-para subiculum	x	✔
stria medullaris	x	✔
stria terminalis	x	✔
striatum	x	✔
subependymale zone or rhinocele	x	✔
superior cerebellar peduncle	x	✔
superior colliculus	x	✔
superior olivary complex	x	✔
thalamus	x	✔
fourth ventricle	x	x
lateral septum	x	x
lateral ventricle	x	x
mammilothalamic tract	x	x
stratum granulosum of hippocampus	x	x
third ventricle	x	x

In KET-DAY mice I found significant differences in FA in 58 of 62 previously analysed ROIs (Figure 24 and Table 31).

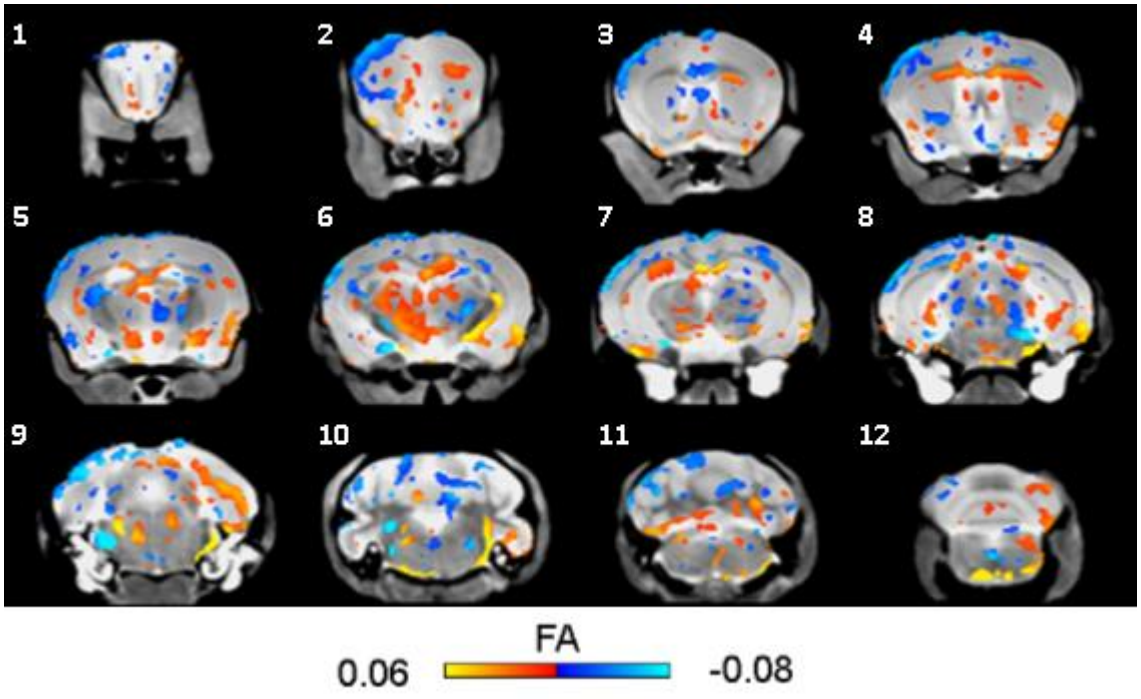

Figure 24. Coronal brain slices displaying fractional anisotropy (FA) differences between KET-DAY and SAL-DAY mice**.** Smaller FA in KET-DAY mice are displayed in blue. Larger FA in KET-DAY mice are displayed in red. Data shown are thresholded at $p<0.05$, FDR corrected at $q=0.05$.

Compared to differences observed in KET-INT mice, differences in FA in KET-DAY mice are restricted to smaller clusters of voxels. In KET-DAY mice there are significant bilateral decreases in FA in clusters of voxels in the corpus callosum and fornix. Further significant decreases in FA in clusters of voxels, in KET-DAY mice, can be seen in the cerebral cortex, right thalamus, midbrain and cerebellar cortex. Whereas examples of clusters of voxels displaying significant increase in FA, in KET-DAY mice, can be seen in the corpus callosum, fornix, left thalamus, right occipital cortex and right medial cerebellar nucleus.

Further comparing results found in KET-INT mice to those found in KET-DAY mice; similar increases in FA can be seen in the corpus callosum (panel 4 in Figures 23&24), fornix (panel 5 in Figures 23&24), left thalamus (panel 6 in Figures 23&24), right occipital lobe (panel 9 in Figures 23&24) and right medial cerebellar nucleus (panel 11 in Figures 23&24). Moreover, similar decreases in FA can be seen in the upper layers of the left cerebral cortex of the frontal lobe (panels 2-4 in Figures 23&24), deeper layers of the

right parietal lobe; somatosensory cortex (panel 7 in Figures 23&24) and in lobule 6 of the cerebellar cortex (panel 11 in Figures 23&24).

These data suggest that repeat ketamine exposure in mice affects the structure of a common series (or network) of brain regions, irrespective of the frequency of administration (daily vs. intermittent). However, the magnitude of these changes does appear to be dependent on the frequency of drug exposure. Specifically, at least for MD, RD and AD, effects of greater magnitude are observed following daily administration, as opposed to intermittent administration. Regarding FA, the larger magnitude changes are found following intermittent, as compared to daily ketamine administration. The reason for these apparent differences, depending on which DTI metric is considered is intriguing, but currently lacks a mechanistic explanation. Nonetheless, this highlights the power of pre-clinical studies where MRI changes can then be explored post-mortem at the cellular level. Indeed, in the context of ketamine effects on brain structure, a testable hypothesis given the data, is whether similar cellular mechanisms may be driving the changes in FA or MD/RD/AD in both KET-INT and KET-DAY mice.

Table 31. Region of interest analysis versus voxel-wise analysis for fractional anisotropy (FA) differences in the daily experiment. Regions where significant ($p<0.05$, FDR $q< 0.05$) changes reside are highlighted in green. Regions where no significant changes reside are highlighted in red.

Region of interest	ROI analysis	Voxel Analysis
amygdala	X	✔
arbor vita of cerebellum	X	✔
basal forebrain	X	✔
bed nucleus of stria terminalis	X	✔
cerebellar cortex	X	✔
cerebral cortex entorhinal cortex	X	✔
cerebral cortex frontal lobe	X	✔
cerebral cortex occipital lobe	X	✔
cerebral cortex parieto-temporal lobe	X	✔
cerebral peduncle	X	✔
corpus callosum	X	✔
corticospinal tract or pyramids	X	✔
dentate gyrus of hippocampus	X	✔
facial nerve (cranial nerve 7)	X	✔
fasciculus retroflexus	X	✔
fimbria	X	✔
fornix	X	✔
fundus of striatum	X	✔
globus pallidus	X	✔
habenular commissure	X	✔
hippocampus	X	✔
hypothalamus	X	✔
inferior cerebellar peduncle	X	✔
inferior colliculus	X	✔
inferior olivary complex	X	✔
internal capsule	X	✔
interpedunclar nucleus	X	✔
lateral olfactory tract	X	✔
lateral septum	X	✔
lateral ventricle	X	✔
mammillary bodies	X	✔
mammilothalamic tract	X	✔
medial lemniscus or medial longitudinal fasciculus	X	✔
medial septum	X	✔
medulla	X	✔
midbrain	X	✔
middle cerebellar peduncle	X	✔
nucleus accumbens	X	✔
olfactory bulbs	X	✔
olfactory tubercle	X	✔
optic tract	X	✔
pars anterior anterior commissure	X	✔
pars posterior anterior commissure	X	✔
periaqueductal grey	X	✔
pons	X	✔
pontine nucleus	X	✔
posterior commissure	X	✔
pre-para subiculum	X	✔
stratum granulosum of hippocampus	X	✔
stria medullaris	X	✔
stria terminalis	X	✔
striatum	X	✔
superior cerebellar peduncle	X	✔
superior colliculus	X	✔
superior olivary complex	X	✔
thalamus	X	✔
third ventricle	X	✔
ventral tegmental decussation	X	✔
cerebral aqueduct	X	X
cuneate nucleus	X	X
fourth ventricle	X	X
subependymale zone or rhinocele	X	X

iv) Comparing the effects of repeat ketamine exposure in mice with repeat ketamine use in humans on changes in brain structure, as seen by DTI

Human studies of the impact of ketamine on brain microstructure as revealed by DTI are very sparse in the literature. To date, only the studies of Liao et al (2010) and Roberts et al (2014), have examined differences in DTI metrics between human repeat ketamine users, with each study focussing only on white matter and no data available on grey matter. These studies do however; find evidence for significant structural alterations in the white matter of the frontal and tempero-parietal lobe. More specifically, Liao and colleagues found decreased FA in white matter tracts of the frontal lobe and temporoparietal lobe (Liao *et al.*, 2010). In contrast, Roberts and colleagues (2014) found reductions in AD in the white matter bundles innervating the grey matter of the cerebral cortex; anterior corona radiata, forceps major, anterior forceps minor, superior longitudinal fasciculus, inferior longitudinal fasciculus, posterior thalamic radiation, and fronto-occipital fasciculus.Although mice and humans have similar gross brain anatomies (e.g. they both have a cerebral cortex and corpus callosum), detailed anatomy differs in complexity by several orders of magnitude between the two species. For example, the human cerebral cortex is highly folded and contains multiple gyri and sulci, the gyri being innervated by white matter fibre bundles. This cerebral architecture is not present in mice and nor are the fibre tracts listed above as displaying significant reductions in AD in the study of Roberts et al (2014). Taken together, this makes any comparison of DTI changes seen in white matter bundles in the brain of human ketamine users to those seen in mice difficult.

Nevertheless, rough comparisons can be made particularly for major white matter tracts or grey matter lobes that are broadly speaking, present in both species. For example, I found clusters of voxels displaying decreased FA in both KET-INT and KET-DAY mice in the grey matter of the frontal lobe and parieto-temporal lobe, both of which are innervated by myelinated fibres arising from the corpus callosum and external capsule. Furthermore, in KET-DAY mice, I found significant decreases in AD in the following cerebral white matter bundles; corpus callosum, cerebral peduncle, fasciculus retroflexus, fimbria, fornix, mammillothalamic tract and stria medullaris. Hence, as the direction of change in FA and AD is the same in the frontal lobe, parieto-temporal lobe and white matter bundles of both mice (given repeat ketamine) and human ketamine

users then there is likely to be a common cellular/molecular mechanism responsible for these changes.

This conclusion is further re-enforced by the rather interesting animal study involving non-human primates; the cynomolgus monkey, in which ketamine induced decreases in FA, similar to those seen in humans, have been reproduced (Li *et al.*, 2017). In this study ten male adolescent cynomolgus monkeys were divided into two groups and given either 1mg/kg of ketamine or saline daily, via intravenous injection for 3 months. The monkeys then underwent DTI scanning and images were compared between the two groups. Like the findings from humans in Liao et al (2010), monkeys given ketamine presented with reduced FA in the left middle temporal gyrus and left frontal gyrus.

The cynomolgus monkey is evolutionarily closer to humans and the monkey brain is more like that of the human brain, in comparison to how similar the mouse brain is to the human brain. The results from Li et al (2017) then support the conclusions drawn in Liao et al (2010); that repeat ketamine administration is responsible for the decrease in FA in white matter bundles of the frontal lobe and temporoparietal lobe. Moreover, these results support a common mechanism, for ketamine-induced decreases in FA, across all three species.

f) Summary

In this chapter I have demonstrated that both daily and intermittent ketamine administration results in significant structural and microstructural re-arrangement of the mouse brain as compared to those mice exposed to vehicle-control. Whilst ketamine exposure affects similar series or networks of brain regions, there are differences in the magnitude of the effect, which appear to be dependent on the frequency of drug administration. For example, with respect to volume change, ketamine appears to have a greater effect when given intermittently and KET-INT mice present with a greater number of large cluster changes in volume, throughout the brain. In contrast, in terms of structure as indexed by DTI, ketamine appears to have a greater effect when given daily on MD, RD and AD, but not FA, the latter being more strongly affected in the KET-INT mice.

Overall, my data suggest that whilst there is some degree of convergent overlap in the directionality of volume changes following repeat ketamine exposure across species,

particularly in the striatum, there is also clearly divergence, particularly regarding the effects of ketamine on the volume of the frontal lobe and nucleus accumbens between mice and humans. Of course, species-specific differences in the response to ketamine cannot be definitively excluded. Nonetheless, it is equally plausible that these differences arise as a function of exposure to additional drugs in the human users. For example a reduction in cerebral volume as has been seen to occur in independent studies for the following drugs, nicotine, alcohol, cocaine and heroin (Lim *et al.*, 2008; Liu *et al.*, 2009; Grodin, Lin, C. A. Durkee, *et al.*, 2013; Li *et al.*, 2015).

The mechanisms driving the observed effects of ketamine at the cellular level are also unclear, but the mouse model offers the opportunity to probe this, guided by the MRI findings, as presented in Chapter 4 of this thesis and discussed in the preceding sections.

It should be noted, however, that all animal studies modelling clinical and/or human conditions need to make approximate choices and thus several limitations and caveats apply. This should be kept in mind when considering the highly contextual nature of MRI data (see Chapter 1). Specifically, it is conceivable that the dose and duration of the ketamine exposure in the mouse model employed in this study is not enough to recapitulate the spectrum of changes in brain volume observed in the human users. Since I did not have access to specific data on these parameters, this is an obvious limitation. Nonetheless, I did find some common effects of ketamine on brain volume across species, supporting my choices about the dose and frequency of ketamine injection. These were based on careful consideration of the available literature and reflect a pragmatic and rational start-point for future studies to address the impact of additional ketamine doses and / or longer duration of exposure on mouse brain structure. These studies should also be extended to include an assessment of the impact of early exposure to ketamine during vulnerable periods of brain development such as adolescence. Indeed, the demographic data on the ketamine users (Chapter 2) strongly suggests that these individuals may have begun using drugs (including alcohol and tobacco) much earlier than the poly-drug controls, as evidenced by the longer duration of exposure, despite matching for age. Animal studies also clearly point to long-term detrimental effects of adolescent ketamine exposure on adult brain function and cognitive behaviour, using a similar dose range to that used in the current study (Featherstone *et al.*, 2012). However, MRI data for these models is currently lacking and

represents an important gap in our knowledge, as does any evidence for sex-specific effects.

A further point to consider in the interpretation of these data is that the effects observed in human ketamine users on brain volume may also very likely reflect complex interactions between drug use and pre-existing genetic variation between individuals, as well as the possibility of additional environmental hits in terms of socio-economic status and so on. Support for this possibility is provided by studies of the effects of cannabis exposure on cortical thickness, which is clearly moderated by individuals genetic pre-disposition, as indexed by the polygenic risk score, indicative of "loading" for a greater or lesser number of single nucleotide polymorphisms in schizophrenia susceptibility genes (French *et al.*, 2015). There is also considerable comorbidity between schizophrenia and substance use disorder, which is partially attributable to shared polygenic liability (Hartz *et al.*, 2017). Notably then, many of the ketamine users in the human data set report at least one family member with a history of mental health problems (see Chapter 2). Since these disorders are highly heritable such gene x environment interactions driving the MRI data are likely, which would not be recapitulated in my mouse model. Future studies are therefore required to explore any potential genetic risk factor x ketamine interactions.

On the other hand, both human ketamine users and mice treated with repeat doses of ketamine present with decreases in FA in the frontal lobe and parieto-temporal lobe, as well as with decreases in AD in cerebral white matter tracts. Hence, it is likely that a common cellular/molecular mechanism is responsible for these changes and this is something, which should be investigated further.

Chapter 4 Cellular correlates of neuroimaging changes seen in two mouse models of repeat ketamine exposure

4.1 Introduction

As discussed elsewhere in this thesis, both human ketamine users (chapter 2) and mice exposed to repeat doses of ketamine (chapter 3) present with decreases in FA in the frontal and parieto-temporal lobe grey matter, accompanied by decreases in AD in cerebral white matter tracts (Liao *et al.*, 2010, 2011; Wang *et al.*, 2013; Edward Roberts *et al.*, 2014). It is therefore plausible that a common cellular mechanism may be responsible for these changes, which requires the cellular correlates of these MR changes be investigated further.

Furthermore, mice repeatedly exposed to ketamine (chapter 3) display changes in the volume of the cerebral cortex, dependent on the frequency of ketamine administration. Specifically, mice exposed to intermittent injections of ketamine (once every 3 days for 30 days) were found to have a significantly larger frontal lobe, as compared to saline controls. A similar effect was present in mice exposed to daily injections of ketamine, be it to a much lesser extent. These data are the exact opposite of what has been previously reported in human ketamine users, which describe a decrease in frontal lobe grey matter volume (Liao *et al.*, 2011; Wang *et al.*, 2013). Whilst the cellular nature of the grey matter loss in humans is unknown, the fact that the opposite occurs in mice, particularly following intermittent drug exposure, is intriguing and requires further investigation.

Acute injections of ketamine induce elevations in glutamate release in the both the mouse and human frontal cortex (Kim *et al.*, 2011a; Stone, Dietrich and Edden, 2012). Similarly, acute ketamine exposure is associated with elevated 2-deoxyglucose (2-DG) uptake, indicative of increased neural activity and functional connectivity between the frontal cortex and several other brain regions, including the thalamus and hippocampus (Dawson *et al.*, 2014). Acute exposure to ketamine also results in elevated cerebral protein synthesis (Autry *et al.*, 2011) and increases in both plasticity (e.g. ARC) and synaptic (e.g. PSD-95) proteins, as well as increased density of dendritic spines (Li *et al.*, 2010). It is therefore plausible that intermittent, but not daily ketamine administration induces a recurrent cerebral plasticity, resulting in a structural adaptation to ketamine exposure, in this case, increased volume in the mouse frontal cortex. Support for this hypothesis also comes from MRI studies on learning in mice, in which morphological

changes detected by MRI associated with learning a behavioural task (e.g. Morris water maze) have been seen to increase synthesis of proteins associated with synaptic plasticity such as GAP-43, BDNF, synaptic and astrocyte proteins (Lerch *et al.*, 2011; Sagi *et al.*, 2012).

Whilst these data offer several testable hypotheses about the effect of ketamine exposure on grey matter, with regards to what cellular changes may underlie ketamine-driven changes in the DTI parameters; FA and AD is much less clear. Indeed, dissecting how changes in DTI metrics relate to specific structural alterations at the cellular level is fraught with difficulty and has multiple possible solutions that may not be mutually exclusive. For example, in the case of FA, a change in this metric may reflect changes in myelin, membrane permeability, axonal number or size, or a combination of all those factors (Jones, Knösche and Turner, 2013). Additional cellular changes may also occur, including, but not limited to; an increase in glial cell number, or an increase in the amount of sub-cellular structures in the neuropil characterised by increased dendritic branching or spine formation, increased glial ramification, or a change in the amount and/or orientation of the cerebral vasculature (Alexander *et al.*, 2007; Beaulieu, 2009; Zatorre, Fields and Johansen-Berg, 2012; Aung, Mar and Benzinger, 2013; Stolp *et al.*, 2018). However, there is a paucity of information on what may underlie ketamine-induced structural changes, detectable by MRI. Given the overlap between DTI findings in humans (Edward Roberts *et al.*, 2014) and the mouse data in this thesis (Chapter 3) such data would be of great interest to the field.

To address the issues, in this chapter, I have conducted an in-depth investigation of the putative cellular correlates underlying structural neuroimaging changes I observed in mice exposed to either daily or intermittent ketamine administration (chapter 3). Such post-mortem work is labour-intensive, and this requires clear a priori hypotheses about regions of interest (ROI) to focus on. I therefore reviewed the neuroimaging data from chapter 3 and chose to focus on two specific brain regions for these investigations, specifically, the mouse frontal cortex and corpus callosum. The rationale for these choices reflects the differences and similarities between the human and mouse MRI data. For example, a larger frontal lobe volume in the mouse, particularly after intermittent administration, compared to decreased volume in humans.

The choice of the corpus callosum, a major white matter tract in the mouse brain, is based on my findings that mice exposed to repeat daily doses of ketamine have smaller callosal volumes, in contrast to those mice given repeat intermittent ketamine, which have larger volumes (section 3.4.b). Furthermore, both daily and intermittent dosing of ketamine in mice resulted in reduced MD, AD and RD values in this region, along with increases in FA (section 3.4.e), consistent with published human data (Liao *et al.*, 2010; Edward Roberts *et al.*, 2014).

4.2 Experimental aims and hypotheses

a) Hypotheses

1. There will be no significant group-level difference in the number of neurons in the frontal lobe.
2. There will be a significant difference in the number of astrocytes and microglia in the frontal lobe and corpus callosum
3. There will be no significant difference in the number of active astrocytes and active microglia in the prefrontal cortex of the frontal lobe and in the corpus callosum
4. There will be a significant difference in the amount of myelin in the prefrontal cortex of the frontal lobe and in the corpus callosum
5. There will be significantly fewer parvalbumin expressing interneurons in the prefrontal cortex of the frontal lobe, in mice repeatedly given ketamine
6. There will be a significant increase in the amount of synaptophysin in the prefrontal cortex of the frontal lobe and in the corpus callosum, of ketamine treated mice

b) Aims

1. To investigate whether there is a group-level difference in cell number in the frontal lobe and/or corpus callosum, between mice repeatedly administered ketamine versus saline. Cell types investigated include:
    a. Neurons

    b. Astrocytes
    c. Microglia
2. To investigate whether there is a group-level difference in the number of activated astrocytes and/or microglia in the prefrontal cortex of the frontal lobe and/or corpus callosum, between mice repeatedly administered ketamine versus saline.
3. To investigate whether there is a group-level difference in the number of axons and amount of myelin content in the prefrontal cortex of the frontal lobe and/or corpus callosum, between mice repeatedly administered ketamine versus saline.
4. To investigate whether there is a group-level difference in the number of parvalbumin expressing interneurons in the prefrontal cortex of the frontal lobe, between mice repeatedly administered ketamine versus saline.
5. To investigate whether there is a group-level difference in the amount of synaptophysin in the prefrontal cortex of the frontal lobe, between mice repeatedly administered ketamine versus saline.

4.3 Materials and methods

a) Tissue processing

After completion of all MR imaging, fixed brains (n=10 per group; KET-INT, SAL-INT, KET-DAY, SAL-DAY) were dissected from the skull, and incubated in 4% PFA / 0.01M PBS for 24 hours, followed by cryoprotection in 30% buffered sucrose solution for 48 hours at +4°C. Brains were then mounted on the stage of a freezing microtome (Microm HM 430, Wallendorf, Germany), coated with Shandon M-1 embedding matrix (ThermoFisher Scientific, Waltham, MA, USA) and 40µm coronal sections were cut and stored sequentially in 96 well plates containing an anti-freeze cryoprotectant solution (TCS: 25% glycerin [vol/vol] 30% ethylene glycol [vol/vol] in 0.2 mol/L phosphate buffer + 0.05% sodium azide), stored at +4°C.

b) Cresyl Fast Violet (Nissl) staining

To visualize neuronal cytoarchitecture, and to facilitate stereological analyses, 40µm brain sections were mounted as a 1 in 6 series on to chrome-gelatin coated slides and left to air-dry overnight at room temperature. The slides were then incubated for 10 minutes in 0.05% cresyl fast violet solution (VWR) with 0.05% acetic acid (VWR) at room temperature. Stained sections were then differentiated through a series of graded Industrial Methylated Spirit (IMS) solutions (70%, 80%, 90%, 95% and 2x100%) before being cleared in Xylene (VWR) and coverslipped with DPX (VWR), a xylene-based mountant.

c) Immunostaining

Either a 1 in 6 (prefrontal cortex) or 1 in 12 (frontal lobe and corpus callosum) series of brain sections were immunostained free-floating for markers of astrocytes, microglia, myelin, axons, interneurons and pre-synaptic proteins (Table 32). Endogenous peroxidase activity was quenched with 1% H_2O_2 in PBS, washed and then blocked in 15% normal serum (Vector Laboratories, Peterborough, UK) diluted in PBS-T. The species of

normal serum was directed against the host species of the secondary antibody. After blocking, sections were incubated overnight at 4°C in primary antibody in 10% normal serum in PBS-T. Sections were then washed and incubated at room temperature in biotinylated secondary antibody at 1:1000 dilution for 2 hours (Table 32) followed by washing and incubation in Vectastain Elite ABC kit (1+1:1000, Vector Laboratories) for 2 hours before visualization by incubation with a 3'3-diaminobenzidine (DAB) peroxidase (HRP) staining kit (Vector Laboratories, Peterborough, UK. Sections were then mounted on to chrome-gelatin coated slides, air-dried overnight, differentiated through a series of graded Industrial Methylated Spirit (IMS) solutions (70%, 80%, 90%, 95% and 2x100%), cleared in xylene (VWR) and coverslipped in DPX (VWR).

Table 32. Primary and secondary antibodies used for immunostaining

	Primary antibody	**Dilution**	**Secondary Antibody**	**Dilution**
Astrocytes	Rabbit anti-GFAP (Dako 20002902)	1 in 20,000	Goat anti rabbit (Vector BA1000)	1 in 1,000
	Rabbit anti-s100b (Abcam 41548)	1 in 2,000	Goat anti rabbit (Vector BA1000)	1 in 1,000
Microglia	Rabbit anti-Iba 1 (Menapath MP-290-CR05)	1 in 1,000	Goat anti rabbit (Vector BA1000)	1 in 1,000
	Rat anti-mouse CD68 (AbD Serotec, MCA 1957)	1 in 1,000	Goat anti rat (Vector BA9400)	1 in 1,000
Myelin	Rat anti myelin basic protein (Abcam 7349)	1 in 1,000	Goat anti rat (Vector BA9400)	1 in 1,000
Axons	Chicken anti-neurofilament (Acris AP31813PU-N)	1 in 500	Goat anti-chicken (Vector 9010)	1 in 1,000
Interneurons	Rabbit anti-parvalbumin (Swant PV25)	1 in 5,000	Swine anti-rabbit (Dako E0353)	1 in 1,000
Pre-synaptic proteins	Mouse anti-synaptophysin (Upstate, ADI-VAM-SV011)	1 in 100	Goat anti-mouse (Vector BA9200)	1 in 1,000

d) Stereology

Design-based stereology enables the accurate measurement of cell counts (Schmitz and Hof, 2005). Design-based stereology is done by first designing a random and systematic sampling scheme such that the objects measured are sampled independent of size, shape, spatial orientation and distribution (West, 2002). This is important, as the measurements of objects will therefore be unbiased to any differences in the

morphology and size of any brain regions being compared. Furthermore, this assumption of three-dimensional spatial independence allows for the reduction of systemic errors in counting, as compared to other counting methods (Gundersen and Jensen, 1987).

To perform design-based stereological measurements, 40µm brain sections at 1 in 6 or 1 in 12 intervals which contained the following regions of interest; Frontal lobe (6 sections between Bregma +0.38mm and +2.8mm), prefrontal cortex (6 sections between Bregma +1.34mm and +2.54mm) and corpus callosum (5 sections between Bregma +1.7mm and +2.7mm) were collected. These sections were stained for specific markers of interest, such as cresyl fast violet for neurons or for markers for astrocytes and microglia. These sections were then compared to the Dorr MRI mouse brain atlas (Dorr *et al.*, 2008) and to a stereological reference atlas of mouse brain anatomy (Paxinos, G. and Franklin, 2001) to accurately draw anatomical boundaries of the regions of interest (Figures 25-27). All stereological measures in this study were carried out using *Stereoinvestigator* software (Microbrightfield Inc.) connected to a *Zeiss Axioskop 2 MOT* (Zeiss) with an *MBF bioscience camera DC1394 (IIDC)*.

Cell counts were performed using an optical fractionator technique (West, 2002). This combines an optical dissector, which is a method used to count nuclei in a three dimensional context with a fractionator, which is a method for systematic and uniform sampling of a two-dimensional area (West, 2002). The optical dissector includes the optical section planes by moving the focal plane along the z-axis and estimates cell numbers without any bias towards their size or shape. The fractionator (Gundersen & Jensen, 1987), applies systematic random sampling sites, thus reducing the total number of cells counted, as well as removing any sampling bias.

To count cells using the optical fractionator, first, data regarding the thickness of the sections and periodicity was recorded. The region of interest was identified in each section and a contour is drawn around it at a low magnification. An appropriately sized grid is then superimposed onto the drawn contour to provide a succession of systematic random sampling sites. A counting frame was then defined at a high magnification such that there was a uniform distribution of counting frames for every sampling site defined by the grid. Gird sizes and counting frame sizes for each marker and ROI are given in table 33.

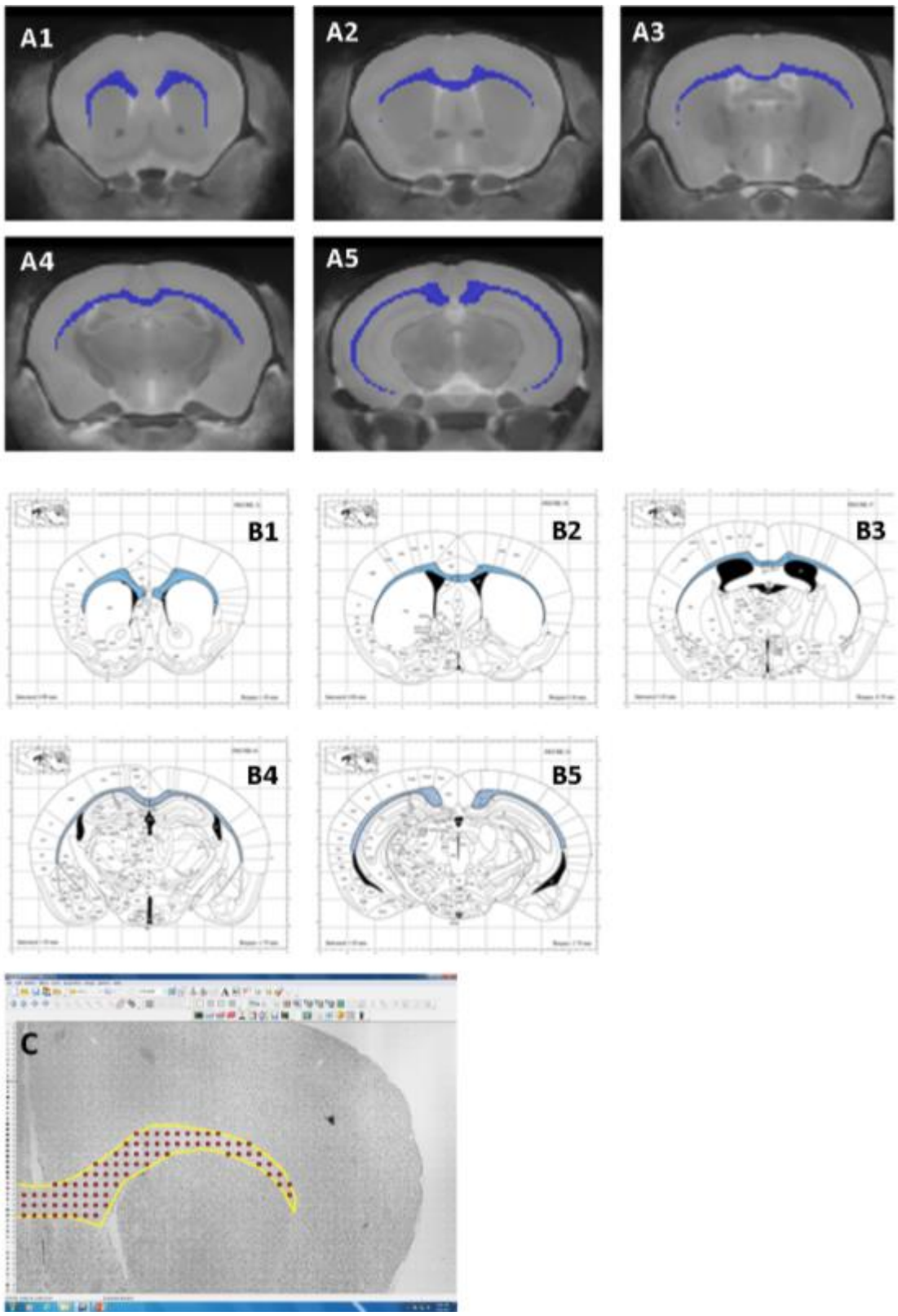

Figure 25.Region of interest identification; corpus callosum. Mouse MR images (A1-5) and serological atlas images (B1-5) of the mouse brain were compared to identify the corpus callosum (shaded in blue) in histological sections (C) for cell counting.

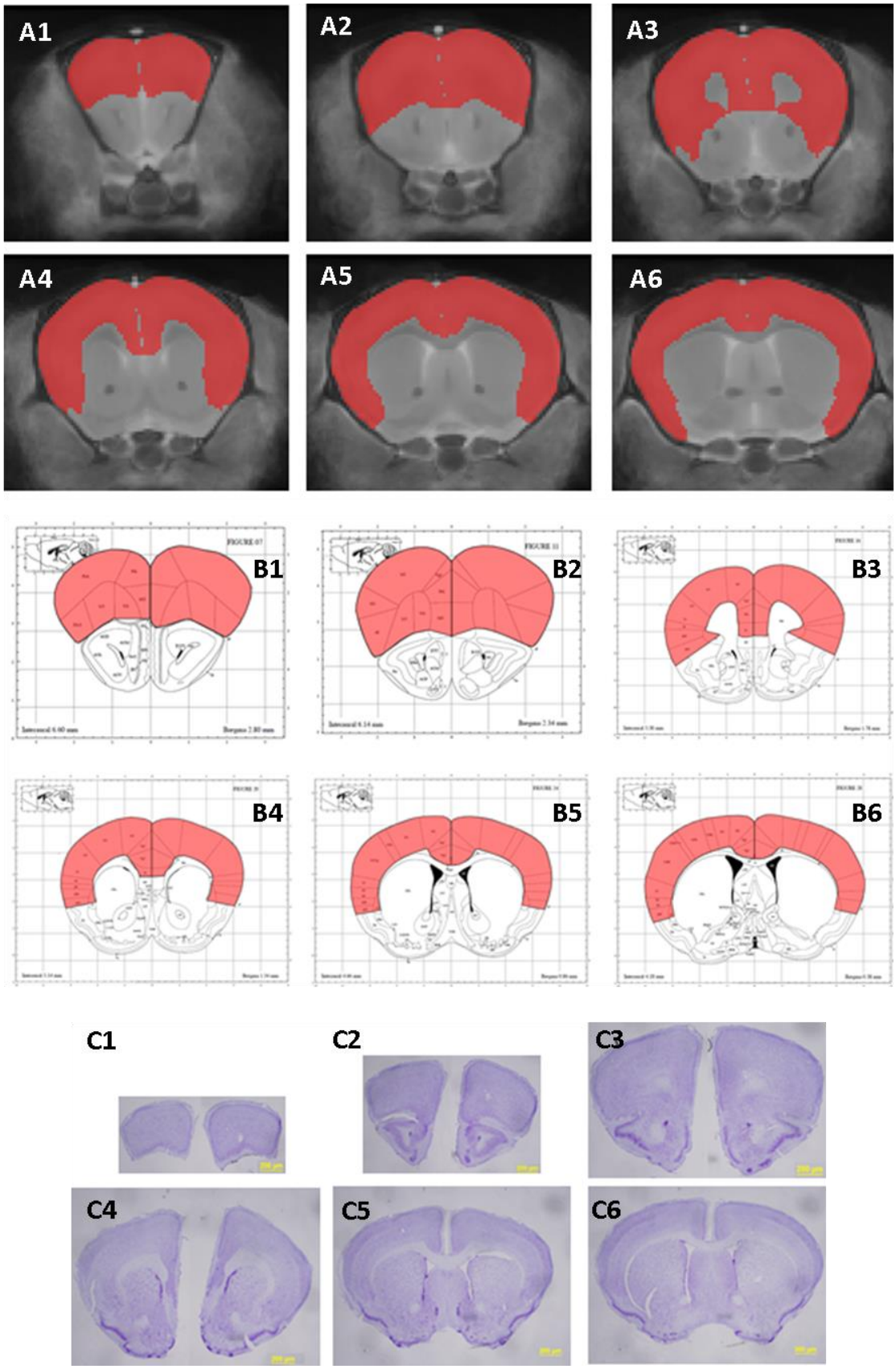

Figure 26.Region of interest identification; frontal lobe. Mouse MR images (A1-6) and serological atlas images (B1-6) of the mouse brain were compared to identify the frontal lobe (shaded in red) in histological sections (C1-6) for cell counting.

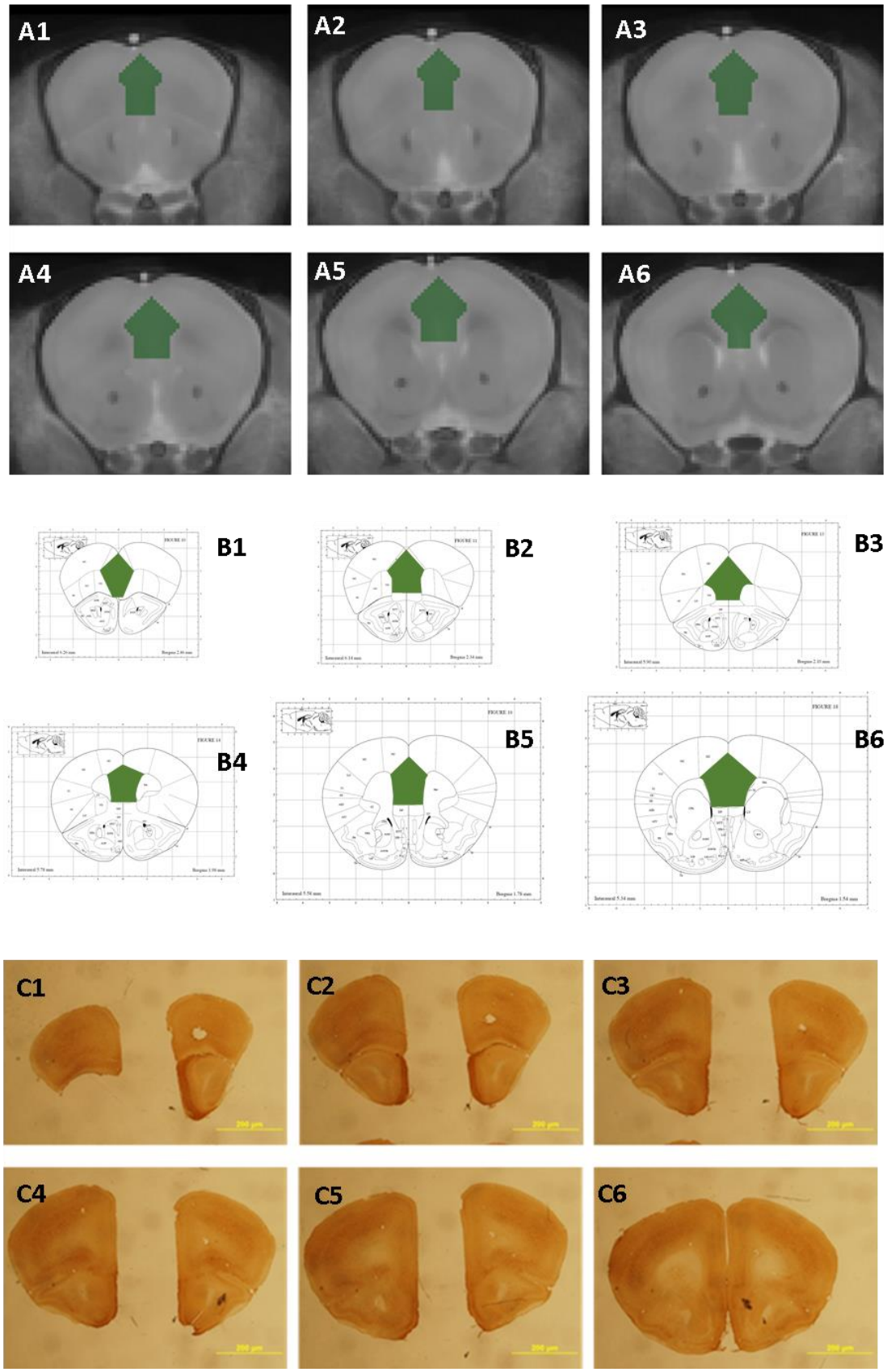

Figure 27.Region of interest identification; prefrontal cortex. Mouse MR images (A1-6) and serological atlas images (B1-6) of the mouse brain were compared to identify the prefrontal cortex (shaded in green) in histological sections (C1-6) for cell counting.

Table 33. Grid sizes and counting frame sizes for stereological cell counting.

	Nissl positive neurons	Iba-1 positive microglia		s100b positive atrocytes
	Fronta lobe	Frontal lobe	Corpus callosum	Frontal lobe
Counting Frame Width (X) (μm)	60	120	100	120
Counting Frame Height (Y) (μm)	60	120	100	120
Sampling Grid (X) (μm)	600	600	200	600
Sampling Grid (Y) (μm)	600	600	200	600

Cells were then counted at each sampling site, to include those within the defined counting frame and those that lie in contact with the upper and right borders (coloured green) of the frame, while excluding those outside the counting frame or in contact with the left and lower borders of the counting frame (coloured red) (Figure 28).Counts obtained by the optical fractionator were within the limits of the Gundersen mean co-efficient of error (COE) of 0.05-0.1.

All cell counts were performed whilst blind to the experimental group the animal belonged to.

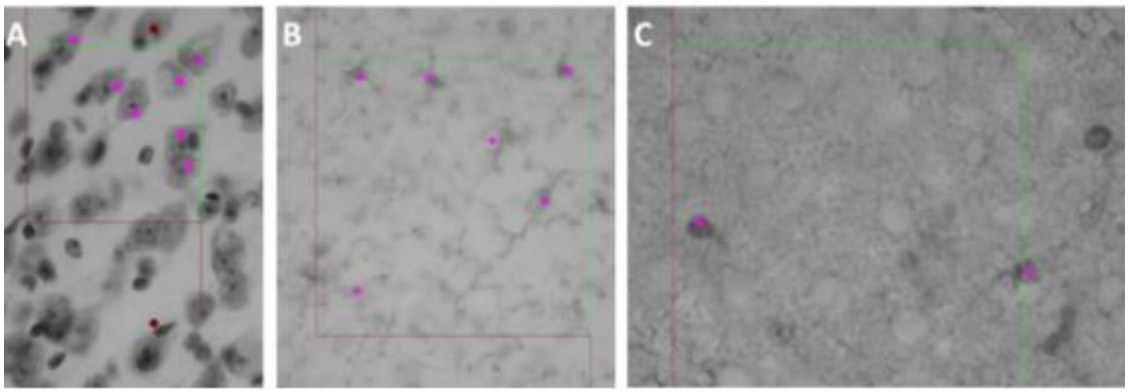

Figure 28. Sample images demonstrating the counting of neurons (A), Iba-1 positive microglia (B) and S100b positive astrocytes (C) within the borders of the counting frame. Cells within the frame and in contact with the green borders were counted (represented by purple dots).

e) Thresholding image analysis

If a protein or marker is densely distributed in a region, the intensity of immunostaining can make it difficult to accurately discriminate individual cells. For example, GFAP staining for fibrous astrocytes within any given region. Therefore, attempts to quantify such staining using counting methods proves difficult. In such cases, semi-automated thresholding image analysis was employed to obtain a measure of the amount of staining per microscope field.

This technique was employed in the current study to quantify the level of glial activation; astrocytes (GFAP) and microglia (CD68), as well as the amount of myelin content (MBP), axon density (neurofilament), parvalbumin expressing interneurons and pre-synaptic protein (synaptophysin). To quantify immunoperoxidase staining for a given marker in each region; non-overlapping images were acquired over 3-6 consecutive sections per region (Table 34). Images were acquired using a *Leica DRMB microscope* (Leica Microscopy & GmBH, Wetzlar, Germany) with a *Lumenera infinity 3 camera*. All images were obtained while maintaining consistent parameters of light intensity, camera setup and calibrations.

Table 34. Number and magnification of images for thresholding analysis.

Immunostain	Region of interst	Number of images per section	Number of sections imaged	Total number of images	Magnification
GFAP	corpus callosum	20	5	100	x63
CD 68	prefrontal cortex	6	3	18	x20
MBP	corpus callosum	16	5	80	x63
	prefrontal cortex	4	3	12	x10
Neurofilament	corpus callosum	16	5	80	x63
	prefrontal cortex	4	3	12	x10
Parvalbumin	prefrontal cortex	4 to 6	6	32	x20
Synaptophysin	prefrontal cortex	15	6	90	x63

Images were analysed using *Image Pro Plus* software (Media Cybernetics, Chicago, IL), to select appropriate thresholds for every region (Figure 29). Thresholds were chosen to best distinguish between specific immunoreactivity for each antigen and the background. Results obtained for each region and each antigen was expressed as % immunoreactivity per image. The mean percentage immunoreactivity per region per animal was then obtained for further analysis.

a) Qualitative image analysis

GFAP staining in the prefrontal cortex was analysed qualitatively, without the need for quantification. Images were taken at x5 and x20 magnification on a *Leica DRMB microscope* (Leica Microscopy & GmBH, Wetzlar, Germany) with a *Lumenera infinity 3 camera*.

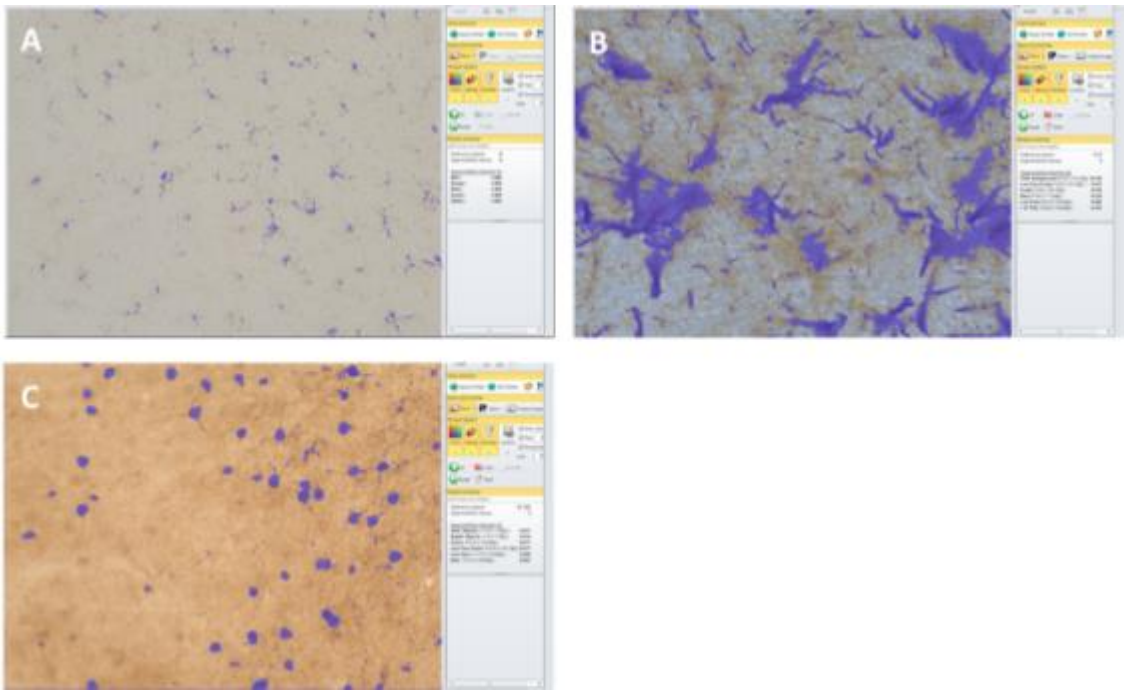

Figure 29. Selecting thresholds for thresholding image analysis. Representative images showing CD68 positive microglia (A), GFAP positive astrocytes (B) and parvalbumin positive interneuron (C) staining, thresholded (blue shading) to accurately discriminate positive immunostaining from background.

b) Quantitative image analysis

All measurements were performed blind to the experimental group. All statistical analysis was performed using *GraphPad Prism* software (GraphPad Software Inc., La Jolla, CA). The mean co-efficient of error for individual measures of cell counts was calculated by the Gundersen method (Gundersen & Jensen, 1987), and was between the recommended range of 0.05 - 0.1. Statistical analyses for measurements of cell counts and thresholding image analysis between two groups was calculated by a two-tailed, unpaired, parametric t-test where $p \leq 0.05$ was considered significant.

4.4 Results and discussion

a) Frontal lobe

To investigate the cellular correlates of MR volume and DTI differences between ketamine and saline treated mice (section 3.4) I began by comparing cell numbers of neurons, astrocytes and microglia in the frontal lobe.

i) Neuron cell counts

Comparing the number of nissl positive neurons within the frontal lobe of mice repeatedly given ketamine versus saline; I found no significant differences between KET-INT mice ($2.09x10^6 \pm 1.16x10^5$, n=9) and SAL-INT mice ($2.26x10^6 \pm 1.16x10^5$, n=10), in my intermittent experiment (t=1.05, p=0.31) (Figure 30), nor between KET-DAY mice ($1.42x10^6 \pm 4.68x10^4$, n=8) and SAL-DAY mice ($1.35x10^6 \pm 6.52x10^4$, n=10), in my daily experiment (t=0.79, p=0.44) (Figure 31).

i) Astrocyte cell counts

Comparing the number of s100b positive astrocytes within the frontal lobe of mice repeatedly given ketamine versus saline; I found no significant differences between KET-INT mice ($2.72x10^5 \pm 1.20x10^4$, n=10) and SAL-INT mice ($2.60x10^5 \pm 1.21x10^4$, n=9), in my intermittent experiment (t=0.71, p=0.49) (Figure 32), nor between KET-DAY mice ($2.52x10^5 \pm 1.15x10^4$, n=10) and SAL-DAY mice ($2.84x10^5 \pm 1.20x10^4$, n=9), in my daily experiment (t=1.94, p=0.07) (Figure 33).

However, there was an indication of a trend towards fewer s100b positive astrocytes in KET-DAY mice versus SAL-DAY mice. Therefore, I decided to correlate the number of s100b positive astrocytes in the frontal lobe, of KET-DAY mice and SAL-DAY mice, with measures of MD, AD and RD; which displayed significant differences in value, at the ROI level, between KET-DAY and SAL-DAY mice (Figure 34).

I did not find any significant correlation between the number of s100b positive astrocytes and measures of MD, AD or RD within KET-DAY mice only (MD; r=-0.011, p=0.98. AD; r=0.023, p=0.95. RD; r=-0.028, p=0.94), SAL-DAY mice only (MD; r=-0.05,

p=0.92. AD; r=0.44, p=0.32. RD; r=-0.032, p=0.70), nor within KET-DAY and SAL-DAY mice together (MD; r=-0.16, p=0.55. AD; r=0.26, p=0.33. RD; r=-0.08, p=0.77).

ii) Microglia cell counts

Comparing the number of Iba-1 positive microglia within the frontal lobe of mice repeatedly given ketamine versus saline; I found no significant differences between KET-INT mice ($3.55x10^5 \pm 6.36x10^3$, n=10) and SAL-INT mice ($3.68x10^5 \pm 5.26x10^3$, n=10), in my intermittent experiment (t=1.59, p=0.13) (Figure 35), nor between KET-DAY mice ($3.62x10^5 \pm 2.23x10^3$, n=9) and SAL-DAY mice ($3.60x10^5 \pm 5.06x10^3$, n=10), in my daily experiment (t=0.36, p=0.72) (Figure 36).

However, there was an indication of a trend towards fewer Iba-1 positive microglia in KET-INT mice versus SAL-INT mice. Therefore, I decided to correlate the number of Iba-1 positive microglia in the frontal lobe, of KET-INT mice and SAL-INT mice, with measures of FA; which displayed significant differences in value, at the ROI level, between KET-INT and SAL-INT mice (Figure 37).

I found a positive trend between fewer Iba-1 positive microglia and lower FA in KET-INT mice only, however this trend was not statistically significant (r=-0.58, p=0.08). Furthermore, I found no significant correlation between the number of Iba-1 positive microglia and FA in SAL-INT mice only, nor in KET-INT and SAL-INT mice together.

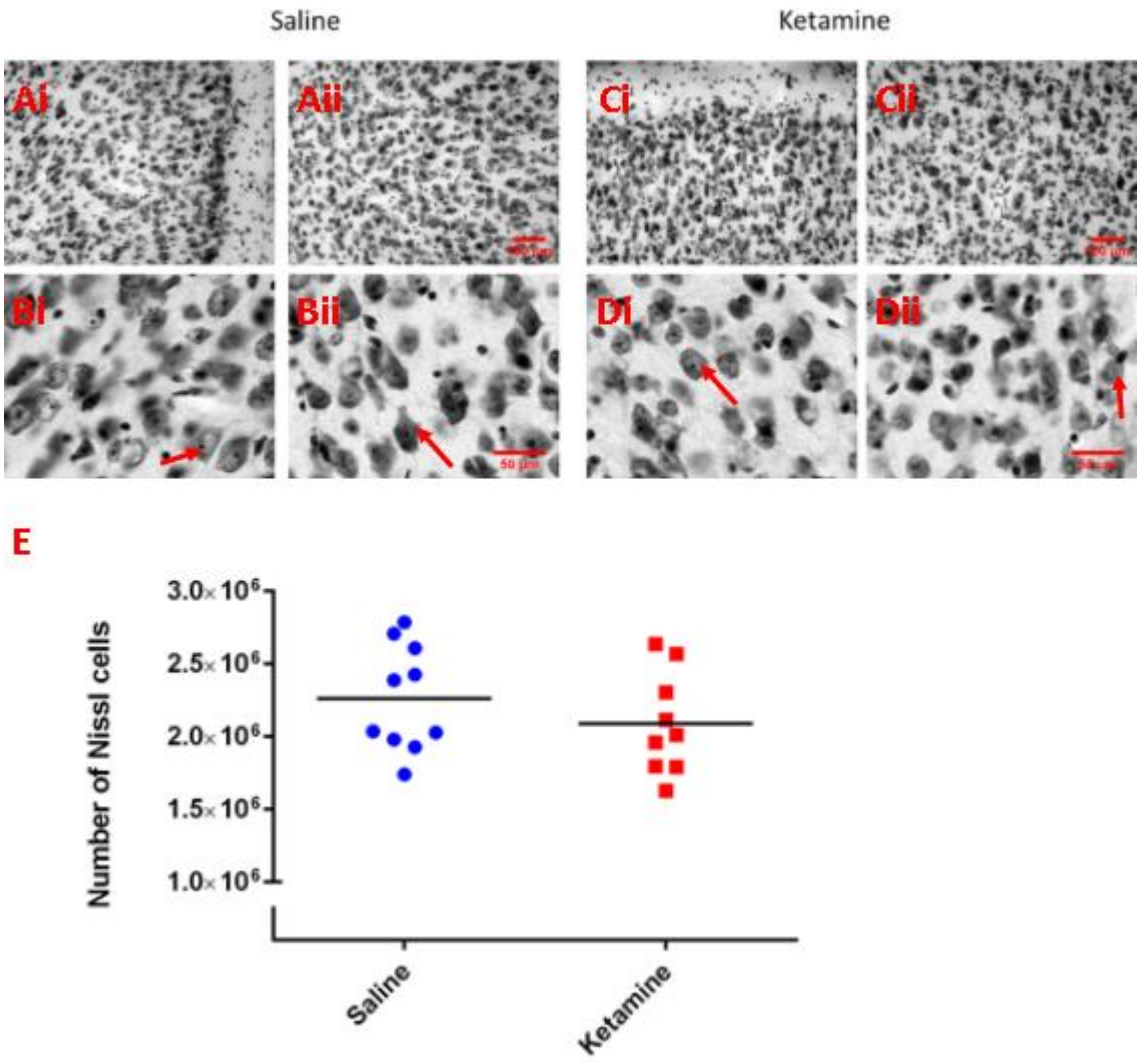

Figure 30. No difference between the number of Nissl positive neurons in the frontal lobe of SAL-INT and KET-INT mice. A&B) Representative images of Nissl positive cells in SAL-INT mice. A) x20 magnification. B) x63 magnification. C&D) Representative images of Nissl positive cells in KET-INT mice. C) x20 magnification. D) x63 magnification. E) Graph of stereological cell counts of Nissl positive neurons in SAL-INT and KET-INT mice. Red arrows point to examples of Nissl positive neurons.

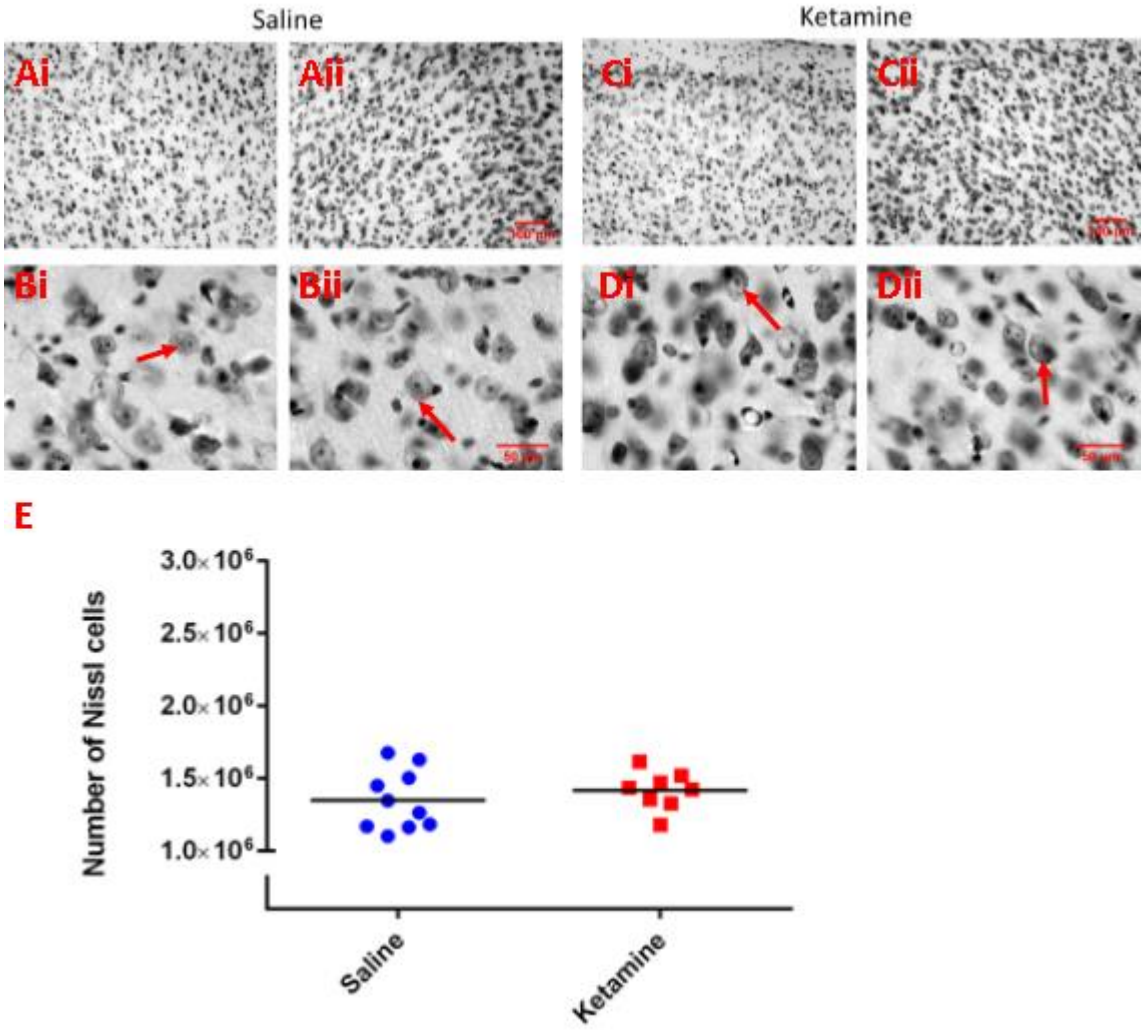

Figure 31. No difference between the number of Nissl positive neurons in the frontal lobe of SAL-DAY and KET-DAY mice. A&B) Representative images of Nissl positive cells in SAL-DAY mice. A) x20 magnification. B) x63 magnification. C&D) Representative images of Nissl positive cells in KET-DAY mice. C) x20 magnification. D) x63 magnification. E) Graph of stereological cell counts of Nissl positive neurons in SAL-DAY and KET-DAY mice. Red arrows point to examples of Nissl positive neurons.

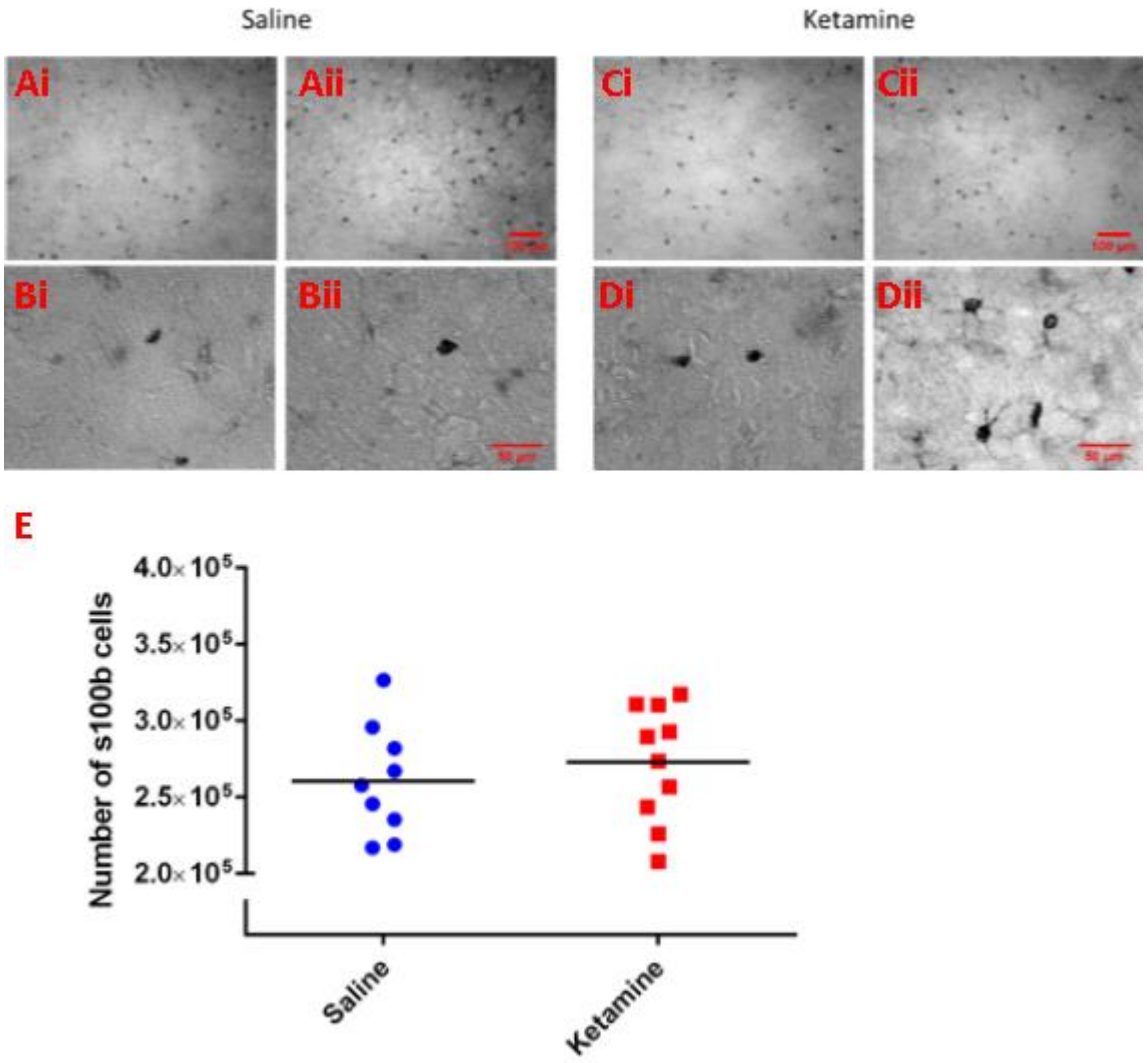

Figure 32. No difference between the number of s100b cells in the frontal lobe of SAL-INT and KET-INT mice. A&B) Representative images of s100b cells in SAL-INT mice. A) x20 magnification. B) x63 magnification. C&D) Representative images of s100b cells in KET-INT mice. C) x20 magnification. D) x63 magnification. E) Graph of stereological cell counts of s100b positive cells in SAL-INT and KET-INT mice.

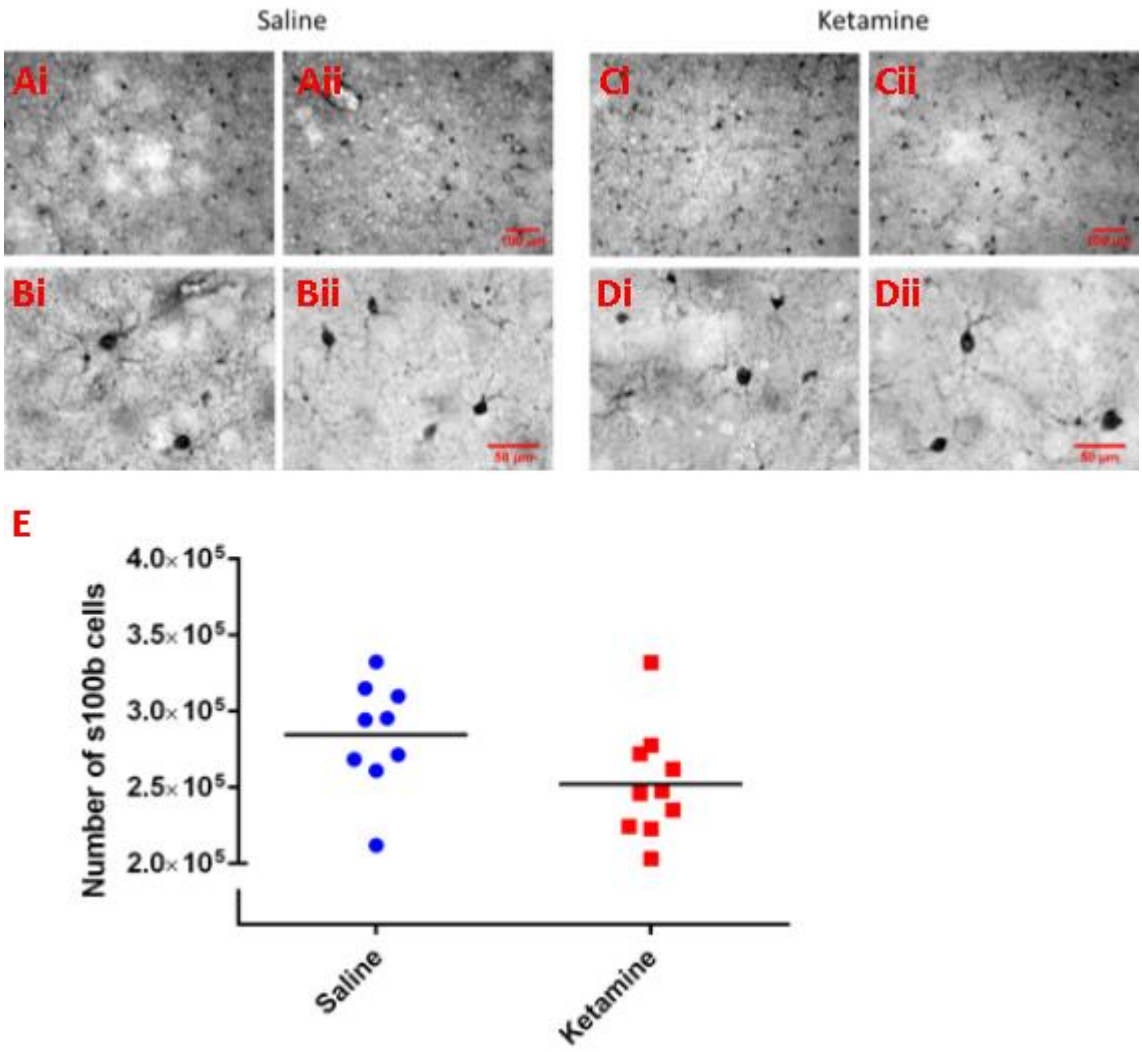

Figure 33. No difference between the number of s100b cells in the frontal lobe of SAL-DAY and KET-DAY mice. A&B) Representative images of s100b cells in SAL-DAY mice. A) x20 magnification. B) x63 magnification. C&D) Representative images of s100b cells in KET-DAY mice. C) x20 magnification. D) x63 magnification. E) Graph of stereological cell counts of s100b positive cells in SAL-DAY and KET-DAY mice.

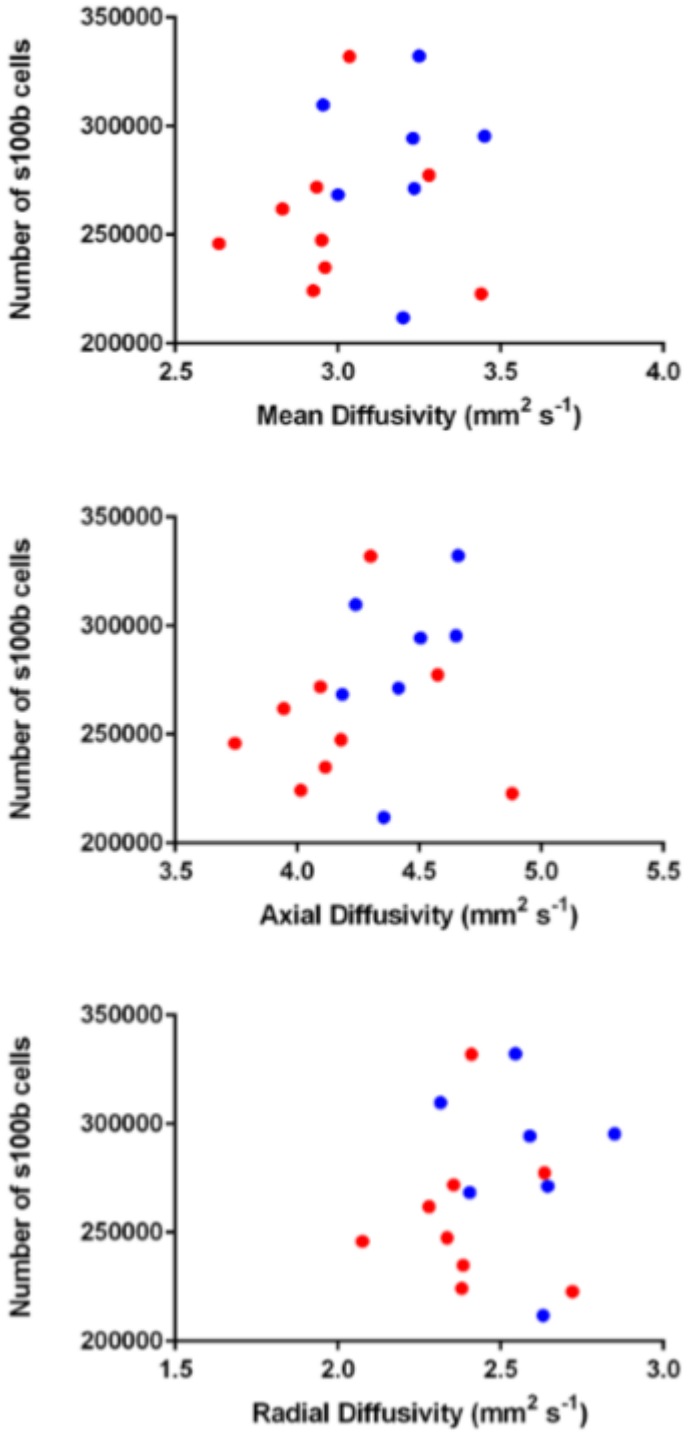

Figure 34. Correlations between the number of s100b positive astrocytes and DTI measures of MD, AD and RD in the frontal lobe of KET-DAY (red dots) and SAL-DAY mice (blue dots).

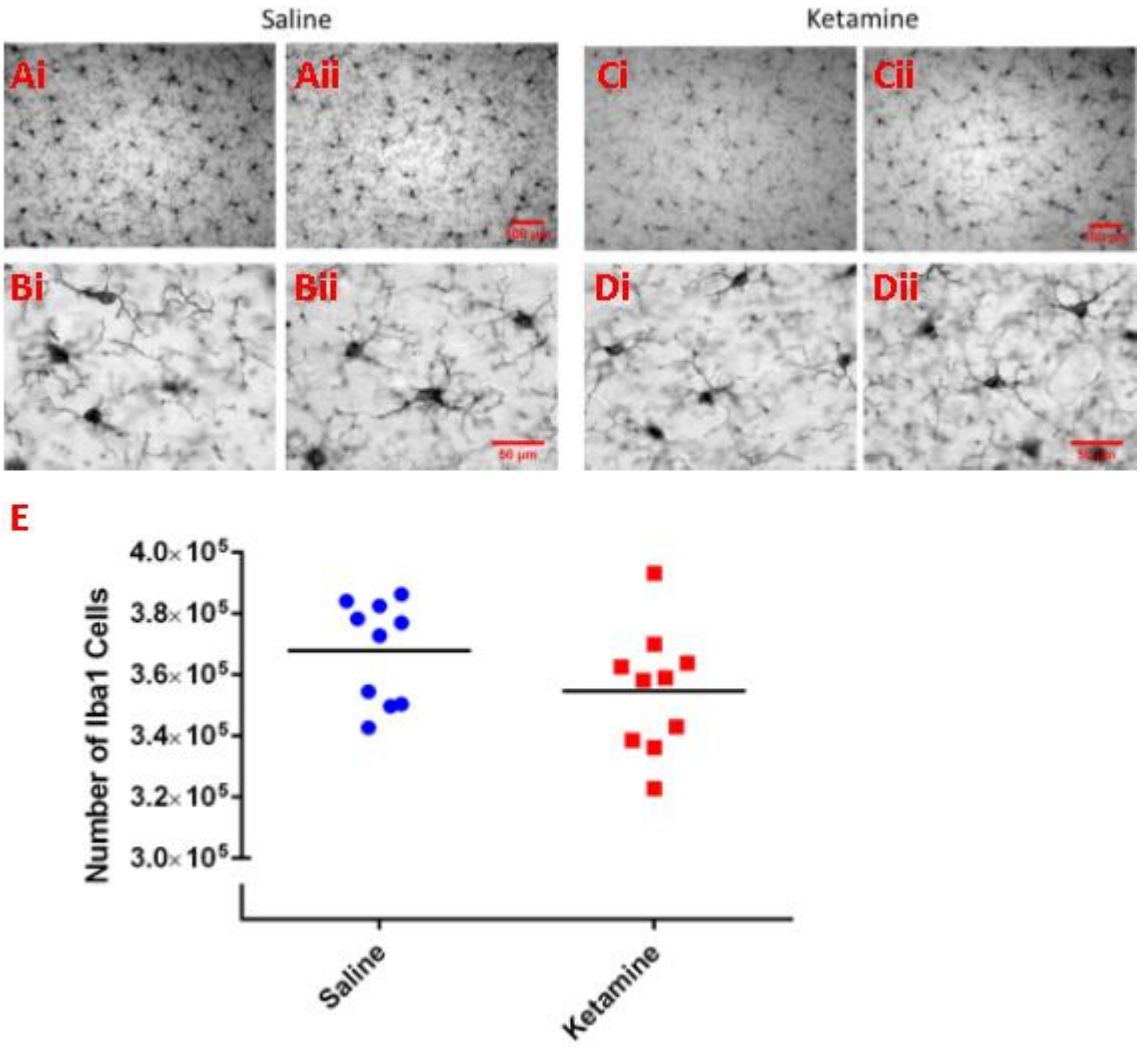

Figure 35. No difference between the number of Iba-1 cells in the frontal lobe of SAL-INT and KET-INT mice. A&B) Representative images of Iba-1 cells in SAL-INT mice. A) x20 magnification. B) x63 magnification. C&D) Representative images of Iba-1 cells in KET-INT mice. C) x20 magnification. D) x63 magnification. E) Graph of stereological cell counts of Iba-1 positive cells in SAL-INT and KET-INT mice.

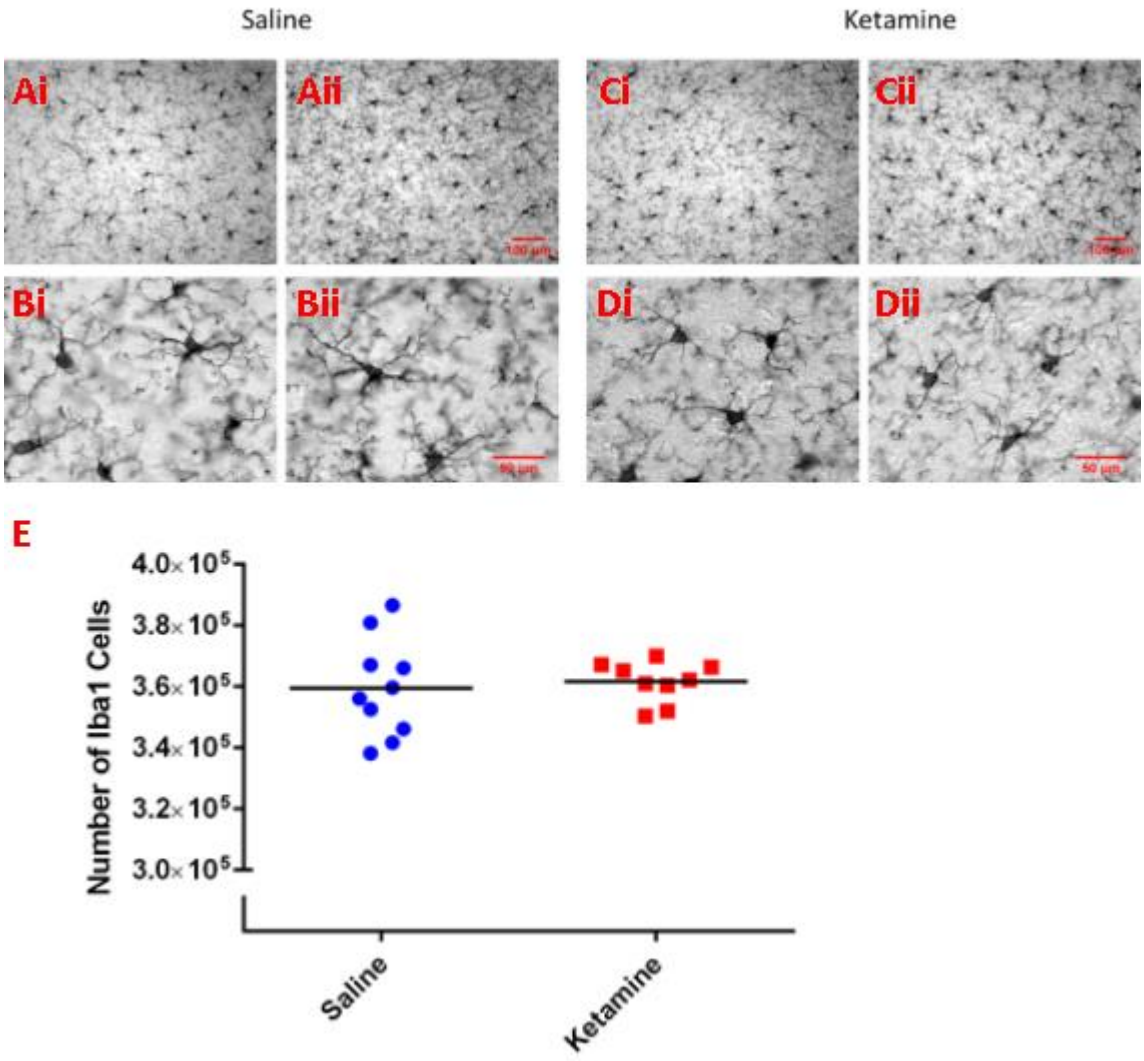

Figure 36. No difference between the number of Iba-1 cells in the frontal lobe of SAL-DAY and KET-DAY mice. A&B) Representative images of Iba-1 cells in SAL-DAY mice. A) x20 magnification. B) x63 magnification. C&D) Representative images of Iba-1 cells in KET-DAY mice. C) x20 magnification. D) x63 magnification. E) Graph of stereological cell counts of Iba-1 positive cells in SAL-DAY and KET-DAY mice.

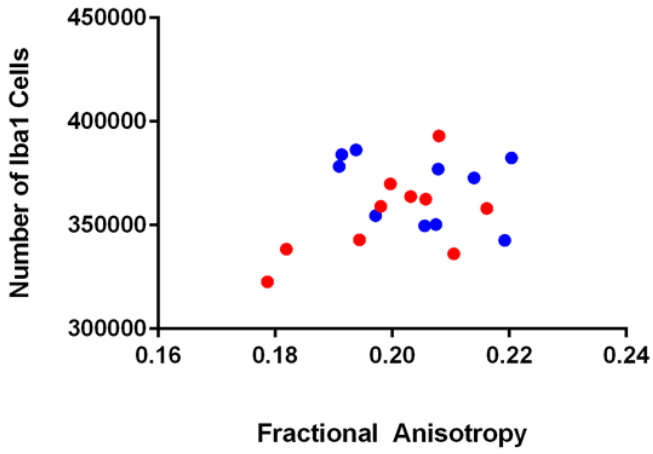

Figure 37. Correlations between the number of Iba-1 positive microglia and DTI measures of FA in the frontal lobe of KET-INT (red dots) and SAL-INT mice (blue dots).

b) Prefrontal cortex

Although I found no significant differences in neuron, astrocyte or microglial number in the frontal lobe, between ketamine treated and saline treated mice, I did see a trend towards fewer astrocytes in KET-Day mice and fewer microglia in KET-INT mice. Furthermore, I found a positive trend between fewer microglia and lower FA in the frontal lobe of KET-INT mice. This suggests that changes to glial cells may, in part, be responsible for structural differences observed in the frontal lobe of ketamine treated and saline treated mice. However, as seen with MRI differences (section 3.4), these glial changes may not be generalised across the entire frontal lobe but may be specifically located in sub regions of the frontal lobe. For example; increased volume of the frontal lobe in KET-INT mice, compared to SAL-INT mice, was shown to be specific to a cluster of voxels within the prefrontal cortex.

I decided to investigate possible cellular correlates of volume and DTI differences, between ketamine mice and saline mice, specifically in the prefrontal cortex. The prefrontal cortex is also an interesting sub-region to investigate as decreases in MD, AD and RD were seen, within this region, in KET-DAY mice (section 3.4.e). FA differences between KET-INT and SAL-INT mice were also observed in the prefrontal cortex (section 3.4.e).

Moreover, as discussed in section 1.5, both single and repeat ketamine administration have been shown to significantly alter the cellular and molecular organisation of neural networks in the prefrontal cortex of rodents. Examples include; a reduction in the number of parvalbumin positive GABAergic interneurons, increased extracellular glutamate levels and glutamatergic disinhibition leading to increased excitatory neural activity (Zhang, Behrens and Lisman, 2008; Quirk *et al.*, 2009; Kim *et al.*, 2011b; Wang *et al.*, 2014). However, the focus in the literature has been on neuronal changes. Therefore, I decided to take a novel approach and focus more on potential glial changes that result from repeat ketamine administration in mice.

i) Activated glial cells

As stated in the introduction to this chapter, I think that repeat ketamine administration may be having a plastic effect on the brain, causing remodelling of neural networks, as opposed to pathology. In the previous section (4.4.a) I have shown that repeat ketamine

administration has no effect on the number of neurons within the frontal lobe, which to a degree indicates a lack of pathology. However, to test my hypothesis further, I decided to investigate if there was any increase in the number of activated glial cells (GFAP positive astrocytes and CD68 positive microglia), in the prefrontal cortex, which would be indicative of pathology (Pekny, Wilhelmsson and Pekna, 2014; Yang and Wang, 2015; Hiragi, Ikegaya and Koyama, 2018; Skaper *et al.*, 2018; Stephenson *et al.*, 2018).

With regards to GFAP positive, fibrous astrocytes, these cells under normal physiological conditions are mainly found in the white matter and only under pathological conditions are they seen in the mouse brain cerebral cortex (Pekny, Wilhelmsson and Pekna, 2014; Yang and Wang, 2015). In my qualitative analysis of GFAP immunoreactivity, in the prefrontal cortex of ketamine treated and saline treated mice, I observed no difference between KET-INT mice and SAL-INT mice (Figure 38) and no difference between KET-DAY and SAL-DAY mice (Figure 39). I, therefore, did not pursue any quantitative analysis.

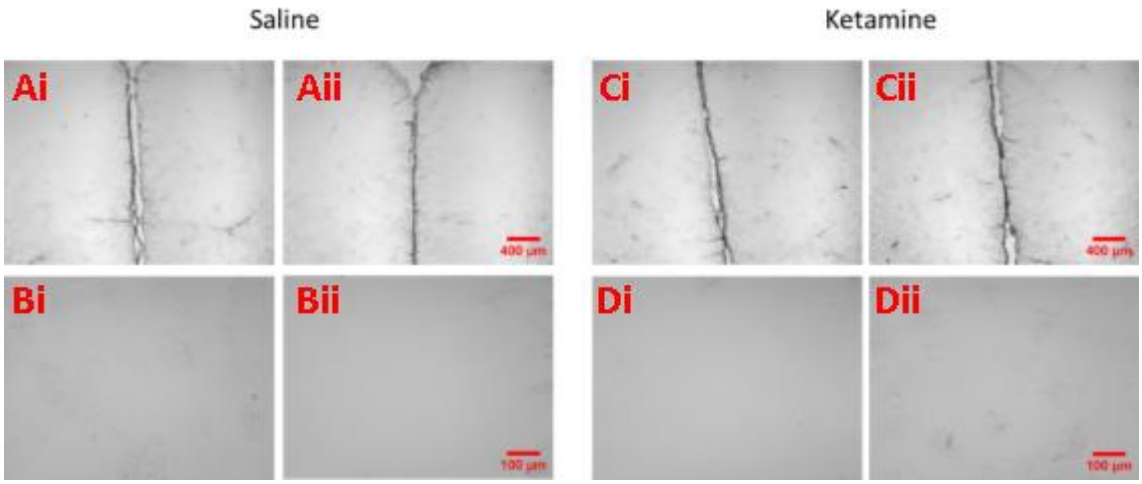

Figure 38. Representative images of GFAP positive staining in the prefrontal cortex of SAL-INT and KET-INT mice. A&B) SAL-INT mice. A) x 5 magnification. B) x20 magnification. C&D) KET-INT mice. C) x 5 magnification. D) x20 magnification.

CD68 is a commonly used marker of microglia activation (Van den Eynde *et al.*, 2014; Hoogland *et al.*, 2015; Lu *et al.*, 2015). I found no significant differences in the amount of CD68 positive microglia in the prefrontal cortex of KET-INT mice (2.35±0.23, n=8) versus SAL-INT mice (2.96±0.35, n=10) , in my intermittent experiment (t=1.47, p=0.16) (Figure 40), nor in KET-DAY mice (1.29±0.07, n=10) versus SAL-DAY mice (1.46±0.14, n=10) from my daily experiment (t= 1.08, p=0.29) (Figure 41).

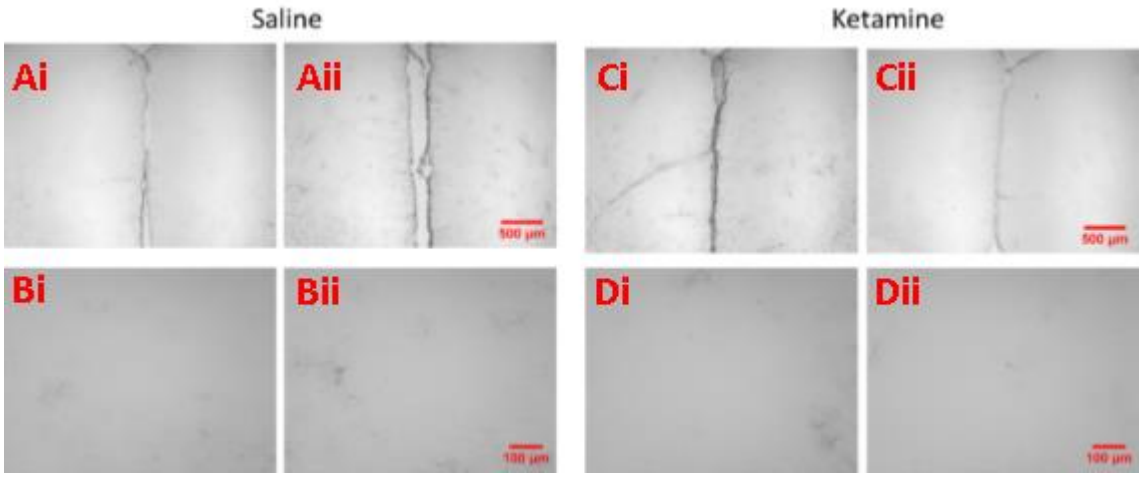

Figure 39. Representative images of GFAP positive staining in the prefrontal cortex of SAL-DAY and KET-DAY mice. A&B) SAL-DAY mice. A) x 5 magnification. B) x20 magnification. C&D) KET-DAY mice. C) x 5 magnification. D) x20 magnification.

The lack of astrocyte or microglial activation between ketamine and saline treated mice further supports my hypothesis that repeat ketamine administration is not having a pathological effect on mouse brain structure, at least in terms of neurogenerative gliosis.

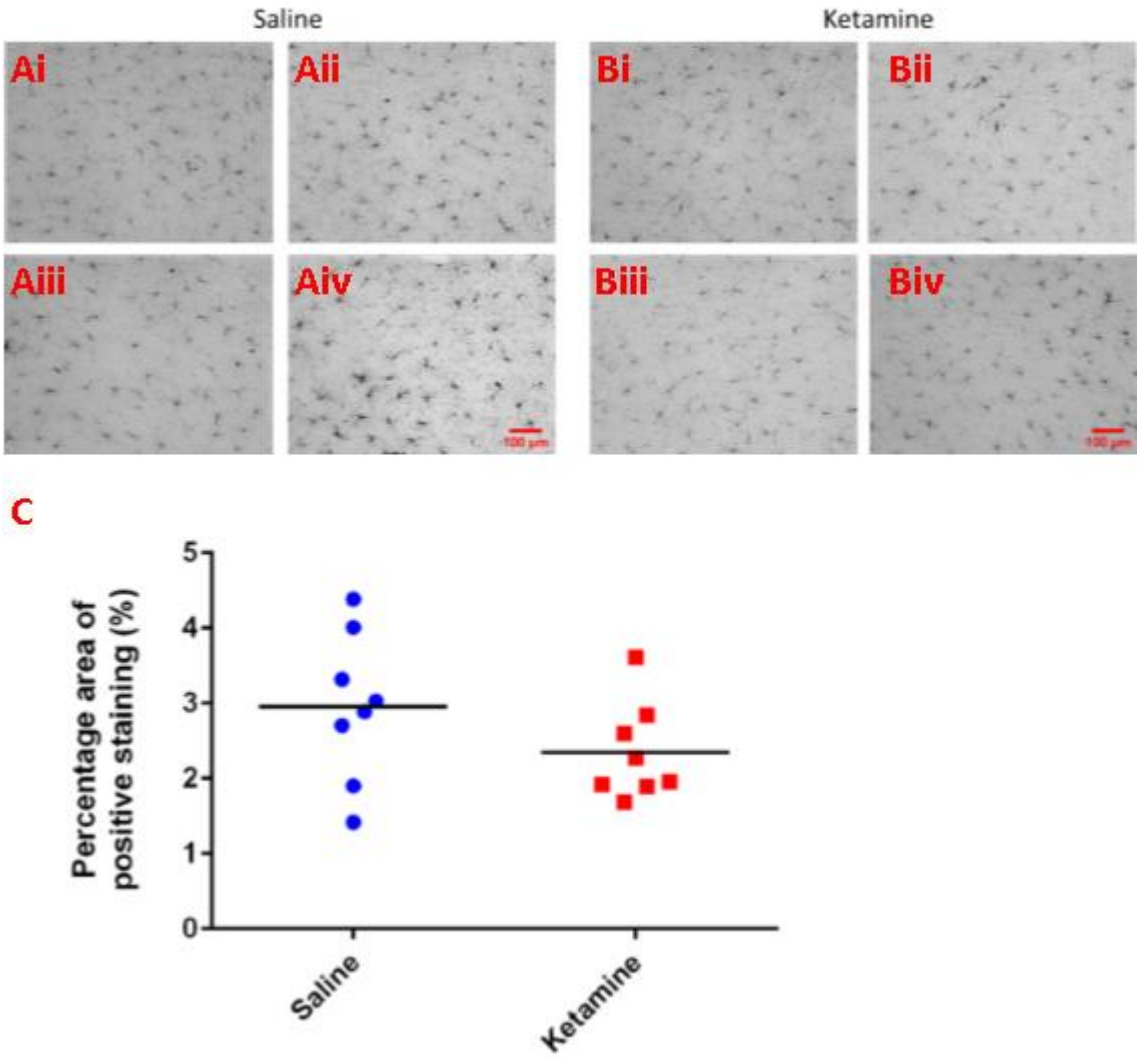

Figure 40. No difference between the percentage area of CD68 positive staining in the prefrontal cortex of SAL-INT and KET-INT mice. A) Representative images of CD68 positive cells in SAL-INT mice. x20 magnification. B) Representative images of CD68 positive cells in KET-INT mice. x20 magnification. C) Graph of the percentage area of CD68 positive staining in SAL-INT and KET-INT mice.

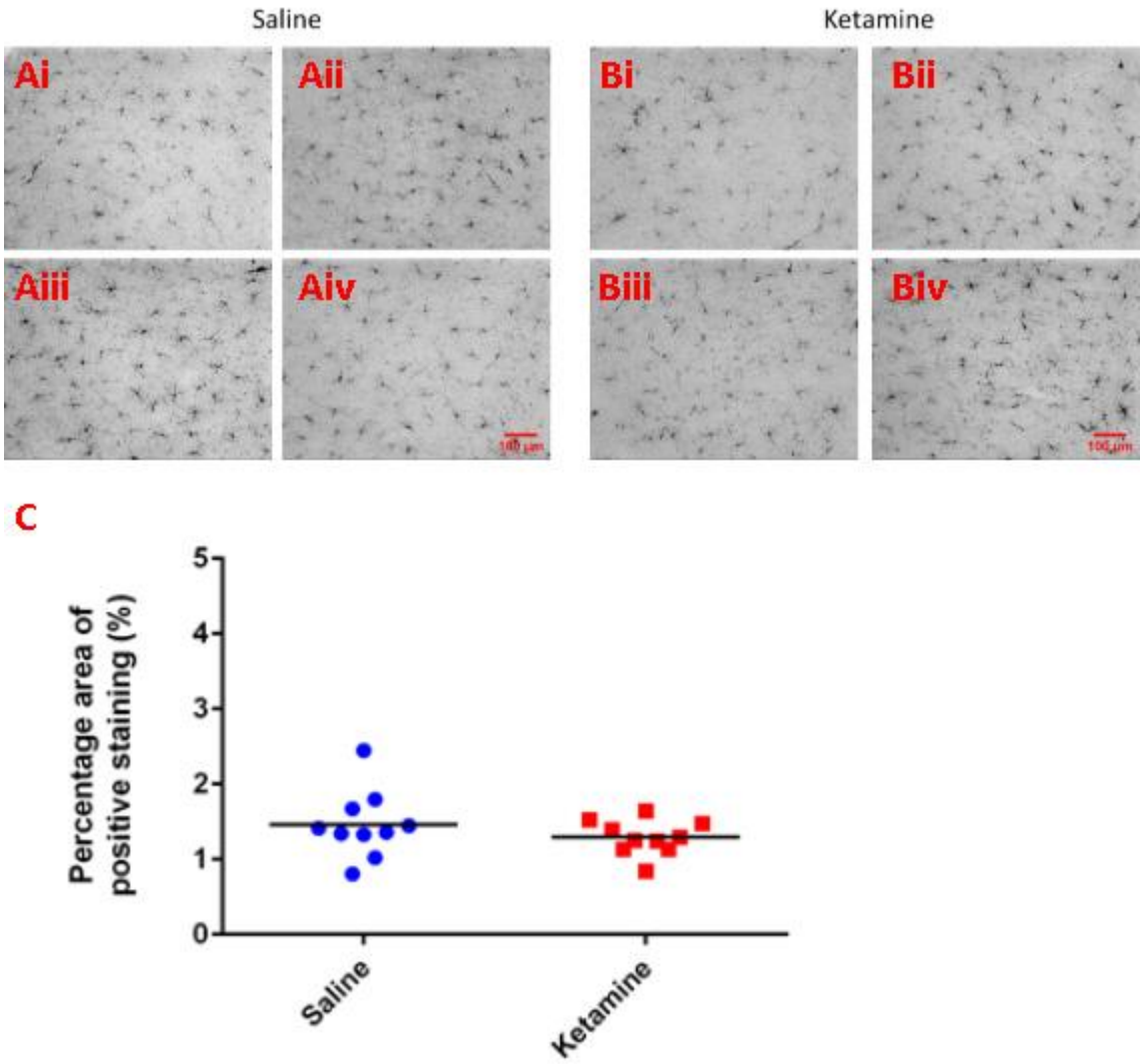

Figure 41. No difference between the percentage area of CD68 positive staining in the prefrontal cortex of SAL-DAY and KET-DAY mice. A) Representative images of CD68 positive cells in SAL-DAY mice. x20 magnification. B) Representative images of CD68 positive cells in KET-DAY mice. x20 magnification. C) Graph of the percentage area of CD68 positive staining in SAL-DAY and KET-DAY mice.

i) Myelin, axons and synapses

Having so far shown no signs of glia pathology, I decided to investigate potential markers of plasticity in the prefrontal cortex of ketamine administered mice. I looked to see whether there was any difference in the amount of myelin basic protein, neurofilament and/or synaptophysin between ketamine and saline treated mice, within the prefrontal cortex. This would tell me, indirectly, whether there was any difference in the amount of myelin, density of axons and/or density of synapses between these groups of mice, within the prefrontal cortex. Changes in myelin content, axon density and the number of synapses have all previously been shown to occur in learning and memory, adaptation to new experiences, as well as repetitive drug use, and are signs of activity dependent remodelling of neural circuits (Bowers, Chen, & Bonci, 2010; Canu, Carnaud, Picquet, & Goutebroze, 2009; Fields, 2008; Johansen-Berg, 2007; Lüscher & Malenka, 2011; Markham, Herting, Luszpak, Juraska, & Greenough, 2009; Nickel & Gu, 2018; Ramirez-Amaya, Escobar, Chao, & Bermidez-Rattoni, 1999; Van den Oever, Spijker, & Smit, 2012; van Huijstee & Mansvelder, 2015; G. Yang, Pan, & Gan, 2009; Zatorre et al., 2012).

I first assessed whether there was any difference in the amount of myelin basic protein (MBP) between KET-INT (1.16±0.01, n=9) and SAL-INT mice (1.17±0.02, n=8). I found no significant difference (t=0.47, p=0.65), Figure 42.

Nor did I find any significant difference in the amount of MBP in the prefrontal cortex between KET-DAY mice (1.10±0.02, n=10) and SAL-DAY mice (1.08±0.02, n=9), (t=1.05, p=0.31), Figure 43.

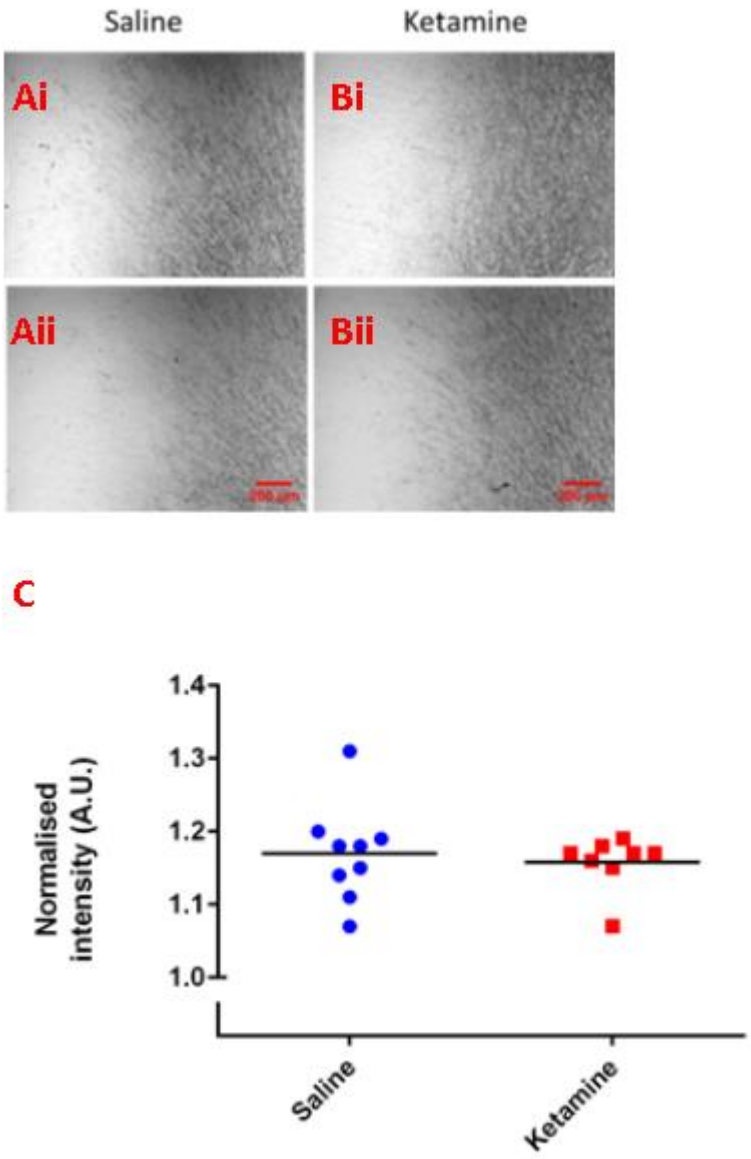

Figure 42. Myelin basic protein (MBP) staining in the prefrontal cortex of SAL-INT and KET-INT mice. A) Representative images of MBP staining in SAL-INT mice. x10 magnification. B) Representative images of MBP staining in KET-INT mice. x10 magnification. C) Graph of normalised MBP staining intensity across the prefrontal cortex.

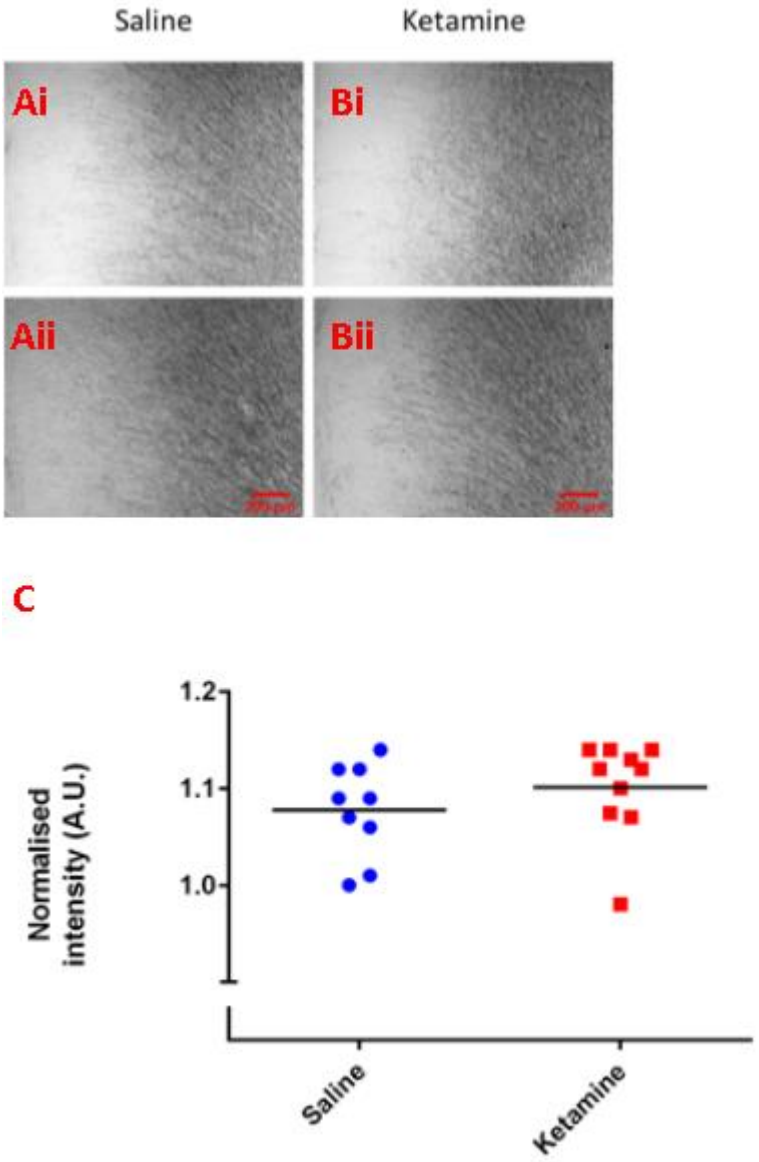

Figure 43. Myelin basic protein (MBP) staining in the prefrontal cortex of SAL-DAY and KET-DAY mice. A) Representative images of MBP staining in SAL-DAY mice. x10 magnification. B) Representative images of MBP staining in KET-DAY mice. x10 magnification. C) Graph of normalised MBP staining intensity across the prefrontal cortex.

Next, I investigated whether there was any difference in the amount of neurofilament staining in the prefrontal cortex of ketamine treated and saline treated mice. I found a significant increase in the amount of neurofilament staining in KET-INT mice (100.9±1.52, n=9) compared to SAL-INT mice (96.21±1.65, n=8), (t=2.11, p=0.05), Figure 44. However, I found no significant difference between KET-DAY mice (97.4±0.86, n=9) and SAL-DAY mice (96.5±1.43, n=7), (t=0.54, p=0.6), Figure 45.

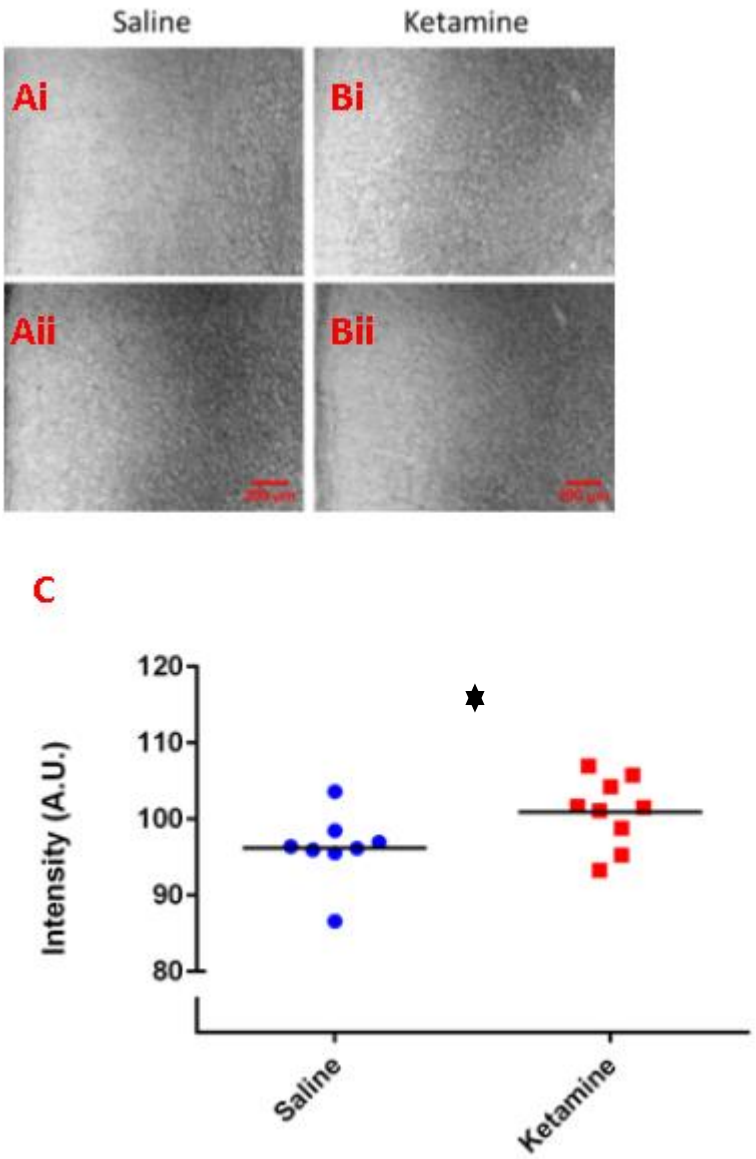

Figure 44. Neurofilament (NF) staining in the prefrontal cortex of SAL-INT and KET-INT mice. A) Representative images of NF staining in SAL-INT mice. x10 magnification. B) Representative images of NF staining in KET-INT mice. x10 magnification. C) Graph of NF staining intensity across the prefrontal cortex. *; $p<0.05$ (T-test).

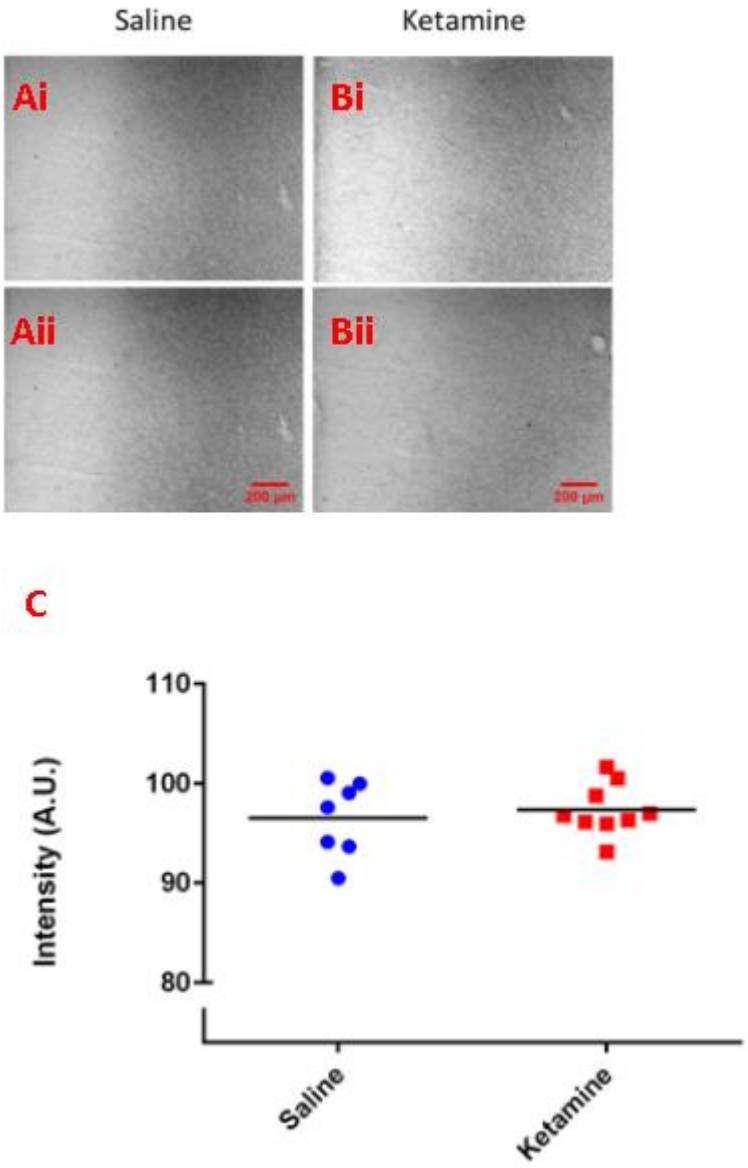

Figure 45. Neurofilament (NF) staining in the prefrontal cortex of SAL-DAY and KET-DAY mice. **A)** Representative images of NF staining in SAL-DAY mice. x10 magnification. **B)** Representative images of NF staining in KET-DAY mice. x10 magnification. **C)** Graph of NF staining intensity across the prefrontal cortex.

I then investigated whether there was any difference in the amount of synaptophysin staining, in the prefrontal cortex, between ketamine and saline treated mice. I found a significant increase in the amount of synaptophysin in KET-INT mice (2.44±0.06, n=7) compared to SAL-INT mice (2.25±0.03, n=6), (t=2.81, p=0.017), Figure 46.

However, I did not find any significant difference in the amount of synaptophysin between KET-DAY mice (2.40±0.05, n=9) and SAL-DAY mice (2.41±0.07, n=9), (t=0.13, p=0.90), Figure 47.

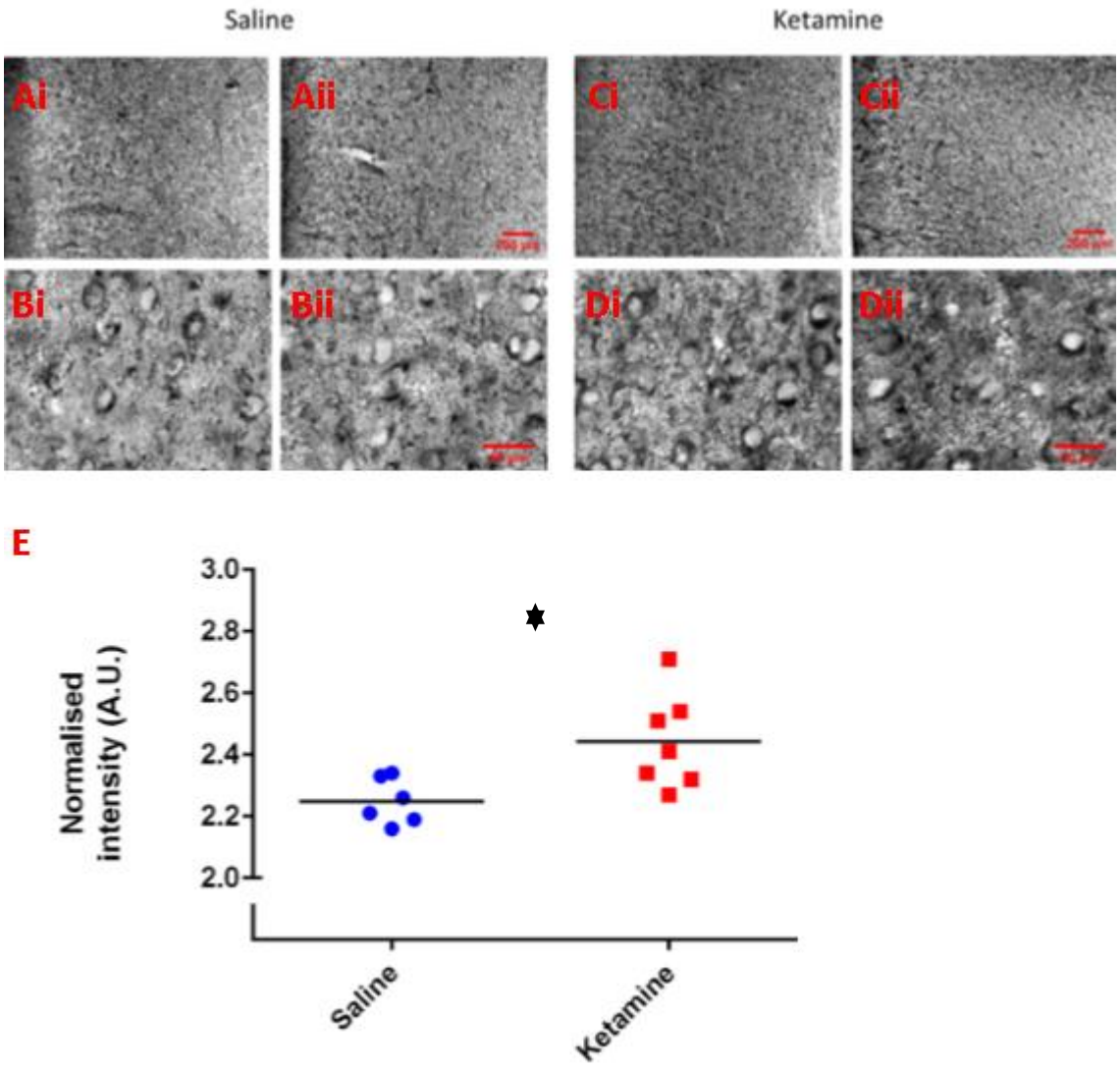

Figure 46. Synaptophysin (Syn) positive staining in the prefrontal cortex of SAL-INT and KET-INT mice. **A&B)** Representative images of Syn positive staining in SAL-INT mice. A) x10 magnification. B) x63 magnification **C&D)** Representative images of Syn positive cells in KET-INT mice. C) x10 magnification. D) x63 magnification. **E)** Graph of normalised Syn staining intensity in SAL-INT and KET-INT mice. *; $p<0.05$ (T-test).

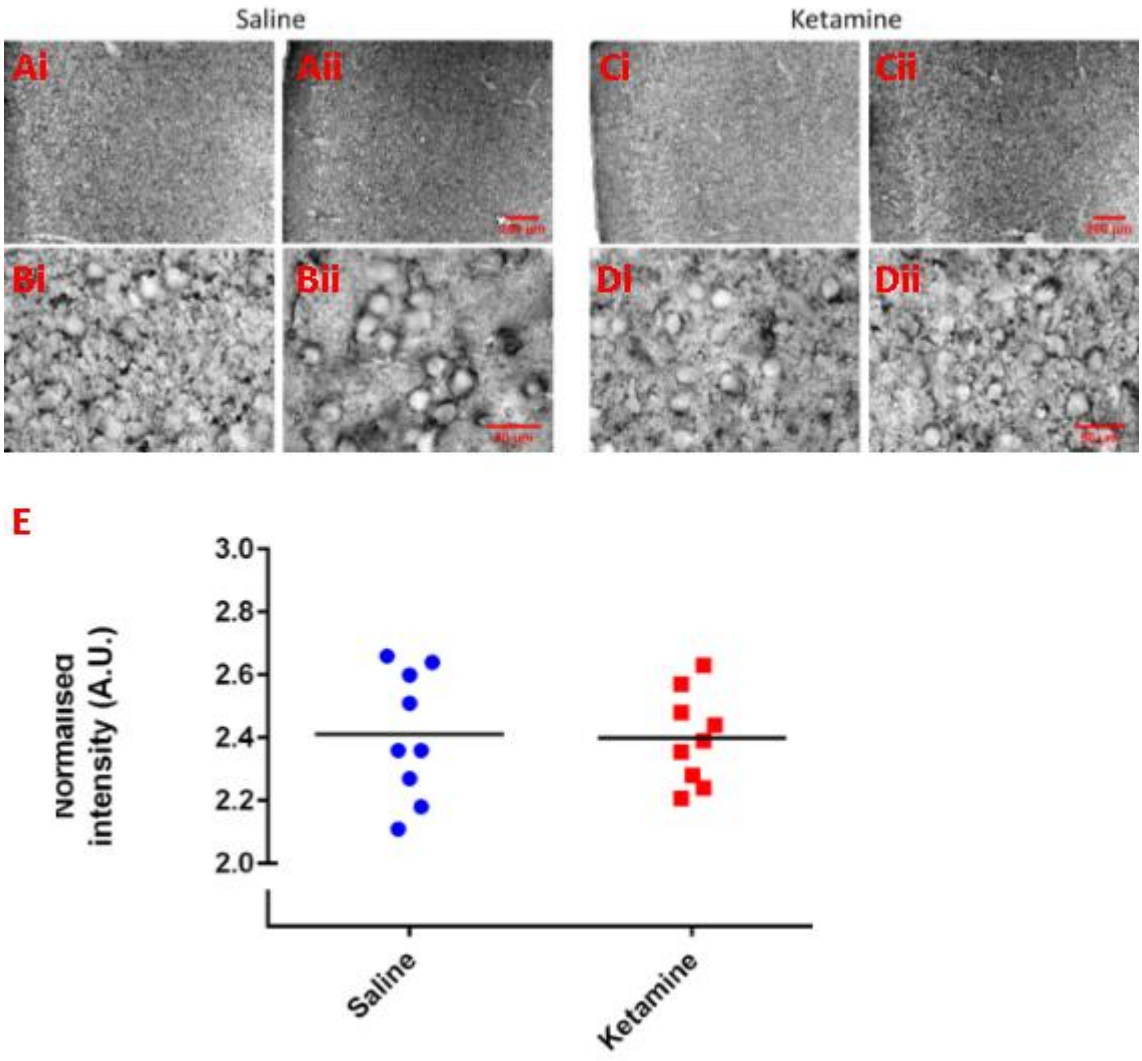

Figure 47. Synaptophysin (Syn) positive staining in the prefrontal cortex of SAL-DAY and KET-DAY mice. **A&B)** Representative images of Syn positive staining in SAL-DAY mice. A) x10 magnification. B) x63 magnification C**&D)** Representative images of Syn positive cells in KET-DAY mice. C) x10 magnification. D) x63 magnification. **E)** Graph of normalised Syn staining intensity in SAL-DAY and KET-DAY mice.

The significant increase in the amount of neurofilament and synaptophysin in the prefrontal cortex of KET-INT mice suggests that ketamine might be having a remodelling effect on neural circuits within this brain region. In turn, this might be responsible for the increase in volume and FA observed in this region. Interestingly, within the literature, increased axon sprouting, and synaptogenesis have been hypothesised to correlate with increases in volume and FA and are indicative of activity-dependent remodelling of neural circuits (Zatorre, Fields and Johansen-Berg, 2012).

As discussed earlier, ketamine administration has been shown to significantly alter excitatory neural activity via a reduction in the number of parvalbumin positive GABAergic interneurons, increased extracellular glutamate levels and glutamatergic disinhibition (Zhang, Behrens and Lisman, 2008; Quirk *et al.*, 2009; Kim *et al.*, 2011b; Wang *et al.*, 2014).

Thus, to investigate whether repeat ketamine administration in my experiments was driving activity dependent remodelling of prefrontal circuits, I decided to assess whether there were any differences in the amount of parvalbumin positive GABAergic interneurons between ketamine and saline treated mice. I decided to focus on the amount of parvalbumin positive staining as a marker of altered neuronal activity as it was one, I could assess using histology.

However, I found no significant difference in the amount of parvalbumin positive interneuron staining between KET-INT (2.68±0.32, n=8) and SAL-INT mice (2.65±0.36, n=9), (t=0.06, p=0.96), Figure48. Nor did I find any significant difference between KET-DAY (2.96±0.24, n=8) and SAL-DAY mice (3.11±0.12, n=12), (t=0.61, p=0.55), Figure 49.

Although it might initially look as if repeat ketamine administration is not inducing any activity dependent plasticity. The lack of any difference in the amount of parvalbumin expressing interneurons, as seen in the literature (Quirk *et al.*, 2009; Wang *et al.*, 2014; Yang *et al.*, 2016), could be attributed to a two-day wash out period used before sacrificing the mice and processing the tissue. In other words, a change in the amount of parvalbumin expressing interneurons might be a temporary one and after two days when there is no ketamine left in the mice, parvalbumin levels might restore to baseline. If this is the case, a temporary reduction in parvalbumin expression may have a functional consequence in terms of a reduction of GABAergic inhibition. This in turn might lead to increased glutamatergic activity within neuronal circuits and changes in behaviour, which subsequently return to baseline. Electrophysiology and the implantation of electrodes into the prefrontal cortex would be a way in which to test whether there is any change in the level of excitatory neuronal activity within the region. These type of experiments can be performed at various time points throughout a ketamine administration experiment and after the cessation of administration, *in-vivo* in freely moving mice (Long and Lee, 2012). Such an experiment would highlight if and when neuronal activity is affected during repeat ketamine exposure. Coupled with

molecular biology techniques, such as western blot, which can more accurately quantify the amount of parvalbumin protein within the region. One could ascertain if and when parvalbumin protein expression is altered and if this leads to a change in functional activity within neuronal networks. One could take sub-groups of ketamine treated mice at different stages of ketamine exposure and/or wash-out and perform western blot experiments to test whether parvalbumin expression is temporarily reduced and then returns to baseline.

Moreover, behavioural experiments could be used at various time points to establish whether changes in parvalbumin expression and functional activity (due to repeat ketamine exposure) within the prefrontal cortex lead to any changes in behaviour.

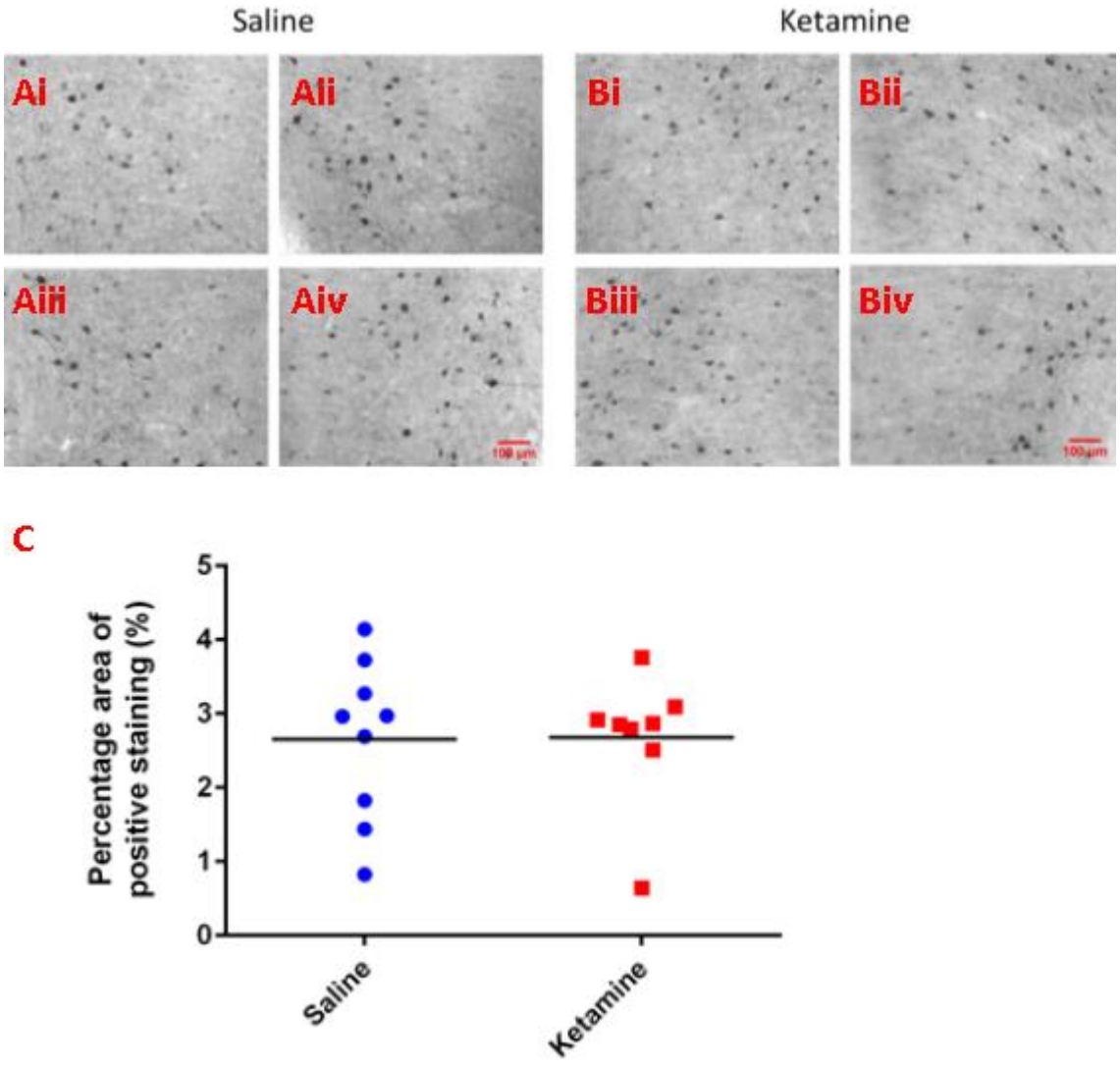

Figure 48. Parvalbumin (PV) positive neurons in the prefrontal cortex. **A)** Representative images of PV positive cells in SAL-INT mice. x20 magnification. **B)** Representative images of PV

positive cells in KET-INT mice. x20 magnification. **C)** Graph of the percentage area of PV positive staining in SAL-INT and KET-INT mice.

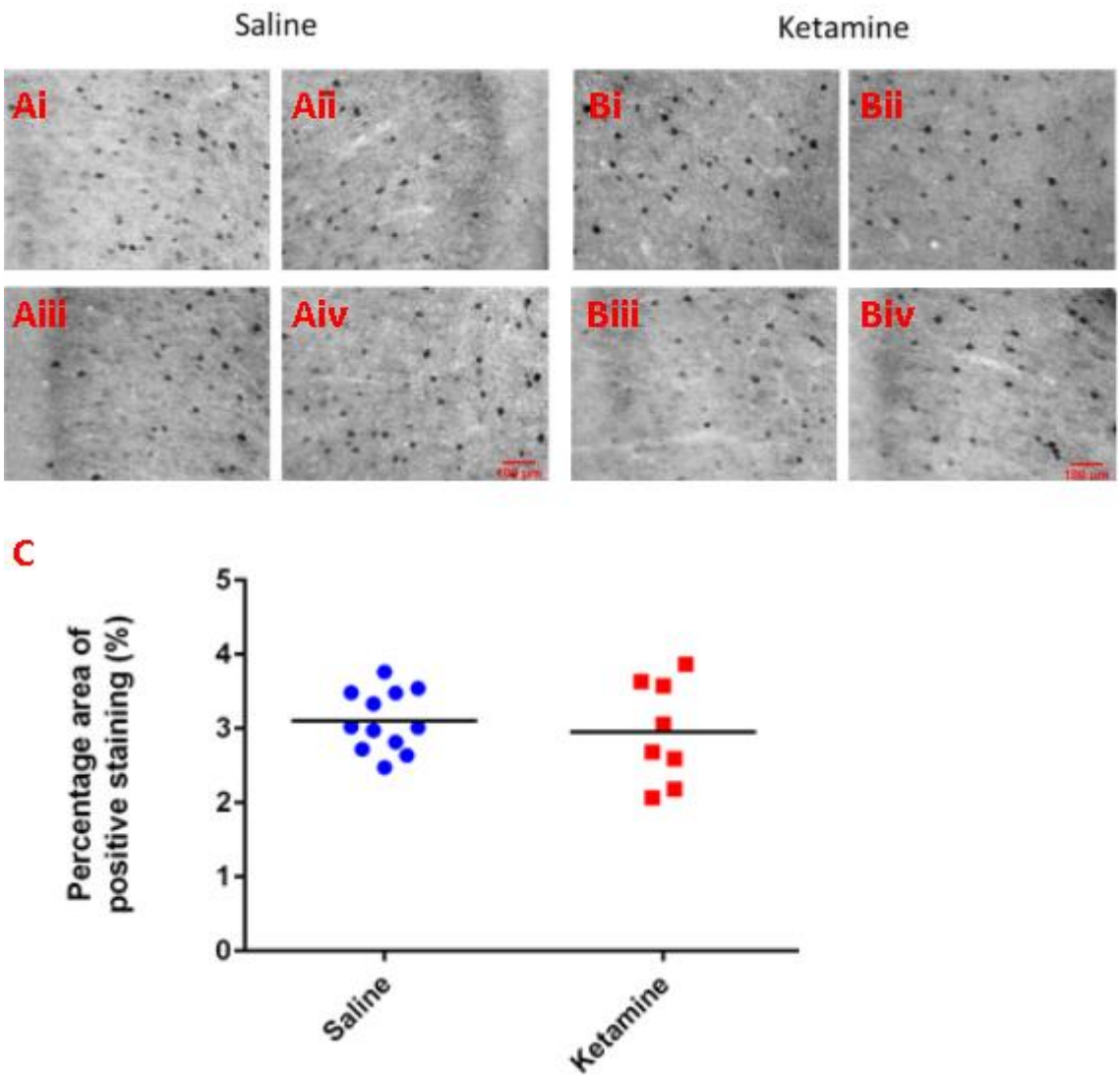

Figure 49. Parvalbumin (PV) positive neurons in the prefrontal cortex. **A)** Representative images of PV positive cells in SAL-DAY mice. x20 magnification. **B)** Representative images of PV positive cells in KET-DAY mice. x20 magnification. **C)** Graph of the percentage area of PV positive staining in SAL-DAY and KET-DAY mice.

c) Corpus callosum

Next, I went on to investigate what cellular differences might be present in ketamine and saline treated mice, within the corpus callosum. As stated in the introduction to this chapter, KET-DAY mice presented with smaller volumes in this region, whereas KET-INT mice presented with larger volumes, as seen using sMRI. Furthermore, both daily and intermittent dosing of ketamine in mice resulted in reduced MD, AD and RD values in this region, along with increases in FA.

Like my approach in the frontal lobe, I first looked to see whether there was any difference in the number of glial cells, in the corpus callosum, between ketamine and saline treated mice.

I found no significant difference in the amount of GFAP positive fibrous astrocytes, which normally reside in the white matter, between KET-INT mice (17.27±1.22, n= 10) and SAL-INT mice (16.32±1.32, n=10), (t=0.53, p=0.60), Figure 50. Nor did I find any significant difference in the amount of GFAP positive astrocytes between KET-DAY mice (5.43±0.97, n=10) and SAL-DAY mice (5.17±1.15, n=10), (t=0.17, p=0.87), Figure 51.

Furthermore, I found no significant difference in the number of Iba-1 positive microglia between KET-INT mice (46502±2003, n=10) and SAL-INT mice (48785±1274, n=10), (t=0.96, p=0.35), Figure 52. Nor did I find any significant difference between the number of Iba-1 positive microglia between KET-DAY (45360±2022, n=9) and SAL-DAY mice (45339±1389, n=10), (t=0.01, =0.99), Figure 53.

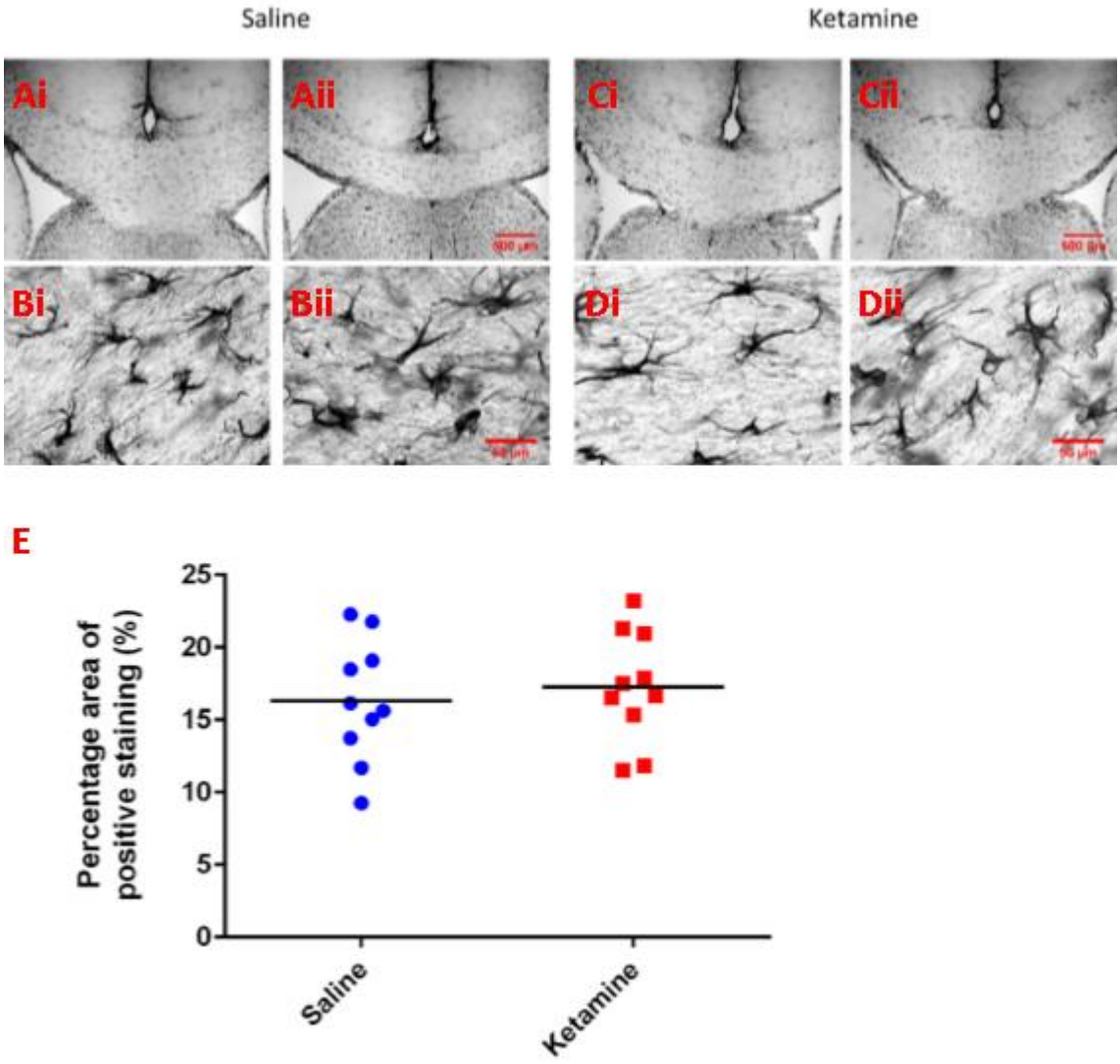

Figure 50. GFAP positive staining in the corpus callosum of SAL-INT and KET-INT mice. **A&B)** Representative images of GFAP positive staining in SAL-INT mice. A) x5 magnification. B) x63 magnification C**&D)** Representative images of GFAP positive cells in KET-INT mice. C) x5 magnification. D) x63 magnification. **E)** Graph of the percentage area of GFAP positive staining in the corpus callosum in SAL-INT and KET-INT mice.

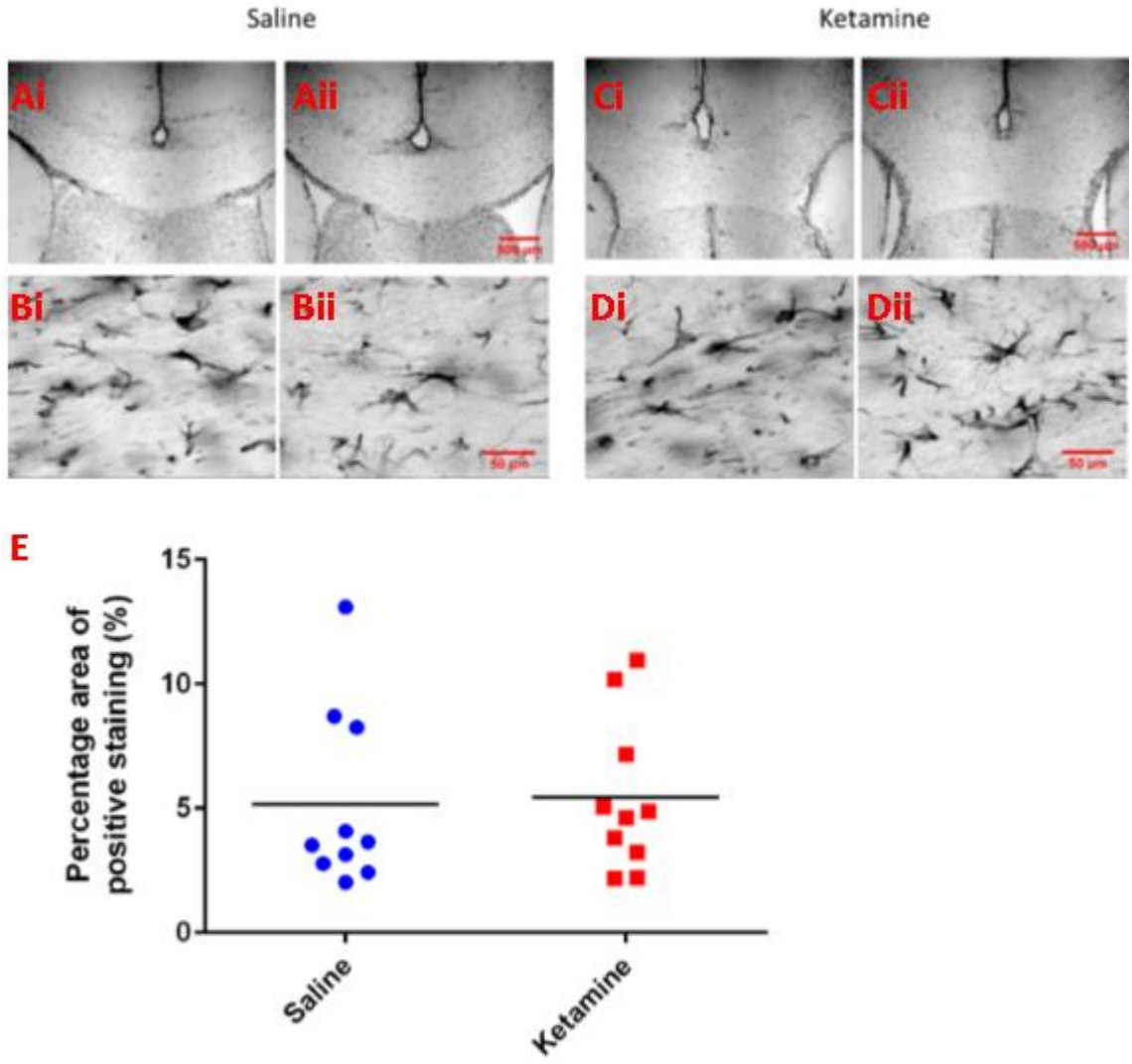

Figure 51. GFAP positive staining in the corpus callosum of SAL-DAY and KET-DAY mice. **A&B)** Representative images of GFAP positive staining in SAL-DAY mice. A) x5 magnification. B) x63 magnification C**&D)** Representative images of GFAP positive cells in KET-DAY mice. C) x5 magnification. D) x63 magnification. **E)** Graph of the percentage area of GFAP positive staining in the corpus callosum in SAL-DAY and KET-DAY mice.

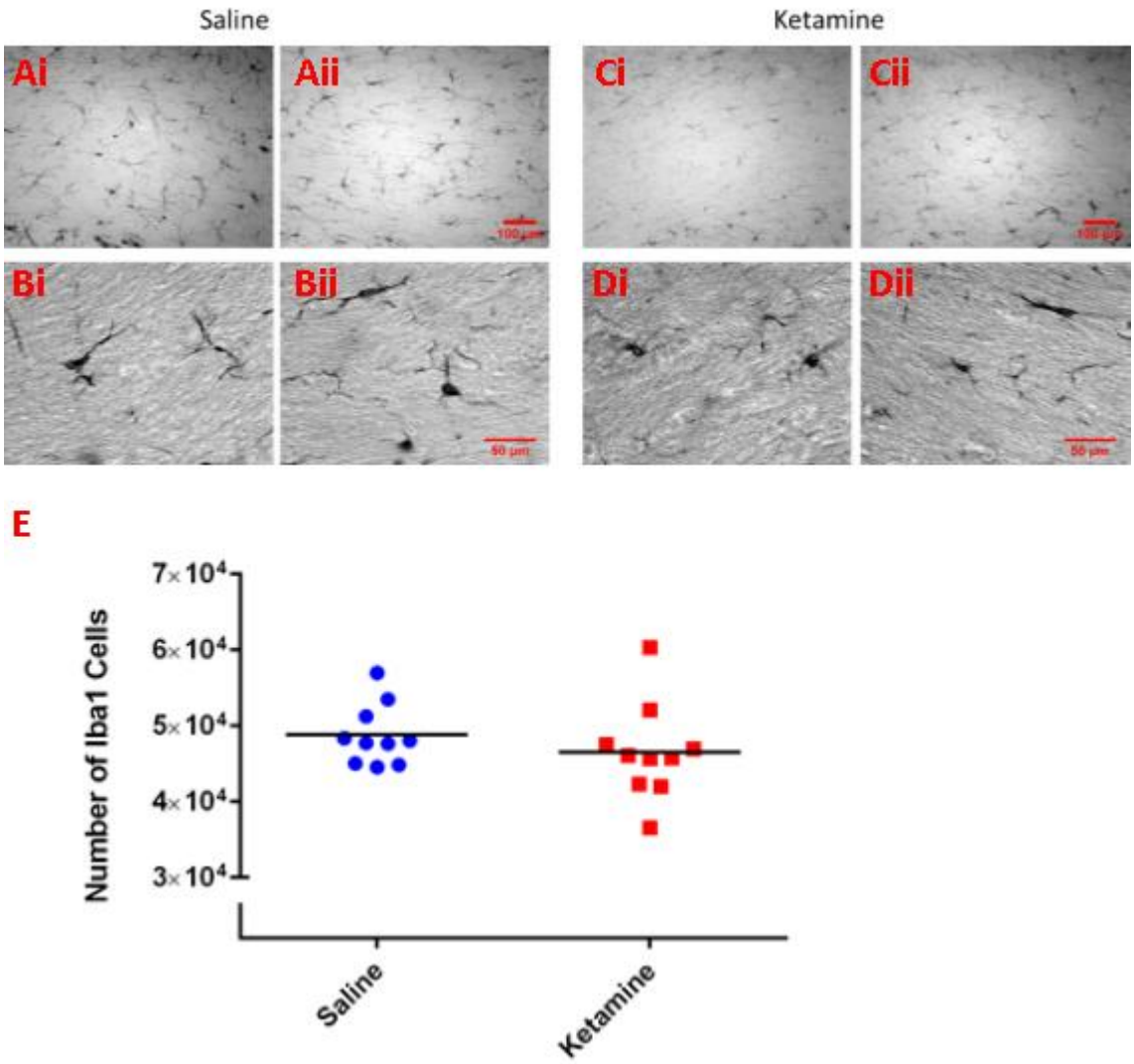

Figure 52. Iba-1 positive staining in the corpus callosum of SAL-INT and KET-INT mice. **A&B)** Representative images of Iba-1 positive staining in SAL-INT mice. A) x20 magnification. B) x63 magnification C**&D)** Representative images of Iba-1 positive cells in KET-INT mice. C) x20 magnification. D) x63 magnification. **E)** Graph of the stereological counts of Iba-1 positive cells in the corpus callosum in SAL-INT and KET-INT mice.

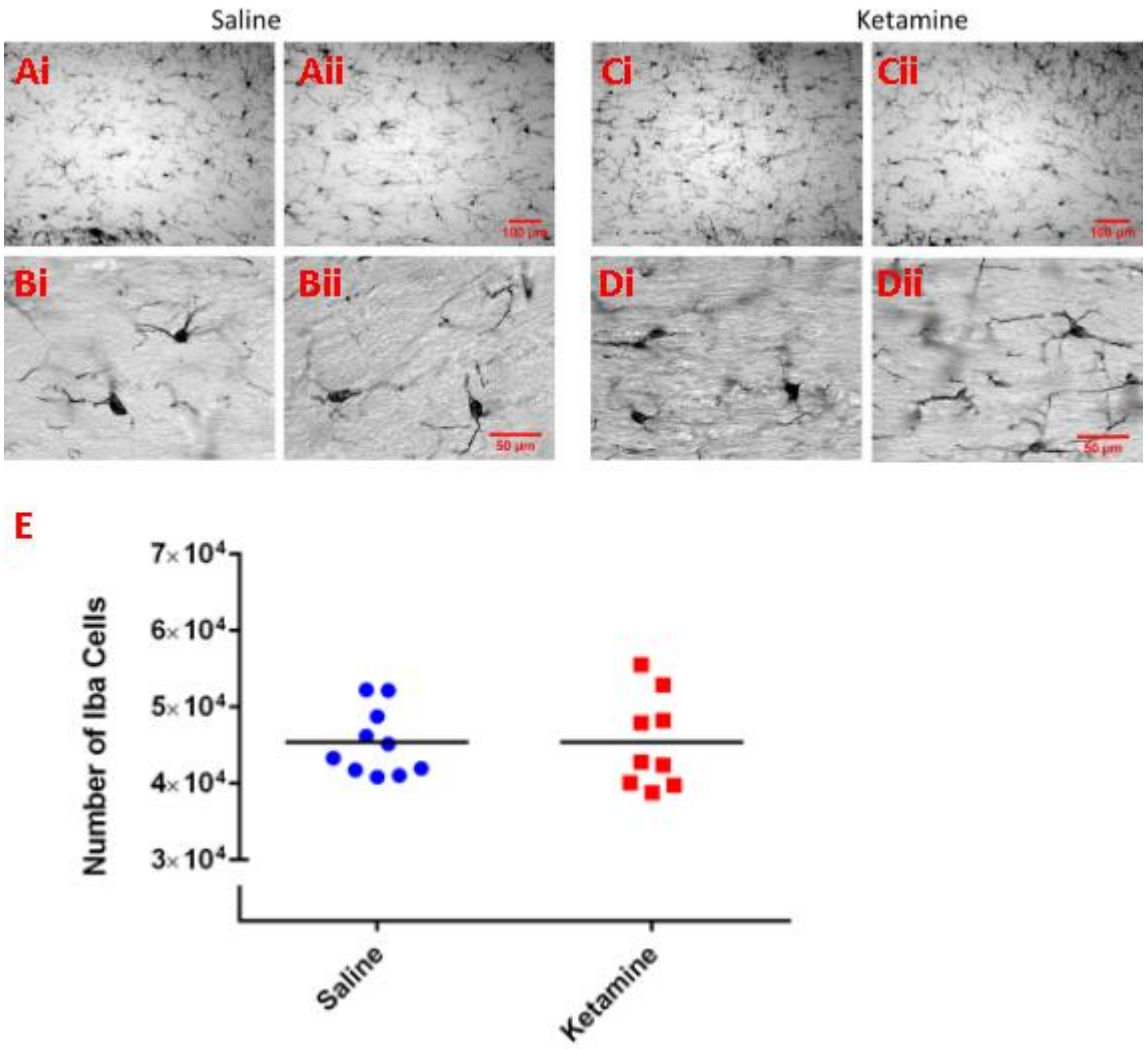

Figure 53. Iba-1 positive staining in the corpus callosum of SAL-DAY and KET-DAY mice. **A&B)** Representative images of Iba-1 positive staining in SAL-DAY mice. A) x20 magnification. B) x63 magnification C**&D)** Representative images of Iba-1 positive cells in KET-DAY mice. C) x20 magnification. D) x63 magnification. **E)** Graph of the stereological counts of Iba-1 positive cells in the corpus callosum in SAL-DAY and KET-DAY mice.

As there was no significant difference in the number of glia in the corpus callosum, between ketamine and saline treated mice, and there was no significant difference in the amount of GFAP reactive astrocytes (a marker of activated astrocytes), I took these results to mean that there was no glial pathology in this region. These results then are like my findings in the frontal lobe and prefrontal cortex.

I next looked to see whether there were any signs of cellular plasticity, and possible remodelling of neural circuits in the corpus callosum, by investigating the amount of MBP and neurofilament in the region.

I found a significant increase in the amount of MBP in KET-INT mice (117.8±3.01, n=10) compared to SAL-INT mice (103.6±1.81, n=10), (t=4.04, p=0.0008), Figure 54.

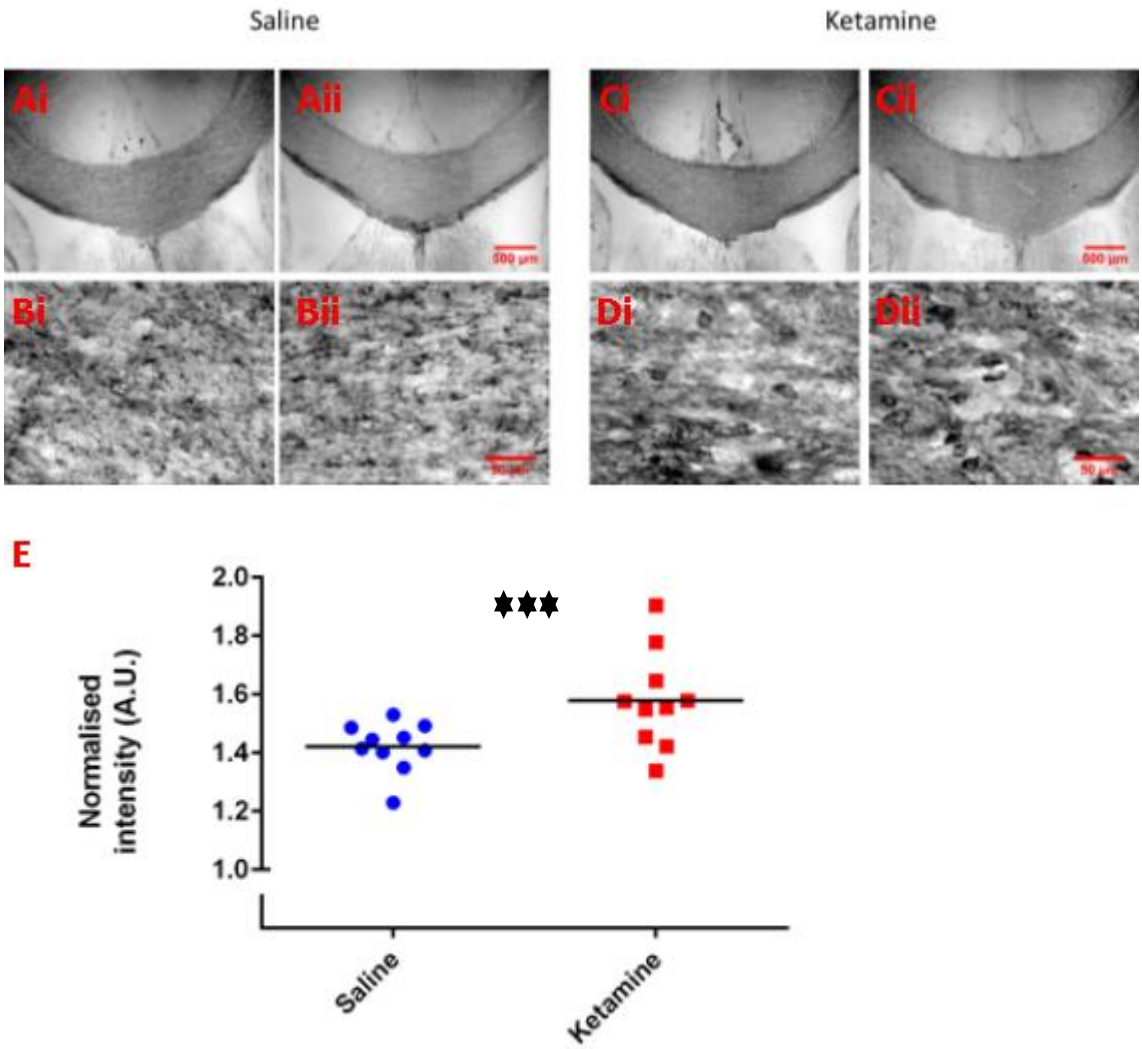

Figure 54. Myelin basic protein (MBP) positive staining in the corpus callosum of SAL-INT and KET-INT mice. **A&B)** Representative images of MBP positive staining in SAL-INT mice. A) x5 magnification. B) x63 magnification C**&D)** Representative images of MBP positive cells in KET-INT mice. C) x5 magnification. D) x63 magnification. **E)** Graph of the percentage area of MBP positive staining in the corpus callosum in SAL-INT and KET-INT mice. ***; p<0.001 (T-test).

However, I found no significant difference in the amount of MBP positive staining between KET-DAY (1.65±0.04, n=10) and SAL-DAY mice (1.62±0.03, n=8), (t=0.54, p=0.60), Figure 55.

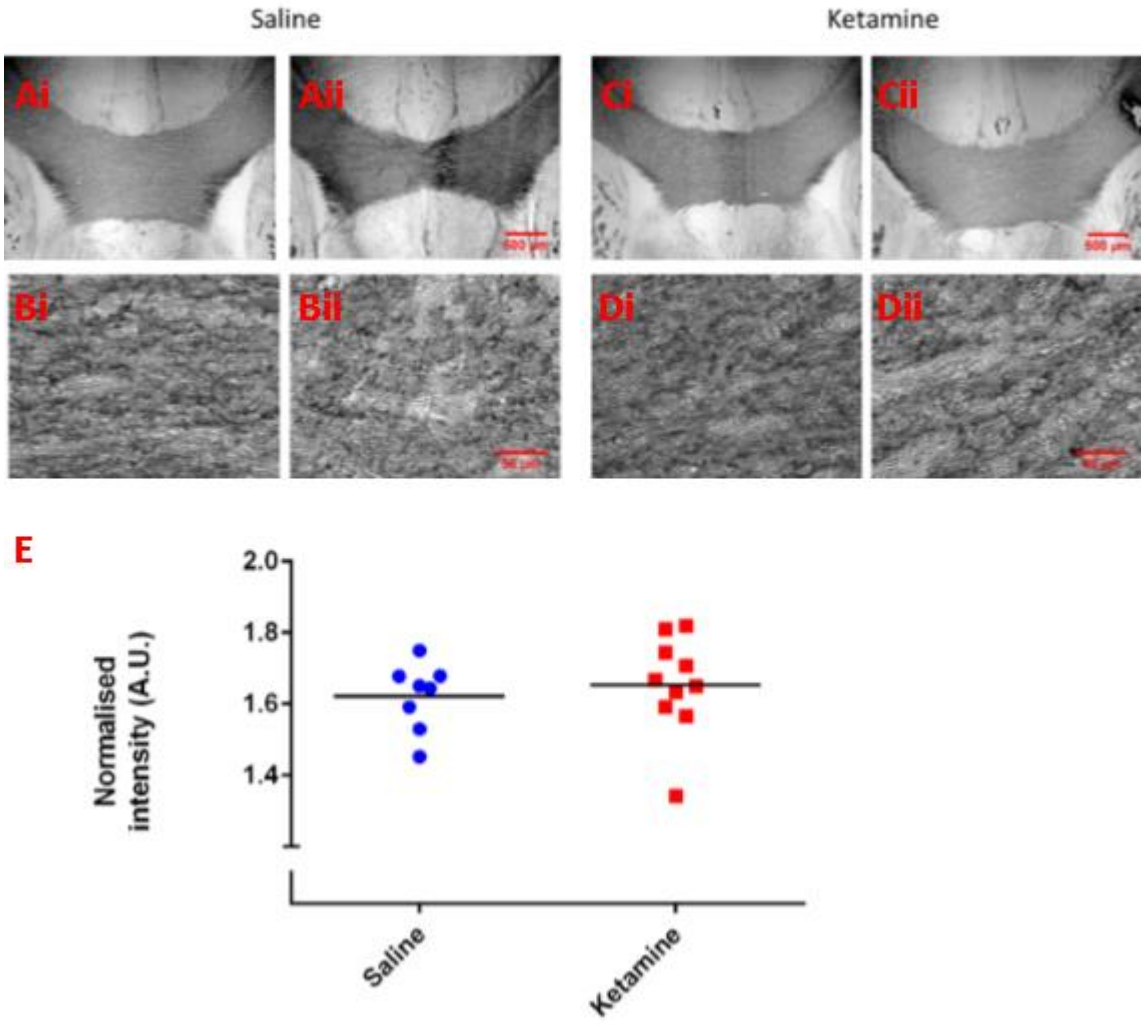

Figure 55. Myelin basic protein (MBP) positive staining in the corpus callosum of SAL-DAY and KET-DAY mice. **A&B)** Representative images of MBP positive staining in SAL-DAY mice. A) x5 magnification. B) x63 magnification **C&D)** Representative images of MBP positive cells in KET-DAY mice. C) x5 magnification. D) x63 magnification. **E)** Graph of the percentage area of MBP positive staining in the corpus callosum in SAL-DAY and KET-DAY mice.

I also found a significant increase in the amount of neurofilament between KET-INT mice (135.9±1.91, n=10) and SAL-INT mice (127.2±2.70, n=10), (t=2.62, p=0.02), Figure 56. However, I did not find any significant difference in the amount of neurofilament positive staining between KET-DAY (116.9±1.15, n=9) and SAL-DAY mice (116.5±1.54, n=10), (t=0.18, p=0.86), Figure 57.

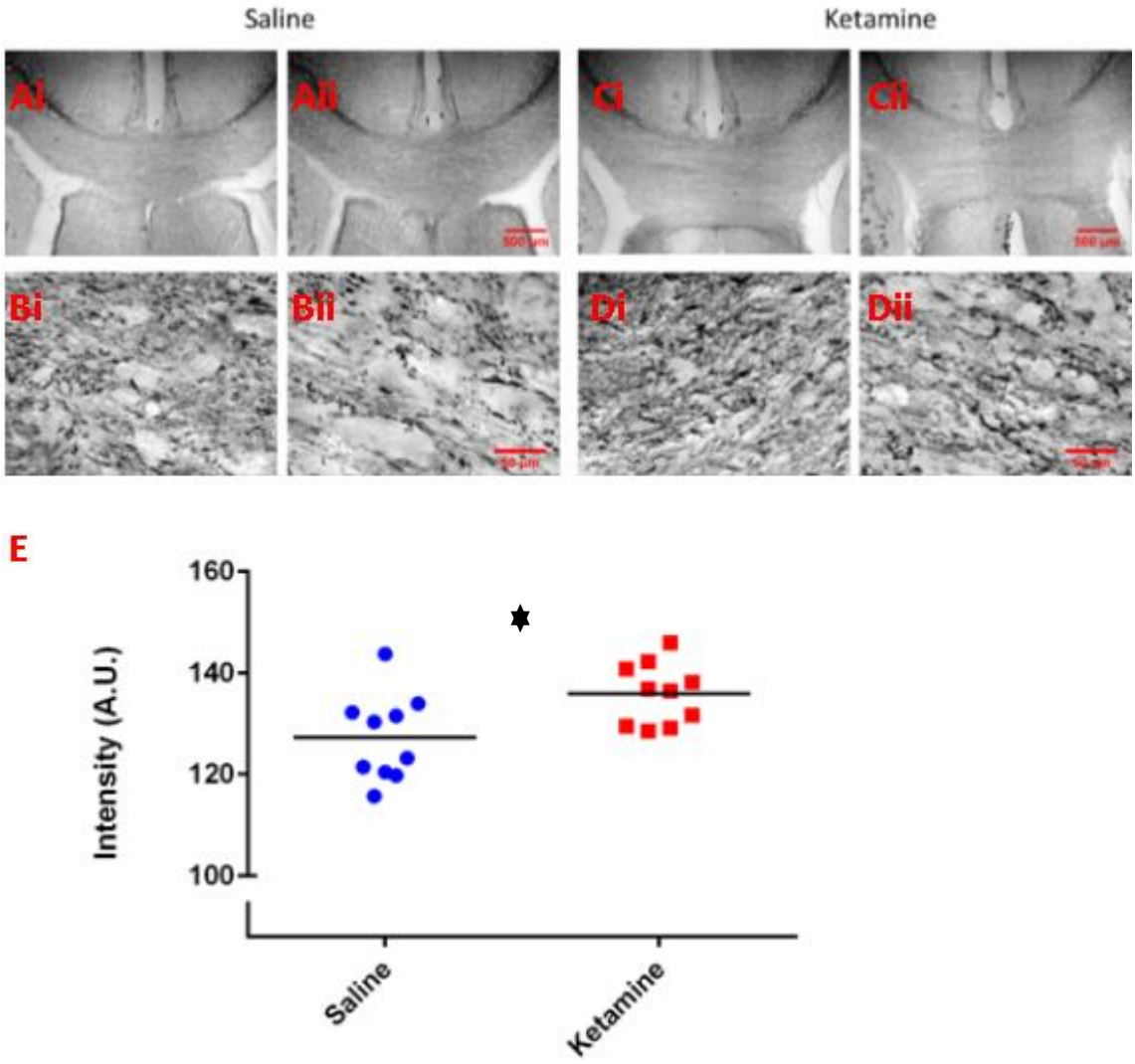

Figure 56. Neurofilament (NF) positive staining in the corpus callosum of SAL-INT and KET-INT mice. **A&B)** Representative images of NF positive staining in SAL-INT mice. A) x5 magnification. B) x63 magnification C**&D)** Representative images of NF positive cells in KET-INT mice. C) x5 magnification. D) x63 magnification. **E)** Graph of the percentage area of NF positive staining in the corpus callosum in SAL-INT and KET-INT mice. *; $p<0.05$ (T-test).

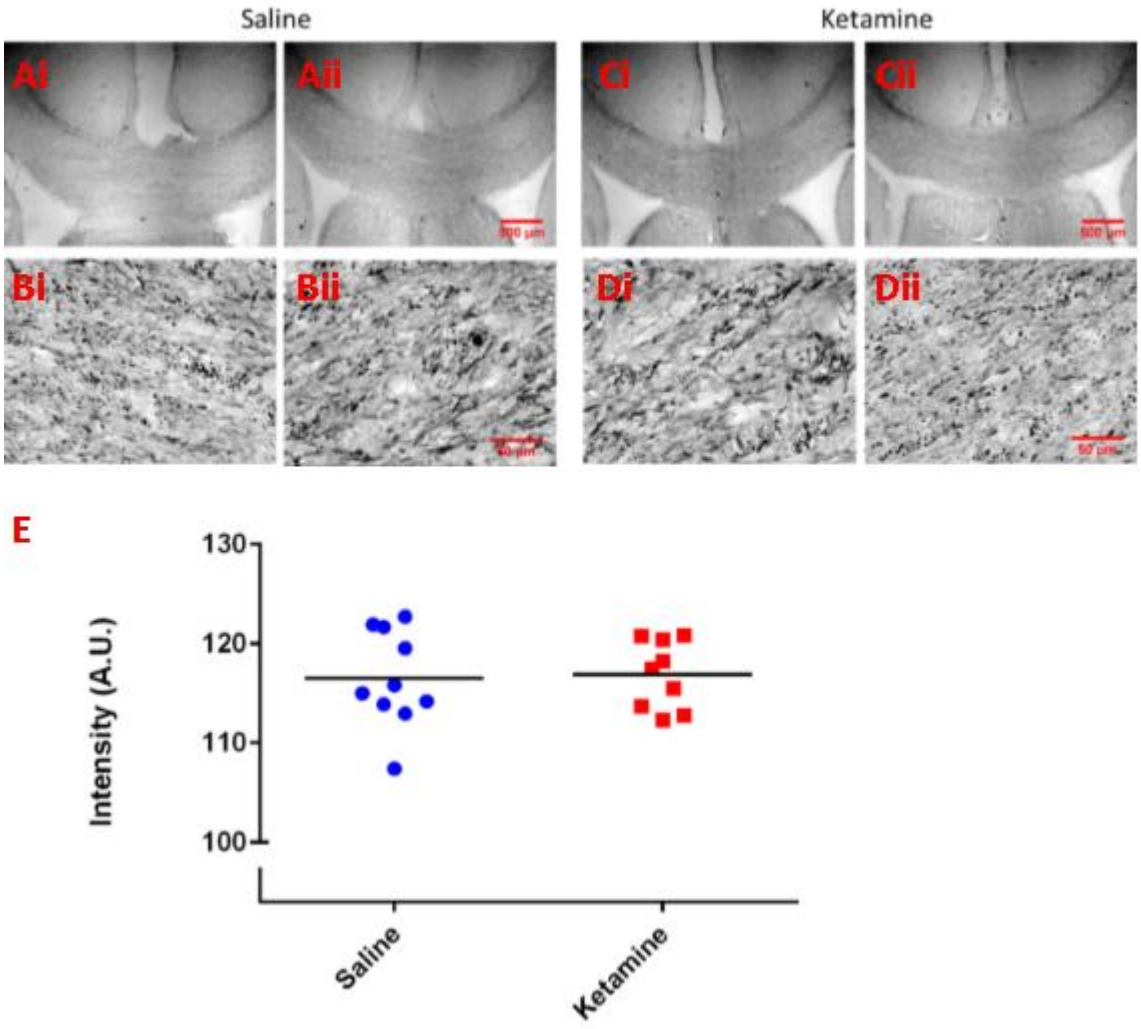

Figure 57. Neurofilament (NF) positive staining in the corpus callosum of SAL-DAY and KET-DAY mice. **A&B)** Representative images of NF positive staining in SAL-DAY mice. A) x5 magnification. B) x63 magnification **C&D)** Representative images of NF positive cells in KET-DAY mice. C) x5 magnification. D) x63 magnification. **E)** Graph of the percentage area of NF positive staining in the corpus callosum in SAL-DAY and KET-DAY mice.

The significant increase in the amount of MBP and neurofilament in KET-INT mice would suggest that, like in the prefrontal cortex, ketamine might be having a remodelling effect on neural circuits within this brain region (Markham *et al.*, 2009; Zatorre, Fields and Johansen-Berg, 2012; Nickel and Gu, 2018). In turn, this might be responsible for the increase in FA observed in this region. Thus, I decided to see whether there was any correlation between FA and the amount of MBP and neurofilament present in the corpus callosum.

I found no significant correlation between FA and the amount of MBP in the corpus callosum; neither in KET-INT mice alone (r=-0.14, p=0.70), SAL-INT mice alone (r=0.02, p=0.96), nor in KET-INT and SAL-INT mice combined (r=0.09, p=0.70), Figure 58.

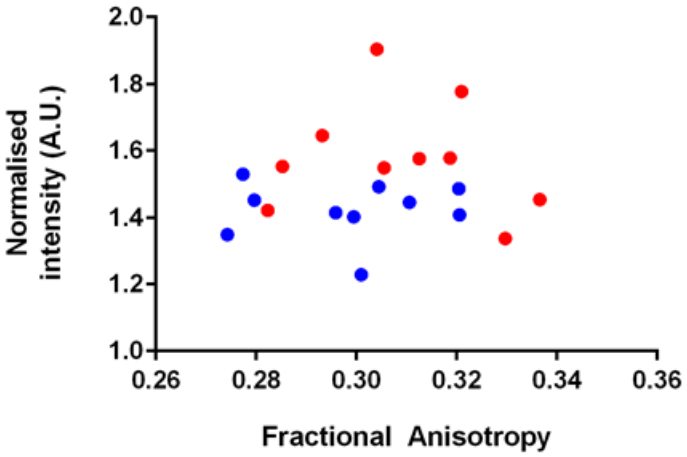

Figure 58. Correlations between the intensity of MBP immunostaining and DTI measures of FA in the corpus callosum of KET-INT (red dots) and SAL-INT mice (blue dots).

However, I did find a significant negative correlation between FA and neurofilament in KET-INT mice alone (r=-0.79, p<0.0017), Figure 59. There was no significant correlation in SAL-INT mice alone (r=0.47, p=0.17), nor in KET-INT and SAL-INT mice combined (r=0.10, p=0.69).

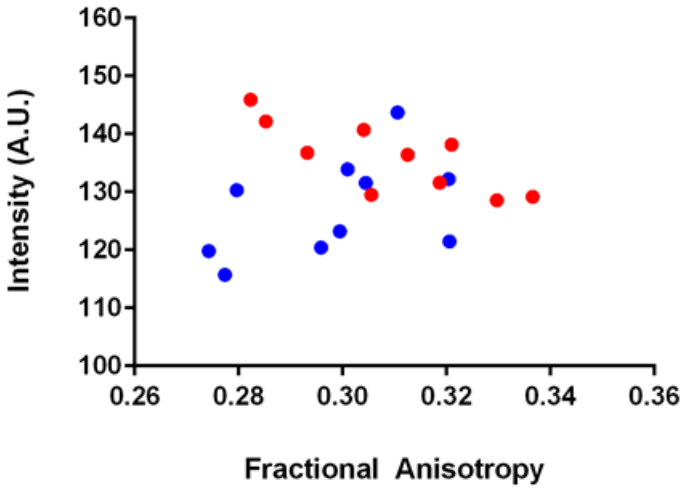

Figure 59. Correlations between the intensity of neurofilament immunostaining and DTI measures of FA in the corpus callosum of KET-INT (red dots) and SAL-INT mice (blue dots).

This correlation suggests that ketamine, through repeat intermittent administration, might be remodelling neural circuitry in the corpus callosum which presents as an increase in the amount of neurofilament, at the cellular level, and an increase in FA at the MR level.

d) Summary

To summarise, in this chapter I have shown that repeat ketamine administration does not induce any change in neuron or glial cell number in the frontal lobe nor corpus callosum. Furthermore, repeat ketamine administration, in mice, be it daily or intermittent, does not induce gliosis. The lack of these changes would suggest that repeat ketamine administration is not having a pathological effect on the mouse brain as it appears to in human ketamine users.

Moreover, I have shown that under repeat intermittent administration, ketamine induces an increase in the amount of neurofilament and synaptophysin in the prefrontal cortex, markers of axons and synapses. These results suggest, indirectly, that repeat intermittent ketamine administration is remodelling neuronal circuitry in this region. Similarly, the increase in MBP and neurofilament in the corpus callosum of mice given repeat ketamine intermittently, suggests rewiring of neuronal circuitry in this region. These structural changes, in both regions, may have functional and behavioural consequences, something which should be investigated further.

As, ketamine was given systemically, it is tempting to speculate that the drug may be rewiring neuronal circuitry in other brain regions as well. This, however, would need further experimental verification. Furthermore, the results presented here are only preliminary and would need further confirmation using other techniques. For example, the increase in synaptophysin staining in KET-INT mice is only an indicator of an increase in one pre-synaptic protein which may or may not correlate with an increase in the size or number of synapses. To understand better what is occurring further experiments should be performed, including a mixture of further histological stainings, coupled with biochemical analysis of the levels of other synaptic proteins and electron microscope investigation of synapse number and distribution. Similarly, these techniques should be applied to investigate further the structural changes behind an increase in

neurofilament (in the prefrontal cortex and corpus callosum) and MBP (in the corpus callosum), which might help establish if and how ketamine is remodelling neural circuitry.

Chapter 5 General discussion

As discussed in the general introduction in chapter 1, ketamine over the last 10-12 years has been used as a revolutionary "off-label" treatment for depression. This has led to the establishment of multiple, specialised ketamine clinics in both the UK and USA. These clinics offer ketamine treatment plans at a cost of £1,200 in the UK and $2400-$4800 in the USA. Unfortunately, these treatment plans are not covered by the NHS in the UK nor medical insurance in the USA. Hence, there is a foreseeable risk of self-medication with ketamine by people suffering with depression. The risk here is that patients will self-medicate with incorrect, too high and too frequent doses of ketamine, which may have unknown long-term detrimental effects on physical and psychological wellbeing.

Currently, there is a lack of understanding as to the long-term effects and safety profile of ketamine treatment for depression, particularly with regards to the effects on brain structure, function and psychological wellbeing. Our best understanding of the long-term effects of ketamine on brain structure and function come from a handful of studies which assessed the effects of repeat ketamine use by poly-drug users. These studies suggest that repeat ketamine use may cause altered neuronal activity in the cortex, alongside cortical atrophy and cognitive deficits. However, these studies are heavily confounded by the fact that other psychotropic drug use is poorly controlled for within these studies. Thus, within the literature, it remains unclear what effects repeat ketamine alone is having on the brain.

The aims of my PhD thesis were to elucidate what effects repeat ketamine exposure, alone, has on brain structure. To investigate this, I contrasted the effects of repeat ketamine use, on brain structure, by recreational users, against repeat ketamine administration (alone) in mice.

My major findings, in humans, were that ketamine users exhibit reduced brain volume in the cerebral cortices, cerebellar cortices and striatum. This is in line with previously published studies showing atrophy in the cerebral cortex frontal lobe and cerebellum (Liao *et al.*, 2011; Wang *et al.*, 2013). Furthermore, ketamine users, in my study, demonstrated reduced psychological wellbeing compared to poly-drug controls, which has been reported previously (Edward Roberts *et al.*, 2014; Morgan *et al.*, 2014). However, the structural changes observed in ketamine users did not correlate with reduced scores of psychological wellbeing. Nor did structural alterations or reduced

scores of psychological wellbeing correlate with either the amount, frequency or duration of ketamine use. Thus, I cannot confidently state that the differences observed in brain structure and psychological wellbeing seen in ketamine users, versus poly-drug controls, is due to ketamine alone. It is my conclusion that other drug use contributes to these changes observed, This is reinforced by studies showing that other psychotropic drugs, used by ketamine users in my study, have been shown to impact on brain structure and psychological wellbeing in similar ways to the results I have observed (Lim *et al.*, 2008; Van Dam, Earleywine and DiGiacomo, 2008b; Compton, Chien and Bollini, 2009; Liu *et al.*, 2009; Fridberg *et al.*, 2011; Baskak *et al.*, 2012; Grodin, Lin, C. a. Durkee, *et al.*, 2013; Li *et al.*, 2015).

Turning to my studies on repeat ketamine administration in mice, I have found both similar and disparate results to those observed in repeat ketamine users. I have seen volume changes in the cerebral cortex, cerebellum and striatum. However, in contrast to volume reductions seen in the frontal lobe of human ketamine users, in mice, I have seen increased cortical volume in the frontal lobe. Furthermore, I have observed clusters of increased volume, as well as clusters of decreased volume, throughout the cerebral cortex of mice given repeat daily or intermittent ketamine. This discrepancy in results observed between humans and mice suggests that other drug use in humans might be confounding the effect of ketamine on brain volume.

In addition to the volume differences observed in mice, I have also observed structural differences, as observed by DTI. These structural differences presented as decreased FA and AD in both KET-INT and KET-DAY mice in the frontal lobe and parieto-temporal lobe. Furthermore, in KET-DAY mice, I found significant decreases in AD in the following cerebral white matter bundles; corpus callosum, cerebral peduncle, fasciculus retroflexus, fimbria, fornix, mammillothalamic tract and stria medullaris. These changes are like those observed in human ketamine users and suggest that a common cellular/molecular mechanism may be responsible for the changes observed (Table 35).

Table 35. Summary of MRI changes observed after repeat ketamine exposure across species

Species	Structural changes	Source
Human	Smaller cerebral cortices: • inferior parietal cortex • temporal pole • supramarginal gyrus • paracentral gyrus • middle temporal gyrus • superior frontal gyrus • isthmus of the cingulate cortex • superior temporal gyrus • banks of the superior temporal sulcus	Chapter 2 of this thesis
	Smaller cerebellar cortices	
	Smaller striatum	
	Smaller cerebral cortex: • superior frontal cortex • middle frontal cortex	Liao et al (2011)
	Cortical atrophy	Wang et al (2013)
	Reduced FA: • frontal cortex • temporoparietal cortex	Liao et al (2010)
	Reduced AD: • frontal cortex • parietal cortex • somatosensory cortex	Roberts et al (2014)
Cynomolgus monkey	Reduced FA • frontal gyrus • middle temporal gyrus	Li et al (2017)
C57BL/6J mice	Larger frontal cortex	Chapter 3 of this thesis
	Reduced FA: • frontal cortex • parieto-temporal cortex	
	Reduced AD: • frontal cortex • parieto-temporal cortex	

I have shown that, within the frontal lobe and corpus callosum, of mice given repeat doses of ketamine, there is no change in the number of neurons nor glia. Furthermore, there is no change in the level of gliosis in these regions. This evidence leads me to conclude, at least in these two regions, that there is a lack of pathology.

Rather, as reinforced by an increase in neurofilament and synaptophysin levels (prefrontal cortex) and neurofilament and MBP (corpus callosum), of mice given repeat intermittent doses of ketamine, ketamine is remodelling neural circuitry. These are only preliminary data, however, and would need further confirmation using other techniques. For example, the increase in synaptophysin staining in KET-INT mice is only an indicator of an increase in one pre-synaptic protein which may or may not correlate with an increase in the size or number of synapses. To understand better what is occurring, further experiments need performing. These could include a mixture of further histological stainings, coupled with biochemical analysis (e.g. western blot) of the levels of other proteins located at the presynaptic terminal / postsynaptic membrane and electron microscope investigation of synapse number and distribution.

Of interest would be to investigate whether the expression of proteins in cell signalling pathways, thought to be involved in the anti-depressant effects of ketamine, are altered following repeat ketamine exposure. As discussed in chapter 1, the primary mechanism of action of ketamine's antidepressant effect is thought to involve the restoration of synaptic connectivity and glutamatergic signalling (which is thought to be disrupted in depression) (Abdallah *et al.*, 2014). This is thought to involve preferential inhibition of NMDA receptors on inhibitory GABAergic interneurons, a widespread prefrontal glutamate surge and activation of post-synaptic AMPA receptors. Combined with ketamine's blockade of extra synaptic NMDA receptors on post-synaptic neurons, this leads to increased BDNF release in the post-synaptic neuron and activation of the mTORC1 signalling pathway. The increase in mTORC1 signalling in turn increases post-synaptic protein synthesis and AMPA cycling. This results in the restoration of AMPA receptors to the post-synaptic membrane (thought to be deficient in depression) and the restoration of glutamatergic neurotransmission to normal levels.

It is my hypothesis that mTORC1 signalling, in KET-INT mice, is increased after each ketamine infusion leading to an increase in AMPA receptors and a strengthening of glutamatergic neurotransmission. In turn, I hypothesise, an increase in BDNF induced

dendritic spine formation and new synapse formation (Wohleb *et al.*, 2017). I further hypothesise that these changes are responsible for the structural MRI changes observed within the frontal cortex of KET-INT mice. Such changes would explain an increase in volume as well as a decrease in AD; a measure of the rate of water diffusion in a given volume (the more structures present in a given volume the greater the impedance of water diffusion).

Moreover, I hypothesise that the increase in MBP and neurofilament; observed within the prefrontal cortex of KET-INT mice, are secondary to an increase in dendritic spine formation and synapse formation. An increase in synapse formation and increased glutamatergic neurotransmission requires a subsequent increase in the rate of action potential propagation. An increase in axon width (neurofilament increase) and an increase in myelin thickness (MBP increase), and thus insulation, would facilitate faster action potential propagation and increased glutamatergic signalling.

Changes in glutamatergic signalling within the prefrontal cortex would subsequently alter neuronal activity in other brain regions, requiring structural changes in those regions. I hypothesise that the increase in MBP and neurofilament, observed within the corpus callosum of KET-INT mice, is reflective of this and the need for faster action potential propagation across the brain; particularly in axonal pathways travelling to the frontal cortex.

In KET-DAY mice changes in synaptophysin, MBP and neurofilament were not observed. In these mice, increased volume was seen in the prefrontal cortex, but this change was not as wide spread as in KET-INT mice. Decreases in FA and AD were also seen in KET-DAY mice, within the frontal cortex, as was observed in KET-INT mice. It might be that cellular and molecular changes are occurring within KET-DAY mice as observed in KET-INT mice but that the histological techniques used in this thesis lack the sensitivity to detect them. In this case, molecular biology techniques; such as western blot or mass spectrometry, can more accurately measure protein expression in a given region. Another factor to consider, is that KET-DAY mice compared to KET-INT mice may have built up greater tolerance to ketamine's effects due to a higher frequency of exposure and therefore the cellular changes observed in KET-INT mice is not detectable using histology. Again, more sensitive molecular biology techniques may help clarify this uncertainty.

Eventually, the functional and behavioural consequences of these potential structural changes require investigation to determine if the outcome is positive or detrimental. This will require a combination of electrophysiological and behavioural experiments in mice give ketamine at different frequencies and for different durations. If the remodelling of neural circuits is positive and not detrimental to brain function or behaviour, then it may be a starting point for further understanding the antidepressant mechanism of depression. It has been demonstrated, in numerous studies now, that acute doses of ketamine, both *in-vitro* and *in-vivo*, increase the number of synapses and dendritic spines within neural circuits, particularly the prefrontal cortex. This rewiring of neural circuits is thought to be the therapeutic base for how ketamine induces anti-depressant effect in patients with depression (Duman and Duman, 2015; Thompson *et al.*, 2015; Wohleb *et al.*, 2017; Zanos *et al.*, 2018).

If it is confirmed that repeat, intermittent doses of ketamine do lead to upregulation of synapses and dendritic spines, and rewiring of neural circuits, without detrimental effects on brain activity and behaviour, then that is one step in the right direction to showing that ketamine is a safe treatment for depression in the long-term.

It would also be good to see experiments in the future being performed on animal models of stress/depression to see whether repeat intermittent ketamine administration has a positive effect in relieving stress/depressive symptoms, and possibly reversing any structural, functional and behavioural pathology without detrimental side effects.

Furthermore, what would be good to see happen in parallel are longitudinal MRI studies of depressed patients being treated with ketamine in ketamine clinics. These studies would show if repeat ketamine infusions ameliorate the structural and psychological pathologies of depressed patients, as well as highlight any long-term side effects. This data could then be compared to that obtained from animal models of depression, and if the same or similar structural, and or functional / behavioural, changes are observed then this would suggest that a common cellular and molecular pathway is affected by ketamine. Ultimately, this may help us to understand better the pathophysiology of depression and the mechanism by which to treat it.

Bibliography – Academic references

Abdallah, C. G. *et al.* (2014) 'Ketamine and Rapid-Acting Antidepressants: A Window into a New Neurobiology for Mood Disorder Therapeutics', *Annual Review of Medicine*, 66(1), pp. 509–523. doi: 10.1146/annurev-med-053013-062946.

Abdallah, C. G., Averill, L. A. and Krystal, J. H. (2015) 'Ketamine as a promising prototype for a new generation of rapid-acting antidepressants', *Annals of the New York Academy of Sciences*, 1344(1), pp. 66–77. doi: 10.1111/nyas.12718.

Al-Harbi, K. S. (2012) 'Treatment-resistant depression: therapeutic trends, challenges, and future directions.', *Patient preference and adherence*. Dove Press, 6, pp. 369–88. doi: 10.2147/PPA.S29716.

Albrecht, J. *et al.* (2010) 'Roles of glutamine in neurotransmission.', *Neuron glia biology*, 6(4), pp. 263–76. doi: 10.1017/S1740925X11000093.

Alexander, A. L. *et al.* (2007) 'Diffusion tensor imaging of the brain.', *Neurotherapeutics : the journal of the American Society for Experimental NeuroTherapeutics*, 4(3), pp. 316–29. doi: 10.1016/j.nurt.2007.05.011.

Alicata, D. *et al.* (2009) 'Higher diffusion in striatum and lower fractional anisotropy in white matter of methamphetamine users.', *Psychiatry research*. Elsevier Ireland Ltd, 174(1), pp. 1–8. doi: 10.1016/j.pscychresns.2009.03.011.

Allman, J. M. *et al.* (2001) 'The anterior cingulate cortex. The evolution of an interface between emotion and cognition.', *Annals of the New York Academy of Sciences*, 935, pp. 107–117. doi: 10.1111/j.1749-6632.2001.tb03476.x.

Almeida, R. G. and Lyons, D. A. (2017) 'On Myelinated Axon Plasticity and Neuronal Circuit Formation and Function', *The Journal of Neuroscience*, 37(42), pp. 10023–10034. doi: 10.1523/JNEUROSCI.3185-16.2017.

Althubaiti, A. (2016) 'Information bias in health research: definition, pitfalls, and adjustment methods.', *Journal of multidisciplinary healthcare*. Dove Press, 9, pp. 211–7. doi: 10.2147/JMDH.S104807.

Anderson, I. M. *et al.* (2017) 'Ketamine augmentation of electroconvulsive therapy to improve neuropsychological and clinical outcomes in depression (Ketamine-ECT): a multicentre, double-blind, randomised, parallel-group, superiority trial', *The Lancet Psychiatry*. doi: 10.1016/S2215-0366(17)30077-9.

Andersson, J. L. R., Skare, S. and Ashburner, J. (2003) 'How to correct susceptibility distortions in spin-echo echo-planar images: application to diffusion tensor imaging', *NeuroImage*, 20(2), pp. 870–888. doi: 10.1016/S1053-8119(03)00336-7.

Angulo, M. C. *et al.* (2004) 'Glutamate released from glial cells synchronizes neuronal activity in the hippocampus.', *The Journal of neuroscience : the official journal of the Society for Neuroscience*, 24(31), pp. 6920–7. doi: 10.1523/JNEUROSCI.0473-04.2004.

Anticevic, A. *et al.* (2013) 'Connectivity, pharmacology, and computation: toward a mechanistic understanding of neural system dysfunction in schizophrenia.', *Frontiers in psychiatry*, 4(December), p. 169. doi: 10.3389/fpsyt.2013.00169.

Arnone, D. *et al.* (2008) 'Corpus callosum damage in heavy marijuana use: Preliminary evidence from diffusion tensor tractography and tract-based spatial statistics', *NeuroImage*, 41(3), pp. 1067–1074. doi: 10.1016/j.neuroimage.2008.02.064.

Artigas, F., Nutt, D. J. and Shelton, R. (2002) 'Mechanism of action of antidepressants.', *Psychopharmacology bulletin*, 36 Suppl 2, pp. 123–32. Available at: http://www.ncbi.nlm.nih.gov/pubmed/12490828 (Accessed: 3 April 2018).

Ashburner, J. (2007) 'A fast diffeomorphic image registration algorithm', *NeuroImage*, 38(1), pp. 95–113. doi: 10.1016/j.neuroimage.2007.07.007.

Ashburner, J. and Friston, K. J. (2000) 'Voxel-based morphometry--the methods.', *NeuroImage*, 11(6 Pt 1), pp. 805–21. doi: 10.1006/nimg.2000.0582.

Ashburner, J. and Friston, K. J. (2000) 'Voxel-Based Morphometry—The Methods', *NeuroImage*, 11(6), pp. 805–821. doi: 10.1006/nimg.2000.0582.

Ashburner, J. and Friston, K. J. (2005) 'Unified segmentation', *NeuroImage*, 26(3), pp. 839–851. doi: 10.1016/j.neuroimage.2005.02.018.

Aung, W. Y., Mar, S. and Benzinger, T. L. (2013) 'Diffusion tensor MRI as a biomarker in axonal and myelin damage', *Imaging in Medicine*, 5(5), pp. 427–440. doi: 10.2217/iim.13.49.

Autry, A. E. *et al.* (2011) 'NMDA receptor blockade at rest triggers rapid behavioural antidepressant responses.', *Nature*, 475(7354), pp. 91–5. doi: 10.1038/nature10130.

Avants, B. B. *et al.* (2010) 'The optimal template effect in hippocampus studies of diseased populations', *NeuroImage*, 49(3), pp. 2457–2466. doi: 10.1016/j.neuroimage.2009.09.062.

Avants, B. B. *et al.* (2011) 'A reproducible evaluation of ANTs similarity metric performance in brain image registration', *NeuroImage*, 54(3), pp. 2033–2044. doi:

10.1016/j.neuroimage.2010.09.025.

Bartha, R. *et al.* (1997) 'Measurement of glutamate and glutamine in the medial prefrontal cortex of never-treated schizophrenic patients and healthy controls by proton magnetic resonance spectroscopy.', *Archives of general psychiatry*, 54(10), pp. 959–65. Available at: http://www.ncbi.nlm.nih.gov/pubmed/9337777 (Accessed: 13 January 2016).

Baskak, B. *et al.* (2012) 'Total exposure duration and proximity of cessation of cannabis use predict severity of sub-clinical psychotic symptoms among former users', *Psychiatry Research*, 198(2), pp. 316–318. doi: 10.1016/j.psychres.2012.01.027.

Beasley, C. L. and Reynolds, G. P. (1997) 'Parvalbumin-immunoreactive neurons are reduced in the prefrontal cortex of schizophrenics.', *Schizophrenia research*, 24(3), pp. 349–55. Available at: http://www.ncbi.nlm.nih.gov/pubmed/9134596 (Accessed: 25 February 2016).

Beaulieu, C. (2009) *The biological basis of diffusion anisotropy*, *Diffusion MRI*. Elsevier Inc. doi: 10.1016/B978-0-12-374709-9.00006-7.

Behrens, M. M. *et al.* (2007) 'Ketamine-induced loss of phenotype of fast-spiking interneurons is mediated by NADPH-oxidase.', *Science (New York, N.Y.)*, 318(5856), pp. 1645–7. doi: 10.1126/science.1148045.

Behrens, M. M., Ali, S. S. and Dugan, L. L. (2008) 'Interleukin-6 mediates the increase in NADPH-oxidase in the ketamine model of schizophrenia.', *The Journal of neuroscience : the official journal of the Society for Neuroscience*, 28(51), pp. 13957–13966. doi: 10.1523/JNEUROSCI.4457-08.2008.

Benarroch, E. E. (2013) 'Microglia: Multiple roles in surveillance, circuit shaping, and response to injury.', *Neurology*, 81(12), pp. 1079–88. doi: 10.1212/WNL.0b013e3182a4a577.

Beumer, W. *et al.* (2012) 'The immune theory of psychiatric diseases: a key role for activated microglia and circulating monocytes.', *Journal of leukocyte biology*, 92(5), pp. 959–75. doi: 10.1189/jlb.0212100.

Le Bihan, D. *et al.* (2001) 'Diffusion tensor imaging: concepts and applications.', *Journal of magnetic resonance imaging : JMRI*, 13(4), pp. 534–46. doi: 10.1002/jmri.1076.

Biswal, B. B. *et al.* (2010) 'Toward discovery science of human brain function.', *Proceedings of the National Academy of Sciences of the United States of America*, 107(10), pp. 4734–9. doi: 10.1073/pnas.0911855107.

Bitanihirwe, B. K. Y. *et al.* (2009) 'Glutamatergic deficits and parvalbumin-containing inhibitory

neurons in the prefrontal cortex in schizophrenia.', *BMC psychiatry*, 9, p. 71. doi: 10.1186/1471-244X-9-71.

Blasi, F. *et al.* (2014) 'Recognition memory impairments after subcortical white matter stroke in mice', *Stroke*, 45(5), pp. 1468–1473. doi: 10.1161/STROKEAHA.114.005324.

Bloemen, O. J. N. *et al.* (2010) 'White-matter markers for psychosis in a prospective ultra-high-risk cohort.', *Psychological medicine*, 40(8), pp. 1297–304. doi: 10.1017/S0033291709991711.

Blot, K., Bai, J. and Otani, S. (2013) 'The effect of non-competitive NMDA receptor antagonist MK-801 on neuronal activity in rodent prefrontal cortex: An animal model for cognitive symptoms of schizophrenia', *Journal of Physiology Paris*. Elsevier Ltd, 107(6), pp. 448–451. doi: 10.1016/j.jphysparis.2013.04.003.

Bokor, G. and Anderson, P. D. (2014) 'Ketamine: an update on its abuse.', *Journal of pharmacy practice*, 27(6), pp. 582–6. doi: 10.1177/0897190014525754.

Bowers, M. S., Chen, B. T. and Bonci, A. (2010) 'AMPA Receptor Synaptic Plasticity Induced by Psychostimulants: The Past, Present, and Therapeutic Future', *Neuron*, 67(1), pp. 11–24. doi: 10.1016/j.neuron.2010.06.004.

Brugger, S. *et al.* (2011) 'Proton Magnetic Resonance Spectroscopy and Illness Stage in Schizophrenia—A Systematic Review and Meta-Analysis', *Biological Psychiatry*. Elsevier Inc., 69(5), pp. 495–503. doi: 10.1016/j.biopsych.2010.10.004.

Byne, W. *et al.* (2006) 'Schizophrenia-associated reduction of neuronal and oligodendrocyte numbers in the anterior principal thalamic nucleus.', *Schizophrenia research*, 85(1–3), pp. 245–53. doi: 10.1016/j.schres.2006.03.029.

Canu, M.-H. *et al.* (2009) 'Activity-dependent regulation of myelin maintenance in the adult rat.', *Brain research*, 1252, pp. 45–51. doi: 10.1016/j.brainres.2008.10.079.

Canuso, C. M. *et al.* (2018) 'Efficacy and Safety of Intranasal Esketamine for the Rapid Reduction of Symptoms of Depression and Suicidality in Patients at Imminent Risk for Suicide: Results of a Double-Blind, Randomized, Placebo-Controlled Study', *American Journal of Psychiatry*, 175(7), pp. 620–630. doi: 10.1176/appi.ajp.2018.17060720.

Carroll, J. B. *et al.* (2011) 'Natural history of disease in the YAC128 mouse reveals a discrete signature of pathology in Huntington disease.', *Neurobiology of disease*, 43(1), pp. 257–65. doi: 10.1016/j.nbd.2011.03.018.

Cheung, V. *et al.* (2008) 'A diffusion tensor imaging study of structural dysconnectivity in

never-medicated, first-episode schizophrenia.', *Psychological medicine*, 38(6), pp. 877–85. doi: 10.1017/S0033291707001808.

Chung, W.-S., Allen, N. J. and Eroglu, C. (2015) 'Astrocytes Control Synapse Formation, Function, and Elimination.', *Cold Spring Harbor perspectives in biology*, 7(9), p. a020370. doi: 10.1101/cshperspect.a020370.

Compton, M. T., Chien, V. H. and Bollini, A. M. (2009) 'Associations between past alcohol, cannabis, and cocaine use and current schizotypy among first-degree relatives of patients with schizophrenia and non-psychiatric controls.', *The Psychiatric quarterly*, 80(3), pp. 143–54. doi: 10.1007/s11126-009-9102-x.

Concha, L. (2014) 'A macroscopic view of microstructure: using diffusion-weighted images to infer damage, repair, and plasticity of white matter.', *Neuroscience*, 276, pp. 14–28. doi: 10.1016/j.neuroscience.2013.09.004.

Cooper, D. *et al.* (2014) 'Multimodal voxel-based meta-analysis of structural and functional magnetic resonance imaging studies in those at elevated genetic risk of developing schizophrenia', *Psychiatry Research: Neuroimaging*. Elsevier, 221(1), pp. 69–77. doi: 10.1016/j.pscychresns.2013.07.008.

Cotel, M.-C. *et al.* (2015) 'Microglial activation in the rat brain following chronic antipsychotic treatment at clinically relevant doses.', *European neuropsychopharmacology : the journal of the European College of Neuropsychopharmacology*, 25(11), pp. 2098–107. doi: 10.1016/j.euroneuro.2015.08.004.

Coyle, C. M. and Laws, K. R. (2015) 'The use of ketamine as an antidepressant: a systematic review and meta-analysis', *Human Psychopharmacology: Clinical and Experimental*, 30(3), pp. 152–163. doi: 10.1002/hup.2475.

Dale, A. M., Fischl, B. and Sereno, M. I. (1999) 'Cortical Surface-Based Analysis', *NeuroImage*, 9(2), pp. 179–194. doi: 10.1006/nimg.1998.0395.

Dale, A. M. and Sereno, M. I. (1993) 'Improved Localizadon of Cortical Activity by Combining EEG and MEG with MRI Cortical Surface Reconstruction: A Linear Approach', *Journal of Cognitive Neuroscience*, 5(2), pp. 162–176. doi: 10.1162/jocn.1993.5.2.162.

Van Dam, N. T., Earleywine, M. and DiGiacomo, G. (2008a) 'Polydrug use, cannabis, and psychosis-like symptoms.', *Human psychopharmacology*, 23(6), pp. 475–85. doi: 10.1002/hup.950.

Van Dam, N. T., Earleywine, M. and DiGiacomo, G. (2008b) 'Polydrug use, cannabis, and

psychosis-like symptoms.', *Human psychopharmacology*, 23(6), pp. 475–85. doi: 10.1002/hup.950.

Danbolt, N. C. (2001) 'Glutamate uptake.', *Progress in neurobiology*, 65(1), pp. 1–105. doi: 10.1016/S0301-0082(00)00067-8.

Daniell, L. C. (1990) 'The noncompetitive N-methyl-D-aspartate antagonists, MK-801, phencyclidine and ketamine, increase the potency of general anesthetics', *Pharmacology Biochemistry and Behavior*, 36, pp. 111–115. doi: 10.1016/0091-3057(90)90134-4.

Davis, K. L. *et al.* (2003) 'White matter changes in schizophrenia: evidence for myelin-related dysfunction.', *Archives of general psychiatry*, 60(5), pp. 443–56. doi: 10.1001/archpsyc.60.5.443.

Dawson, N. *et al.* (2014) 'Subanesthetic Ketamine Treatment Promotes Abnormal Interactions between Neural Subsystems and Alters the Properties of Functional Brain Networks', *Neuropsychopharmacology*, 39(7), pp. 1786–1798. doi: 10.1038/npp.2014.26.

Deakin, J. F. W. *et al.* (2008) 'Glutamate and the neural basis of the subjective effects of ketamine: a pharmaco-magnetic resonance imaging study.', *Archives of general psychiatry*, 65(2), pp. 154–64. doi: 10.1001/archgenpsychiatry.2007.37.

Delgado, P. L. (2000) 'Depression: the case for a monoamine deficiency.', *The Journal of clinical psychiatry*, 61 Suppl 6, pp. 7–11. Available at: http://www.ncbi.nlm.nih.gov/pubmed/10775018 (Accessed: 14 January 2018).

Deoni, S. C. L. *et al.* (2008) 'Gleaning multicomponent T1 and T2 information from steady-state imaging data', *Magnetic Resonance in Medicine*, 60(6), pp. 1372–1387. doi: 10.1002/mrm.21704.

Desikan, R. S. *et al.* (2006) 'An automated labeling system for subdividing the human cerebral cortex on MRI scans into gyral based regions of interest', *NeuroImage*, 31(3), pp. 968–980. doi: 10.1016/j.neuroimage.2006.01.021.

DiazGranados, N. *et al.* (2010) 'Rapid Resolution of Suicidal Ideation After a Single Infusion of an *N* -Methyl- <scp>D</scp> -Aspartate Antagonist in Patients With Treatment-Resistant Major Depressive Disorder', *The Journal of Clinical Psychiatry*, 71(12), pp. 1605–1611. doi: 10.4088/JCP.09m05327blu.

Domingues, A. M. de J., Taylor, M. and Fern, R. (2010) 'Glia as transmitter sources and sensors in health and disease.', *Neurochemistry international*, 57(4), pp. 359–66. doi: 10.1016/j.neuint.2010.03.024.

Domino, E. F. (2010) 'Taming the ketamine tiger. 1965.', *Anesthesiology*, 113(3), pp. 678–684. doi: 10.1097/ALN.0b013e3181ed09a2.

Dorr, a. E. *et al.* (2008) 'High resolution three-dimensional brain atlas using an average magnetic resonance image of 40 adult C57Bl/6J mice', *NeuroImage*, 42, pp. 60–69. doi: 10.1016/j.neuroimage.2008.03.037.

Doyle, O. M. *et al.* (2013a) 'Quantifying the attenuation of the ketamine pharmacological magnetic resonance imaging response in humans: a validation using antipsychotic and glutamatergic agents.', *The Journal of pharmacology and experimental therapeutics*, 345(1), pp. 151–60. doi: 10.1124/jpet.112.201665.

Doyle, O. M. *et al.* (2013b) 'Quantifying the attenuation of the ketamine pharmacological magnetic resonance imaging response in humans: a validation using antipsychotic and glutamatergic agents.', *The Journal of pharmacology and experimental therapeutics*, 345(1), pp. 151–60. doi: 10.1124/jpet.112.201665.

Driesen, N., McCarthy, G. and Bhagwagar, Z. (2013) 'Relationship of resting brain hyperconnectivity and schizophrenia-like symptoms produced by the NMDA receptor antagonist ketamine in humans', *Molecular …*, 18(11), pp. 1–16. doi: 10.1038/mp.2012.194.Relationship.

Driesen, N. R. *et al.* (2013) 'The impact of NMDA receptor blockade on human working memory-related prefrontal function and connectivity.', *Neuropsychopharmacology : official publication of the American College of Neuropsychopharmacology*, 38, pp. 2613–22. doi: 10.1038/npp.2013.170.

Duman, C. H. and Duman, R. S. (2015) 'Spine synapse remodeling in the pathophysiology and treatment of depression', *Neuroscience Letters*, 601, pp. 20–29. doi: 10.1016/j.neulet.2015.01.022.

Duman, R. S. *et al.* (2012) 'Signaling pathways underlying the rapid antidepressant actions of ketamine.', *Neuropharmacology*. Elsevier Ltd, 62(1), pp. 35–41. doi: 10.1016/j.neuropharm.2011.08.044.

Edward Roberts, R. *et al.* (2014) 'Abnormalities in white matter microstructure associated with chronic ketamine use.', *Neuropsychopharmacology : official publication of the American College of Neuropsychopharmacology*. Nature Publishing Group, 39(2), pp. 329–38. doi: 10.1038/npp.2013.195.

Ellegood, J. *et al.* (2014) 'Neuroanatomical phenotypes in a mouse model of the 22q11.2

microdeletion.', *Molecular psychiatry*. NIH Public Access, 19(1), pp. 99–107. doi: 10.1038/mp.2013.112.

Enwright, J. F. *et al.* (2016) 'Reduced Labeling of Parvalbumin Neurons and Perineuronal Nets in the Dorsolateral Prefrontal Cortex of Subjects with Schizophrenia.', *Neuropsychopharmacology : official publication of the American College of Neuropsychopharmacology*. doi: 10.1038/npp.2016.24.

Ernst, T. *et al.* (2000) 'Evidence for long-term neurotoxicity associated with methamphetamine abuse: A 1H MRS study.', *Neurology*, 54(6), pp. 1344–9. Available at: http://www.ncbi.nlm.nih.gov/pubmed/10746608 (Accessed: 13 January 2016).

Eroglu, C. and Barres, B. A. (2010) 'Regulation of synaptic connectivity by glia', *Nature*, 468(7321), pp. 223–231. doi: 10.1038/nature09612.

Van den Eynde, K. *et al.* (2014) 'Hypolocomotive behaviour associated with increased microglia in a prenatal immune activation model with relevance to schizophrenia', *Behavioural Brain Research*, 258, pp. 179–186. doi: 10.1016/j.bbr.2013.10.005.

Eyo, U. B. and Dailey, M. E. (2013) 'Microglia: key elements in neural development, plasticity, and pathology.', *Journal of neuroimmune pharmacology : the official journal of the Society on NeuroImmune Pharmacology*, 8(3), pp. 494–509. doi: 10.1007/s11481-013-9434-z.

Fan, N. *et al.* (2015) 'Relationship of serum levels of TNF-α, IL-6 and IL-18 and schizophrenia-like symptoms in chronic ketamine abusers', *Schizophrenia research*. doi: 10.1016/j.schres.2015.11.006.

Fang, Y. X. *et al.* (2006) 'Recent trends in drug abuse in China', *Acta Pharmacologica Sinica*, 27(2), pp. 140–144. doi: 10.1111/j.1745-7254.2006.00270.x.

Featherstone, R. E. *et al.* (2012) 'Subchronic ketamine treatment leads to permanent changes in EEG, cognition and the astrocytic glutamate transporter EAAT2 in mice.', *Neurobiology of disease*. Elsevier B.V., 47(3), pp. 338–46. doi: 10.1016/j.nbd.2012.05.003.

Featherstone, R. E. *et al.* (2014) 'Juvenile exposure to ketamine causes delayed emergence of EEG abnormalities during adulthood in mice.', *Drug and alcohol dependence*. Elsevier Ireland Ltd, 134, pp. 123–7. doi: 10.1016/j.drugalcdep.2013.09.017.

Feifel, D. (2016) 'Breaking Sad: Unleashing the Breakthrough Potential of Ketamine's Rapid Antidepressant Effects.', *Drug development research*. doi: 10.1002/ddr.21347.

Feighner, J. P. (1999) 'Mechanism of action of antidepressant medications.', *The Journal of*

clinical psychiatry, 60 Suppl 4, pp. 4-11; discussion 12–3. Available at: http://www.ncbi.nlm.nih.gov/pubmed/10086478 (Accessed: 3 April 2018).

Fellin, T. *et al.* (2004) 'Neuronal synchrony mediated by astrocytic glutamate through activation of extrasynaptic NMDA receptors.', *Neuron*, 43(5), pp. 729–43. doi: 10.1016/j.neuron.2004.08.011.

Fields, R. D. (2008) 'White matter in learning, cognition and psychiatric disorders', *Trends in Neurosciences*, 31(June), pp. 361–370. doi: 10.1016/j.tins.2008.04.001.

Finlay, C. J., Duty, S. and Vernon, A. C. (2014) 'Brain morphometry and the neurobiology of levodopa-induced dyskinesias: current knowledge and future potential for translational pre-clinical neuroimaging studies.', *Frontiers in neurology*, 5, p. 95. doi: 10.3389/fneur.2014.00095.

Fischl, B. *et al.* (2002) 'Whole brain segmentation: automated labeling of neuroanatomical structures in the human brain.', *Neuron*, 33(3), pp. 341–55. Available at: http://www.ncbi.nlm.nih.gov/pubmed/11832223 (Accessed: 8 December 2016).

Fischl, B., van der Kouwe, A., *et al.* (2004) 'Automatically parcellating the human cerebral cortex.', *Cerebral cortex (New York, N.Y. : 1991)*, 14(1), pp. 11–22. Available at: http://www.ncbi.nlm.nih.gov/pubmed/14654453 (Accessed: 12 December 2016).

Fischl, B., Salat, D. H., *et al.* (2004) 'Sequence-independent segmentation of magnetic resonance images.', *NeuroImage*, 23 Suppl 1, pp. S69-84. doi: 10.1016/j.neuroimage.2004.07.016.

Fischl, B. *et al.* (no date) 'High-Resolution Intersubject Averaging and a Coordinate System for the Cortical Surface'.

Fischl, B. and Dale, A. M. (2000) 'Measuring the thickness of the human cerebral cortex from magnetic resonance images', *Proceedings of the National Academy of Sciences*, 97(20), pp. 11050–11055. doi: 10.1073/pnas.200033797.

Fischl, B., Liu, A. and Dale, A. M. (2001) 'Automated manifold surgery: constructing geometrically accurate and topologically correct models of the human cerebral cortex', *IEEE Transactions on Medical Imaging*, 20(1), pp. 70–80. doi: 10.1109/42.906426.

Fischl, B., Sereno, M. I. and Dale, A. M. (1999) 'Cortical Surface-Based Analysis', *NeuroImage*, 9(2), pp. 195–207. doi: 10.1006/nimg.1998.0396.

French, L. *et al.* (2015) 'Early Cannabis Use, Polygenic Risk Score for Schizophrenia and Brain Maturation in Adolescence', *JAMA Psychiatry*, 72(10), pp. 1002–1011. doi:

10.1001/jamapsychiatry.2015.1131.

Fridberg, D. J. *et al.* (2011) 'Cannabis users differ from non-users on measures of personality and schizotypy', *Psychiatry Research*, 186(1), pp. 46–52. doi: 10.1016/j.psychres.2010.07.035.

Frohlich, J. and Van Horn, J. D. (2014) 'Reviewing the ketamine model for schizophrenia.', *Journal of psychopharmacology (Oxford, England)*, 28(4), pp. 287–302. doi: 10.1177/0269881113512909.

Fu, Y. *et al.* (2009) 'Glutamate excitotoxicity inflicts paranodal myelin splitting and retraction.', *PloS one*, 4(8), p. e6705. doi: 10.1371/journal.pone.0006705.

Fusar-Poli, P. *et al.* (2012) 'Neuroanatomical Maps of Psychosis Onset: Voxel-wise Meta-Analysis of Antipsychotic-Naive VBM Studies', *Schizophrenia Bulletin*, 38(6), pp. 1297–1307. doi: 10.1093/schbul/sbr134.

Garver, D. L., Holcomb, J. a and Christensen, J. D. (2008) 'Compromised myelin integrity during psychosis with repair during remission in drug-responding schizophrenia.', *The international journal of neuropsychopharmacology / official scientific journal of the Collegium Internationale Neuropsychopharmacologicum (CINP)*, 11(1), pp. 49–61. doi: 10.1017/S1461145707007730.

Gaser, C. and Dahnke, R. (2012) 'CAT - A Computational Anatomy Toolbox for the Analysis of Structural MRI Data', 32(7), p. 7743.

Genovese, C. R., Lazar, N. a and Nichols, T. (2002) 'Thresholding of statistical maps in functional neuroimaging using the false discovery rate.', *NeuroImage*, 15(4), pp. 870–8. doi: 10.1006/nimg.2001.1037.

Giuliani, N. R. *et al.* (2005) 'Voxel-based morphometry versus region of interest: A comparison of two methods for analyzing gray matter differences in schizophrenia', *Schizophrenia Research*, 74(2–3), pp. 135–147. doi: 10.1016/j.schres.2004.08.019.

Glausier, J. R., Fish, K. N. and Lewis, D. A. (2014) 'Altered parvalbumin basket cell inputs in the dorsolateral prefrontal cortex of schizophrenia subjects.', *Molecular psychiatry*, 19(1), pp. 30–6. doi: 10.1038/mp.2013.152.

Glickman, M. E., Rao, S. R. and Schultz, M. R. (2014) 'False discovery rate control is a recommended alternative to Bonferroni-type adjustments in health studies', *Journal of Clinical Epidemiology*, 67(8), pp. 850–857. doi: 10.1016/j.jclinepi.2014.03.012.

Goldstein, R. Z. and Volkow, N. D. (2002) 'Drug addiction and its underlying neurobiological basis: neuroimaging evidnce for the involvement of the frontal cortex', *American Journal of*

Psychiatry, 159(10), pp. 1642–1652. doi: 10.1176/appi.ajp.159.10.1642.

Gonzalez-Burgos, G. and Lewis, D. a (2012) 'NMDA receptor hypofunction, parvalbumin-positive neurons, and cortical gamma oscillations in schizophrenia.', *Schizophrenia bulletin*, 38(5), pp. 950–7. doi: 10.1093/schbul/sbs010.

Good, C. D. *et al.* (2001) 'A voxel-based morphometric study of ageing in 465 normal adult human brains.', *NeuroImage*, 14, pp. 21–36. doi: 10.1006/nimg.2001.0786.

Green, a R. *et al.* (2012) 'Lost in translation: preclinical studies on 3,4-methylenedioxymethamphetamine provide information on mechanisms of action, but do not allow accurate prediction of adverse events in humans.', *British journal of pharmacology*, 166(5), pp. 1523–36. doi: 10.1111/j.1476-5381.2011.01819.x.

Grodin, E. N., Lin, H., Durkee, C. a., *et al.* (2013) 'Deficits in cortical, diencephalic and midbrain gray matter in alcoholism measured by VBM: Effects of co-morbid substance abuse', *NeuroImage: Clinical*. The Authors, 2, pp. 469–476. doi: 10.1016/j.nicl.2013.03.013.

Grodin, E. N., Lin, H., Durkee, C. A., *et al.* (2013) 'Deficits in cortical, diencephalic and midbrain gray matter in alcoholism measured by VBM: Effects of co-morbid substance abuse', *NeuroImage: Clinical*, 2, pp. 469–476. doi: 10.1016/j.nicl.2013.03.013.

Gujar, S. K. *et al.* (2005) 'Magnetic resonance spectroscopy.', *Journal of neuro-ophthalmology : the official journal of the North American Neuro-Ophthalmology Society*, 25(3), pp. 217–26. Available at: http://www.ncbi.nlm.nih.gov/pubmed/16148633 (Accessed: 8 July 2018).

Gundersen, H. J. and Jensen, E. B. (1987) 'The efficiency of systematic sampling in stereology and its prediction.', *Journal of microscopy*, 147(Pt 3), pp. 229–63. Available at: http://www.ncbi.nlm.nih.gov/pubmed/3430576 (Accessed: 13 April 2018).

Gundersen, V., Storm-Mathisen, J. and Bergersen, L. H. (2015) 'Neuroglial Transmission', *Physiological Reviews*, 95(3), pp. 695–726. doi: 10.1152/physrev.00024.2014.

Han, X. *et al.* (2006) 'Reliability of MRI-derived measurements of human cerebral cortical thickness: The effects of field strength, scanner upgrade and manufacturer', *NeuroImage*, 32(1), pp. 180–194. doi: 10.1016/j.neuroimage.2006.02.051.

Han, Y. *et al.* (2016) 'Efficacy of ketamine in the rapid treatment of major depressive disorder: a meta-analysis of randomized, double-blind, placebo-controlled studies.', *Neuropsychiatric disease and treatment*. Dove Press, 12, pp. 2859–2867. doi: 10.2147/NDT.S117146.

Harris, J. and Attwell, D. (2012) 'The energetics of CNS white matter.', 32(1), pp. 356–371. doi:

10.1523/JNEUROSCI.3430-11.2012.

Harrison, D. M. *et al.* (2015) 'Thalamic lesions in multiple sclerosis by 7T MRI: Clinical implications and relationship to cortical pathology.', *Multiple sclerosis (Houndmills, Basingstoke, England)*, 21(9), pp. 1139–50. doi: 10.1177/1352458514558134.

Hartz, S. M. *et al.* (2017) 'Association Between Substance Use Disorder and Polygenic Liability to Schizophrenia.', *Biological psychiatry*, 82(10), pp. 709–715. doi: 10.1016/j.biopsych.2017.04.020.

Haselhorst, R. *et al.* (2002) 'Frontocortical N-acetylaspartate reduction associated with long-term i.v. heroin use.', *Neurology*, 58(2), pp. 305–7. Available at: http://www.ncbi.nlm.nih.gov/pubmed/11805264 (Accessed: 13 January 2016).

Heckers, S. and Konradi, C. (2014) 'GABAergic mechanisms of hippocampal hyperactivity in schizophrenia.', *Schizophrenia research*. Elsevier B.V. doi: 10.1016/j.schres.2014.09.041.

Héja, L. *et al.* (2009) 'Glutamate uptake triggers transporter-mediated GABA release from astrocytes.', *PloS one*, 4(9), p. e7153. doi: 10.1371/journal.pone.0007153.

Héja, L. *et al.* (2012) 'Astrocytes convert network excitation to tonic inhibition of neurons', *BMC Biology*, 10(1), p. 26. doi: 10.1186/1741-7007-10-26.

Hinman, J. R. *et al.* (2013) 'Ketamine disrupts theta synchrony across the septotemporal axis of the CA1 region of hippocampus.', *Journal of neurophysiology*, 109(2), pp. 570–9. doi: 10.1152/jn.00561.2012.

Hiragi, T., Ikegaya, Y. and Koyama, R. (2018) 'Microglia after Seizures and in Epilepsy', *Cells*, 7(4), p. 26. doi: 10.3390/cells7040026.

Hirschfeld, R. M. (2000) 'History and evolution of the monoamine hypothesis of depression.', *The Journal of clinical psychiatry*, 61 Suppl 6, pp. 4–6. Available at: http://www.ncbi.nlm.nih.gov/pubmed/10775017 (Accessed: 14 January 2018).

Hof, P. R. *et al.* (2003) 'Loss and altered spatial distribution of oligodendrocytes in the superior frontal gyrus in schizophrenia', *Biological Psychiatry*, 53(12), pp. 1075–1085. doi: 10.1016/S0006-3223(03)00237-3.

Holmes, H. E. *et al.* (2017) 'Comparison of In Vivo and Ex Vivo MRI for the Detection of Structural Abnormalities in a Mouse Model of Tauopathy', *Frontiers in Neuroinformatics*, 11(March), p. 20. doi: 10.3389/fninf.2017.00020.

Honey, G. D. *et al.* (2008) 'Individual differences in psychotic effects of ketamine are predicted

by brain function measured under placebo.', *The Journal of neuroscience : the official journal of the Society for Neuroscience*, 28(25), pp. 6295–6303. doi: 10.1523/JNEUROSCI.0910-08.2008.

Honey, R. a E. *et al.* (2004) 'Acute ketamine administration alters the brain responses to executive demands in a verbal working memory task: an FMRI study.', *Neuropsychopharmacology : official publication of the American College of Neuropsychopharmacology*, 29(6), pp. 1203–1214. doi: 10.1038/sj.npp.1300438.

Honjin, R., Sakato, S. and Yamashita, T. (1977) 'Electron microscopy of the mouse optic nerve: a quantitative study of the total optic nerve fibers.', *Archivum histologicum Japonicum = Nihon soshikigaku kiroku*, 40(4), pp. 321–32. Available at: http://www.ncbi.nlm.nih.gov/pubmed/597007 (Accessed: 13 January 2016).

Hoogland, I. C. M. *et al.* (2015) 'Systemic inflammation and microglial activation: systematic review of animal experiments', *Journal of Neuroinflammation*, 12(1), p. 114. doi: 10.1186/s12974-015-0332-6.

Hou, Y. *et al.* (2013) 'Neuronal injury, but not microglia activation, is associated with ketamine-induced experimental schizophrenic model in mice.', *Progress in neuro-psychopharmacology & biological psychiatry*. Elsevier Inc., 45, pp. 107–16. doi: 10.1016/j.pnpbp.2013.04.006.

Howells, F. M. *et al.* (2014) '1H-magnetic resonance spectroscopy (1H-MRS) in methamphetamine dependence and methamphetamine induced psychosis', *Schizophrenia Research*. Elsevier B.V., 153(1–3), pp. 122–128. doi: 10.1016/j.schres.2014.01.029.

Howes, O., McCutcheon, R. and Stone, J. (2015) 'Glutamate and dopamine in schizophrenia: An update for the 21st century', *J Psychopharmacol*, 29(2), pp. 97–115. doi: 10.1177/0269881114563634.

Huang, Y. H. and Bergles, D. E. (2004) 'Glutamate transporters bring competition to the synapse.', *Current opinion in neurobiology*, 14(3), pp. 346–52. doi: 10.1016/j.conb.2004.05.007.

van Huijstee, A. N. and Mansvelder, H. D. (2015) 'Glutamatergic synaptic plasticity in the mesocorticolimbic system in addiction', *Frontiers in Cellular Neuroscience*, 8, p. 466. doi: 10.3389/fncel.2014.00466.

Ionescu, D. F., Rosenbaum, J. F. and Alpert, J. E. (2015) 'Pharmacological approaches to the challenge of treatment-resistant depression.', *Dialogues in clinical neuroscience*. Les Laboratoires Servier, 17(2), pp. 111–26. Available at: http://www.ncbi.nlm.nih.gov/pubmed/26246787 (Accessed: 3 April 2018).

Jagannathan, N. R., Desai, N. G. and Raghunathan, P. (1996) 'Brain metabolite changes in alcoholism: An in vivo proton magnetic resonance spectroscopy (MRS) study', *Magnetic Resonance Imaging*, 14(5), pp. 553–557. doi: 10.1016/0730-725X(96)00048-3.

Jenkinson, M. *et al.* (2012) 'FSL', *NeuroImage*, 62(2), pp. 782–790. doi: 10.1016/j.neuroimage.2011.09.015.

Jo, S. *et al.* (2014) 'GABA from reactive astrocytes impairs memory in mouse models of Alzheimer's disease.', *Nature medicine*. Nature Publishing Group, 20(8), pp. 886–96. doi: 10.1038/nm.3639.

Joe-Laidler, K. and Hunt, G. (2008) 'Sit down to float', *Addiction Research & Theory*, 16(3), pp. 259–271. doi: 10.1080/16066350801983673.Sit.

Johansen-Berg, H. (2007) 'Structural plasticity: rewiring the brain.', *Current biology : CB*, 17(4), pp. R141-4. doi: 10.1016/j.cub.2006.12.022.

Jones, D. K., Knösche, T. R. and Turner, R. (2013) 'White matter integrity, fiber count, and other fallacies: the do's and don'ts of diffusion MRI.', *NeuroImage*, 73, pp. 239–54. doi: 10.1016/j.neuroimage.2012.06.081.

Jovicich, J. *et al.* (2006) 'Reliability in multi-site structural MRI studies: Effects of gradient non-linearity correction on phantom and human data', *NeuroImage*, 30(2), pp. 436–443. doi: 10.1016/j.neuroimage.2005.09.046.

Káradóttir, R. *et al.* (2005) 'NMDA receptors are expressed in oligodendrocytes and activated in ischaemia.', *Nature*, 438(7071), pp. 1162–6. doi: 10.1038/nature04302.

Keilhoff, G. *et al.* (2004) 'Repeated application of ketamine to rats induces changes in the hippocampal expression of parvalbumin, neuronal nitric oxide synthase and cFOS similar to those found in human schizophrenia.', *Neuroscience*, 126(3), pp. 591–8. doi: 10.1016/j.neuroscience.2004.03.039.

Kennerley, S. W. *et al.* (2006) 'Optimal decision making and the anterior cingulate cortex', *Nature Neuroscience*, 9(7), pp. 940–947. doi: 10.1038/nn1724.

Kennerley, S. W. and Wallis, J. D. (2009) 'Encoding of reward and space during a working memory task in the orbitofrontal cortex and anterior cingulate sulcus.', *Journal of neurophysiology*, 102, pp. 3352–3364. doi: 10.1152/jn.00273.2009.

Khakh, B. S. and Sofroniew, M. V (2015) 'Diversity of astrocyte functions and phenotypes in neural circuits', *Nature Neuroscience*, 18(7), pp. 942–952. doi: 10.1038/nn.4043.

Kim, J. H., Renden, R. and von Gersdorff, H. (2013) 'Dysmyelination of auditory afferent axons increases the jitter of action potential timing during high-frequency firing.', *The Journal of neuroscience : the official journal of the Society for Neuroscience*, 33(22), pp. 9402–7. doi: 10.1523/JNEUROSCI.3389-12.2013.

Kim, S.-Y. *et al.* (2011a) 'In vivo and ex vivo evidence for ketamine-induced hyperglutamatergic activity in the cerebral cortex of the rat: Potential relevance to schizophrenia.', *NMR in biomedicine*, 24(10), pp. 1235–42. doi: 10.1002/nbm.1681.

Kim, S.-Y. *et al.* (2011b) 'In vivo and ex vivo evidence for ketamine-induced hyperglutamatergic activity in the cerebral cortex of the rat: Potential relevance to schizophrenia.', *NMR in biomedicine*, 24(10), pp. 1235–42. doi: 10.1002/nbm.1681.

Kim, Y. B. *et al.* (2012) 'Connectivity of thalamo-cortical pathway in rat brain: combined diffusion spectrum imaging and functional MRI at 11.7 T.', *NMR in biomedicine*, 25(7), pp. 943–52. doi: 10.1002/nbm.1815.

Kirby, T. (2015) 'Ketamine for depression: the highs and lows', *The Lancet Psychiatry*. Elsevier, 2(9), pp. 783–784. doi: 10.1016/S2215-0366(15)00392-2.

Kittelberger, K. *et al.* (2012) 'Comparison of the effects of acute and chronic administration of ketamine on hippocampal oscillations: relevance for the NMDA receptor hypofunction model of schizophrenia.', *Brain structure & function*, 217(2), pp. 395–409. doi: 10.1007/s00429-011-0351-8.

Kraus, C. *et al.* (2017) 'Administration of ketamine for unipolar and bipolar depression', *International Journal of Psychiatry in Clinical Practice*, pp. 1–12. doi: 10.1080/13651501.2016.1254802.

Kraus, M. F. *et al.* (2007) 'White matter integrity and cognition in chronic traumatic brain injury: a diffusion tensor imaging study.', *Brain : a journal of neurology*, 130(Pt 10), pp. 2508–19. doi: 10.1093/brain/awm216.

Krystal, J. H. *et al.* (1994) 'Subanesthetic effects of the noncompetitive NMDA antagonist, ketamine, in humans. Psychotomimetic, perceptual, cognitive, and neuroendocrine responses.', *Archives of general psychiatry*, 51(3), pp. 199–214. Available at: http://www.ncbi.nlm.nih.gov/pubmed/8122957 (Accessed: 12 January 2016).

Krystal, J. H. *et al.* (2005) 'Preliminary evidence of attenuation of the disruptive effects of the NMDA glutamate receptor antagonist, ketamine, on working memory by pretreatment with the group II metabotropic glutamate receptor agonist, LY354740, in healthy human subjects',

Psychopharmacology, 179, pp. 303–309. doi: 10.1007/s00213-004-1982-8.

Kumra, S. *et al.* (2012) 'Parietal Lobe Volume Deficits in Adolescents With Schizophrenia and Adolescents With Cannabis Use Disorders', *Journal of the American Academy of Child & Adolescent Psychiatry*, 51(2), pp. 171–180. doi: 10.1016/j.jaac.2011.11.001.

Lahti, a C. *et al.* (2001) 'Effects of ketamine in normal and schizophrenic volunteers.', *Neuropsychopharmacology : official publication of the American College of Neuropsychopharmacology*, 25(4), pp. 455–67. doi: 10.1016/S0893-133X(01)00243-3.

Lahti, A. C., Holcomb, H. H., *et al.* (1995) 'Ketamine activates psychosis and alters limbic blood flow in schizophrenia.', *Neuroreport*, 6(6), pp. 869–72. Available at: http://www.ncbi.nlm.nih.gov/pubmed/7612873 (Accessed: 20 February 2016).

Lahti, A. C., Koffel, B., *et al.* (1995) 'Subanesthetic doses of ketamine stimulate psychosis in schizophrenia.', *Neuropsychopharmacology : official publication of the American College of Neuropsychopharmacology*, 13(1), pp. 9–19. doi: 10.1016/0893-133X(94)00131-I.

Lahti, A. C. *et al.* (1999) 'NMDA-sensitive glutamate antagonism: A human model for psychosis', *Neuropsychopharmacology*, 21(6 SUPPL. 2). doi: 10.1016/S0893-133X(99)00132-3.

Lambert, O. and Bourin, M. (2002) 'SNRIs: mechanism of action and clinical features', *Expert Review of Neurotherapeutics*, 2(6), pp. 849–858. doi: 10.1586/14737175.2.6.849.

Lang, E. J. and Rosenbluth, J. (2003) 'Role of myelination in the development of a uniform olivocerebellar conduction time.', *Journal of neurophysiology*, 89, pp. 2259–2270. doi: 10.1152/jn.00922.2002.

Lapidus, K. A. B. *et al.* (2014) 'A Randomized Controlled Trial of Intranasal Ketamine in Major Depressive Disorder', *Biological Psychiatry*. Elsevier, 76(12), pp. 970–976. doi: 10.1016/j.biopsych.2014.03.026.

Laskaris, L. E. *et al.* (2015) 'Microglial activation and progressive brain changes in schizophrenia', *British Journal of Pharmacology*. doi: 10.1111/bph.13364.

Lerch, J. P., Carroll, J. B., Spring, S., *et al.* (2008) 'Automated deformation analysis in the YAC128 Huntington disease mouse model.', *NeuroImage*, 39(1), pp. 32–9. doi: 10.1016/j.neuroimage.2007.08.033.

Lerch, J. P., Carroll, J. B., Dorr, A., *et al.* (2008) 'Cortical thickness measured from MRI in the YAC128 mouse model of Huntington's disease.', *NeuroImage*, 41(2), pp. 243–51. doi: 10.1016/j.neuroimage.2008.02.019.

Lerch, J. P. *et al.* (2011) 'Maze training in mice induces MRI-detectable brain shape changes specific to the type of learning', *NeuroImage*. Elsevier Inc., 54(3), pp. 2086–2095. doi: 10.1016/j.neuroimage.2010.09.086.

Lerch, J. P. *et al.* (2012) 'Wanted dead or alive? The tradeoff between in-vivo versus ex-vivo MR brain imaging in the mouse', *Frontiers in Neuroinformatics*, 6(March), pp. 1–9. doi: 10.3389/fninf.2012.00006.

Leung, K.-S. *et al.* (2008) 'Dinosaur girls, candy girls, and Trinity: voices of Taiwanese club drug users.', *Journal of ethnicity in substance abuse*, 7(3), pp. 237–57. doi: 10.1080/15332640802313205.

Lewis, D. A. *et al.* (2012) 'Cortical parvalbumin interneurons and cognitive dysfunction in schizophrenia.', *Trends in neurosciences*, 35(1), pp. 57–67. doi: 10.1016/j.tins.2011.10.004.

Li, N. *et al.* (2010) 'mTOR-dependent synapse formation underlies the rapid antidepressant effects of NMDA antagonists.', *Science (New York, N.Y.)*, 329(5994), pp. 959–64. doi: 10.1126/science.1190287.

Li, Q. *et al.* (2017) 'Chronic Ketamine Exposure Causes White Matter Microstructural Abnormalities in Adolescent Cynomolgus Monkeys', *Frontiers in Neuroscience*, 11(May), pp. 1–9. doi: 10.3389/fnins.2017.00285.

Li, Y. *et al.* (2015) 'Reduced frontal cortical thickness and increased caudate volume within fronto-striatal circuits in young adult smokers.', *Drug and alcohol dependence*. Elsevier Ireland Ltd, 151, pp. 211–219. doi: 10.1016/j.drugalcdep.2015.03.023.

Liao, Y. *et al.* (2010) 'Frontal white matter abnormalities following chronic ketamine use: a diffusion tensor imaging study.', *Brain : a journal of neurology*, 133(Pt 7), pp. 2115–22. doi: 10.1093/brain/awq131.

Liao, Y. *et al.* (2011) 'Reduced dorsal prefrontal gray matter after chronic ketamine use.', *Biological psychiatry*. Elsevier Inc., 69(1), pp. 42–8. doi: 10.1016/j.biopsych.2010.08.030.

Liao, Y. *et al.* (2012) 'Alterations in regional homogeneity of resting-state brain activity in ketamine addicts', *Neuroscience Letters*. Elsevier Ireland Ltd, 522(1), pp. 36–40. doi: 10.1016/j.neulet.2012.06.009.

Lieberman, J. A. *et al.* (2018) 'Hippocampal dysfunction in the pathophysiology of schizophrenia: a selective review and hypothesis for early detection and intervention', *Molecular Psychiatry*. doi: 10.1038/mp.2017.249.

Lim, A. L., Taylor, D. A. and Malone, D. T. (2012) 'Consequences of early life MK-801 administration: Long-term behavioural effects and relevance to schizophrenia research', *Behavioural Brain Research*. Elsevier B.V., 227(1), pp. 276–286. doi: 10.1016/j.bbr.2011.10.052.

Lim, K. O. *et al.* (2008) 'Brain macrostructural and microstructural abnormalities in cocaine dependence', *Drug and Alcohol Dependence*, 92(1–3), pp. 164–172. doi: 10.1016/j.drugalcdep.2007.07.019.

Lin, J. H. and Lu, A. Y. (1997) 'Role of pharmacokinetics and metabolism in drug discovery and development.', *Pharmacological reviews*, 49(4), pp. 403–49. Available at: http://www.ncbi.nlm.nih.gov/pubmed/9443165 (Accessed: 24 February 2016).

Lindahl, J. S. *et al.* (2008) 'In utero PCP exposure alters oligodendrocyte differentiation and myelination in developing rat frontal cortex.', *Brain research*, 1234, pp. 137–47. doi: 10.1016/j.brainres.2008.06.126.

Liu, H. *et al.* (2008) 'Disrupted white matter integrity in heroin dependence: a controlled study utilizing diffusion tensor imaging.', *The American journal of drug and alcohol abuse*, 34(January 2016), pp. 562–575. doi: 10.1080/00952990802295238.

Liu, H. *et al.* (2009) 'Frontal and cingulate gray matter volume reduction in heroin dependence: Optimized voxel-based morphometry: Regular article', *Psychiatry and Clinical Neurosciences*, 63, pp. 563–568. doi: 10.1111/j.1440-1819.2009.01989.x.

Liu, J. *et al.* (2012) 'Impaired adult myelination in the prefrontal cortex of socially isolated mice.', *Nature neuroscience*, 15(12), pp. 1621–3. doi: 10.1038/nn.3263.

Long, M. A. and Lee, A. K. (2012) 'Intracellular recording in behaving animals.', *Current opinion in neurobiology*. NIH Public Access, 22(1), pp. 34–44. doi: 10.1016/j.conb.2011.10.013.

Lu, J.-Y. *et al.* (2015) 'Intrathecal enzyme replacement therapy improves motor function and survival in a preclinical mouse model of infantile neuronal ceroid lipofuscinosis', *Molecular Genetics and Metabolism*, 116(1–2), pp. 98–105. doi: 10.1016/j.ymgme.2015.05.005.

Lua, A. C. *et al.* (2003) 'Profiles of urine samples from participants at rave party in Taiwan: prevalence of ketamine and MDMA abuse', *Forensic Science International*, 136(1–3), pp. 47–51. doi: 10.1016/S0379-0738(03)00261-5.

De Luca, M. T. *et al.* (2012) 'The role of setting for ketamine abuse: Clinical and preclinical evidence', *Reviews in the Neurosciences*, 23(5–6), pp. 769–780. doi: 10.1515/revneuro-2012-0078.

Lüscher, C. and Malenka, R. C. (2011) 'Drug-evoked synaptic plasticity in addiction: from molecular changes to circuit remodeling.', *Neuron*. NIH Public Access, 69(4), pp. 650–63. doi: 10.1016/j.neuron.2011.01.017.

Ma, J., Tai, S. K. and Leung, L. S. (2012) 'Septohippocampal GABAergic neurons mediate the altered behaviors induced by n-methyl-D-aspartate receptor antagonists.', *Hippocampus*, 22(12), pp. 2208–18. doi: 10.1002/hipo.22039.

Makinodan, M. *et al.* (2009) 'Demyelination in the juvenile period, but not in adulthood, leads to long-lasting cognitive impairment and deficient social interaction in mice.', *Progress in neuro-psychopharmacology & biological psychiatry*, 33(6), pp. 978–85. doi: 10.1016/j.pnpbp.2009.05.006.

Makinodan, M. *et al.* (2012) 'A Critical Period for Social Experience-Dependent Oligodendrocyte Maturation and Myelination', *Science*, 337(6100), pp. 1357–1360. doi: 10.1126/science.1220845.

Malhotra, A. K. *et al.* (1996) 'NMDA receptor function and human cognition: the effects of ketamine in healthy volunteers.', *Neuropsychopharmacology : official publication of the American College of Neuropsychopharmacology*, 14(5), pp. 301–7. doi: 10.1016/0893-133X(95)00137-3.

Malone, I. B. *et al.* (2015) 'Accurate automatic estimation of total intracranial volume: A nuisance variable with less nuisance', *NeuroImage*, 104, pp. 366–372. doi: 10.1016/j.neuroimage.2014.09.034.

Manjón, J. V. *et al.* (2010) 'Adaptive non-local means denoising of MR images with spatially varying noise levels', *Journal of Magnetic Resonance Imaging*, 31(1), pp. 192–203. doi: 10.1002/jmri.22003.

Mariachiara, B. and Bramanti, P. (2014) 'Pharmacogenomics Exploring effects of EAAT polymorphisms', 5, pp. 925–932.

Markham, J. A. *et al.* (2009) 'Myelination of the corpus callosum in male and female rats following complex environment housing during adulthood', *Brain Research*. Elsevier B.V., 1288, pp. 9–17. doi: 10.1016/j.brainres.2009.06.087.

Marsman, A. *et al.* (2013) 'Glutamate in Schizophrenia: A Focused Review and Meta-Analysis of 1H-MRS Studies', *Schizophrenia Bulletin*, 39(1), pp. 120–129. doi: 10.1093/schbul/sbr069.

Matute, C. (2006) 'Oligodendrocyte NMDA receptors: a novel therapeutic target', *Trends in molecular medicine*, 12(7), pp. 289–292. doi: 10.1016/j.molmed.2006.05.003.

Mcdonald, J., Althomsons, S. and Hyrc, K. (1998) 'Oligodendrocytes from forebrain are highly vulnerable to AMPA/kainate receptor-mediated excitotoxicity', *Nature medicine*. Available at: http://www.nature.com/nm/journal/v4/n3/abs/nm0398-291.html (Accessed: 15 October 2014).

McDonald, J. W., Levine, J. M. and Qu, Y. (1998) 'Multiple classes of the oligodendrocyte lineage are highly vulnerable to excitotoxicity', *NeuroReport*, 9(12), pp. 2757–2762. doi: 10.1097/00001756-199808240-00014.

McIntyre, R. S. *et al.* (2014) 'Treatment-resistant depression: Definitions, review of the evidence, and algorithmic approach', *Journal of Affective Disorders*, 156, pp. 1–7. doi: 10.1016/j.jad.2013.10.043.

McKenna, M. C. (2007) 'The glutamate-glutamine cycle is not stoichiometric: fates of glutamate in brain.', *Journal of neuroscience research*, 85(15), pp. 3347–58. doi: 10.1002/jnr.21444.

Mighdoll, M. I. *et al.* (2014) 'Myelin, myelin-related disorders, and psychosis', *Schizophrenia Research*. Elsevier B.V. doi: 10.1016/j.schres.2014.09.040.

Moghaddam, B. *et al.* (1997) 'Activation of glutamatergic neurotransmission by ketamine: a novel step in the pathway from NMDA receptor blockade to dopaminergic and cognitive disruptions associated with the prefrontal cortex.', *The Journal of neuroscience : the official journal of the Society for Neuroscience*, 17(8), pp. 2921–2927.

Morgan, C. J. A. *et al.* (2014) 'Long-term heavy ketamine use is associated with spatial memory impairment and altered hippocampal activation', 5(December), pp. 1–11. doi: 10.3389/fpsyt.2014.00149.

Morgan, C. J. a, Mofeez, A., *et al.* (2004) 'Acute effects of ketamine on memory systems and psychotic symptoms in healthy volunteers.', *Neuropsychopharmacology : official publication of the American College of Neuropsychopharmacology*, 29(1), pp. 208–18. doi: 10.1038/sj.npp.1300342.

Morgan, C. J. a, Riccelli, M., *et al.* (2004) 'Long-term effects of ketamine: evidence for a persisting impairment of source memory in recreational users.', *Drug and alcohol dependence*, 75(3), pp. 301–8. doi: 10.1016/j.drugalcdep.2004.03.006.

Morgan, C. J. a and Curran, H. V. (2006) 'Acute and chronic effects of ketamine upon human memory: a review.', *Psychopharmacology*, 188(4), pp. 408–24. doi: 10.1007/s00213-006-0572-3.

Morgan, C. J. a, Muetzelfeldt, L. and Curran, H. V. (2010) 'Consequences of chronic ketamine self-administration upon neurocognitive function and psychological wellbeing: a 1-year longitudinal study.', *Addiction (Abingdon, England)*, 105(1), pp. 121–33. doi: 10.1111/j.1360-0443.2009.02761.x.

Mori, S. and Zhang, J. (2006) 'Principles of diffusion tensor imaging and its applications to basic neuroscience research.', *Neuron*, 51(5), pp. 527–39. doi: 10.1016/j.neuron.2006.08.012.

Morris, B. J., Cochran, S. M. and Pratt, J. a (2005) 'PCP: from pharmacology to modelling schizophrenia.', *Current opinion in pharmacology*, 5(1), pp. 101–6. doi: 10.1016/j.coph.2004.08.008.

Muetzelfeldt, L. *et al.* (2008) 'Journey through the K-hole: Phenomenological aspects of ketamine use', *Drug and Alcohol Dependence*, 95, pp. 219–229. doi: 10.1016/j.drugalcdep.2008.01.024.

Müller, N. *et al.* (2015) 'The role of inflammation in schizophrenia', *Frontiers in Neuroscience*, 9(OCT). doi: 10.3389/fnins.2015.00372.

Muñoz Maniega, S. *et al.* (2008) 'A diffusion tensor MRI study of white matter integrity in subjects at high genetic risk of schizophrenia', *Schizophrenia Research*. Elsevier B.V., 106(2–3), pp. 132–139. doi: 10.1016/j.schres.2008.09.016.

Murrough, J. W. *et al.* (2013) 'Rapid and longer-term antidepressant effects of repeated ketamine infusions in treatment-resistant major depression.', *Biological psychiatry*, 74(4), pp. 250–6. doi: 10.1016/j.biopsych.2012.06.022.

Nave, K.-A. (2010) 'Myelination and support of axonal integrity by glia.', *Nature*, 468(7321), pp. 244–252. doi: 10.1038/nature09614.

Nickel, M. and Gu, C. (2018) 'Regulation of Central Nervous System Myelination in Higher Brain Functions', *Neural Plasticity*, 2018, pp. 1–12. doi: 10.1155/2018/6436453.

Van den Oever, M. C., Spijker, S. and Smit, A. B. (2012) 'The Synaptic Pathology of Drug Addiction', in *Advances in experimental medicine and biology*, pp. 469–491. doi: 10.1007/978-3-7091-0932-8_21.

Olney, J. W., Labruyere, J. and Price, M. T. (1989) 'Pathological changes induced in cerebrocortical neurons by phencyclidine and related drugs', *Science*, 244(4910), pp. 1360–1362. doi: 10.1126/science.2660263.

Pagliaccio, D. *et al.* (2015) 'Shared Predisposition in the Association Between Cannabis Use and

Subcortical Brain Structure', *JAMA Psychiatry*, 63130(10), pp. 1–8. doi: 10.1001/jamapsychiatry.2015.1054.

Pajevic, S., Basser, P. J. and Fields, R. D. (2014) 'Role of myelin plasticity in oscillations and synchrony of neuronal activity', *Neuroscience*. IBRO, 276, pp. 135–147. doi: 10.1016/j.neuroscience.2013.11.007.

Papaseit, E. *et al.* (2014) 'Emerging drugs in Europe', *Current Opinion in Psychiatry*, 27(4), pp. 243–250. doi: 10.1097/YCO.0000000000000071.

Parks, M. H. *et al.* (2002) 'Longitudinal brain metabolic characterization of chronic alcoholics with proton magnetic resonance spectroscopy.', *Alcoholism, clinical and experimental research*, 26(9), pp. 1368–1380. doi: 10.1097/01.ALC.0000029598.07833.2D.

Parlapani, E. *et al.* (2009) 'Association between myelin basic protein expression and left entorhinal cortex pre-alpha cell layer disorganization in schizophrenia.', *Brain research*. Elsevier B.V., 1301, pp. 126–34. doi: 10.1016/j.brainres.2009.09.007.

Pascual, O. *et al.* (2012) 'PNAS Plus: Microglia activation triggers astrocyte-mediated modulation of excitatory neurotransmission', *Proceedings of the National Academy of Sciences*, 109(4), pp. E197–E205. doi: 10.1073/pnas.1111098109.

Pedrini, M. *et al.* (2012) 'Similarities in serum oxidative stress markers and inflammatory cytokines in patients with overt schizophrenia at early and late stages of chronicity.', *Journal of psychiatric research*, 46(6), pp. 819–24. doi: 10.1016/j.jpsychires.2012.03.019.

Pekny, M., Wilhelmsson, U. and Pekna, M. (2014) 'The dual role of astrocyte activation and reactive gliosis', *Neuroscience Letters*, 565, pp. 30–38. doi: 10.1016/j.neulet.2013.12.071.

Peng, P. *et al.* (2018) 'Brain Structure Alterations in Respect to Tobacco Consumption and Nicotine Dependence: A Comparative Voxel-Based Morphometry Study', *Frontiers in Neuroanatomy*, 12, p. 43. doi: 10.3389/fnana.2018.00043.

Pennington, D. L. *et al.* (2015) 'Alcohol Use Disorder with and without Stimulant Use: Brain Morphometry and Its Associations with Cigarette Smoking, Cognition, and Inhibitory Control', *PLOS ONE*. Edited by H. de Wit, 10(3), p. e0122505. doi: 10.1371/journal.pone.0122505.

Peters, B. D. *et al.* (2013) 'Polyunsaturated fatty acid concentration predicts myelin integrity in early-phase psychosis', *Schizophrenia Bulletin*, 39(4), pp. 830–838. doi: 10.1093/schbul/sbs089.

Pfefferbaum, A. *et al.* (2009) 'Degradation of Association and Projection White Matter Systems in Alcoholism Detected with Quantitative Fiber Tracking', *Biological Psychiatry*. Society of

Biological Psychiatry, 65(8), pp. 680–690. doi: 10.1016/j.biopsych.2008.10.039.

Pomarol-Clotet, E. *et al.* (2006) 'Psychological effects of ketamine in healthy volunteers. Phenomenological study.', *The British journal of psychiatry : the journal of mental science*, 189, pp. 173–179. doi: 10.1192/bjp.bp.105.015263.

Pomarol-Clotet, E. *et al.* (2010) 'Medial prefrontal cortex pathology in schizophrenia as revealed by convergent findings from multimodal imaging.', *Molecular psychiatry*, 15(8), pp. 823–830. doi: 10.1038/mp.2009.146.

Portmann, T. *et al.* (2014) 'Behavioral abnormalities and circuit defects in the basal ganglia of a mouse model of 16p11.2 deletion syndrome.', *Cell reports*. NIH Public Access, 7(4), pp. 1077–1092. doi: 10.1016/j.celrep.2014.03.036.

Potvin, S. *et al.* (2008) 'Inflammatory Cytokine Alterations in Schizophrenia: A Systematic Quantitative Review', *Biological Psychiatry*, 63(8), pp. 801–808. doi: 10.1016/j.biopsych.2007.09.024.

Price, R. B. *et al.* (2014) 'EFFECTS OF KETAMINE ON EXPLICIT AND IMPLICIT SUICIDAL COGNITION: A RANDOMIZED CONTROLLED TRIAL IN TREATMENT-RESISTANT DEPRESSION', *Depression and Anxiety*, 31(4), pp. 335–343. doi: 10.1002/da.22253.

Quirk, M. C. *et al.* (2009) 'A defined network of fast-spiking interneurons in orbitofrontal cortex: responses to behavioral contingencies and ketamine administration.', *Frontiers in systems neuroscience*, 3(November), p. 13. doi: 10.3389/neuro.06.013.2009.

Raine, A. (1991) 'The SPQ: a scale for the assessment of schizotypal personality based on DSM-III-R criteria.', *Schizophrenia bulletin*, 17(4), pp. 555–564. doi: 10.1093/schbul/17.4.555.

Ram&#xFFFD;rez-Amaya, V. *et al.* (1999) 'Synaptogenesis of mossy fibers induced by spatial water maze overtraining', *Hippocampus*, 9(6), pp. 631–636. doi: 10.1002/(SICI)1098-1063(1999)9:6<631::AID-HIPO3>3.0.CO;2-3.

Reagan-Shaw, S., Nihal, M. and Ahmad, N. (2008) 'Dose translation from animal to human studies revisited.', *The FASEB journal : official publication of the Federation of American Societies for Experimental Biology*, 22(3), pp. 659–661. doi: 10.1096/fj.07-9574LSF.

Regenold, W. T. *et al.* (2007) 'Myelin staining of deep white matter in the dorsolateral prefrontal cortex in schizophrenia, bipolar disorder, and unipolar major depression.', *Psychiatry research*, 151(3), pp. 179–88. doi: 10.1016/j.psychres.2006.12.019.

Reis Marques, T. *et al.* (2014) 'White matter integrity as a predictor of response to treatment

in first episode psychosis.', *Brain : a journal of neurology*, 137(Pt 1), pp. 172–82. doi: 10.1093/brain/awt310.

Reuter, M., Rosas, H. D. and Fischl, B. (2010) 'Highly accurate inverse consistent registration: A robust approach', *NeuroImage*, 53(4), pp. 1181–1196. doi: 10.1016/j.neuroimage.2010.07.020.

Reynaud-Maurupt, C. *et al.* (2007) 'Characteristics and Behaviors of Ketamine Users in France in 2003', *Journal of Psychoactive Drugs*, 39(1), pp. 1–11. doi: 10.1080/02791072.2007.10399859.

Richetto, J. *et al.* (2016) 'Genome-Wide Transcriptional Profiling and Structural Magnetic Resonance Imaging in the Maternal Immune Activation Model of Neurodevelopmental Disorders', *Cerebral Cortex*, pp. 1–17. doi: 10.1093/cercor/bhw320.

Rowland, L. M. *et al.* (2005) 'Effects of ketamine on anterior cingulate glutamate metabolism in healthy humans: a 4-T proton MRS study.', *The American journal of psychiatry*, 162(2), pp. 394–6. doi: 10.1176/appi.ajp.162.2.394.

Sagi, Y. *et al.* (2012) 'Learning in the Fast Lane: New Insights into Neuroplasticity', *Neuron*, 73(6), pp. 1195–1203. doi: 10.1016/j.neuron.2012.01.025.

Salami, M. *et al.* (2003) 'Change of conduction velocity by regional myelination yields constant latency irrespective of distance between thalamus and cortex.', *Proceedings of the National Academy of Sciences of the United States of America*, 100, pp. 6174–6179. doi: 10.1073/pnas.0937380100.

Sanacora, G. *et al.* (2017) 'A Consensus Statement on the Use of Ketamine in the Treatment of Mood Disorders', *JAMA Psychiatry*, 74(4), p. 399. doi: 10.1001/jamapsychiatry.2017.0080.

Sassano-Higgins, S. *et al.* (2016) 'a Review of Ketamine Abuse and Diversion', *Depression and Anxiety*, 33(8), pp. 718–727. doi: 10.1002/da.22536.

Schacter, D. L., Guerin, S. A. and St Jacques, P. L. (2011) 'Memory distortion: an adaptive perspective.', *Trends in cognitive sciences*. NIH Public Access, 15(10), pp. 467–74. doi: 10.1016/j.tics.2011.08.004.

Schak, K. M. *et al.* (2016) 'Potential Risks of Poorly Monitored Ketamine Use in Depression Treatment.', *The American journal of psychiatry*, 173(3), pp. 215–8. doi: 10.1176/appi.ajp.2015.15081082.

Schmitt, S., Cantuti Castelvetri, L. and Simons, M. (2014) 'Metabolism and functions of lipids in myelin', *Biochimica et Biophysica Acta (BBA) - Molecular and Cell Biology of Lipids*. Elsevier B.V.

doi: 10.1016/j.bbalip.2014.12.016.

Schmitz, C. and Hof, P. R. (2005) 'Design-based stereology in neuroscience', *Neuroscience*, 130(4), pp. 813–831. doi: 10.1016/j.neuroscience.2004.08.050.

Schnieder, T. P. and Dwork, A. J. (2011) 'Searching for neuropathology: gliosis in schizophrenia.', *Biological psychiatry*, 69(2), pp. 134–9. doi: 10.1016/j.biopsych.2010.08.027.

Schobel, S., Chaudhury, N. and Khan, U. (2013) 'Imaging patients with psychosis and a mouse model establishes a spreading pattern of hippocampal dysfunction and implicates glutamate as a driver', *Neuron*, 78(1), pp. 81–93. doi: 10.1016/j.neuron.2013.02.011.Imaging.

Segal, D. *et al.* (2007) 'Oligodendrocyte pathophysiology: a new view of schizophrenia.', *The international journal of neuropsychopharmacology / official scientific journal of the Collegium Internationale Neuropsychopharmacologicum (CINP)*, 10(4), pp. 503–11. doi: 10.1017/S146114570600722X.

Ségonne, F. *et al.* (2004) 'A hybrid approach to the skull stripping problem in MRI', *NeuroImage*, 22(3), pp. 1060–1075. doi: 10.1016/j.neuroimage.2004.03.032.

Segonne, F., Pacheco, J. and Fischl, B. (2007) 'Geometrically Accurate Topology-Correction of Cortical Surfaces Using Nonseparating Loops', *IEEE Transactions on Medical Imaging*, 26(4), pp. 518–529. doi: 10.1109/TMI.2006.887364.

Serafini, G. *et al.* (2014) 'The role of ketamine in treatment-resistant depression: a systematic review.', *Current neuropharmacology*. Bentham Science Publishers, 12(5), pp. 444–61. doi: 10.2174/1570159X12666140619204251.

Shackman, A. J. *et al.* (2011) 'The integration of negative affect, pain and cognitive control in the cingulate cortex', *Nature Reviews Neuroscience*. Nature Publishing Group, 12(3), pp. 154–167. doi: 10.1038/nrn2994.

Short, B. *et al.* (2017) 'Review Side-effects associated with ketamine use in depression: a systematic review', *The Lancet Psychiatry*, 5, pp. 65–78. doi: 10.1016/S2215-0366(17)30272-9.

Short, B. *et al.* (2018) 'Side-effects associated with ketamine use in depression: a systematic review.', *The lancet. Psychiatry*. Elsevier, 5(1), pp. 65–78. doi: 10.1016/S2215-0366(17)30272-9.

Sierra, C. (2014) 'Essential hypertension, cerebral white matter pathology and ischemic stroke.', *Current medicinal chemistry*, 21(19), pp. 2156–64. Available at: http://www.ncbi.nlm.nih.gov/pubmed/24372222 (Accessed: 22 February 2016).

Sigal, T. *et al.* (2012) 'Diffusion tensor imaging of corpus callosum integrity in multiple sclerosis: correlation with disease variables.', *Journal of neuroimaging : official journal of the American Society of Neuroimaging*, 22(1), pp. 33–7. doi: 10.1111/j.1552-6569.2010.00556.x.

De Simoni, S. *et al.* (2013) 'Test-retest reliability of the BOLD pharmacological MRI response to ketamine in healthy volunteers.', *NeuroImage*. Elsevier Inc., 64, pp. 75–90. doi: 10.1016/j.neuroimage.2012.09.037.

Singh, I. *et al.* (2017a) 'Ketamine treatment for depression: opportunities for clinical innovation and ethical foresight', *The Lancet Psychiatry*, 4(5), pp. 419–426. doi: 10.1016/S2215-0366(17)30102-5.

Singh, I. *et al.* (2017b) 'Ketamine treatment for depression: Opportunities for clinical innovation and ethical foresight', *The Lancet Psychiatry*. Elsevier Ltd, 0366(17), pp. 1–8. doi: 10.1016/S2215-0366(17)30102-5.

Skaper, S. D. *et al.* (2018) 'An Inflammation-Centric View of Neurological Disease: Beyond the Neuron', *Frontiers in Cellular Neuroscience*, 12, p. 72. doi: 10.3389/fncel.2018.00072.

Sled, J. G., Zijdenbos, A. P. and Evans, A. C. (1998) 'A nonparametric method for automatic correction of intensity nonuniformity in MRI data', *IEEE transactions on medical imaging*, 17(1), pp. 87–97. doi: 10.1109/42.668698.

Song, S.-K. *et al.* (2003) 'Diffusion tensor imaging detects and differentiates axon and myelin degeneration in mouse optic nerve after retinal ischemia.', *NeuroImage*, 20(3), pp. 1714–22. Available at: http://www.ncbi.nlm.nih.gov/pubmed/14642481 (Accessed: 13 January 2016).

Song, S.-K. *et al.* (2005) 'Demyelination increases radial diffusivity in corpus callosum of mouse brain.', *NeuroImage*, 26(1), pp. 132–40. doi: 10.1016/j.neuroimage.2005.01.028.

Song, X. *et al.* (2013) 'Elevated levels of adiponectin and other cytokines in drug naïve, first episode schizophrenia patients with normal weight.', *Schizophrenia research*, 150(1), pp. 269–73. doi: 10.1016/j.schres.2013.07.044.

Spangaro, M. *et al.* (2012) 'Cognitive dysfunction and glutamate reuptake: Effect of EAAT2 polymorphism in schizophrenia', *Neuroscience Letters*. Elsevier Ireland Ltd, 522(2), pp. 151–155. doi: 10.1016/j.neulet.2012.06.030.

Steeds, H., Carhart-Harris, R. L. and Stone, J. M. (2014) 'Drug models of schizophrenia', *Therapeutic Advances in Psychopharmacology*, 5, pp. 43–58. doi: 10.1177/2045125314557797.

Steen, R. G., Hamer, R. M. and Lieberman, J. A. (2005) 'Measurement of Brain Metabolites by

1H Magnetic Resonance Spectroscopy in Patients with Schizophrenia: A Systematic Review and Meta-Analysis', *Neuropsychopharmacology*, 30(11), pp. 1949–1962. doi: 10.1038/sj.npp.1300850.

Stephenson, J. *et al.* (2018) 'Inflammation in CNS Neurodegenerative Diseases', *Immunology*. doi: 10.1111/imm.12922.

Stolp, H. B. *et al.* (2018) 'Voxel-wise comparisons of cellular microstructure and diffusion-MRI in mouse hippocampus using 3D Bridging of Optically-clear histology with Neuroimaging Data (3D-BOND)', *Scientific Reports*, 8(1). doi: 10.1038/s41598-018-22295-9.

Stone, J. *et al.* (2015) 'Perceptual distortions and delusional thinking following ketamine administration are related to increased pharmacological MRI signal changes in the parietal lobe.', *Journal of psychopharmacology (Oxford, England)*, pp. 8–11. doi: 10.1177/0269881115592337.

Stone, J., Dietrich, C. and Edden, R. (2012) 'Ketamine effects on brain GABA and glutamate levels with 1H-MRS: relationship to ketamine-induced psychopathology - supplementary', *Molecular …*, (1). Available at: http://www.ncbi.nlm.nih.gov/pmc/articles/PMC3883303/ (Accessed: 20 November 2014).

Stone, J. M. *et al.* (2009) 'Glutamate dysfunction in people with prodromal symptoms of psychosis: relationship to gray matter volume.', *Biological psychiatry*. Elsevier Inc., 66(6), pp. 533–9. doi: 10.1016/j.biopsych.2009.05.006.

Stone, J. M. *et al.* (2012) 'Ketamine effects on brain GABA and glutamate levels with 1H-MRS: relationship to ketamine-induced psychopathology.', *Molecular psychiatry*. Nature Publishing Group, 17(7), pp. 664–5. doi: 10.1038/mp.2011.171.

Stone, J. M. *et al.* (2014) 'Glutamate, N-acetyl aspartate and psychotic symptoms in chronic ketamine users.', *Psychopharmacology*, 231(10), pp. 2107–16. doi: 10.1007/s00213-013-3354-8.

Stone, J. M., Morrison, P. D. and Pilowsky, L. S. (2007) 'Glutamate and dopamine dysregulation in schizophrenia--a synthesis and selective review.', *Journal of psychopharmacology (Oxford, England)*, 21(4), pp. 440–52. doi: 10.1177/0269881106073126.

Sturrock, R. R. 'Myelination of the mouse corpus callosum.', *Neuropathology and applied neurobiology*, 6(6), pp. 415–20. Available at: http://www.ncbi.nlm.nih.gov/pubmed/7453945 (Accessed: 13 January 2016).

Sun, L. *et al.* (2011) 'Permanent deficits in brain functions caused by long-term ketamine

treatment in mice.', *Human & experimental toxicology*, 30(9), pp. 1287–1296. doi: 10.1177/0960327110388958.

Takahashi, N. *et al.* (2011) 'Linking oligodendrocyte and myelin dysfunction to neurocircuitry abnormalities in schizophrenia.', *Progress in neurobiology*, 93(1), pp. 13–24. doi: 10.1016/j.pneurobio.2010.09.004.

Tanaka, H. *et al.* (2009) 'Mice with Altered Myelin Proteolipid Protein Gene Expression Display Cognitive Deficits Accompanied by Abnormal Neuron-Glia Interactions and Decreased Conduction Velocities', *Journal of Neuroscience*, 29(26), pp. 8363–8371. doi: 10.1523/JNEUROSCI.3216-08.2009.

Taylor, C. *et al.* (2005) 'Mechanisms of action of antidepressants: from neurotransmitter systems to signaling pathways.', *Cellular signalling*. NIH Public Access, 17(5), pp. 549–57. doi: 10.1016/j.cellsig.2004.12.007.

Taylor, M. J. *et al.* (2012) 'Lack of effect of ketamine on cortical glutamate and glutamine in healthy volunteers: a proton magnetic resonance spectroscopy study.', *Journal of psychopharmacology (Oxford, England)*, 26(5), pp. 733–7. doi: 10.1177/0269881111405359.

Théberge, J. *et al.* (2004) 'Duration of untreated psychosis vs. N-acetylaspartate and choline in first episode schizophrenia: a 1H magnetic resonance spectroscopy study at 4.0 Tesla.', *Psychiatry research*, 131(2), pp. 107–14. doi: 10.1016/j.pscychresns.2004.04.002.

Thompson, P. M. (2004) 'Structural Abnormalities in the Brains of Human Subjects Who Use Methamphetamine', *Journal of Neuroscience*, 24(26), pp. 6028–6036. doi: 10.1523/JNEUROSCI.0713-04.2004.

Thompson, S. M. *et al.* (2015) 'An excitatory synapse hypothesis of depression', *Trends in Neurosciences*, 38(5), pp. 279–294. doi: 10.1016/j.tins.2015.03.003.

Tibbo, P. *et al.* (2004) '3-T proton MRS investigation of glutamate and glutamine in adolescents at high genetic risk for schizophrenia.', *The American journal of psychiatry*, 161(6), pp. 1116–8. doi: 10.1176/appi.ajp.161.6.1116.

Tohka, J., Zijdenbos, A. and Evans, A. (2004) 'Fast and robust parameter estimation for statistical partial volume models in brain MRI', *NeuroImage*, 23(1), pp. 84–97. doi: 10.1016/j.neuroimage.2004.05.007.

Tomassy, G. S. *et al.* (2014) 'Distinct profiles of myelin distribution along single axons of pyramidal neurons in the neocortex.', *Science (New York, N.Y.)*, 344(June), pp. 319–24. doi: 10.1126/science.1249766.

Tustison, N. J. *et al.* (2010) 'N4ITK: Improved N3 Bias Correction', *IEEE Transactions on Medical Imaging*, 29(6), pp. 1310–1320. doi: 10.1109/TMI.2010.2046908.

Uranova, N. a *et al.* (2004) 'Oligodendroglial density in the prefrontal cortex in schizophrenia and mood disorders: a study from the Stanley Neuropathology Consortium.', *Schizophrenia research*, 67(2–3), pp. 269–75. doi: 10.1016/S0920-9964(03)00181-6.

Vernon, A. C. *et al.* (2011) 'Effect of chronic antipsychotic treatment on brain structure: a serial magnetic resonance imaging study with ex vivo and postmortem confirmation.', *Biological psychiatry*. Elsevier Inc., 69(10), pp. 936–44. doi: 10.1016/j.biopsych.2010.11.010.

Vernon, A. C. *et al.* (2012) 'Contrasting effects of haloperidol and lithium on rodent brain structure: a magnetic resonance imaging study with postmortem confirmation.', *Biological psychiatry*. Elsevier Inc., 71(10), pp. 855–63. doi: 10.1016/j.biopsych.2011.12.004.

Vernon, A. C. *et al.* (2014) 'Reduced cortical volume and elevated astrocyte density in rats chronically treated with antipsychotic drugs-linking magnetic resonance imaging findings to cellular pathology.', *Biological psychiatry*. Elsevier, 75(12), pp. 982–90. doi: 10.1016/j.biopsych.2013.09.012.

Vicente, R. *et al.* (2008) 'Dynamical relaying can yield zero time lag neuronal synchrony despite long conduction delays.', *Proceedings of the National Academy of Sciences of the United States of America*, 105(44), pp. 17157–17162. doi: 10.1073/pnas.0809353105.

Volterra, A. and Meldolesi, J. (2005) 'Astrocytes, from brain glue to communication elements: the revolution continues.', *Nature reviews. Neuroscience*, 6(8), pp. 626–40. doi: 10.1038/nrn1722.

Vande Voort, J. L. *et al.* (2016) 'Antisuicidal Response Following Ketamine Infusion Is Associated With Decreased Nighttime Wakefulness in Major Depressive Disorder and Bipolar Disorder', *The Journal of Clinical Psychiatry*. doi: 10.4088/JCP.15m10440.

Walhovd, K. B., Johansen-Berg, H. and Karadottir, R. T. (2014) 'Unravelling the secrets of white matter - bridging the gap between cellular, animal and human imaging studies.', *Neuroscience*, 276, pp. 2–13. doi: 10.1016/j.neuroscience.2014.06.058.

Walton, M. E. *et al.* (2007) 'Adaptive decision making and value in the anterior cingulate cortex.', *NeuroImage*. Elsevier Inc., 36 Suppl 2(3), pp. T142-54. doi: 10.1016/j.neuroimage.2007.03.029.

Wang, C. *et al.* (2013) 'Brain damages in ketamine addicts as revealed by magnetic resonance imaging.', *Frontiers in neuroanatomy*, 7(July), p. 23. doi: 10.3389/fnana.2013.00023.

Wang, J. J. *et al.* (2009) 'MRSI and DTI: a multimodal approach for improved detection of white matter abnormalities in alcohol and nicotine dependence', *NMR in Biomedicine*, 22(5), pp. 516–522. doi: 10.1002/nbm.1363.

Wang, N. *et al.* (2014) 'Downregulation of Neuregulin 1-ErbB4 Signaling in Parvalbumin Interneurons in the Rat Brain May Contribute to the Antidepressant Properties of Ketamine.', *Journal of molecular neuroscience : MN*, 54(2), pp. 211–8. doi: 10.1007/s12031-014-0277-8.

Wang, S. and Young, K. M. (2014) 'White matter plasticity in adulthood.', *Neuroscience*. IBRO, 276, pp. 148–60. doi: 10.1016/j.neuroscience.2013.10.018.

Weiland, B. J. *et al.* (2015) 'Daily Marijuana Use Is Not Associated with Brain Morphometric Measures in Adolescents or Adults', *The Journal of Neuroscience* , 35(4), pp. 1505–1512. doi: 10.1523/JNEUROSCI.2946-14.2015.

West, M. J. (2002) 'Design-based stereological methods for counting neurons.', *Progress in brain research*, 135, pp. 43–51. doi: 10.1016/S0079-6123(02)35006-4.

Wilkinson, S. T. *et al.* (2017) 'A Survey of the Clinical, Off-Label Use of Ketamine as a Treatment for Psychiatric Disorders', *American Journal of Psychiatry*, 174(7), pp. 695–696. doi: 10.1176/appi.ajp.2017.17020239.

Wohleb, E. S. *et al.* (2017) 'Molecular and Cellular Mechanisms of Rapid-Acting Antidepressants Ketamine and Scopolamine.', *Current neuropharmacology*, 15(1), pp. 11–20. Available at: http://www.ncbi.nlm.nih.gov/pubmed/26955968 (Accessed: 20 May 2018).

Wolff, K. and Winstock, A. R. (2006) 'Ketamine : from medicine to misuse.', *CNS drugs*, 20(3), pp. 199–218. Available at: http://www.ncbi.nlm.nih.gov/pubmed/16529526.

Wood, S. J. *et al.* (2007) 'Evidence for neuronal dysfunction in the anterior cingulate of patients with schizophrenia: a proton magnetic resonance spectroscopy study at 3 T.', *Schizophrenia research*, 94(1–3), pp. 328–31. doi: 10.1016/j.schres.2007.05.008.

Wood, T. C. *et al.* (2016) 'Whole-brain ex-vivo quantitative MRI of the cuprizone mouse model', *PeerJ*, 4, p. e2632. doi: 10.7717/peerj.2632.

Wu, H. *et al.* (2016) 'NMDA receptor antagonism by repetitive MK801 administration induces schizophrenia-like structural changes in the rat brain as revealed by voxel-based morphometry and diffusion tensor imaging', *Neuroscience*, 322, pp. 221–233. doi: 10.1016/j.neuroscience.2016.02.043.

Wu, Y. *et al.* (2015) 'Microglia: Dynamic Mediators of Synapse Development and Plasticity',

Trends in Immunology, 36(10), pp. 605–613. doi: 10.1016/j.it.2015.08.008.

Wu, Z. *et al.* (2014) 'Tonic inhibition in dentate gyrus impairs long-term potentiation and memory in an Alzheimer's [corrected] disease model.', *Nature communications*, 5, p. 4159. doi: 10.1038/ncomms5159.

Xia, M. *et al.* (2014) 'Behavioral sequelae of astrocyte dysfunction: focus on animal models of schizophrenia.', *Schizophrenia research*. doi: 10.1016/j.schres.2014.10.044.

Xiu, Y. *et al.* (2014) 'White matter injuries induced by MK-801 in a mouse model of schizophrenia based on NMDA antagonism.', *Anatomical record (Hoboken, N.J. : 2007)*, 297(8), pp. 1498–507. doi: 10.1002/ar.22942.

Xiu, Y. *et al.* (2015) 'The myelinated fiber loss in the corpus callosum of mouse model of schizophrenia induced by MK-801', *Journal of Psychiatric Research*, 63, pp. 132–140. doi: 10.1016/j.jpsychires.2015.02.013.

Xu, H. *et al.* (2009) 'Behavioral and neurobiological changes in C57BL/6 mice exposed to cuprizone.', *Behavioral neuroscience*, 123(2), pp. 418–29. doi: 10.1037/a0014477.

Yang, C. *et al.* (2016) 'Loss of parvalbumin-immunoreactivity in mouse brain regions after repeated intermittent administration of esketamine, but not R-ketamine', *Psychiatry Research*, 239, pp. 281–283. doi: 10.1016/j.psychres.2016.03.034.

Yang, G., Pan, F. and Gan, W.-B. (2009) 'Stably maintained dendritic spines are associated with lifelong memories.', *Nature*, 462(7275), pp. 920–4. doi: 10.1038/nature08577.

Yang, Z. and Wang, K. K. W. (2015) 'Glial fibrillary acidic protein: from intermediate filament assembly and gliosis to neurobiomarker', *Trends in Neurosciences*, 38(6), pp. 364–374. doi: 10.1016/j.tins.2015.04.003.

Yoo, S. Y. *et al.* (2009) 'Proton magnetic resonance spectroscopy in subjects with high genetic risk of schizophrenia: investigation of anterior cingulate, dorsolateral prefrontal cortex and thalamus.', *Schizophrenia research*. Elsevier B.V., 111(1–3), pp. 86–93. doi: 10.1016/j.schres.2009.03.036.

Yu, H. J. *et al.* (2012) 'Multiple white matter tract abnormalities underlie cognitive impairment in RRMS.', *NeuroImage*, 59(4), pp. 3713–22. doi: 10.1016/j.neuroimage.2011.10.053.

Yücel, D. I. *et al.* (2007) 'Neuropsychological Perspective', *Australiain and New Zealand Journal of Psychiatry*, 41, pp. 957–968.

Yung, A. R. *et al.* (2005) 'Mapping the onset of psychosis: the Comprehensive Assessment of

At-Risk Mental States.', *The Australian and New Zealand journal of psychiatry*. SAGE Publications, 39(11–12), pp. 964–71. doi: 10.1111/j.1440-1614.2005.01714.x.

Yung, A. R. *et al.* (2005) 'Mapping the onset of psychosis: The comprehensive assessment of at risk mental states (CAARMS)', *Australian and New Zealand Journal of Psychiatry*, 39(December 2004), pp. 964–971. doi: 10.1016/S0920-9964(03)80090-7.

Zanos, P. *et al.* (2018) 'Convergent Mechanisms Underlying Rapid Antidepressant Action', *CNS Drugs*, 32(3), pp. 197–227. doi: 10.1007/s40263-018-0492-x.

Zarate, C. and Singh, J. (2006) 'A randomized trial of an N-methyl-D-aspartate antagonist in treatment-resistant major depression', *Archives of …*, 63. Available at: http://archneur.jamanetwork.com/article.aspx?articleid=668195 (Accessed: 9 October 2014).

Zatorre, R. J., Fields, R. D. and Johansen-Berg, H. (2012) 'Plasticity in gray and white: neuroimaging changes in brain structure during learning', *Nature Neuroscience*. Nature Publishing Group, 15(4), pp. 528–536. doi: 10.1038/nn.3045.

Zhang, D. *et al.* (2012) 'Preclinical experimental models of drug metabolism and disposition in drug discovery and development', *Acta Pharmaceutica Sinica B*. Elsevier, 2(6), pp. 549–561. doi: 10.1016/j.apsb.2012.10.004.

Zhang, M. W., Harris, K. M. and Ho, R. C. (2016) 'Is Off-label repeat prescription of ketamine as a rapid antidepressant safe ? Controversies , ethical concerns , and legal implications', *BMC Medical Ethics*. BMC Medical Ethics, pp. 1–8. doi: 10.1186/s12910-016-0087-3.

Zhang, M. W., Harris, K. M. and Ho, R. C. (2016) 'Is Off-label repeat prescription of ketamine as a rapid antidepressant safe? Controversies, ethical concerns, and legal implications', *BMC Medical Ethics*, 17(1), p. 4. doi: 10.1186/s12910-016-0087-3.

Zhang, R. *et al.* (2012) 'Myelination deficit in a phencyclidine-induced neurodevelopmental model of schizophrenia.', *Brain research*. Elsevier, 1469, pp. 136–43. doi: 10.1016/j.brainres.2012.06.003.

Zhang, Y., Behrens, M. M. and Lisman, J. E. (2008) 'Prolonged exposure to NMDAR antagonist suppresses inhibitory synaptic transmission in prefrontal cortex.', *Journal of neurophysiology*, 100(2), pp. 959–65. doi: 10.1152/jn.00079.2008.

Zhou, Y. and Danbolt, N. C. (2013) 'GABA and Glutamate Transporters in Brain.', *Frontiers in endocrinology*, 4(November), p. 165. doi: 10.3389/fendo.2013.00165.

Zhou, Y. and Danbolt, N. C. (2014) 'Glutamate as a neurotransmitter in the healthy brain',

Journal of Neural Transmission, 121(8), pp. 799–817. doi: 10.1007/s00702-014-1180-8.

Zhu, S. *et al.* (2014) 'Chronic Phencyclidine Induces Inflammatory Responses and Activates GSK3?? in Mice', *Neurochemical Research*, 39(12), pp. 2385–2393. doi: 10.1007/s11064-014-1441-9.

Zhu, W. *et al.* (2016) 'Risks Associated with Misuse of Ketamine as a Rapid-Acting Antidepressant', *Neuroscience Bulletin*, 32(6), pp. 557–564. doi: 10.1007/s12264-016-0081-2.

Bibliography – News articles and websites

BBC News. (2017, April 6). *Ketamine depression treatment 'should be rolled out'*. Retrieved from bbc.co.uk/news: http://www.bbc.co.uk/news/health-39501566

Codrea-Racio, A. (2016, April 13). *Here's everything you need to know about ketamine*. Retrieved from vice.com: https://thump.vice.com/en_us/article/kb575a/ketamine-club-drug-explainer

Daly, M. (2016, February 18). *How ketamine has made its way back into the uk*. Retrieved from vice.com: https://www.vice.com/en_uk/article/bnp48a/return-of-ketamine-uk-china-labs

Daly, M. (2016, June 12). *Why do Brits love ketamine so much?* Retrieved from vice.com: https://www.vice.com/en_uk/article/nnkjed/why-do-the-british-love-ketamine-so-much

Forster, K. (2017, April 5). *Independent*. Retrieved from independent.co.uk: https://www.independent.co.uk/news/health/ketamine-depression-treatment-cure-nothing-else-works-oxford-university-rupert-mcshane-a7668441.html

Forster, K. (2017, July 25). *Ketamine has 'truly remarkable' effect on depression and is effective in elderly patients, scientists say*. Retrieved from independent.co.uk: https://www.independent.co.uk/news/health/ketamine-elderly-patients-severe-depression-effect-benefit-horse-tranquiliser-study-colleen-loo-new-a7859511.html

Hatton, C. (2015, Juy 10). *The Ketamine Connection*. Retrieved from BBC.co.uk/news: http://www.bbc.co.uk/news/resources/idt-bc7d54e7-88f6-4026-9faa-2a36d3359bb0

Ketamine Advocacy Network. (2015). *Cost*. Retrieved from ketamineadvocacynetwork.org: http://www.ketamineadvocacynetwork.org/cost/

Ketamine Health Centres. (n.d.). Retrieved from ketaminehealthcentres.com: http://ketaminehealthcenters.com/

Ketamine Wellness Centres. (2018). *Ketamine treatments*. Retrieved from ketaminewellnesscentres.com: https://www.ketaminewellnesscenters.com/

Labu, N. (2017, October 25). *Smugglers use towes to move ketamine to Spain*. Retrieved from dhakatribune.com: http://www.dhakatribune.com/bangladesh/crime/2017/10/25/bangladeshi-smugglers-spray-g-ketamine-white-towels-smuggle-spain-courier/

Malta Independent. (2010, June 25). *Maltese facing ketamine trafficking charges in Italy*. Retrieved from Independent.com: http://www.independent.com.mt/articles/2010-06-25/news/maltese-facing-ketamine-trafficking-chargesin-italy-276364/

Marsh, S. (2017, June 2). *Ketamine could help thousands with severe depression, doctors say*. Retrieved from guardian.com: https://www.theguardian.com/society/2017/jun/02/ketamine-help-thousands-severe-depression-doctors

Mind. (2016, June). *Treatment*. Retrieved from Mind.org.uk: https://www.mind.org.uk/information-support/types-of-mental-health-problems/depression/treatment/#.WsPscC7wa2Q

NHS. (2016, October 5). *Treatment*. Retrieved from NHS.uk: https://www.nhs.uk/conditions/clinical-depression/treatment/

NY Ketamine Infusions LLC. (2018). *Depression*. Retrieved from nyketamine.com: http://nyketamine.com/depression/

Oaklander, M. (2017, July 27). *New Hope for Depression*. Retrieved from time.com: http://time.com/4876098/new-hope-for-depression/

Oliver, S. (2017, December 13). *My life as an international ketamine smuggler*. Retrieved from vice.com: https://www.vice.com/en_uk/article/5959zk/my-life-as-an-international-ketamine-smuggler

Oxford Health. (2017, August 16). *Ketamine service for depression*. Retrieved from oxfordhealth.nhs.uk: https://www.oxfordhealth.nhs.uk/service_description/ketamine-clinic-for-depression/

Portland Ketamine Clinic. (n.d.). *PKC*. Retrieved from portlandketamineclinic.com: http://portlandketamineclinic.com/PKC/

Survey, G. D. (2011, August 30). *k-hole*. Retrieved from globaldrugsurvey.com: https://www.globaldrugsurvey.com/k-hole/